Redox controls on Cr isotopes in natural waters



Qiong Zhang

Department of Earth Sciences & St Anne's College

University of Oxford

A thesis submitted for the degree of

Doctor of Philosophy in Geology and Mineralogy

Trinity Term 2016

Supervised by Prof. Don Porcelli and Prof. Ian Thompson

Abstract

Redox controls on Cr isotopes in natural waters

Qiong Zhang
St Anne's College, Oxford

Trinity Term, 2016

Shifts in Cr isotope fractionations due to microbial activity provide valuable insights into the mechanisms of its cycling, and can be used to quantify biogeochemically mediated redox processes in the environment. In my thesis, microbial Cr isotope fractionations were determined, with a broad range of experimental variables, including species, electron donors, Cr concentration, pH and respiration pathways, and the information can be used to understand the natural environment. Cr isotopes are found to be very sensitive to the types of electron donors and bacterial respiration pathways, indicating that the bacteria employed different metabolic pathways to reduce Cr under those conditions. These also suggest the potential to develop Cr isotopes as a new tool to probe specific biological processes. Cr isotope fractionation in metal-microbe-mineral interactions is also studied. The addition of the minerals did not lead to a significant change on bacterial Cr isotope fractionations, though Cr reduction rates were significantly impacted. This indicates that although metabolic rates were altered by the interactions with the minerals, similar reduction pathways were still used by the bacteria. Based on these studies, the potential of combining a whole cell bioreporter, which can be used to assess the toxicity of Cr, and Cr isotope techniques, which can be applied in monitoring bio-reduction processes in contaminated sites, were explored. The whole cell bioreporter was found to be efficient in indicating Cr toxicity at different concentration levels and Cr isotopes were independent of toxicity levels. Therefore, it can be used to monitor bioremediation processes of Cr(VI) with different concentrations.

Extended Abstract

Redox controls on Cr isotopes in natural waters

Qiong Zhang

St Anne's College, Oxford

Trinity Term, 2016

Shifts in Cr isotope fractionations due to microbial activity provide valuable insight into the mechanisms of Cr cycling, and can be used to quantify biogeochemically mediated redox processes in the environment. However, little is known of the environmental conditions and microbial activity that determine Cr isotope fractionation. In the first study, the metabolism of Cr by two facultative anaerobic bacteria, *Pseudomonas fluorescens* LB 300 and *Shewanella oneidensis* MR-1, was investigated to determine the conditions under which Cr(VI) is reduced and the corresponding isotope signatures that are generated. The present study considered the effects of a broad range of parameters, including microbial species, electron donors, pH and respiration pathways, on Cr isotope fractionation.

Both bacteria were able to reduce Cr(VI) within the experimental period and incubation conditions, and in all cases the $^{53}Cr/^{52}Cr$ isotope ratio of the remaining Cr(VI) increased, indicating that the reduced Cr was isotopically lighter. In the aerobic reduction experiments conducted at a range of different pH (pH=4, 6 and 8), the greatest reduction rate occurred at pH = 8, while under all pH conditions progressive reduction increased the isotope ratio of Cr(VI) by Rayleigh distillation with a fractionation factor of ε = -3.1‰, indicating that pH had lit-

tle impact on isotope fractionation. Experiments using different electron donors demonstrated that citrate promoted the greatest Cr(VI) reduction rate (15.1×10^{-10} mg·L^{-1}·$hour^{-1}$·$cell^{-1}$) compared with glucose (6.6×10^{-10} mg·L^{-1}·$hour^{-1}$·$cell^{-1}$), acetate (4.9×10^{-10} mg·L^{-1}·$hour^{-1}$·$cell^{-1}$) and propionate (4.8×10^{-10} mg·L^{-1}·$hour^{-1}$·$cell^{-1}$). Under aerobic conditions, although Cr(VI) reduction rates varied substantially under different experimental settings, the isotope fractionation factors were constant for all the environmental conditions examined ($\varepsilon = 3.1$); with the exception of citrate (ε = -4.3 ‰).

Cr(VI) reduction rates were generally much faster under anaerobic conditions for both bacteria investigated. Under anaerobic conditions, the utilisation of different electron donors resulted in the same Cr(VI) reduction rates by the bacteria, but fractionated Cr with a broad range of isotope fractionation factors; -4.6 ‰ for citrate, -3.2 ‰ for acetate, -5.0 ‰ for glucose and -1.5 ‰ for propionate; possibly reflects different reduction pathways. No clear relationship between the reduction rates and fractionation factors was observed in this study.

The Cr isotope fractionation factors ε are insensitive to pH and substrate concentration, but dependant on the type of electron donors and respiration pathways of bacteria. This indicates that isotope variations may be used to investigate metabolic processes, by clearly distinguishing different biological pathways. Although having been proposed in many previous studies, an inverse relationship between reduction rates and fractionation factors were not observed in this study. The ε value from all experimental conditions examined ranged between 1.5 to 5 ‰, with a mean value at -3.3 ‰. This is valuable information for assessing the behaviour of Cr in the environment, and helps further to establish isotopic fractionation as an environmental diagnostic tool.

The second study mainly focuses on the interactions between Cr, Fe minerals and bacteria. Microbes interact with metals and minerals in the environments, altering their physical and chemical state whilst in turn the metals and minerals af-

fect microbial growth, activity and survival. Cr(VI) reduction experiments with two iron-reducing bacteria, *Pseudomonas fluorescens* LB 300 and *Shewanella oneidensis* MR 1, were conducted, in the presence of two iron oxide minerals, goethite and haematite, which are common in the environment. Both minerals were found to inhibit Cr(VI) reduction rates by *Pseudomonas*, but accelerated those by *Shewanella*. The Cr isotopic fractionation factors generated by *Shewanella* was independent of the presence of both minerals (ε = -2.3 ‰). For *Pseudomonas*, the ε value was the same in both the presence and absence of goethite (-3.3 ‰), however, it was much higher (ε = -4.3 ‰) with the presence of haematite. This indicates that the type of minerals in the environment may have significant impact on bacterial Cr isotope fractionation and must be taken into consideration when using Cr isotope data to estimate the extent of reduction.

Aqueous Fe(III) in the solution had no detectable impact on either bacterial Cr(VI) reduction rates nor the isotopic fractionation factors, indicating that the reduction of Cr(VI) occurred prior to that of Fe(III). The presence of aqueous Fe(II) induced rapid abiotic reduction of Cr(VI), but had little impact on bacterial Cr(VI) reduction rates or isotope fractionation. The evidence suggests that the different impacts that Fe minerals had were related to the way bacteria attached to the minerals and the difference in the reduction pathways. SEM images confirmed that *Pseudomonas* were much more tightly packed on the mineral surfaces than were *Shewanella*. The images also confirmed that *Shewanella* produced nanowires. The results indicate that the dominant Cr(VI) reduction pathway for *Pseudomonas fluorescens* LB 300 is through membrane-bound enzymes, while for *Shewanella oneidensis* MR 1 is through extracellular electron transfer.

In the third study of my thesis, I used a whole cell bioreporter *Acinetobacter baylyi* ADPWH-*rec*A to indicate the toxicity of different species of Cr over a range of initial concentrations, and used Cr isotope techniques to study the impacts of different Cr(VI) concentration and its toxicity on the reduction processes by *Pseu-*

domonas fluorescens LB 300 (LB 300). The whole cell bioreporter *Acinetobacter baylyi* ADPWH-*rec*A was efficient in indicating the genotoxicity of Cr(VI) at low concentration levels and cytotoxicity at high concentration levels. High concentrations (> 100 mg/L) of Cr(III) could also strongly induce the luminescence in the bioreporter, indicating it could cause DNA damage at such concentration level. *Pseudomonas fluorescens* LB 300 was found to be effective in reducing Cr(VI) even when the concentration was high (40 mg/L), however, complete Cr(VI) reduction was only observed at low concentration level (< 5 mg/L), reflecting that the toxicity of high concentration of Cr(VI) would impact on its reduction process by the bacteria. With its reduction, Cr isotope fractionated, the δ^{53}Cr value increased in Cr(VI) species, indicating that the product was isotopically lighter. The calculated fractionation factor by bacterial Cr(VI) reduction process (ε) was 3.1 ‰ when its initial concentration was less than 20 mg/L, and was 2.6 ‰ when the Cr(VI) concentration was 40 mg/L. The small variation of the ε values generated from different experiments indicates that initial Cr(VI) concentration is not an important factor to consider when use Cr isotope data to indicate the extent of reduction in the environment or during bioremediation.

The contents of this thesis are all my own work, except where otherwise stated. The views and opinions expressed herein are mine and not necessarily those of any other person or body unless so attributed.

Acknowledgements

I would like thank many people without whom this thesis would never have been possible. First, I would like to offer my sincerest gratitude to both of my supervisors, Professor Don Porcelli and Professor Ian Thompson, for their guidance and support, their criticism, and their endless encouragement throughout the duration of my PhD.

This research was funded by the EU Framework 7 Marie Curie Initial training Network MetTrans. Many thanks to all the senior researchers in the network for sharing their vast knowledge in different areas and offering their support and advice to my research, especially Prof Don Porcelli, Prof Johan Ingri, Dr. Per Andersson, Dr. Ian Burke, Dr. Sam Shaw, and Dr. Sander Van Den Boorn. Great thanks to all the metTrans fellows for their support and encouragement over the years and for those fun times we spent together: Dr. Mel Murphy, Hanna Wouters, Sarah Conrad, Giada Trezzi, Lindsay Krall, Becca Neely, Catherine Hirst, Nicola Pallavicini, Marco Agnelli, Andrea Perez, Scott Hawley, Lina Hällström, Joachim Katchinoff and Arola Moreras Marti. I also want to thank Naoual Assar and Maria Petrunova who did a great administrative job for MetTrans.

Many thanks to Dr. Ken Amor for his expertise in Cr isotope analysis and many helpful discussions about my research, Dr. Steve Galar for many practical advice and useful comments on my work, Dr. Song Yizhi for his advice in toxicity evaluation and Raman-spectrometry analysis. Thanks too, to Phil Holdship, Alan Hsieh, Steve Wyatt, Jon Wade, and Jane Barling for their great support in all the lab work in the Department of Earth Sciences. Special thanks to Mel Murphy for her

great support on my research, and also for all the delicious cakes she made! Many thanks to Pierre Bonnand for many useful advice and discussions. I also would like to acknowledge Prof. YiTin Wang (University of Washington), who kindly gave me the most important material for my study: my lovely bugs! Thanks to prof. Heather Bouman, Dr. Alex Dickson, and prof. Chris Ballentine for many useful comments and suggestions during my Transfer and Confirmation of Status. Thanks to prof. Ros Rickaby for many great advice for future studies and prof. Jon Lloyd who agrees to examine my viva and provides me many useful comments on my thesis.

Many thanks are due to my colleagues in Chemical Engineering group in Begbroke Science Park. I would like to thank Dr. Helen Townley and Dr. Wei Huang for many useful discussions and advice on my research. Thanks to Dr. Duan Ager for his support in the lab. Many thanks to Lakshmi Manjoosha Adapa, Licheng Shen, Shivashkar Singh, Cordelia Rampley, Fozia Parveen, Anna Evison, Patrick Thill, Ana Castro-Castellon, Cindy Huang, Catherine Fan, Gabriella Gadelha, Jiabao Xu, Ke Yang, Marimar Bravo, Meg Uapipatanakul, Naomi Wise, Pingqian Shen, Rachel Morrison, Xiafu Shi and Yaldah Azimi for their company.

I would also like to thank my friends at the Department of Earth Sciences, my officemates Allison Bryan, Ash Norris, danielle kondla, Cesar Espinoza Campuzano, Xinyuan Zheng, and Lan Chen, with whom I had all those interesting chatting and gossip with. Thanks to my fellow Postgrad12s: Yu, Weimu, Qingfeng, Helen, Nikita, Hanna, Renee, Fern, Brendan, Will, Ash, Dave, Tim and Mike for always being supportive. Many thanks are also due to the 'ultimate Frisbee group', especially John Hooker, who always sends out interesting advertisements for the game. Thanks Steve Usher for those interesting chatting and delicious chocolates, Cornelius Vermaak for his help, Micha Ruhl for those lovely cuisines he made. I also want to thank everyone in the clean lab community and all the computing, administrative and technical staff for their great efforts in keeping this department a great place to work in.

Thanks to all my friends who make my life in Oxford enjoyable: Chuang, Yang, Yilun and Xue, Xiaochen and Ran, Yishu, Weidi, Mengjiao, Shuo, Steven, Kwok, Mengyin, and a cast of thousands more. To my closest friends and those I consider family: Ula and Jerry, Ming, Kimi, Fan, Chao and Jin, Xinyuan, Jie, Weimu, Feifei and Yujia, thank you so much for always being supportive. I couldn't have done it without you!

Special thanks to Yu, for all those delicious cheesecakes he made, all his support and advice, all those interesting places we visited, and all the great time we spent together.

Lastly, I would like to thank my amazing family for their endless love and patience, especially my dear parents, who are always encouraging and supporting me. It is to my family that I dedicate this thesis.

Contents

Abstract i

Extended Abstract ii

Contents **x**

List of Figures **xv**

List of Tables **xx**

1 Introduction **1**

1.1 Chromium in the nature environment 1

1.1.1 Source of chromium 1

1.1.2 Toxicity of chromium 3

1.1.2.1 Toxicity effects in humans 3

1.1.2.2 Toxicity effects in cellular levels 4

1.1.2.3 The impact of Cr toxicity on the environment 5

1.1.3 Chromium behaviours and its isotopes 6

1.1.3.1 The effects of oxygen and pH levels 6

1.1.3.2 Reduction/oxidation of Cr 7

1.1.3.3 Adsorption of Cr 8

1.1.3.4 Microbial activity 9

1.1.3.5 Cr isotopes 9

1.2 Mechanisms of microbial Cr reduction 13

1.2.1 Aerobic reduction 14
1.2.2 Anaerobic reduction 15
1.2.3 Long distance electron transport 16
1.3 Mechanisms of Stable Isotope Fractionation 17
1.3.1 Equilibrium effects 17
1.3.2 Kinetic effects 19
1.3.3 Mathematical calculations 20
1.4 Bacterial sulphur reduction and isotope fractionation 22
1.5 Aims and overview of the thesis 25

2 Methodology **27**
2.1 Microbial reduction of chromium under various conditions 28
2.1.1 Bacteria strains 28
2.1.2 Strain stock and storage 28
2.1.3 Growth medium and general culturing condition 30
2.1.4 Growth curve 32
2.2 Chromium toxicity test 33
2.2.1 Preparation of the strain 33
2.2.2 Chromium sample preparation 34
2.2.3 Bioreporter response measurements 34
2.3 High Performance Ion Chromatography 35
2.3.1 Cr(VI) measurement 35
2.4 Chromium isotope measurement 38
2.4.1 Ion exchange separation of chromium for stable isotope mass spectrometric analysis 38
2.4.2 Further purification of chromium through liquid-liquid separation 40
2.4.3 Thermal Ionization Mass Spectrometry (TIMS) 41
2.4.4 The mass-dependent instrumental bias 43

2.4.5 Double spike method 45
2.4.6 Optimising the double spike 48
2.4.7 Reproducibility and accuracy of Cr isotopic measurements . . 50
2.5 SEM imaging of the microbial samples 50

3 The Cr isotope proxy for bacterial reduction processes 55
3.1 Introduction 55
3.2 Materials and Methods 59
3.2.1 Bacteria 59
3.2.2 Growth medium and general culturing condition 59
3.2.3 Cr reduction experiments 61
3.2.4 Cr Isotope Analysis 62
3.3 Results 62
3.3.1 Biosorption and bioreduction 62
3.3.2 Electron Donors and Respiration Pathways 63
3.3.3 Electron Donor Concentration 67
3.3.4 pH 68
3.4 Discussion 70
3.4.1 Electron Donors and Respiration Pathways 70
3.4.2 Electron Donor Concentration 73
3.4.3 pH 74
3.4.4 Bacterial species 75
3.5 Conclusion 76

4 Cr isotope fractionation during metal-mineral-microbe interactions 79
4.1 Introduction 79
4.2 Materials and Methods 83
4.2.1 Bacteria 83
4.2.2 Cr reduction experiments 84

4.2.3 Cr isotope analysis . . . 86
4.2.4 Characterization of bacteria-mineral interaction by SEM . . . 87
4.3 Results . . . 87
4.3.1 Fe minerals . . . 87
4.3.2 Aqueous Fe(III) . . . 97
4.3.3 Fe(II) . . . 98
4.3.4 SEM Analysis . . . 99
4.4 Discussion . . . 103
4.4.1 Is biogenic Fe(II) contributing to Cr(VI) reduction? . . . 103
4.4.2 Microbe-mineral interactions . . . 105
4.4.3 The impact of iron . . . 109
4.5 Conclusions . . . 111

5 Monitor Cr toxicity and remediation process-combining a whole-cell bioreporter and Cr isotope techniques 113

5.1 Introduction . . . 113
5.2 Materials and methods . . . 118
5.2.1 Chromium toxicity tests . . . 118
5.2.1.1 Preparation of the bioreporter . . . 119
5.2.1.2 chromium sample preparation . . . 119
5.2.1.3 Bioreporter response measurement . . . 119
5.2.2 Cr reduction experiments . . . 120
5.2.3 Cr isotope measurements . . . 121
5.3 Results . . . 121
5.3.1 Determination of Cr toxicity . . . 121
5.3.2 Bacterial Cr(VI) reduction experiments . . . 125
5.3.3 The application of Cr isotopes . . . 126
5.4 Discussion . . . 129
5.5 Conclusion . . . 134

6 Synthesis and Directions for Future Research **136**

6.1 Summary of previous studies 136

6.2 Directions of future study 140

6.2.1 Intracellular or extracellular reactions? 144

6.2.1.1 Study of intracellular pathways-the role of metals . . 146

6.2.1.2 Study of extracellular pathways 147

6.2.2 Applications 148

References **149**

Appendix **171**

List of Figures

1.1 the Eh-pH diagram showing the aqueous inorganic Cr species in soil-water environments. 7

2.1 Flasks from microbial aerobic reduction experiments 31
2.2 Bottles from microbial anaerobic reduction experiments. 31
2.3 Growth curve for *Pseudomonas fluorescens* LB 300. 32
2.4 96-well microplate used for the toxicity test. 35
2.5 The Cr (VI) ion chromatography peak at 530 nm wavelength for a 2.5 mg/L standard 37
2.6 Cr (VI) Standard Curve for Ion Chromatography measurements . . . 38
2.7 Efficiency calibration for the anion column 39
2.8 Contour plot of error in α for the ^{50}Cr - ^{54}Cr double spike. 49
2.9 Plot of the error in α against the proportion p of double spike in the double spike-sample mixture. 50
2.10 The long-term reproducibility of δ^{53}Cr for the Cr standard. 51
2.11 SEM photos for bacteria 54

3.1 Cr reduction experiments by *Pseudomonas fluorescens* LB 300 under aerobic conditions (a) and anaerobic conditions (b), using different compounds as electron donors. 63
3.2 The impact of different electron donors on Cr isotope fractionation by *Pseudomonas fluorescens* LB 300. Under aerobic conditions 65

3.3 The impact of different respiration pathways on Cr isotope fractionation by *Pseudomonas fluorescens* LB 300. 66
3.4 Comparison of the aerobic and anaerobic reduction and isotope fractionation of Cr (VI) by *Shewanella oneidensis* MR 1 67
3.5 The impact of glucose concentration on Cr reduction and isotope fractionation by *Pseudomonas fluorescens* LB 300 68
3.6 The impact of pH on Cr reduction and isotope fractionation by *Pseudomonas fluorescens* LB 300 69
3.7 Comparison of Cr isotope fractionation by different species of bacteria and from abiotic reactions 77

4.1 Raman spectra of the minerals phases used in this study. 89
4.2 XRD spectrum of the minerals used in this study. 90
4.3 Control experiments with bacteria and minerals 94
4.4 Microbial Cr reduction experiments in the presence of different forms of iron. 95
4.5 Observed isotope fractionation during microbial Cr reduction experiments. 96
4.6 The impact of Fe(II) on Cr(VI) reduction and isotope fractionation. . 100
4.7 SEM images for bacteria-mineral interactions 101
4.8 SEM image for *Shewanella oneidensis* MR 1 102
4.9 Three possible pathways for microbial Cr(VI) reduction. 108

5.1 Growth curve of the ADPWH_*rec*A. 122
5.2 Induction ratios of bioluminence of the bioreporter. 123
5.3 Growth curve of the ADPWH_*rec*A with different concentrations (< 5 mg/L) of $K_2Cr_2O_7$ and K_2CrO_4. 124
5.4 Response of ADPWH_*rec*A to different low concentrations of $K_2Cr_2O_7$ and K_2CrO_4 at 6 hours of experiment. 125

5.5 Bacterial Cr reduction experiments with different Cr initial concentrations 127

5.6 Bacterial Cr isotope fractionation experiments with different Cr initial concentrations 128

5.7 The response of ADPWH_*rec*A to different concentrations of $K_2Cr_2O_7$ (A) and K_2CrO_4 (B) after 6 hours of exposure and the response of ADPWH_*rec*A to different concentration of Cr(III) (C) in solution at time 0 and after 6 hours. 131

6.1 The relationship between Cr isotope fractionation factors and the half life of the reaction for abiotic Cr reduction experiments. 139

2 $\ln f$ vs. $\ln(\delta^{53}Cr/1000+1)$ for aerobic Cr(VI) reduction by *Pseudomonas* with glucose as the electron donor. 173

3 $\ln f$ vs. $\ln(\delta^{53}Cr/1000+1)$ for aerobic Cr(VI) reduction by *Pseudomonas* with citrate as the electron donor. 175

4 $\ln f$ vs. $\ln(\delta^{53}Cr/1000+1)$ for aerobic Cr(VI) reduction by *Pseudomonas* with acetate as the electron donor. 177

5 $\ln f$ vs. $\ln(\delta^{53}Cr/1000+1)$ for aerobic Cr(VI) reduction by *Pseudomonas* with propionate as the electron donor. 179

6 $\ln f$ vs. $\ln(\delta^{53}Cr/1000+1)$ for anaerobic Cr(VI) reduction by *Pseudomonas* with glucose as the electron donor. 181

7 $\ln f$ vs. $\ln(\delta^{53}Cr/1000+1)$ for anaerobic Cr(VI) reduction by *Pseudomonas* with citrate as the electron donor. 183

8 $\ln f$ vs. $\ln(\delta^{53}Cr/1000+1)$ for both aerobic and anaerobic Cr(VI) reduction by *Pseudomonas* with citrate as the electron donor. 184

9 $\ln f$ vs. $\ln(\delta^{53}Cr/1000+1)$ for anaerobic Cr(VI) reduction by *Pseudomonas* with acetate as the electron donor. 186

10 $\ln f$ vs. $\ln(\delta^{53}Cr/1000+1)$ for both aerobic and anaerobic Cr(VI) reduction by *Pseudomonas* with acetate as the electron donor. 187

11 $\ln f$ vs. $\ln(\delta^{53}Cr/1000+1)$ for anaerobic Cr(VI) reduction by *Pseudomonas* with propionate as the electron donor. 189

12 $\ln f$ vs. $\ln(\delta^{53}Cr/1000+1)$ for aerobic Cr(VI) reduction by *Shewanella* with succinate as the electron donor. 191

13 $\ln f$ vs. $\ln(\delta^{53}Cr/1000+1)$ for anaerobic Cr(VI) reduction by *Shewanella* with succinate as the electron donor. 193

14 $\ln f$ vs. $\ln(\delta^{53}Cr/1000+1)$ for Cr(VI) reduction by *Pseudomonas* at pH 4. 196

15 $\ln f$ vs. $\ln(\delta^{53}Cr/1000+1)$ for Cr(VI) reduction by *Pseudomonas* at pH 6. 198

16 $\ln f$ vs. $\ln(\delta^{53}Cr/1000+1)$ for Cr(VI) reduction by *Pseudomonas* at pH 8. 200

17 $\ln f$ vs. $\ln(\delta^{53}Cr/1000+1)$ for Cr(VI) reduction by *Pseudomonas* at different pH. 201

18 $\ln f$ vs. $\ln(\delta^{53}Cr/1000+1)$ for Cr(VI) reduction by *Pseudomonas* without any minerals or aqueous Fe species. 203

19 $\ln f$ vs. $\ln(\delta^{53}Cr/1000+1)$ for Cr(VI) reduction by *Pseudomonas* in the presence of goethite. 205

20 $\ln f$ vs. $\ln(\delta^{53}Cr/1000+1)$ for Cr(VI) reduction by *Pseudomonas* in the presence of haematite. 207

21 $\ln f$ vs. $\ln(\delta^{53}Cr/1000+1)$ for Cr(VI) reduction by *Pseudomonas* in the presence of aqueous Fe(III). 209

22 $\ln f$ vs. $\ln(\delta^{53}Cr/1000+1)$ for Cr(VI) reduction by *Pseudomonas* in the presence of aqueous Fe(II). 211

23 $\ln f$ vs. $\ln(\delta^{53}Cr/1000+1)$ for Cr(VI) reduction by *Pseudomonas* in the presence of both Fe(II) and goethite (excluding abiotic reduction by Fe(II)). 213

24 $\ln f$ vs. $\ln(\delta^{53}Cr/1000+1)$ for Cr(VI) reduction by *Pseudomonas* in the presence of both Fe(II) and Haematite (excluding abiotic reduction by Fe(II)). 215

25 $\ln f$ vs. $\ln(\delta^{53}Cr/1000+1)$ for Cr(VI) abiotic reduction by Fe(II). . . 216

26 $\ln f$ vs. $\ln(\delta^{53}Cr/1000+1)$ for Cr(VI) reduction by *Shewanella* without any minerals or aqueous Fe species. 218

27 $\ln f$ vs. $\ln(\delta^{53}Cr/1000+1)$ for Cr(VI) reduction by *Shewanella* in the presence of aqueous Fe(III). 220

28 $\ln f$ vs. $\ln(\delta^{53}Cr/1000+1)$ for Cr(VI) reduction by *Shewanella* in the presence of goethite. 222

29 $\ln f$ vs. $\ln(\delta^{53}Cr/1000+1)$ for Cr(VI) reduction by *Shewanella* in the presence of haematite. 224

30 $\ln f$ vs. $\ln(\delta^{53}Cr/1000+1)$ for Cr(VI) reduction by *Pseudomonas* with high initial Cr concentration (40 mg/L). 226

31 $\ln f$ vs. $\ln(\delta^{53}Cr/1000+1)$ for Cr(VI) reduction by *Pseudomonas* with low initial Cr concentration (5 mg/L). 228

32 $\ln f$ vs. $\ln(\delta^{53}Cr/1000+1)$ for Cr(VI) reduction by *Pseudomonas* with both low (5 mg/L) and medium (20 mg/L) initial Cr concentration. 229

List of Tables

1.1 Commonly observed chromium concentrations in the environment [*Bradl*, 2005] 2

1.2 Enrichment Factors for Metals in the Tissues of Phytoplankton and Brown Algae [*Libes*, 1992] 10

2.1 Lab conditions for the aerobic microbiological experiments. 29

2.2 Chromium spike composition (ng/g) 39

4.1 Cell specific reduction rates and isotopic fractionation factors 92

1 Aerobic Cr(VI) reduction by *Pseudomonas fluorescens* LB 300 with glucose as the electron donor 172

2 Aerobic Cr(VI) reduction by *Pseudomonas fluorescens* LB 300 with citrate as the electron donor 174

3 Aerobic Cr(VI) reduction by *Pseudomonas fluorescens* LB 300 with acetate as the electron donor 176

4 Aerobic Cr(VI) reduction by *Pseudomonas fluorescens* LB 300 with propionate as the electron donor 178

5 Anaerobic Cr(VI) reduction by *Pseudomonas fluorescens* LB 300 with glucose as the electron donor 180

6 Anaerobic Cr(VI) reduction by *Pseudomonas fluorescens* LB 300 with citrate as the electron donor 182

7 Anaerobic Cr(VI) reduction by *Pseudomonas fluorescens* LB 300 with acetate as the electron donor 185
8 Anaerobic Cr(VI) reduction by *Pseudomonas fluorescens* LB 300 with propionate as the electron donor 188
9 Aerobic Cr(VI) reduction by *Shewanella* with succinate as the electron donor 190
10 Anaerobic Cr(VI) reduction by *Shewanella* with succinate as the electron donor 192
11 Aerobic Cr(VI) reduction by *Pseudomonas fluorescens* LB 300 with different concentrations of glucose as the electron donor (data at 48 hours) 194
12 Aerobic Cr(VI) reduction by *Pseudomonas fluorescens* LB 300 at pH 4 195
13 Aerobic Cr(VI) reduction by *Pseudomonas fluorescens* LB 300 at pH 6.1 197
14 Aerobic Cr(VI) reduction by *Pseudomonas fluorescens* LB 300 at pH 8 199
15 Anaerobic Cr(VI) reduction by *Pseudomonas fluorescens* LB 300 without any mineral or aqueous iron species 202
16 Anaerobic Cr(VI) reduction by *Pseudomonas fluorescens* LB 300 in the presence of goethite 204
17 Anaerobic Cr(VI) reduction by *Pseudomonas fluorescens* LB 300 in the presence of haematite 206
18 Anaerobic Cr(VI) reduction by *Pseudomonas fluorescens* LB 300 aqueous Fe(III) in the medium 208
19 Anaerobic Cr(VI) reduction by *Pseudomonas fluorescens* LB 300 aqueous Fe(II) in the medium 210
20 Anaerobic Cr(VI) reduction by *Pseudomonas fluorescens* LB 300 with both aqueous Fe(II) and goethite in the medium 212
21 Anaerobic Cr(VI) reduction by *Pseudomonas fluorescens* LB 300 with both aqueous Fe(II) and haematite in the medium 214

22 Anaerobic Cr(VI) reduction by *Shewanella oneidensis* MR-1 without any mineral or aqueous iron species 217

23 Anaerobic Cr(VI) reduction by *Shewanella oneidensis* MR-1 with aqueous Fe(III) in the medium 219

24 Anaerobic Cr(VI) reduction by *Shewanella oneidensis* MR-1 with goethite in the medium 221

25 Anaerobic Cr(VI) reduction by *Shewanella oneidensis* MR-1 with haematite in the medium 223

26 Aerobic Cr(VI) reduction by *Pseudomonas fluorescens* LB 300 with different initial Cr(VI) concentration 225

27 Aerobic Cr(VI) reduction by *Pseudomonas fluorescens* LB 300 with different initial Cr(VI) concentration 227

28 Aerobic Cr(VI) reduction by *Pseudomonas fluorescens* LB 300 with different initial Cr(VI) concentration 230

Chapter 1

Introduction

1.1 Chromium in the nature environment

1.1.1 Source of chromium

Chromium is abundant in the earth's crust and ranks 21^{st} among the elements in crustal abundance. It is naturally occurring in the environment by weathering and leaching from rocks and cycling by wet precipitation, dry fallout from atmosphere and run off from terrestrial systems. Cr can exist in many different forms with oxidation states from 0 to VI, but only two of them, trivalent and hexavalent Cr, are stable in the environment [*Kota and Stasicka*, 2000].

The major oxidation state of chromium in igneous rocks are Cr (III), which is insoluble and surface-reactive, and so immobilized, but Manganese oxides, the known dominant natural oxidants of Cr (III), are common in various environments and are often impartial in controlling Cr transport and fate [*Feng et al.*, 2006; *Landrot et al.*, 2012]. When Cr (III) is oxidized to Cr (VI), its solubility and bio-availability both increase. Naturally, Cr concentrations are 0.5 to 100 nM in rivers and lakes, and 0.1 to 16 nM in seawaters. The commonly observed chromium concentrations in various environmental media are shown in Table. 1.1 [*Bradl*, 2005].

Compared to natural sources, anthropogenic sources contribute a higher content

Table 1.1: Commonly observed chromium concentrations in the environment [*Bradl*, 2005]

Material	**Average Concentration mg/kg**	**Range mg/kg**
Continental crust	125	80-200
Ultramafic igneous	1800	1000-3400
Basaltic igenous	200	40-600
Granific igneous	20	2-90
Limestone	10	<1-120
Coal	20	10-1000
Fly ash	247	37-651
Phosphate fertilizers	-	30-3000
Sewage sludges	74	2-1100
Soils	40	10-150
Freshwater (μg/L)	1	0.1-6
Seawater(μg/L)	0.3	0.2-50

of chromium in the environment. Chromium has been used by human activity for a long time. Over 2000 years ago, chromium oxide was already being used for coating metal weapons by the Chinese in the Qin dynasty. In the western world, it was first discovered in the 18 century and was initially used as a pigment.

In recent times, chromium has been exploited in an even broader range of applications. It can be used to induce hardness, toughness and chemical resistance in steel. The 'stainless steel' is made by alloying Fe with Cr. When chromium alloyed with iron and nickel, nichrome is produced, which is resistant to high temperatures and can be employed making heating units. Thin Cr alloy coatings (chrome plating) are widely used for auto parts or other products. The super-alloys made by chromium and nickel was found to perform well in the hot, corrosive and high stress environment of jet engines.

Chromite is the only ore of chromium. It is an oxide mineral composed of chromium, iron and oxygen ($FeCr_2O_4$). Chromite occurs in basic and ultrabasic igneous rocks, and also is found in metamorphic and sedimentary rocks that are

produced when chromite-bearing rocks are altered by heat or weathering. About two fifths of chromite ores in the world are produced in South Africa.

Because it is widely used in many industries, including those for iron and steel production, electroplating, metal finishing, petroleum refining, textile manufacturing, leather tanning and paper production, Cr concentration in wastewater discharges from these industries have been reported to be very high [*Sultan and Hasnain*, 2012], and Cr contamination becomes a serious environmental problem all over the world.

Wastewater and industrial emissions often pollute soils with Cr, which can accumulate gradually from sources with even relatively low concentrations. For example, soils from chromium waste dump sites show a considerable concentration of chromium. For example, up to about 1500 mg/kg chromium was found in soils near the "Warszawa" smelter and up to 1000 mg/kg was found near the "Radoskor" Tannery [*Baralkiewicz and Siepak*, 1999a]. Chromium is found mainly concentrated at surface levels in polluted soils [*Baralkiewicz and Siepak*, 1999b].

1.1.2 Toxicity of chromium

1.1.2.1 Toxicity effects in humans

Chromium is an essential micronutrient for living organisms. Cr(III) is known for its particular role in the maintenance of normal carbohydrate metabolism in mammals and yeasts. Studies on human and experimental animals demonstrated that 50 to 200 μg/day of Cr(III) is needed for the maintenance of normal glucose metabolism. Moreover, Cr(III) is also suggested to be involved in the tertiary structure of proteins and in the conformation of cell RNA and DNA [*Zayed and Terry*, 2003]. However, trivalent chromium has low bioavailability in most cases. Approximately 99% of the orally dosed chromic chloride to humans was recovered in faeces, with about 94% recovered after duodenal administration. Only less than 0.5% was found excreted

in urine, indicating poor absorption of Cr(III). Poor absorption of Cr(III) was also found in studies with experimental animals [*Dayan and Paine*, 2001]. Another form of chromium, hexavalent chromium, is very soluble and bioavailable: assessment following oral administration of sodium chromate in humans revealed that about 10% of the dose had been absorbed in the gastrointestinal tract [*Dayan and Paine*, 2001]. Twenty four hours after duodenal administration, about half of the dose was found to be absorbed and contained in faecal excretion while 10% was detected in the urine [*Dayan and Paine*, 2001]. Respiratory exposure of Cr(VI) resulted in detectable urinary excretion of it, which occurred in welders and in workers in the chrome plating industry. Animal studies also indicate that Cr-rich stainless steel welding fumes induce more lung injury and inflammation compared to mild steel welding fumes that are mainly composed with Fe [*Antonini and Roberts*, 2007]. During the transport in the blood, Cr(VI) was found to be reduced and only Cr(III) was present in the urine [*Dayan and Paine*, 2001]. For human beings, the lethal oral dose of soluble chromate is considered to be 50 - 70 mg/kg body weight. Acute poisoning of Cr(VI) can induce vomiting, diarrhoea, haemorrhage and blood loss into the gastrointestinal tract, which can cause cardiovascular shock. The longer toxic effect in humans are liver and kidney necrosis [*Dayan and Paine*, 2001].

1.1.2.2 Toxicity effects in cellular levels

The mechanism of Cr toxicity has been studied with different types of cells. Various studies on genetic effects of Cr(VI) confirm that it induces oxidative stress in cells, causing DNA damage, gene mutation, sister chromatid exchange, chromosomal aberrations, cell transformation and dominant lethal mutations in a number of targets in both animal and human cells [*Dayan and Paine*, 2001; *Xu et al.*, 2004, 2005].

When Cr(VI) enters the cells, it reacts spontaneously with intracellular reductants and generates short lived intermediates of Cr(V) and/or Cr(IV) and ultimately

reduces to Cr(III) [*Xu et al.*, 2004, 2005]. In the cytoplasm, Cr(V) can be partially re-oxidized to Cr(VI) to produce a reactive oxygen species (ROS) that can easily combine with DNA-protein complexes; Cr(IV) is able to bind to cellular material, altering their physiological functions. Studies have demonstrated that Cr(VI) can be transported through mammalian cell membranes by the carboxylate, sulphate and phosphate carrier systems, and generate free radicals inside the cells [*Bopp and Ehrlich*, 1988; *Michel et al.*, 2003; *Ramirez-diaz et al.*, 2008].

1.1.2.3 The impact of Cr toxicity on the environment

In the environment, Cr(VI) pollution can alter the structure of the soil microbial community, reduce microbial growth and enzymatic activity. Some lab based studies have shown that it can cause cellular oxidative stress in cells, and cellular defense against the toxicity that involved activation of antioxidant mechanisms [*Ackerley et al.*, 2006]. Its toxicity towards microorganisms can also inhibit the biodegradation of other organic pollutants. In one study of natural samples, a viable anaerobic bacterial community was found, but Cr(VI) altered its composition, so impacting on the soil biodegradation potential [*Kourtev et al.*, 2006]. In a study of microbial community responses to different dosages of chromate in soils, the researchers found that the soil microbial community structure, metabolic activity and also the selection of Cr(VI) resistance have been altered [*Viti et al.*, 2006]. It was also found that *Pseudomonas* strains can resist up to 40 mM Cr(VI), however, cyanobacteria were more sensitive to chromium [*Viti et al.*, 2006].

On reduction, Cr(VI) is converted to Cr(III), and although it is a nutritional requirement for effective sugar and fat metabolism, some studies have shown that it could also be toxic to microbes by causing DNA damage [*Plaper et al.*, 2002] or changing pH [*Garcia et al.*, 1994] in the surrounding environment. Although at the extracellular level, Cr(III) is relatively innocuous as a consequence of its inability to cross cell membranes, it can generate toxic effects by its ability to bind to phosphates

in DNA.

1.1.3 Chromium behaviours and its isotopes

Cr(III) and Cr(VI) are the two most stable oxidation states in natural waters. Under salt water conditions, at a pH of approximately 8, the Cr^{+4} cation may also be present. The ratio between these forms depends on many different processes, such as microbial activity, chemical redox transformation by aqueous reactants, precipitation/dissolution process, adsorption/desorption reactions and redox reactions with minerals. For example, if organic matter is present in large quantities, Cr(VI) may be reduced to Cr(III), which can be easily adsorbed on the particulate matter. If not adsorbed, Cr(III) can form large, polynucleate complexes that are not soluble. These complexes can still be transported to the ocean as colloidal suspensions, or precipitate in the sediment, although, a proportion of Cr(III) may be re-mobilised in the form of soluble Cr(III)-organic complexes [*Whalley et al.*, 1999].

Once it enters into aquatic systems, most of the chromium will ultimately be deposited in the sediment. Soluble chromium, mostly Cr(VI) and soluble Cr(III) complexes, only accounts for a very small percentage of the total chromium in both the water column and sediments. Oxygen levels and pH were found to be essential in determining chromium species in the natural environment [*Pourbaix*, 1974; *Trama and Benoit*, 1960; *Zink et al.*, 2010].

1.1.3.1 The effects of oxygen and pH levels

Cr(VI) predominates under highly oxidizing conditions, such as shallow aquifers, whereas Cr(III) predominates under reducing conditions, such as deeper groundwaters. In anoxic and suboxic conditions, Cr(III) is the only form present [*Kota and Stasicka*, 2000]. In oxygenated aqueous solutions, Cr(III) is predicted to be stable when pH$\leq$6, while Cr(VI) is predominate when pH$\geq$7 [*Campanella*, 1996]. The major dissolved species of Cr(III) are Cr^{3+}, $CrOH^{2+}$, $Cr(OH)_3^0$, and $Cr(OH)_4^-$. Cr^{3+}

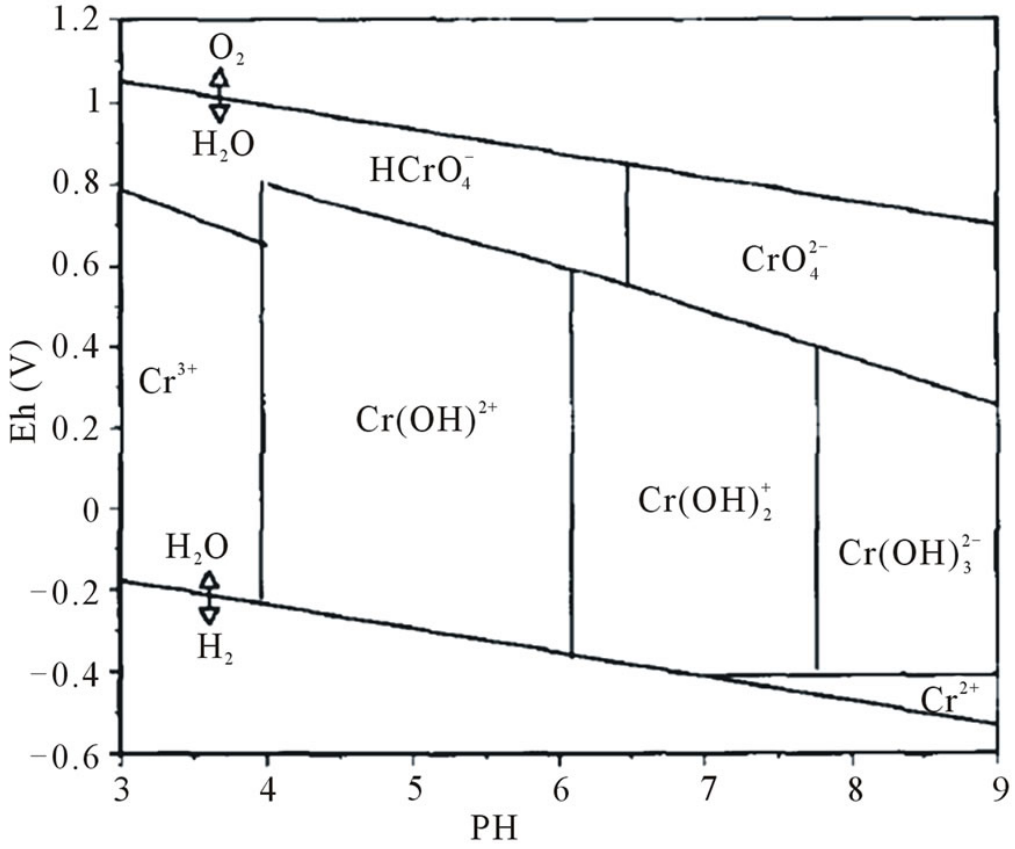


Figure 1.1: the Eh-pH diagram showing the aqueous inorganic Cr species in soil-water environments.

is prevalent only at pH below 3.6-3.8 and $Cr(OH)_4^-$ is dominant only at high pH (above 10-11.5). The dominant species are $CrOH^{2+}$ when pH is ranged in 6.3-6.5, and are $Cr(OH)_3^0$ when pH is between 6.3-7 and 10-11.5 [*Campanella*, 1996]. In natural groundwater, the pH is typically 6 to 8 and CrO_4^{2-} is the predominant species of chromium in the hexavalent oxidation state, whereas $Cr(OH)_2^+$ will be the dominant species in the trivalent oxidation state. In seawater, Cr(VI) is generally more stable [*Libes*, 1992]. Fig. 1.1 is the Eh-pH diagram showing the aqueous inorganic Cr species in soil-water environments [*Ciavatta et al.*, 2012].

1.1.3.2 Reduction/oxidation of Cr

In an aqueous environment, many other factors other than pH and oxygen may also play an important role in affecting the speciation of chromium; Cr undergoes

relatively rapid reduction or oxidation, making the determination of its various species difficult. For instances, many reports have been published about Cr(VI) reduction by aqueous Fe(II) [*Kitchen et al.*, 2012], hydrogen peroxide [*Rock et al.*, 2001], and organic matter such as humic acid, glucuronic, and alginic acids [*Kantar et al.*, 2008; *Kitchen et al.*, 2012]. The reduction of Cr(VI) by S^{2-} or Fe^{2+} ions under anaerobic conditions is usually very fast, and the reduction half-lives range from seconds to several days [*Basu and Johnson*, 2012; *Kitchen et al.*, 2012]. Minerals in the environment may significantly accelerate the Cr(VI) reduction by Fe(II), and this is found to be driven by the high reactivity of adsorbed Fe(II) [*Buerge and Hug*, 1999; *Fengdorf*, 1995]. However, reduction by organic sediments or soils were reported to be much slower and dependent on the type and amount of organic materials, also the redox condition of the water [*Ellis et al.*, 2002; *Stewart et al.*, 2010]. The reduction process was generally more rapid under anaerobic than aerobic conditions. The photochemical generation of Cr (III) has also been suggested in a number of reports [*Kieber and Helz*, 1992].

Cr(III) is found to be stable in soil and aquatic environments, and its oxidation to Cr(VI) is rare even in the presence of dissolved oxygen; the only reported pathway to oxidise Cr(III) is by Mn(III,IV) hydroxides [*Landrot et al.*, 2012]. However, in the environment, Cr(III) is typically less soluble and more inert to oxidation, and $Cr(OH)_3$ precipitates may form on surfaces of Mn minerals. These processes can be accelerated with the participation of specific bacterial activity [*Banerjee and Nesbitt*, 1999; *Feng et al.*, 2006]. Moreover, Cr(III) oxidation is generally considered to be slower than Cr(VI) reduction, because in most environments, Cr(III) oxidants are less abundant than potential Cr(VI) reductants [*Bradl*, 2005].

1.1.3.3 Adsorption of Cr

In seawater, the concentrations of dissolved metals, such as chromium, appears to be determined by the rate of removal, by means of adsorption or precipitation onto

particles or by incorporation into biogenic materials [*Libes*, 1992]. Such processes have been termed as "The Great Particle Conspiracy". Cr can be immobilised by the adsorption processes. The predominant forms of Cr(VI) in the environment ($HCrO_4^-$, CrO_4^{2-} or $Cr_2O_7^{2-}$, depending on pH) generally adsorb more at lower pH on clays such as kaolinite and montmorillonite, iron hydroxide, goethite and alumina. Redox reactions can also occur on the surface of minerals, and it is usually very difficult to separate the effects by these reactions from those by adsorption. In some cases, Cr(VI) was found to adsorb onto clay minerals, followed by reduction. Because clays may contain a fraction of reduced Fe, which can work as a reductant, and Cr(VI) can be reduced by Fe(II) as shown in the following equation:

$$3Fe(II)O + 6H^+ + Cr(VI) = Cr(III) + 3Fe(III) + 3H_2O \tag{1.1}$$

1.1.3.4 Microbial activity

Chromium is classified as a micronutrient because it is essential to the growth of phytoplankton. It is important in the enzyme systems which catalyse biochemical reactions. The enrichment of the trace metals in the marine organisms can be expressed by an enrichment factor (EF):

$$EF = \frac{Metal\ concentration\ in\ biogenic\ material}{Metal\ concentration\ in\ seawater} \tag{1.2}$$

The enrichment factors for some trace metals in the tissues of phytoplankton are shown in the above table.

1.1.3.5 Cr isotopes

Chromium has 4 stable isotopes: ^{50}Cr (4.35%), ^{52}Cr (83.8%), ^{53}Cr (9.50%) and ^{54}Cr (2.37%)[*Rotaru et al.*, 1992]. When Cr is distributed between 2 forms by redox reactions, the lighter isotopes are enriched in the product and heavier isotopes in the

Table 1.2: Enrichment Factors for Metals in the Tissues of Phytoplankton and Brown Algae [*Libes*, 1992]

Element	**Plankton**	**Brown Algae**
Al	25,000	1550
Cd	910	890
Co	4600	650
Cr	17,000	6500
Cu	17,000	920
Fe	87,000	17,000
I	1200	6200
Mg	0.59	0.96
Mn	9400	6500
Mo	25	11
N	19,000	7500
Na	0.14	0.78
Ni	1700	140
P	15,000	10,000
Pb	41,000	70,000
S	1.7	3.4
Si	17,000	120
Sn	2900	92
V	620	250
Zn	65,000	3400

original pool, because the lighter isotopes are found to be more reactive in most conditions [*Ellis et al.*, 2002]. This is the underlying principle behind my entire thesis, and is explained in many places in the following chapters. Changes in isotopic composition can be used as an indicator of redox conditions in the environment, with oxidised Cr isotopically heavier as evidence of removal of Cr by reduction. Likewise, isotopic compositions enable differentiation of natural sources of Cr and those introduced by anthropogenic activity [*Ellis et al.*, 2002; *Izbicki et al.*, 2012; *Johnson and Bullen*, 2004], and assessment of the effectiveness of remedial intervention.

Chromium isotopes are not only useful as indicators of redox conditions prevailing in the modern environment, they can also be used to provide indications of prevailing conditions over geological time. Their distinctive profiles in the sedimentary deposits can reflect water and atmospheric oxygen levels in the past [*Frei and Polat*, 2013; *Frei et al.*, 2013; *Rotaru et al.*, 1992].

In order to more effectively develop the use of Cr isotopic variations as environmental indicators, a database containing the relationship between isotope variations and specific environmental parameters is essential for establishing isotopic fractionation as a diagnostic tool.

The dominant processes that control Cr behaviour include biotic and abiotic reduction, together with interaction with mineral surfaces and precipitation.

Cr isotope fractionation in abiotic processes

Abiotic reduction occurs both in the aqueous phase and also on mineral surfaces. *Zink et al.* [2010] reported Cr reduction by H_2O_2 in aqueous media under both highly acidic and circum-neutral conditions; the fractionation factors were found to be -3.5 ‰ and -5.0 ‰, respectively. The presence of elements such as iron in its various chemical forms is known to have the potential to alter the chemical state of Cr. *Dossing et al.* [2011] reported ε of -3.0 ‰ to - 4.4 ‰ for reduction by aqueous Fe(II) at circum-neutral pH, and -1.5 ‰ when reduced by dissolved Fe(II) and Fe(II)+Fe(III) green rust together. *Basu and Johnson* [2012] have conducted

Cr(VI) reduction experiments with Fe(II)-doped goethite, FeS, green rust, siderite ($FeCO_3$) and artificially reduced sediments from a permeable reactive barrier. The fractionation factors were found to be -2.11 ‰ to -3.91 ‰, respectively. In addition to redox reactions, adsorption is also an important process that may induce chromium isotope fractionation. However, *Ellis et al.* [2004] have investigated the effects of sorption during transport of Cr(VI) and found that stable isotope fractionation caused by equilibrium adsorption onto γ-Al_2O_3 and goethite was negligible (0.04 ‰). The isotopic effects of adsorption on other phases are not known.

Cr isotope fractionation in microbial processes

Microbes are usually found to be very active in various environments, and their activity is the predominant factor that controls the transportation of many different elements in the environment. In waters, Cr(VI) is readily bio-accumulated by phytoplankton and zooplankton. Many different bacteria isolated from industrial effluent or chromium contaminated soil are found to be resistant to high concentrations of Cr [*Sultan and Hasnain*, 2012; *Yahya et al.*, 2012]. Some populations are also very effective in reducing Cr(VI) to Cr (III) both in water and soil [*Cheng et al.*, 2010; *Naik et al.*, 2012], and therefore can be applied in bio-remediation of chromium in the environment. Although Cr(III) is a very important micro nutrient, its bioavailability is low, and it has been used as a tracer to help measure efflux rates in biota in many previous studies [*Wang and Zhang*, 2013; *Zhang et al.*, 2011].

Shifts in isotope fractionations due to microbial activities provide valuable insight into the mechanisms of metal cycling, and can be used to quantify biogeochemically mediated redox processes in the environment [*Basu et al.*, 2014; *Han et al.*, 2012; *Sikora et al.*, 2008]. There are many factors that can influence the microbial processing of Cr and some of these can be moderated by the immediate environment, such as the presence of specific electron donors and their respective concentrations.

Previous studies have mostly focused on microbial Cr(VI) reduction under anaerobic conditions. *Sikora et al.* [2008] were the first to investigate the impact of

microbes on Cr isotopic fractionation. They conducted anaerobic reduction experiments with *Shewanella oneidensis* MR 1 and found that the chromium isotope fractionation factor ε ranged from -4.0 to -4.5 ‰ when reduction rates were low and -1.8 ‰ when the reduction rate was much greater. *Han et al.* [2012] reported Cr isotope data during reduction by *Pseudomonas stutzeri* RCH2 under both aerobic and denitrifying conditions, and reported it to be -2 ‰ under aerobic and -0.4 ‰ under denitrifying, conditions. *Basu et al.* [2014] reported chromium reduction by a metabolically diverse group of bacteria, and also suggested that stronger isotopic fractionations were induced during Cr(VI) reduction under electron donor poor conditions.

However, despite these reports and compared to other elements such as microbially mediated sulphate [*Habicht and Canfield*, 1997; *Kaplan and Rittenberg*, 1964] reduction, information is still limited in terms of the environmental conditions and microbial activities on determination of Cr isotopic fractionations. Such information would be of significant value since it would help establish isotopic fractionation as an effective means to provide insight into the prevailing conditions in the environment such as redox, pH or concentration and help further establish the technique as an effective environmental diagnostic tool.

1.2 Mechanisms of microbial Cr reduction

Since the first discovery of Cr reducing bacteria in the 1970s, research focused on Cr-reducing microorganisms has been enthusiastically pursued as a way to immobilise contaminant Cr, and diverse bacterial species were found to be capable of reducing Cr(VI) [*Basu et al.*, 2014; *Wang and Xiao*, 1995]. The reduction may be through both intracellular and extracellular pathways and may occur under both aerobic or anaerobic conditions. Generally, microbial reduction of Cr(VI) to Cr(III) can be considered as an additional chromate resistance mechanism [*Joutey et al.*, 2015;

Ramirez-diaz et al., 2008; *Viti et al.*, 2014].

1.2.1 Aerobic reduction

For aerobes, pseudomonad resistance to Cr(VI) has been well investigated. Cr(VI) resistance in *Pseudomonas fluorescens* is attributed to the decreased uptake and enhanced efflux of Cr(VI) by the cell membrane. In many cases, resistance genes are located on the plasmid; the loss of this plasmid results in the loss of chromate resistance [*Bopp et al.*, 1983]. However, further study has revealed that Cr(VI) reduction activities were maintained in both sensitive (wild type) and resistant (mutant) strains, indicating that the capability of Cr(VI) reduction did not depend solely upon Cr(VI) resistance of the bacteria [*Bopp and Ehrlich*, 1988]. The reductase of Cr(VI) was found to be membrane associated and can mediate the transfer of electrons from NADH to chromate [*Bopp and Ehrlich*, 1988]. Many bacteria in other genera, such as *Bacillus* spp., *E. coli* ATCC 33456, *Shewanella alga* BrY-MT and some unidentified strains are also capable of reducing Cr(VI) and the reductases in most of these bacteria were found to be soluble in the cytosol [*Cheung and Gu*, 2007].

ChrR, one of the best studied reductase of *Pseudomonas putida*, is a soluble flavin mononucleotide-binding protein [*Ackerley et al.*, 2004a]. It functions as a 50-kDa dimer and shows a NADH-dependent reductase activity that protects against chromate toxicity. In the reduction process, ChrR transiently reduces Cr(VI) with a one-electron shuttle to form Cr(V), followed by a two electron transfer to generate Cr(III) [*Ackerley et al.*, 2004b]. At the same time, ChrR also expresses a quinone reductase activity that generates a flavin semiquinone and transfers over 25% of the NADH electrons to superoxide anion [*Ackerley et al.*, 2004a]. A proportion of the Cr(V) intermediate are reoxidized spontaneously to generate ROS (reactive oxygen species), but its reduction through a two electron transfer catalyzed by ChrR and an additional mechanism of quinones reduction provides shielding against ROS and

reduces the opportunity for production of harmful radicals [*Ackerley et al.*, 2004b].

YieF Cr(VI) reductase is another well characterised protein present in *E.coli*. It is similar to ChrR in terms of kinetic and physicochemical properties; it is also soluble and is a member of a widely distributed family of proteins. Other than Cr(VI), YieF can also reduce many different substrates such as ferricyanide, V(V), Mo(VI) and 2,6-dichloroindophenol [*Ackerley et al.*, 2004b]. It is unique in that it catalyzes the direct reduction of Cr(VI) to Cr(III) through a four-electron transfer, in which three electrons are consumed in reducing Cr(VI) to Cr(III) and the other one is transferred to molecular oxygen, generating ROS. YieF is regarded as a more effective enzyme than ChrR in reducing Cr(VI) [*Ackerley et al.*, 2004a; *He et al.*, 2011].

Both ChrR and YieF need to use alternative substrates in addition to Cr(VI), indicating that the reduction activity has been an adaptive mechanism promoted by recent chromate exposure.

1.2.2 Anaerobic reduction

A number of facultative anaerobes are capable of reducing Cr(VI). The reduction activity by these anaerobes were found to be associated with their electron transfer systems that catalyzed the electron flow along the respiratory chains [*Guha et al.*, 2001]. In the absence of oxygen, Cr(VI) can serve as a terminal electron acceptor for many electron donors, such as carbohydrates, proteins, fats, hydrogen, and even endogenous electron reserves [*Chirwa and Wang*, 2000; *Xu et al.*, 2011].

Under anaerobic conditions, the cytochrome families are frequently shown to be involved in the enzymatic reduction of different metals, such as Fe(III) and Cr(VI). The c-type cytochromes are very important and well studied electron transfer proteins, and are commonly found in many organisms, such as yeast, horse and bacteria. For example, a soluble c_3 cytochrome was found to be responsible for Cr(VI) reduction in *D. vulgaris* [*Lovley*, 1995]. *Sundararajan et al.* [2011] proposed that the

mechanism of Cr(VI) reduction by cytochrome c7 proteins using Density functional theory calculations and suggested that both electron transfer from the heme and proton transfer from the lysines occur, followed by a disproportionation mechanism involving Cr(V). Other than multiheme cytochromes, metallo-enzymes containing hemes or (Fe/S) centres with low redox petentials are also found to possess a metal reductase activity, and some bacteria are found to generate cytochrome c and [Fe] hydrogenase simultaneously [*Michel et al.*, 2001, 2003].

Other than directly enzymatic Cr(VI) reduction, natural metabolites of anaerobes such as H_2S produced by sulphate reducing bacteria, can also reduce Cr(VI) under an anoxic environment. The anaerobic Cr(VI) reduction process was also found to generate energy for bacterial growth [*Fein et al.*, 2002].

1.2.3 Long distance electron transport

In the past decade, increasing numbers of studies have focused on microbial extracellular electron transport pathways, revealing a different perspective on how biogeochemical processes are directly coupled across the entire scale of the system studied.

The study by *Gorby et al.* [2006] reported that some bacteria, including metal-reducing bacteria *Shewanella oneidensis* MR-1, the oxygenic phototrophic cyanobacterium *Synechocystis* PCC6803, and the thermophilic fermentative bacterium *Pelotomaculum thermopropionicum*, can produce electrically conductive pilus-like appendages called bacterial nanowires in direct response to electron acceptor limitation. These nanowires have been demonstrated to be highly electrically conductive and therefore the cells are able to transfer electrons extracellularly [*El-Naggar et al.*, 2010; *Gorby et al.*, 2006].

Specific cultivation conditions may impact on the production of nanowires. *Gorby et al.* [2006] reported that the samples with cells cultivated in nutrient-rich media or under high agitation conditions contained abundant cellular debris and relatively

few intact structures resembling nanowires. *Pirbadian et al.* [2014] demonstrated that the nanowires produced by *Shewanella oneidensis* MR-1 were extensions of the outer membrane and periplasm that include the multi-heme cytochromes responsible for extracellular electron transfer. They also reported that the production of bacterial nanowires is correlated with an increase in cellular reductase activity.

Although the spatial domain for electron transfer was once defined at the nanometer scale, today we can directly observe centrimeter-scale nanowires or cable bacteria for long distance electron transfer [*Pfeffer et al.*, 2012; *Pirbadian et al.*, 2014]. These findings add a new dimension to the understanding of biogeochemical process in the natural environment. *Risgaard-Petersen et al.* [2012] and *Pfeffer et al.* [2012] demonstrated that sulfide in marine sediments can be microbially oxidized when pulses of oxygen are introduced centimeters above. They revealed that the long, filamentous bacteria (e.g. *Desulfobulbacea*) were the native conductors that carry electric currents across centimetre-wide zones. When the electrons are transferred, steep gradients in pH, sulphate, calcium and iron are formed, which drive ion migration across suboxic zones and induce changes in mineral solubility [*Risgaard-Petersen et al.*, 2012].

Other than in the field of geochemistry, extracellular electron-transport processes are also of great interest for their technological applications, such as in bioremediation or help to design microbial fuel cells.

1.3 Mechanisms of Stable Isotope Fractionation

1.3.1 Equilibrium effects

Isotopic fractionation can occur in equilibrated systems that comprise two or more phases that contain a common element. It is caused by a quantum mechanical effect, which induces a different zero-point energy of the isotopes. According to the quantum mechanics theory, the energy of a diatomic molecule (E) at absolute zero

has a finite value that depends on its vibrational frequency v [*Hoefs*, 2004]

$$E = \frac{1}{2}hv \tag{1.3}$$

Where h is Planck's constant, equal to 6.626176×10^{-34}J/Hz. The vibrational frequency (v) decreases if the light isotope of an element in a diatomic molecule is replaced by a heavier isotope of the same element, which causes a decrease of the energy of the molecule. The molecules containing the heavy isotope of an element are more stable than the same molecules would be if they contain the lighter isotope, i.e. molecules containing heavy isotopes are less reactive than molecules containing light isotopes.

The basis for a qualitative guide to stable isotope fractionations in all elements, derived originally by *Bigeleisen and Mayer* [1947] and extended by *Schauble* [2004], are listed below:

1. Equilibrium isotopic fractionations usually decrease as temperature increases, roughly in proportion to $1/T^2$ for most substances.

2. Isotopic fractionations are largest for light elements and for isotopes with very different masses if all else are equal. They scale roughly as $(m_{heavy} - m_{light})/(m_{light}m_{heavy})$ (approximately equal to $\Delta m/m^2$) where m_{light} and m_{heavy} are the masses of two isotopes of an element, Δm is the difference between their masses (m is the average atomic mass of the element).

3. At equilibrium, the heavy isotopes of an element will tend to be concentrated in substances where that element forms the stiffest bonds. Bond stiffness is greatest for short and strong chemical bonds. These properties are associated with:

1) high oxidation state in the element of interest;

2) high oxidation state in the atoms to which the element of interest is bonded for anions, such as Cl^-, Se^{2-} and O^{2-};

3) bonds involving elements near the top of the periodic table;

4) the presence of highly covalent bonds between atoms with similar electronegativities

5) for transition elements, low-spin electronic configurations, also d^3 or d^8 electronic structure for octahedrally-coordinated atoms

6) low coordination number

4. when the element of interest is directly bonded to hydrogen, or is part of a low-mass molecule, it may not be as enriched in heavy isotopes as would be expected from the last rule.

Large equilibrium fractionations usually occur at low temperatures between substances with markedly different oxidation states, bond partners, electronic configurations or coordination numbers. It tends to become zero at extremely high temperatures.

1.3.2 Kinetic effects

The kinetic effect occurs only in unidirectional and incomplete processes like evaporation, biologically mediated reactions and diffusion. They are caused by the different rates of various isotopic components in a chemical reaction, which depend on the amount of energy required to break their bonds with other atoms. The lighter isotopes have lower dissociation energies. Therefore, one common feature in many kinetic fractionations is that the lighter isotopes are more reactive and are concentrated in the reaction products. Such features were observed in both many non-biological and biological reactions [*Basu and Johnson*, 2012; *Kitchen et al.*, 2012; *Zink et al.*, 2010].

1.3.3 Mathematical calculations

The isotopic compositions of samples are often expressed as deviations from the composition of a reference standard:

$$\delta_{spl} = \frac{R_{spl} - R_{std}}{R_{std}} \times 1000‰ \tag{1.4}$$

Where R_{spl} value refers to the respective isotope ratio measurement and R_{std} is the defined isotope ratio of a standard. The use of a standard can minimise the systematic errors in measurements made on different mass spectrometers.

Since the R value usually represents the heavier isotope/ lighter isotope ratio, a positive δ value indicates that the sample is enriched in heavier isotopes relative to the standard. A negative δ value indicates that the samples has lower R value than the standard and that it is depleted in the heavier isotope relative to the standard.

In the case of isotope fractionation between two phases a and b in isotopic equilibrium, the isotope composition of an element in phases a and b are:

$$\begin{aligned} \delta_a &= (\frac{R_a - R_{std}}{R_{std}}) \times 1000‰ \\ \delta_b &= (\frac{R_b - R_{std}}{R_{std}}) \times 1000‰ \end{aligned} \tag{1.5}$$

They can be solved for R_a and R_b:

$$\begin{aligned} R_a &= \frac{R_{std}(\delta_a + 1000)}{1000} \\ R_b &= \frac{R_{std}(\delta_b + 1000)}{1000} \end{aligned} \tag{1.6}$$

The extent of isotope fractionation that takes place during a change in state is expressed quantitatively by the isotope fractionation factor α defined by the relation

$$\alpha_b^a = \frac{R_a}{R_b} \tag{1.7}$$

Substitute equation 1.6, it can be expressed as:

$$\alpha_b^a = \frac{\delta_a + 1000}{\delta_b + 1000} \tag{1.8}$$

The ε notation is also widely used :

$$\varepsilon_b^a = (\alpha_b^a - 1) \times 1000‰ \tag{1.9}$$

If subtract 1 from both sides of Eq. 1.8, the following equation can be obtained:

$$\alpha_b^a - 1 = \frac{\delta_a - \delta_b}{\delta_b + 1000} \tag{1.10}$$

In most cases, $\delta_b \ll 1000$, which permits the approximation that δ_b+1000=1000, and so:

$$(\alpha_b^a - 1) \times 1000 = \delta_a - \delta_b \tag{1.11}$$

In which case the ε can also be expressed as:

$$\varepsilon = \delta_a - \delta_b \tag{1.12}$$

In biologically mediated redox reactions, for instance, microbial Cr reduction processes, microbes progressively reduce Cr(VI) to Cr(III), and the products will never re-equilibrate with the original reactants. Since the lighter isotopes of Cr are enriched in the products, they will be progressively depleted in the original Cr(VI) pool. This scenario can be described by means of one of the Rayleigh equations [*Rayleigh*, 1896].

$$R_{Cr(VI)} = R^0_{Cr(VI)} f^{\alpha-1} \tag{1.13}$$

Where

$R_{Cr(VI)} = \frac{^{53}Cr}{^{52}Cr}$ in the remaining Cr(VI)

$R^0_{Cr(VI)} = \frac{^{53}Cr}{^{52}Cr}$ in the original Cr(VI) pool

α = isotope fractionation factor, where $\alpha = (^{53}\mathrm{Cr}/^{52}\mathrm{Cr})_{Cr(III)}/(^{53}\mathrm{Cr}/^{52}\mathrm{Cr})_{Cr(VI)}$

f = fraction of the Cr(VI) that was remaining after reduction.

The isotope ratio of the product Cr(III) at a specified value of f is:

$$R_{Cr(III)} = R^0_{Cr(VI)} \alpha f^{\alpha-1} \tag{1.14}$$

Where all the variables have the same meaning as in equation 1.13.

Equation 1.13 can be rearranged to:

$$\frac{R_{Cr(VI)}}{R^0_{Cr(VI)}} = f^{\alpha-1} \tag{1.15}$$

if we consider the phase a as Cr(VI) remaining in the system and the phase b is the initial Cr(VI) pool, then substitute Eq. 1.7 and Eq. 1.8 into Eq. 1.15,

$$\frac{\delta_{Cr(VI)} + 10^3}{\delta^0_{Cr(VI)} + 10^3} = f^{\alpha-1} \tag{1.16}$$

1.4 Bacterial sulphur reduction and isotope fractionation

Isotope are used in many studies focused on other elements, for example, sulphur. Sulphur and chromium both can be electron acceptors in microbial metabolic processes. Although sulphate reduction process is far more complex with more oxidation states, in the absence of a better model some parallels can be drawn. For example, the lighter isotopes are more reactive in the reduction process for both Cr and S; the electron transfer process for both Cr(VI) and S(VI) have multiple steps and involve

many different kinds of enzymes. Furthermore, the methods and considerations had in S isotope studies provide valuable information to interpret Cr isotope studies. Of course, the complexities of S reduction processes can be much greater than that of Cr in many environments. Compared with Cr, S has been studied in much greater detail. Sulphate reduction can be conducted by a large group of organisms, over 100 species of which are known so far [*Hoefs*, 2004]. Sulphate reducers are widely distributed in anoxic environments. They are able to gain energy for growth by reducing sulphate while oxidizing organic carbon (or H_2), and can tolerate temperatures over a wide range (-1.5 to over 100 °C, [*Canfield*, 2001]). Microbial sulphate reduction can yield quite large mass-dependent fractionations between sulphate and sulphide; the products are depleted in heavy isotopes, which are enriched in the residual sulphate. Previous studies have investigated the effects of different environmental conditions, including those within the common physiological ranges (e.g. temperature between 4 to 30 °C) as well as extreme environments (e.g. over 100 °C), on microbial sulphate reduction rates (SRRs) and the associated isotope fractionation factors (ε). However, the factors that determine the magnitude of sulphur isotope fractionation during bacterial sulphate reduction are still under debate. The first data about microbial S isotope fractionation was reported by *Thode et al.* [1951], in which it was demonstrated that the sulphide released during sulphate reduction by growing cells of *Desulfovibrio desulfuricans* was enriched in the lighter isotope of sulphur (^{32}S) by a factor of 10 to 12 ‰. A number of different conditions have been tested to determine their impact on biological S fractionation. *Harrison and Thode* [1958] reported that the degree of S isotope fractionation was inversely proportional to the rate of reduction (controlled by temperature and electron donor concentration), and was impacted by sulphate concentration only at limited conditions. *Kaplan and Rittenberg* [1964] demonstrated that fractionation of sulphur during bacterial reduction was influenced by different electron donors: it was inversely proportional to the rate of reduction when lactate and ethanol were electron donors and directly

proportional when molecular hydrogen was the electron donor. It was also reported that temperature and sulphate concentration only influenced the rate of reduction, but not the fractionation of the isotopes [*Kaplan and Rittenberg*, 1964].

Many studies have attempted to explain the mechanism controlling fractionation during sulphate and sulphite reduction. *Harrison and Thode* [1958] suggested two rate controlling steps: the entrance of sulphate into the cell and the breaking of the sulphur-oxygen bonds during reduction of sulphate to sulphite. The first step was assumed to have a very small isotope effect and to regulate fractionation only when S reduction rates or S concentration are very high. The second step was believed to have a kinetic isotope effect. However, this model did not fully explain all the data available. Enzymatic studies on S isotope fractionation have been conducted in many different bacteria [*Sim et al.*, 2011, 2012], and based on those studies, quantitative models have been proposed to predict S isotope fractionation factors under various conditions [*Druhan et al.*, 2014; *Wing and Halevy*, 2014]. Most of these models are based on the assumptions that the S isotope fractionation factors depend on the cellular specific rate ($\text{cell}^{-1}\cdot\text{time}^{-1}$) and the S concentration. However, the influence of both these factors are not clear [*Hoefs*, 2004].

There are similarities between Cr(VI) reduction and sulphate reduction processes. For example, *Myers et al.* [2000] reported that one possible pathway for Cr(VI) reduction by *Shewanella oneidensis* MR 1 requires enzymes located in the inner-most cell membrane of the bacteria. Accordingly, the first step of this pathway is transporting of Cr(VI) into the cell, which is similar to the sulphate reduction process. During Cr(VI) reduction, a Cr(V) intermediate was detected, suggesting that at least two distinctive steps are involved [*Myers et al.*, 2000]. Similarly, a multiple-steps strategy was also detected in bacterial sulphate reduction [*Canfield*, 2001]. Overall, the scientific findings with microbial sulphate reduction processes may provide some insights into microbial Cr(VI) reduction processes.

1.5 Aims and overview of the thesis

Chromium isotopic signatures can potentially be employed as indicators of prevailing environmental conditions, where isotope variations can be shown to be diagnostic of specific processes. Before it can be widely used, the isotope fractionation factors of different reactions have to be determined and characterised and the range of differences established. Other than the abiotic reactions, microbial activity is believed to play a central role in controlling Cr migration in the environment, but limited information is available to date concerning the microbial Cr(VI) reduction and the associated isotope fractionation processes. The aim of this study was to fill this knowledge gap by determining Cr isotope fractionation factors associated with microbial activity under different culture conditions, to understand the range of isotope signatures generated by bacteria and the factors that have the greatest impact on them. Specifically the aim was to determine the influence of bacterial species, type of the electron donors, mode of bacterial metabolism (aerobic and anaerobic), initial Cr concentration, bacterial cell density, and microbe-mineral interactions on both the rates of reduction and isotopic signatures generated. From such analysis the factors that should to be taken into consideration when interpreting Cr isotope signatures will be more apparent and informative.

Chapter 2 describes the methodology of the study, including the methods for culturing bacteria, the laboratory conditions employed for the Cr reduction experiments, and the techniques for determining Cr concentrations and isotopic compositions.

Chapter 3 reports on a series of studies to determine the key parameters influencing bacterial Cr reduction processes and isotope fractionations, thus providing some calibration of isotopic fractions generated in the environment.

Chapter 4 examines the influence of aqueous Fe and Fe minerals on microbial Cr reduction processes.

Chapter 5 presents a novel combination of a whole cell bioreporter and Cr isotope techniques to provide insights into Cr toxicity and microbial reduction processes occurring over a wide range of different concentrations.

Chapter 6 discusses the contribution of the research aimed at improving understanding of the cycling of redox metals in the environment and the role of microbes in the processes.

Chapter 2

Methodology

In my thesis, a series of experiments were performed to determine the rates of microbial reduction of Cr(VI) to Cr(III), and the associated isotope fractionation. In each experiment, dissolved Cr(VI) was combined with the microbial culture under different conditions, for instance, under different pH conditions, with several electron donors, and with or without the presence of diverse minerals. The experiments ran for the duration while Cr(VI) was reduced. The remaining Cr(VI) in solution was separated using anion exchange chromatography and the isotope composition was measured by thermal ionisation mass spectrometry (TIMS). To compensate for the variations of biological processes, every experiment in my study was done with triplicate samples in each group. It was crucial to keep everything 'clean' in my study: all equipment needs to be sterilised before use to prevent contamination from other microbes, and all beakers, flasks, pipette tips, and tubes etc. need to be cleaned with acids to keep the chemical blank as low as possible. The detailed methods used are stated in this chapter.

2.1 Microbial reduction of chromium under various conditions

In this study, Cr reduction experiments were undertaken with two facultative anaerobes, *Pseudomonas fluorescens* LB 300 and *Shewanella oneidensis* MR 1, under various well controlled lab conditions shown in Table 2.1. Most of the experiments were done under aerobic conditions, while the experiments with different electron donors were done both aerobically and anaerobically.

2.1.1 Bacteria strains

Bacterial strains in this study were selected because of their abilities to reduce chromium under various conditions [*Sikora et al.*, 2008; *Wang and Shen*, 1995; *Zhang et al.*, 2016]. The bacteria *Shewanella oneidensis* MR-1 (MR-1) was purchased from NCIMB Ltd (NCIMB 14063) and *Pseudomonas fluorescens* LB 300 (LB 300) was kindly provided by Prof. Yi-Tin Wang from the Department of Civil Engineering, University of Kentucky [*Wang and Shen*, 1995].

2.1.2 Strain stock and storage

The strain stock culturing and storage methods employed for both these bacteria were the same. Generally, a culture tube containing Luria Bertani Medium (LB medium) with fresh inoculum was prepared and incubated at 30 °C over night to ensure that the cultures were in late log or stationary phase. One mL of bacterial culture was then taken and added into a sterile cryovial with 225 μL of sterile 80% glycerol. The tube was shaken thoroughly and stored at -80 °C. To recover the cells before the experiments, a sterile toothpick was used to scrape off the ice and to streak the cells in the LB medium.

Table 2.1: Lab conditions for the aerobic microbiological experiments. LB 300: *Pseudomonas fluorescens* LB 300; MR 1: *Shewanella oneidensis* MR 1

Electron Donors	**Concentration (g/L)**	**Chromium (mg/L)**	**Cell Density cells/mL**	**pH**	**Strains**
Electron donors					
Glucose	5	20	10^{10}	7	LB 300
Citrate	5	20	10^{10}	7	LB 300
Acetate	5	20	10^{10}	7	LB 300
Propionate	5	20	10^{10}	7	LB 300
Experiments varying electron donor concentration					
Glucose	0	20	10^{10}	7	LB 300
Glucose	0.5	20	10^{10}	7	LB 300
Glucose	2	20	10^{10}	7	LB 300
Glucose	10	20	10^{10}	7	LB 300
Experiments varying initial chromium concentration					
Glucose	5	5	10^{10}	7	LB 300
Glucose	5	20	10^{10}	7	LB 300
Glucose	5	40	10^{10}	7	LB 300
Experiments varying cell density					
Glucose	5	20	10^{7}	7	LB 300
Glucose	5	20	10^{10}	7	LB 300
Experiments varying pH					
Glucose	5	20	10^{10}	4	LB 300
Glucose	5	20	10^{10}	6	LB 300
Glucose	5	20	10^{10}	8	LB 300
Experiments varying bacteria species					
Glucose	5	20	10^{10}	7	LB 300
Succinate	5	20	10^{10}	7	MR 1

2.1.3 Growth medium and general culturing condition

Two growth media were employed in the aerobic reduction study: The LB (Luria Bertani) Broth (Sigma Aldrich) and a Minimal salts medium (0.03 g NH_4Cl, 0.03 g K_2HPO_4, 0.05 g KH_2PO_4, 0.01 g NaCl and 0.01 g $MgSO_4$ in 1 L of Milli-Q water). The anaerobic growth medium and cell suspension medium for *Shewanella oneidensis* MR-1 was similar to those described by *Myers and Nealson* [1988], and modified by adding different electron donors and accepters. The composition of the growth medium was as follows: 15mM Sodium succinate, 9.0 mM $(NH_4)_2SO_4$, 5.7 mM K_2HPO_4, 3.3 mM KH_2PO_4, 2.0 mM $NaHCO_3$, 1.01 mM $MgSO_4$, $CaCl_2$, 67.2 μM Na_2EDTA, 56.6 μM H_3BO_3, 10.0 μM NaCl, 5.4 μM $FeSO_4$, 5.0 μM $Ni(NH_4)_2(SO_4)_2$, 5.0 μM $CoSO_4$, 3.87 μM Na_2MoO_4, 1.5 μM Na_2SeO_4, 1.26 μM $MnSO_4$, 1.04 μM $ZnSO_4$, 0.2 μM $CuSO_4$, 20 μg L-arginine HCl, 20 μg L-glutamine, and 40μg DL-serine, in milli-Q water. The cell suspension medium contains: 1.9 mM K_2HPO_4, 2.5 mM KH_2PO_4, 1.0 mM $MgCl_2$, and 3.2 mM NaCl.

All aerobic reduction experiments were conducted in Erlenmeyer flasks (Fig. 2.1). Bacteria were first incubated in LB medium at 30 °C and 120 rpm. When cells reached the late exponential state, they were collected by centrifugation at 4100 rpm and 4 °C for 20 minutes, and washed 3-4 times using 0.9 % sterile NaCl solution before adding to 50 mL of freshly autoclaved minimal salts medium. Cell density was controlled to be between 10^9 - 10^{10}/mL. All the electron donor solutions were sterilised by passing through 0.22 μm membranes. A Cr solution was prepared by dissolving potassium di-chromate in sterilised Milli-Q water and filtering through a 0.22 μm membrane before the experiments. The pH was adjusted using 1 M HCl or NaOH. The medium were then incubated at 30 °C and 120 rpm.

All anaerobic experiments were conducted in serum bottles closed with thick blue butyl rubber stoppers and aluminum crimp seals (Fig. 2.2). The prepared anaerobic media were flushed with 0.22 μm filtered N_2 for at least 30 min, until the



Figure 2.1: Flasks from microbial aerobic reduction experiments



Figure 2.2: Bottles from microbial anaerobic reduction experiments. The colours of the redox indicator show the redox potential in the medium. Blue: fully aerobic; Pink: redox potential above -51 mV; Colourless: redox potential below -110 mV.

redox indicator (resazurin) turned colourless during the procedure. Resazurin used in the experiment is the most commonly used redox indicator, which is generally non-toxic to bacteria and effective at very low concentrations (0.5 to 1 mg/L). The indicator is blue in its inactive form. At neutral pH, it reduces to resorufin (pink) when reducing conditions are reached, and then forms hydroresorufin (colourless) when the redox potential is below -110 mV. However, if the redox potential rises back up to above -51mV, it regains a pink color.

To transfer medium or chemicals, all syringes were flushed with N_2 prior to use and N_2 was injected into bottles to compensate for subsequent sample withdrawals.

At each time point during an experiment, 1000 μL of sample was taken and centrifuged at 9000 rpm at 4 °C for 10 min. The supernatant was sterilised by passing through a 0.22 μm filter, and then transferred into a clean Eppendorf tube and stored at -80°C before further treatment.

2.1.4 Growth curve

All the reduction experiments were done when cells were in the late logarithmic or early stationary phase. Therefore, the first step of the microbiological experiments was to determine the growth kinetics for each of the bacteria. In this study, both optical density measurement and plate counting were applied to monitor the growth of the cells. Optical density measurements revealed that *Pseudomonas fluorescens* LB 300 reached the late exponential phase after 72 hours of culturing, while plating results showed that there was no significant increase of cells between samples taken from 48 hours and 72 hours of culturing (Fig. 2.3). The increase of living cells between 48 hours and 72 hours was caused by a mixing of both living and dead cells, so after 48 hours, LB 300 has already reached its late exponential phase, and all experiments were conducted at this time point. The same experiments were also done for *Shewanella oneidensis* MR-1, and the cells were also found to reach the late log phase after 48 hours. In this study, cell density was determined by plating.

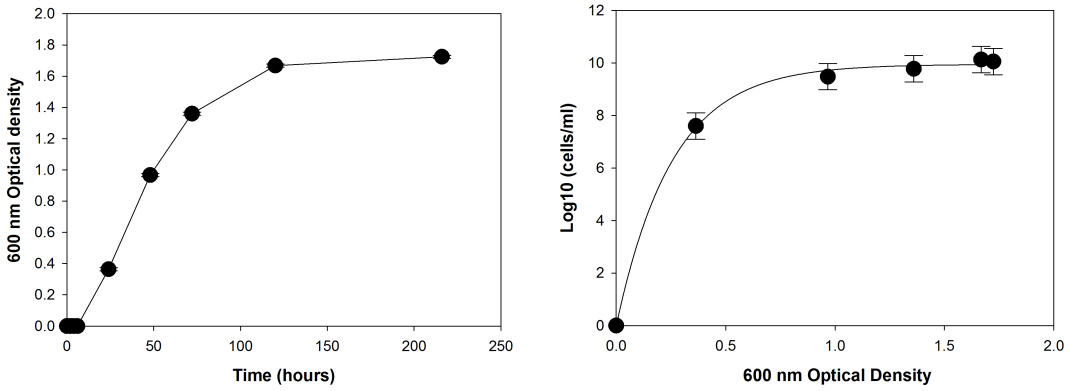


Figure 2.3: Left panel: Growth curve for *Pseudomonas fluorescens* LB 300 based on optical density measurement. Right panel: The relationship between the number of cells and the optical density measured.

2.2 Chromium toxicity test

To determine the right range of Cr initial concentrations for bacterial reduction experiments, a chromium toxicity test was done by using a whole cell bioreporter, *Acinetobacter baylyi* ADPWH_*rec*A. Bacterial whole cell bioreporters are an efficient, cost-effective and sensitive means of determining toxic materials bioavailability and genotoxicity [*van der Meer and Belkin*, 2010]. *A. baylyi* ADPWH_*rec*A has a chromosomal insertion of the promoterless *lux*CDABE cassette form *Photorhabdus luminescens* [*Huang et al.*, 2005] which is controlled by the SOS-inducible *rec*A promoter [*Song et al.*, 2009]. It has been reported to be useful in semi-quantitatively detecting and evaluating genotoxic compounds in the environment.

The method was established by *Jiang et al.* [2015]; *Song et al.* [2009, 2014], to evaluate the toxicity of different compounds using this bioreporter. This is now described briefly as follows:

2.2.1 Preparation of the strain

All chemicals in this study were analytical-grade reagents (Sigmal Aldrich, USA). LB medium (Luria-Bertani medium) and LBK medium (LB medium with 10 μg kanamycin mL^{-1}) were used for the cultivation of strains and in the induction studies.

The strains were first recovered from -80 °C and incubated on LB agar plate (supplemented with 10 μg kanamycin mL^{-1}) at 30 °C overnight. One colony was taken and incubated in 5 mL LBK medium in a rotary shaking incubator at 120 rpm, 30 °C, for 12-14 hours. The strain was harvested by centrifugation at 4100 rpm for 20 minutes. The cells were then resuspended in 5 mL fresh LB medium and diluted 10 times for the experiments.

2.2.2 Chromium sample preparation

Potassium dichromate, potassium chromate and chromium chloride solutions with Cr concentrations of 50, 200, 400 and 1000 mg/L (in terms of chromium) were prepared. Milli-Q water with no Cr was used in one group as the blank control (negative control), and Mitomycin C from streptomyces caespitosus was applied as the positive control in the experiment.

2.2.3 Bioreporter response measurements

Aliquots of 180 μl ADPWH_*rec*A and 20 μl chromium solutions were transferred to, and mixed in, a 96-well microplate (black with clear bottom, Greiner, Germany), the final concentrations in the wells were 0, 5, 20, 40 and 100 mg/L for all of the three different chromium species (Fig 2.4). Milli-Q water and mitomycin C (1×10^{-6} M) were used as the negative and positive controls. Bioluminescent intensity and optical density were both measured with a Bio-tek Synergy 2 HT plate reader every 30 minutes at 30 °C over 6 hours. Each group in this experiment contained triplicate samples and every measurement was done three times.

The bacteria used in this study can generate bio-luminescence. In this study, the intensity of bio-luminescence expressed by the control group was considered as the baseline. The toxicity of Cr was evaluated using the induction ratio, which can be calculated using the following equation:

$$The\ induction\ ratio = \frac{Bioluminescent\ intensity_{The\ induced\ treatment}}{Bioluminescent\ intensity_{The\ negtive\ control}} \tag{2.1}$$

The detection limit is defined as the lowest concentration of Cr(VI) causing a significant induction ratio response relative to the negative control (p<0.01).

In the presence of a DNA damaging compound that causes genotoxicity to cells, the intensity of bio-luminescence increases with the toxicity level. In this case, the



Figure 2.4: 96-well microplate used for the toxicity test.

induction ratio is greater than 1. However, when the toxicity level is exceeded to the extent that seriously damages cell functions, the bio-luminescence will decrease, and in this case, the induction ratio is less than 1.

2.3 High Performance Ion Chromatography

2.3.1 Cr(VI) measurement

I have set up the methods for Cr measurement based on Dionex Application Notes (Application update 165), and modified it according to my study. I tested it for the proper range of Cr(VI) and Cr(III) concentration that can be accurately measured by the instrument.

In the present study, a Thermo scientific^{TM} dionex^{TM} ICS−3000 HPLC/IC instrument was used to measure Cr (VI) concentrations. A Dionex IonPac CG5A (4 × 50mm) guard column, Dionex IonPac CS5A (4 × 250 mm) column, 375 μL reaction coil and an UV/Visible HPLC Detector were used.

The Eluent contained 2 mM Pyridine-2,6-dicarboxylic acid (PDCA), 2 mM Na_2HPO_4, 10 mM NaI, 50 mM $CH_3CO_2NH_4$ and 2.8 mM LiOH. To prepare it, a concentrated stock of 10 × Eluent was made first, by dissolving 3.34 g pyridine-2,6-dicarboxylic acid (PDCA), 5.36 g disodium hydrogen phosphate heptahydrate, 15 g sodium iodide, 38.5 g ammonium acetate, and 1.1 g lithium hydroxide monohydrate in 1 L of Milli−Q water. Before each measurement, fresh eluent was prepared by adding 100 mL of the concentrated eluent stock to a 1 L volumetric flask and bringing up to 1 L with Milli-Q water. The pH of the solution was between 6.7 and 6.8.

Postcolumn reagent contained 2 mM DPC, 10% CH_3OH and 0.9 N H_2SO_4. To prepare it, 0.5 g 1,5-diphenylcarbohydrazide (DPC) was dissolved in 100 mL HPLC grade methanol in a volumetric flask. 500 mL Milli−Q water with 25 mL 96% sulfuric acid was then added and diluted to 1 L with Milli-Q water.

Chromate is subjected to postcolumn derivatisation with DPC (1,5-diphenylcarbohydrazide). Therefore, the flow rates of Eluent (1 mL/min) and postcolumn reagent (0.5 mL/min) are critical in the measurement and need to be well controlled. The measurements for Cr(VI) are done at a wavelength of 530 nm and the retention time was 4.7 to 8 minutes (peak 7 in Fig. 2.5, Absorption units (AU) vs. Retention Time). A calibration curve was done at the beginning of each measurement. This was accomplished by measuring a series of Cr(VI) standard samples at concentrations of 0.5, 1.0, 1.5, 2.0, and 2.5 mg/L prior to any sample measurement. A linear relationship between the areas of Cr(VI) peaks and their concentrations can be found (Fig. 2.6). The standard solutions were prepared by diluting a Cr(VI) standard stock solution into Milli-Q water.

Cr(III) can also be measured with the same instrument, but the sample treatment methods are different. A Cr(VI) solution passed through a 0.22 μm membrane can be measured directly (530nm wavelength). The detection limit was 0.1 mg/L for Cr(VI). However, Cr(III) samples need to be boiled with Eluent stock and 0.1 ‰

nitric acid prior to the measurement with a UV detector (335 nm wavelength).

This method used the PDCA based eluent system, in which Cr(III) is separated as the $Cr(PDCA)^2$ complex (formed by sample treatment), while Cr(VI) is separated as the chromate anion. Cr(III)-PDCA complex does not react with DPC in the postcolumn reagent, but it can still be detected at 530 nm. Cr(VI) and the DPC reaction can also be detected at 335 nm. Therefore, although it is convenient to measure both Cr(VI) and Cr(III) in the sample, there are interference with both species which decrease the accuracy of the measurement, and the detection limit for Cr(III) was over 1 mg/L, which was too high for my study. So in this study, I did not treat my samples to form the Cr(III)-PDCA complex, and Cr(III) was not detected by the instrument. This permits an accurate measurement of Cr(VI). In a preliminary reduction experiment, I measured total Cr concentrations with a Quad-ICP-MS throughout the experiment, and it remained constant over the reduction period, which means that throughout the reduction, both Cr(VI) and Cr(III) were in the solution. After measuring Cr(VI) concentrations with HPIC, Cr(III) concentrations can then be calculated by mass balance.

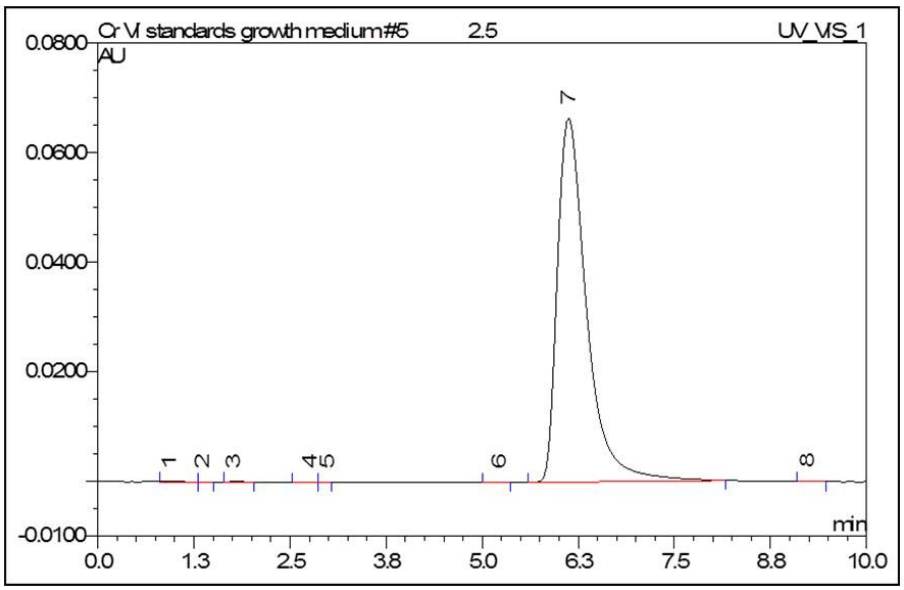


Figure 2.5: The Cr (VI) ion chromatography peak at 530 nm wavelength for a 2.5 mg/L standard

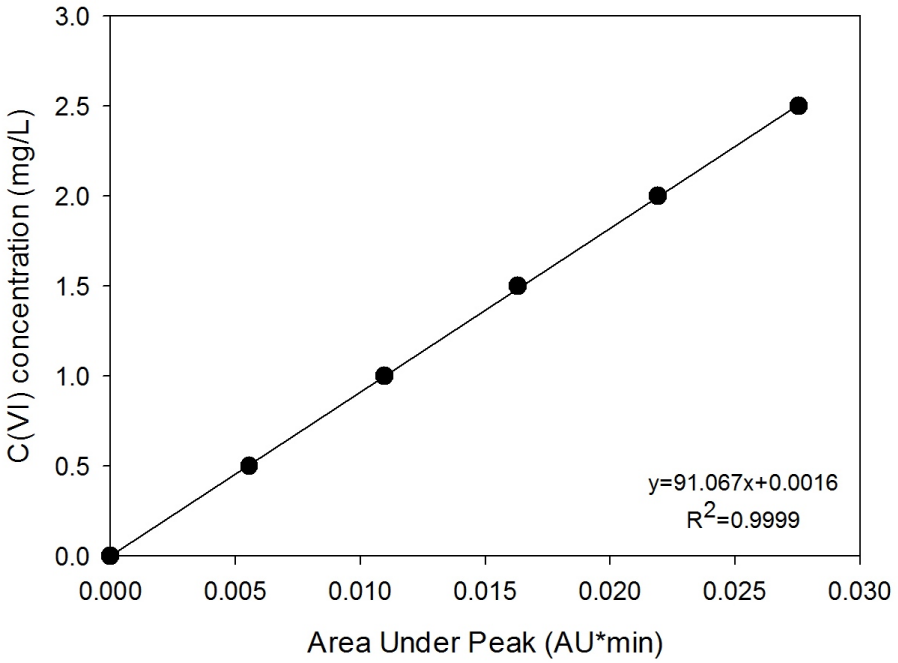


Figure 2.6: Cr (VI) Standard Curve for Ion Chromatography measurements

2.4 Chromium isotope measurement

2.4.1 Ion exchange separation of chromium for stable isotope mass spectrometric analysis

The preparation of samples for determination of the ^{53}Cr/^{52}Cr ratio was modified from the methods of *Ellis et al.* [2002]. We used a double isotope spike approach for correction of isotopic fractionation occurring during sample preparation and mass spectrometry steps. After determining Cr (VI) concentration in the samples by IC, an accurately measured aliquot containing approximately 500 ng of Cr (VI) was taken from each sample and 500 ng ^{50}Cr-^{54}Cr spike was added to it. For this study, the double spike was in the Cr(VI) oxidation state (Table 2.2) in this study. In order to extract Cr (VI) from the sample matrix, an anion exchange chromatography method was employed. The mixture was loaded carefully onto a 2 mL pre-cleaned BioRad AG1-X8 anion resin bed. Cations and weak acids were flushed from the column using 10 mL Milli-Q water while Cr(VI) sticks on the resin. Cr (VI) was

Table 2.2: Chromium spike composition (ng/g)

^{50}**Cr**	48.43115
^{52}**Cr**	1.358566
^{53}**Cr**	0.181261
^{54}**Cr**	50.02902

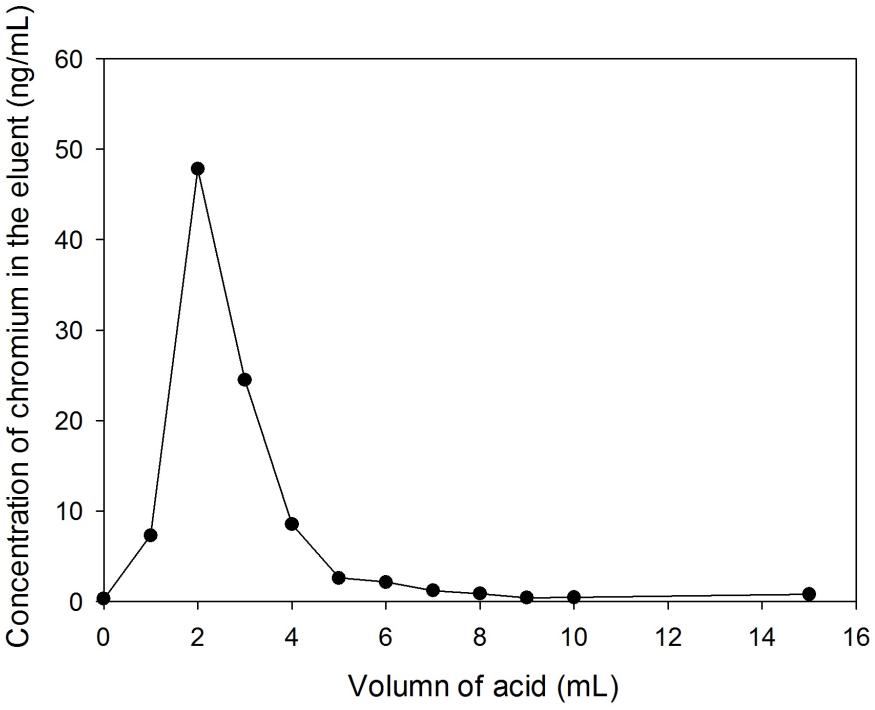


Figure 2.7: Efficiency calibration for the anion column

then reduced and eluted by using 10 mL 4N HNO_3, which was dried down on a hotplate.

The columns were calibrated with the standard Cr solution before processing any samples (Fig. 2.7). The yield from this chromatography method is higher than 95%.

2.4.2 Further purification of chromium through liquid-liquid separation

After the ion exchange separation step, some organic residues from the resin may contaminate the Cr samples. The residue can interfere with Cr isotope measurements on TIMS. To remove any organic residue from the column chemistry, Cr samples were further purified by a liquid-liquid separation method modified from *Bni et al.* [2007]. Cr samples were dried down after the ion exchange separation step, and then re-oxidized by adding 1 mL of ammonium persulfate solution and reacting at 100 °C for approximately 2 hours to ensure all of the Cr was fully oxidized. The sample was then cooled down and mixed with 1 μL H_2O_2 and 1 mL ethyl acetate under 10 °C at a specific pH condition (1.7 ± 0.1). In this step, Cr (VI) reacted with H_2O_2 and formed a blue Cr-peroxo complex which can dissolve into ethyl acetate. The extraction of the solution was performed as soon as possible because Cr(VI) in the water phase is not stable for a long time under these conditions [*Bni et al.*, 2007]. If it reduces to Cr (III), it will stay in the water phase and the extraction efficiency will decrease significantly. After shaking the mixture intensely for 30 seconds, the water phase is removed and the ethyl acetate was then mixed with 1 mL of NH_3 water (5 μL of 28 % NH_3 into 40 mL of Milli-Q water) for another 30 seconds. In this step, Cr (VI) was reduced to Cr (III) and dissolved into the water phase, so the water phase was extracted and dried down on a hotplate. The yields for the liquid-liquid separation step were between 70 % to 80 %. Although *Bni et al.* [2007] suggested using an ultrasonic bath to help the mixing of NH_3 water and the ethyl acetate to facilitate the extraction, it is not recommended in this study, because an ultrasonic bath will increase the fraction of ethyl acetate dissolved in water, which is not removed during the separation process. During sample loading onto rhenium filaments, the carbon from the ethyl acetate would make the filament turn black and therefore interfere with the isotope measurement.

2.4.3 Thermal Ionization Mass Spectrometry (TIMS)

Thermal ionization mass spectrometry (TIMS) is widely used for isotopic analysis of metals because thermal ionization can produce an ion beam with a very small kinetic energy spread (≈0.5 eV), and only a magnetic mass analyzer is needed to resolve different isotopes.

In our study, a single rhenium filament was required for ionisation of Cr samples in TIMS. The samples are typically in the form of nitrate salts. The single filament acts as both the vaporization and ionization filament.

Mass spectrometry was performed on a Thermo Finnigan Triton TIMS instrument. The dried sample was dissolved in 1 μL 0.1 M HNO_3, and carefully loaded onto a Re filament that was cleaned by boiling in H_2O_2 and degassed in high vacuum (10^{-6} Torr, T 1600 °C, at 3.2 A for 45 min). The Cr sample was dried by passing a low current through the filament (around 0.6 A). One μL of activator, containing silica gel, H_3BO_3 and Al was then added on top of the Cr sample under the same conditions. After this was fully dried, the mixture was first heated to around 1.2 A to burn off the ammonia salts and then to 1.8 A for 30 seconds to form a glass, which helps to enhance Cr^+ emission and stabilize small ion-beams. Ionisation efficiency for Cr in my study is around 1/1000.

The Data acquisition method was modified from *Trinquier et al.* [2008], and described briefly here. In the mass spectrometer, filaments were slowly heated to final temperatures of between 1170 °C and 1230 °C. $^{50}Cr/^{52}Cr$, $^{53}Cr/^{52}Cr$ and $^{54}Cr/^{52}Cr$ ratios were determined by simultaneous measurement of the ion beams on a multiple collector array.

Isobaric interferences on Cr masses are possible from 50V (0.24 % relative abundance of V), 50Ti (5.25 %), and 54Fe (5.83 %). However, the concentration of V and Ti in samples from this study were expected to be extremely low, and to be completely removed by the purification process. Moreover, the presence of V and Ti

during the run was monitored and corrected for using mass 51 (99.76 % of V) and 48 (73.98 % of Ti). For Fe, although its concentrations in the samples in some experiments of this study were high (1 mg/L in the study stated in chapter 4), the ion exchange chromatography separation and liquid liquid separation can also remove it. A test for the presence of Fe interference was made on mass 56 (91.66 % of Fe) [*May and Wiedmeyer*, 1998] and was found to be negligible.

Measured $^{53}Cr/^{52}Cr$ ratios were reported as relative deviations from the standard (NIST SRM 979) in parts per thousand (per mil or ‰):

$$\delta^{53}Cr = [\frac{(^{53}Cr/^{52}Cr)_{sample}}{(^{53}Cr/^{52}Cr)_{standard}} - 1] \times 1000‰ \tag{2.2}$$

The isotope fractionation factor can be quantified as:

$$\alpha = \frac{(^{53}Cr/^{52}Cr)_{product}}{(^{53}Cr/^{52}Cr)_{reactant}} \tag{2.3}$$

which can also be expressed using ε notation:

$$\varepsilon = (\alpha - 1) \times 1000‰ \tag{2.4}$$

In this study, Cr (VI) reduction experiments were done in a well mixed, closed environment; a Rayleigh distillation equation (Eq. 1.13) can be used to calculate the δ^{53} value of the remaining Cr (VI), which can also be expressed as follows:

$$\delta(t) = (\delta_0 + 1000)(\frac{c(t)}{c_0})^{\alpha-1} - 1000 \tag{2.5}$$

which can also be rearranged to a linear form:

$$\ln(\delta(t) + 1000) = (\alpha - 1)\ln[c(t) + [ln(\delta_0 + 1000) - (\alpha - 1)\ln(c_0)]] \tag{2.6}$$

where c(t) and δ(t) are the concentration and isotopic composition of Cr(VI) at time

t; c_0 and δ_0 are their initial values. The best-fit α values can be found by plotting $\ln(\delta^{53}Cr + 1000‰)$ vs. $\ln[c(t)]$ and using linear regression for the plots to obtain a value of the slope of α-1 [*Kitchen et al.*, 2012]. Uncertainties can be calculated as 2×standard errors of the best fit slopes.

During thermal ionisation, the light isotope is preferentially evaporated, thus producing an instrumental mass-dependent fractionation. In the initial stages, the analysed material is isotopically lighter relative to the true isotope composition, and at the end, it is isotopically heavier. Corrections for these instrumentally produced mass fractionation that preserve natural mass dependent fractionation can be approached in two ways: a double spike method or an empirical adjustment. The double spike method allows for rigorous calculation of instrumental mass fractionation. The empirical method compares the measurement of samples with the isotopic analysis of a standard, base on the assumption that standards and samples fractionate to the same extent during isotopic analysis under carefully controlled analytical conditions.

In this study, a double spike method was applied for corrections of the mass-dependent instrumental bias.

2.4.4 The mass-dependent instrumental bias

Instrumental mass-dependent fractionation can be described by different mass fractionation laws.

The linear law is probably the most intuitive of all the mass fractionation laws.

By introducing the conventional notation δ defined as $\delta = 1000\ (\frac{r_i}{R_i}$ - 1) where r_i and R_i stand for the measured and true isotopic ratio, respectively. The following equation can be obtained:

$$\frac{\delta_i}{\delta_j} = \frac{M_i - M_k}{M_j - M_k} \tag{2.7}$$

In which M_i, M_k and M_j are the masses for different isotopes. This equation describes the linear relationship between the isotopic ratios in the delta notation predicted by the linear mass fractionation law.

Other than the linear law, the power law and the exponential law are also considered in previous studies.

The power law can be expressed by the following equation:

$$r_i \approx R_i g^{M_i - M_k} \tag{2.8}$$

where r_i and R_i stand for the measured and true isotopic ratio, respectively, and M_i and M_k are the masses for the isotopes. g is defined as the mass bias factor.

For thermal ionization mass spectrometry, the exponential law appears to be the best model that describes the mass dependent fractionation in the TIMS source for many different elements [*Beard and Johnson*, 1999; *Hart and Zindler*, 1989; *Russel et al.*, 1978]. Therefore it was used for the double spike correction.

The exponential law can be expressed as:

$$r_i \approx R_i (\frac{M_i}{M_k})^{\beta} \tag{2.9}$$

where r_i and R_i stand for the measured and true isotopic ratio, respectively, and M_i and M_k are the masses for the isotopes. β is the mass bias factor.

From the exponential law, linear alignments can be obtained in log-log plots in which one measured isotopic ratio is plotted against another. For example, with different isotopic ratio R_i and R_j of the same element, the exponential law can be changed to the form of:

$$\frac{\ln r_i - \ln R_i}{\ln r_j - \ln R_j} = \frac{\ln M_i/M_k}{\ln M_j/M_k} \tag{2.10}$$

2.4.5 Double spike method

The double spike method has been widely used in many isotope systems, such as Fe and Mo [*Johnson and Beard*, 1999; *Siebert et al.*, 2001]. It involves measuring the relative amount of four isotopes, two of which are enhanced by the addition of enriched isotopic spikes to the sample. From the knowledge of the double spike composition it is possible to invert the measurements to obtain the true composition of the sample corrected for instrumental mass fractionation.

The principle of double spiking works for triple or multiple spikes as well [*Galer*, 1999].Mass dependent fractionation occurs both in the mass spectrometer and in nature. As was discussed previously, natural variations in stable isotope ratios can be expressed in terms of a mass fraction factor from a standard isotope composition, which can be directly converted to a standard δ' notation. In this study, for $^{53}Cr/^{52}Cr$ the exponential fractional law between sample (N) and standard (n) is:

$$(\frac{^{53}Cr}{^{52}Cr})_N = (\frac{^{53}Cr}{^{52}Cr})_n(\frac{52.9406}{51.9405})^{-\alpha} \tag{2.11}$$

where 52.9406 and 51.9405 are the atomic weights of ^{53}Cr and ^{52}Cr, respectively. The isotope variations can be expressed as δ'^{53}Cr:

$$\delta'^{53}Cr = 1000 \log \frac{(^{53}Cr/^{52}Cr)_N}{(^{53}Cr/^{52}Cr)_n} = -1000\alpha \log \frac{52.9406}{51.9405} \tag{2.12}$$

Similarly, a fractionation factor β describes the mass fractionation occurring in the instrument during measurement of the double spike sample mixture,

$$(\frac{^{53}Cr}{^{52}Cr})_N = (\frac{^{53}Cr}{^{52}Cr})_n(\frac{52.9406}{51.9405})^{-\beta} \tag{2.13}$$

The double spike (T) and sample (N) are mixed to form the mixture (M), and for each isotope, M can be expressed in terms of a proportion p per mole of element of double spike to 1-p of sample. For example, the mixing law for ^{53}Cr in the mixture

is

$$(^{53}Cr)_M = p(^{53}Cr)_T + (1-p)(^{53}Cr)_N \tag{2.14}$$

Given the double spike composition T, measurement of the mixture m and the composition of the standard n, it is possible to invert to find the true composition of the sample N, the mixture M, double spike to sample proportion p, and the fractionation factors α and β.

In nature, sample N is fractionated from the standard n by a factor of α. The sample was then mixed with a double spike T, which has a known composition of Cr. When measured on TIMS, an instrumental fractionation occurs to the mixture M by a factor of β, and what we obtained is the measured composition after instrumental fractionation of the mixture. The composition of the double spike in this study is listed in the Table 2.2 and the standard composition n is the composition of the NIST SRM 979.

The inversion involves the solution of simultaneous non-linear equations of three isotopic ratios with a common denominator for the unknowns p, α, and β. It does not matter which isotope of the four is chosen as the common denominator, because the answer will be the same for all isotopes. In this study, ^{52}Cr is chosen as the common denominator, and the double spike inversion is based on the following equations.

Exponential mass fractionation law for the sample with mass fractionation factor α:

$$n_i = N_i e^{\alpha P_i} \tag{2.15}$$

Exponential mass fractionation law for the mixture with mass fractionation factor β:

$$m_i = M_i e^{\beta P_i} \tag{2.16}$$

The mixing relationship in isotope ratio space between double spike and sample:

$$M_i = \lambda T_i + (1-\lambda) N_i \tag{2.17}$$

In these equations, N_i refers to the ith isotopic ratio of the sample (i=1, 2, 3). M_i, m_i, and T_i are defined similarly. P_i is the natural log of the atomic masses ratio. According to the equation 2.14, λ is related to the proportion p by mole in which the double spike and sample mix, as follows:

$$p = (1 + \frac{1-\lambda}{\lambda}(\frac{1+\sum_k N_k}{1+\sum_k T_k}))^{-1} \tag{2.18}$$

where $\sum_k$ is the sum of the all isotope ratios for the element. The value of λ depends on the denominator employed in the study.

When combining the equations with n_i, m_i, and M_i, the following equation can be obtained:

$$F_i(\lambda, \alpha, \beta, n, m, T) = \lambda T_i + (1-\lambda) n_i e^{-\alpha P_i} - m_i e^{-\beta P_i} = 0 \tag{2.19}$$

When α and β are small ($\ll$1), the equations can be linearised to:

$$F_i(\lambda, \alpha, \beta, n, m, T) \approx n_i - m_i + \lambda(T_i - n_i) - (1-\lambda)\alpha n_i P_i + \beta m_i P_i \tag{2.20}$$

which can be written in matrix form as:

$$\mathbf{F(x,n,m,T)} \approx -\mathbf{b} + A\mathbf{x} \tag{2.21}$$

where: $A = \begin{pmatrix} T_1 - n_1 & -n_1 P_1 & m_1 P_1 \\ T_2 - n_2 & -n_2 P_2 & m_2 P_2 \\ T_3 - n_3 & -n_3 P_3 & m_3 P_3 \end{pmatrix}$, $b = \begin{pmatrix} m_1 - n_1 \\ m_2 - n_2 \\ m_3 - n_3 \end{pmatrix}$, $x = \begin{pmatrix} \lambda \\ (1-\lambda)\alpha \\ \beta \end{pmatrix}$.

α and β can be obtained by solving the equations:

$$F(x, n, m, T) = 0 \tag{2.22}$$

2.4.6 Optimising the double spike

A good double spike should produce low errors for the measurement. In this study, the error in α with the double spike employed was calculated, according to the methods of *Rudge et al.* [2009], in which the compositions of the double spike and the standard were assumed to have no error, and they were due to Johnson-Nyquist noise of the impedance amplifiers (thermal noise of the electronic baseline and the counting statistic of the ion beam intensity.

Fig. 2.8 represent a contour plot of the error in α for a ^{50}Cr - ^{54}Cr double spike. Finding the optimum double spike is to locate the minimum error (shown as the cross in the figure). The optimum spike is 57.77% of ^{50}Cr and 42.23% of ^{54}Cr, and the optimum proportion of the spike in the mixture is 28.64 %. However, in reality, it is hardly possible to mix the spike with sample in exactly the proportions we would like, therefore it is very important to understand how the error varies in the vicinity of the optimum. The contour figure can provide an idea of the robustness of the optimal double spike.

For a double spike with known compositions, we can calculate the optimum double spike - sample mixing proportions. Fig. 2.9 indicates that our double spike is robust with a broad range of spike-sample proportions. The spike-sample proportion used in this study was around 0.5.

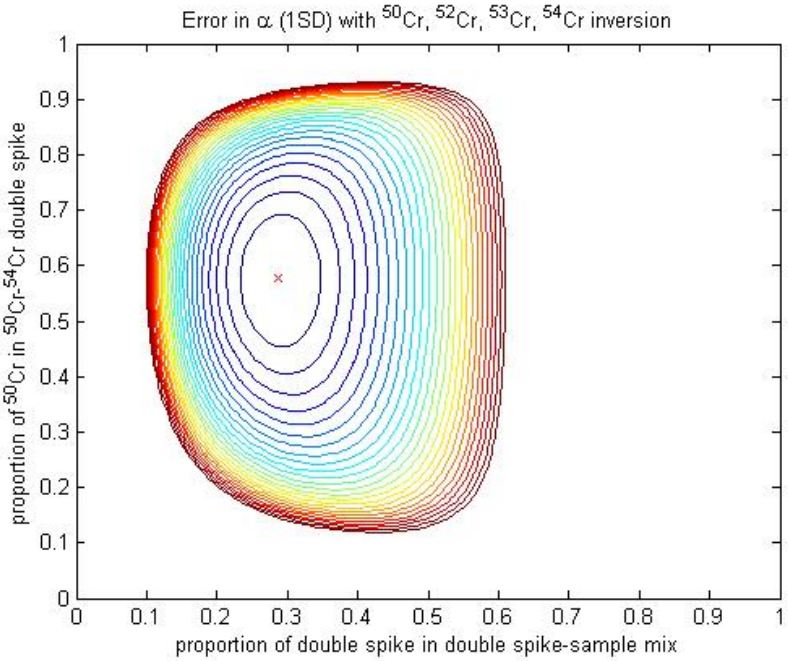


Figure 2.8: Contour plot of error in α for the ^{50}Cr - ^{54}Cr double spike. The horizontal axis gives the proportion p of double spike in the double spike - sample mixture, and the vertical axis gives the proportion q of ^{50}Cr in the double spike. The optimum is marked by a cross. Only contours within 25 % of the error are shown in this figure, with internal 1% of the optimal error on α. There is a broad region around the optimum where low errors are found.

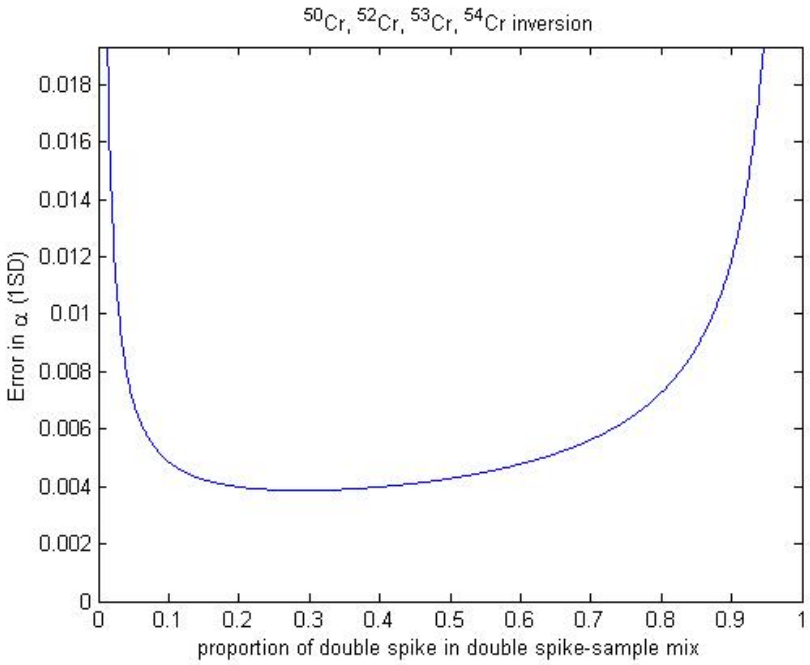


Figure 2.9: Plot of the error in α against the proportion p of double spike in the double spike-sample mixture. The spike composition is shown in Table. 2.2. The errors are small (< 0.005) for quite a broad range of spike-sample mixing proportions (0.15 to 0.55).

2.4.7 Reproducibility and accuracy of Cr isotopic measurements

The long-term instrumental reproducibility was determined by measuring a spiked Cr standard (Fig. 2.10). The mean δ^{53}Cr value over a long period of measurement is slightly negative compared to the reported NIST SRM 979 Cr standard value. The internal error (2S.D.) of the measurement is 0.049 ‰.

2.5 SEM imaging of the microbial samples

A JEOL JSM-6390 Scanning Eletron Microscope (SEM) was employed in this study to assess bacterial-mineral interactions.

Sample preparation followed the standard SEM protocol, which is described as follows:

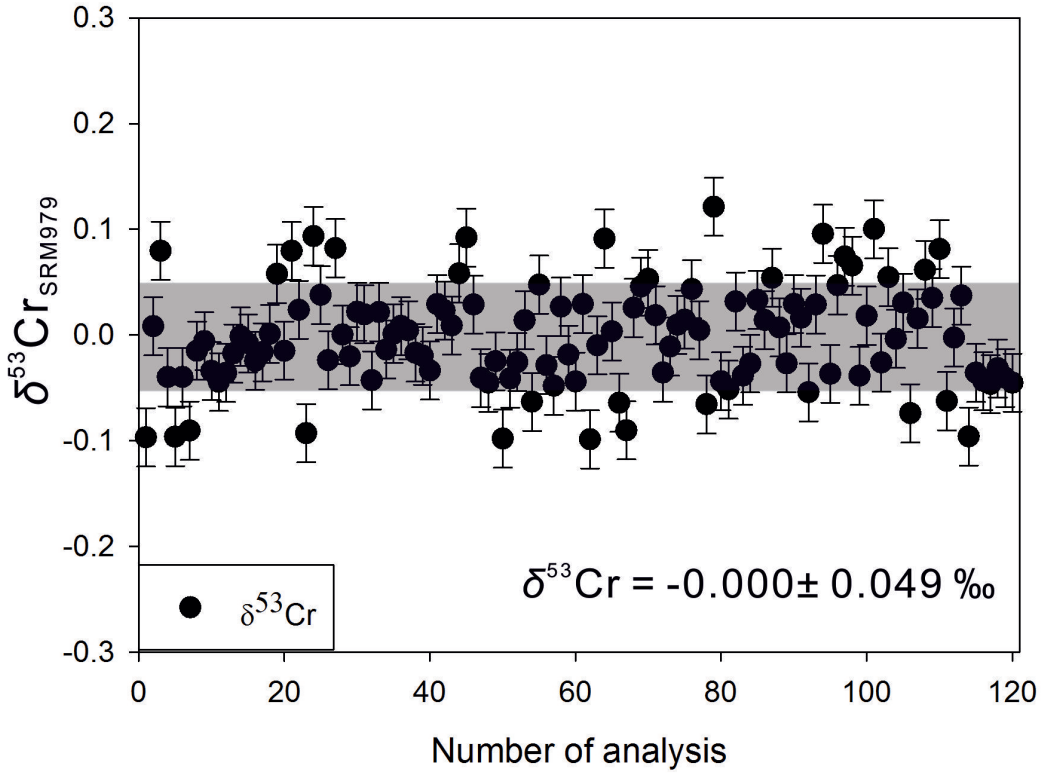


Figure 2.10: The long-term reproducibility of δ^{53}Cr for the Cr standard. Each data point represents analysis of a spiked standard deconvolved using double-spike correction. Error bars are shown as 2 × standard errors of an individual analysis, which consists of measurement of 200 isotope ratios. The grey area represents the 2 × standard deviation envelope for the average $\delta^{53}Cr$ values for the standard.

1. **Primary fixation.** The primary fixative (2.5 % glutaraldehyde in 0.1 M phosphate buffer at pH 7.2-7.4 for cells or animal tissue) was added. Samples were incubated at room temperature for 1 hour.

2. **Rinse.** The specimens were rinsed in 0.1 M Phosphate Buffer (3 changes of fresh buffer, 5 min each).

3. **Secondary fixation.** Aliquot of 0.5 ml of 0.2 M Phosphate Buffer and 0.5 ml of 2 % OsO4 were added to samples (for a final concentration of 1 % OsO4, 0.1 M Phosphate Buffer), and then the samples were incubated at 4 °C for approximately 1 hour.

4. **Rinse.** The specimens were rinsed in Milli-Q water (3 changes of fresh water, 5 min each).

5. **Dehydration.** The samples were incubated in 50 % EtOH for 10 min, in 70 % EtOH for 10 min, in 90 % EtOH for 10 min, in 95 % EtOH for 10 min, and in 100 % EtOH for 20 min. All the procedures were repeated 3 times.

6. **Drying.** There are two ways to dry the sample: using hexamethyldisilazane (HMDS) as drying agent or using Critical Point Drying (CPD). In this study, the former was used. In a fume hood the EtOH was removed and 0.5ml HMDS was quickly added to the sample vial. The mixture was incubated for 3 mins. Then, the HMDS was removed and sample vials were left (with lid open) overnight in the fumehood for the HMDS fumes to evaporate.

7.The samples were mounted on carbon adhesive tape on an SEM stub, sputter coated with 10-15 nm thickness of gold or gold/palladium.

After fixation, the samples were then imaged at 10 kV. The sample pictures are in Fig. 2.11, where suspended cells of *Pseudomonas fluorescens* LB 300 and *Shewanella oneidensis* MR 1 are shown. *Pseudomonas fluorescens* LB 300 have rough surfaces and possess multiple polar flagella (Fig. 2.11A, white arrows), which aid the mobility of cells. *Shewanella oneidensis* MR 1 have much smoother surfaces than *Pseudomonas fluorescens* LB 300 and can produce "nano-wires" that are re-

ported to facilitate an extracellular electron transfer processes (Fig. 2.11B, white arrows,[*Gorby et al.*, 2006]).

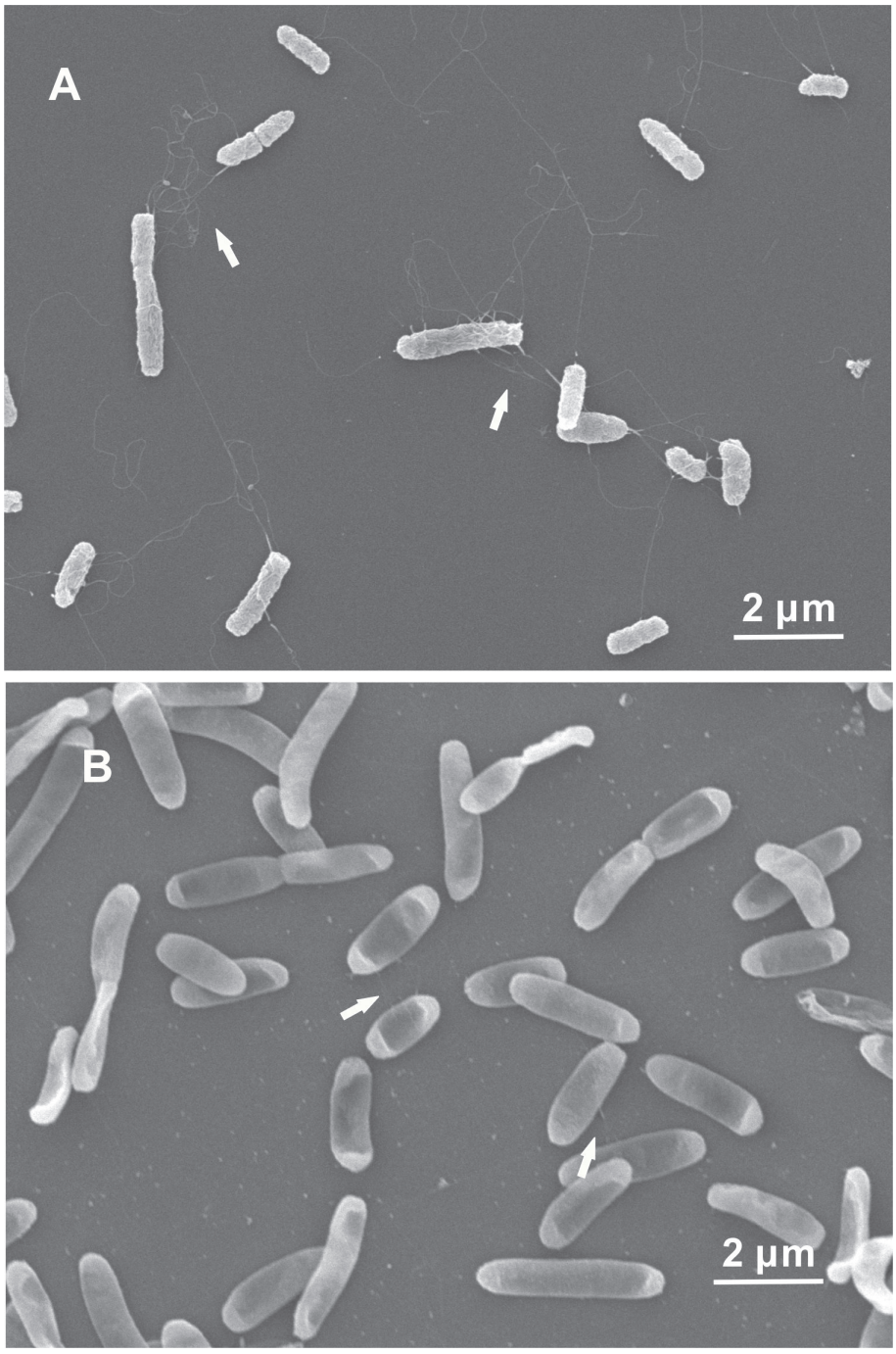


Figure 2.11: A: Suspended cells of *Pseudomonas fluorescens* LB 300, which have multiple flagella to aid mobility. B: Suspended cells of *Shewanella oneidensis* MR 1. The cells were flat and have thick polars.

Chapter 3

The Cr isotope proxy for bacterial reduction processes

3.1 Introduction

Chromium is abundant in the earth's crust [*Rudnick and Gao*, 2003] and can naturally occur in the environment by weathering and leaching from rocks. Cr exists in many different oxidation states (0 to VI), but only two of them, trivalent and hexavalent Cr, are stable in the environment [*Kota and Stasicka*, 2000].

The predominant oxidation state in igneous and metamorphic rocks is Cr (III), which is generally insoluble and less reactive, and so relatively immobile in the environment. Manganese oxides, which are able to oxidise Cr (III), are a dominant inorganic control of Cr in oxic environments [*Feng et al.*, 2006; *Landrot et al.*, 2012]. When Cr is oxidized to Cr (VI), its solubility increases significantly, and as a consequence its mobility. Cr naturally occurs in rivers and lakes at concentrations of 0.5 to 100 nM, and about 0.1 to 16 nM in seawater [*Bradl*, 2005]. In addition to inputs from natural sources, the presence of high levels of Cr can also be a consequence of its widespread use in industrial processes such as leather tanning, making stainless steel and preventing engine corrosion.

Because Cr is spread widely in the environment, has high toxicity, and is able to exert quite distinctive physio-chemical characteristics under different redox conditions, it is important to be able to effectively monitor Cr and identify the abiotic and biotic conditions that determine its chemical states. This is aided by the fact that Cr has 4 stable isotopes, and redox reactions are known to enrich the lighter isotopes in the products since they are more reactive [*Ellis et al.*, 2002]. Thus, changes in isotopic composition may be used as indicators to track the progress of redox conditions in the environment. Likewise, isotopic compositions enable differentiation between natural local sources of Cr from those introduced by anthropogenic activity [*Ellis et al.*, 2002; *Izbicki et al.*, 2012; *Johnson and Bullen*, 2004], and to assess the effectiveness of remedial interventions.

Chromium isotope data are usually reported as relative deviations from the standard (NIST SRM 979) in parts per thousand (per mil or ‰):

$$\delta^{53}Cr = [\frac{(^{53}Cr/^{52}Cr)_{sample}}{(^{53}Cr/^{52}Cr)_{standard}} - 1] \times 1000‰ \tag{3.1}$$

The isotope fractionation factor is:

$$\alpha = \frac{(^{53}Cr/^{52}Cr)_{productflux}}{(^{53}Cr/^{52}Cr)_{reactant}} \tag{3.2}$$

which can also be expressed using ε notation:

$$\varepsilon = (\alpha - 1) \times 1000‰ \tag{3.3}$$

Cr(VI) reduction reactions, such as those undertaken by microbial communities, result in reaction of lighter isotopes at a faster rate than heavier ones, leaving diminished concentration of Cr(VI) that are isotopically heavy. In contrast, dilution of Cr(VI) does not change the δ^{53}Cr value. An understanding of the mechanism by which the isotopic ratios of Cr are modified may enable the monitoring and predictions of the fate of Cr(VI) in contaminated sites [*Berna et al.*, 2010] or in the

natural environment [*Ellis et al.*, 2002; *Gao and Schulze*, 2010; *Raddatz et al.*, 2010; *Wanner et al.*, 2012].

Chromium isotopes are not only useful as indicators of redox conditions prevailing in modern environments, but may also be used as a proxy of prevailing oxygenation conditions over geological time. The isotopic composition of Cr in sedimentary deposits can reflect oxygen levels in the hydrosphere and atmosphere in the past [*Frei and Polat*, 2013; *Frei et al.*, 2013; *Rotaru et al.*, 1992].

In order to develop more effectively the use of Cr isotopic variations as environmental indicators, a database calibrating them with specific parameters is essential for establishing isotopic fractionation as a diagnostic tool.

The dominant environmental processes that control Cr cycling include both biotic and abiotic reaction. Isotopic fractionation factors determined from abiotic reactions are valuable and can help understand Cr behaviour under various environmental conditions. It is useful to compare isotope signatures generated from biotic and abiotic reactions, and use these signatures to help determine whether or not different processes can be distinguished. *Zink et al.* [2010] have reported Cr reduction by H_2O_2 in aqueous media under both highly acidic and circum-neutral conditions; the fractionation factors were found to be -3.5 ‰ and -5.0 ‰, respectively. The presence of elements such as iron in its various chemical forms is known to have the potential to alter the chemical state of Cr. *Dossing et al.* [2011] reported ε of -3.0 ‰ to - 4.4 ‰ for reduction by aqueous Fe(II) at circum-neutral pH, and -1.5 ‰ when simultaneously reduced by dissolved Fe(II) and Fe(II)+Fe(III) green rust. *Basu and Johnson* [2012] have conducted Cr(VI) reduction experiments with Fe(II)-doped goethite, FeS, green rust, siderite($FeCO_3$) and artificially reduced sediments from a permeable reactive barrier. The fractionation factors were found to vary from -2.1 ‰ to -3.9 ‰. In addition to redox reactions, adsorption is also an important process that may induce chromium isotope fractionation. *Ellis et al.* [2004] investigated the effects of sorption of Cr(VI) onto goethite and $\gamma - Al_2O_3$,

and found that equilibrium fractionation of Cr stable isotope during adsorption is negligible. Cr(VI) isotope fractionation during adsorption on other phases have not been determined.

Shifts in isotope fractionations due to microbial activities provide valuable insight into the mechanisms of metal cycling, and can be used to quantify biogeochemically mediated redox processes in the environment [*Basu et al.*, 2014; *Han et al.*, 2012; *Sikora et al.*, 2008]. There are many factors that can impact the microbial processing of Cr and some of these can be moderated by the immediate environment, such as the presence of specific electron donors and Cr concentration.

Previous studies have mostly focused on microbial Cr(VI) reduction under anaerobic conditions. *Sikora et al.* [2008] were the first to investigate the impact of microbial factors on Cr isotopic fractionation. They conducted anaerobic reduction experiments with *Shewanella oneidensis* MR 1 and determined a chromium isotope fractionation factor ε that ranged from 4.0 to 4.5 ‰ when reduction rates were low but was 1.8 ‰ at greater reduction rate. *Han et al.* [2012] reported Cr isotope data during reduction by *Pseudomonas stutzeri* RCH2 under both aerobic (2 ‰) and denitrifying conditions (0.4 ‰). *Basu et al.* [2014] reported chromium reduction by a metabolically diverse group of bacteria, and suggested that stronger isotopic fractionation was induced during Cr(VI) reduction under electron donor poor conditions.

Chromium and sulphur have many similarities: they are both known as redox sensitive elements, they both can be electron acceptors in microbial metabolic processes, and large isotope fractionation by bacterial processes were found for both elements. The scientific findings with microbial sulphate reduction processes may provide insights of microbial Cr(VI) reduction processes. It has been demonstrated that different environmental conditions may have a great impact on microbial S isotope fractionation [*Habicht and Canfield*, 1997; *Kaplan and Rittenberg*, 1964]. However, information is still limited on the environmental conditions and microbial

activity that determine Cr isotopic fractionation.

Information about the impacts of different environmental conditions on microbial activity and corespondent isotope fractionation process would be enormously valuable in establishing isotopic fractionation as an effective means to provide insight of the prevailing conditions in the habitat such as redox, pH or concentration and help further establish the technique for identifying environmental processes. Thus the objective of this study is to investigate the impact of bacterial species, the nature of the electron donors, and the mode of bacteria metabolism (aerobic and anaerobic), on both the rates of reduction and the shift in the isotopic signature.

3.2 Materials and Methods

3.2.1 Bacteria

The bacterial strains selected in this study were *Shewanella oneidensis* MR-1 (MR-1) and *Pseudomonas fluorescens* LB 300 (LB 300), both of which are typical and common in the environment and are reported to reduce Cr under specific conditions. The two bacteria are both facultative anaerobes, so both have the potential to reduce Cr (VI) to Cr (III) both aerobically and anaerobically. The fractionation of chromium isotopes was determined under both these conditions. *Shewanella oneidensis* MR-1 (MR-1) was purchased from NCIMB Ltd (NCIMB 14063) and *Pseudomonas fluorescens* LB 300 (LB 300) was kindly provided by Prof. Yi-Tin Wang from department of Civil Engineering, University of Kentucky [*Wang and Shen*, 1995].

3.2.2 Growth medium and general culturing condition

Two Growth media were employed in the aerobic reduction study: LB (Luria Bertani) Broth (Sigma Aldrich) and the Minimal salts medium (0.03g NH_4Cl, 0.03g

K_2HPO_4, 0.05g KH_2PO_4, 0.01g NaCl and 0.01 g $MgSO_4$ in 1 L of Milli-Q water). The anaerobic growth medium and cell suspension medium for Shewanella oneidensis MR-1, described by *Myers and Nealson* [1988], was modified by adding different electron donors and accepters. The composition of the growth medium was as follows: 9.0 mM $(NH_4)_2SO_4$, 5.7 mM K_2HPO_4, 3.3 mM KH_2PO_4, 2.0 mM $NaHCO_3$, 1.01 mM $MgSO_4$, $CaCl_2$, 67.2 μM Na_2EDTA, 56.6 μM H_3BO_3, 10.0 μM NaCl, 5.4 μM $FeSO_4$, 5.0 μM $Ni(NH_4)_2(SO_4)_2$, 5.0 μM $CoSO_4$, 3.87 μM Na_2MoO_4, 1.5 μM Na_2SeO_4, 1.26 μM $MnSO_4$, 1.04 μM $ZnSO_4$, 0.2 μM $CuSO_4$, 20μg L-arginine HCl, 20 μg L-glutamine, 40μg DL-serine in milli-Q water. All the electron donor solutions were sterilised by passing through a 0.22 μm membrane. A Cr (VI) solution was prepared by dissolving potassium di-chromate in sterilized Milli-Q water and also filtering through 0.22 μm membrane before the experiments.

Before the aerobic reduction experiments, bacteria were cultured by transfer of a single colony grown aerobically in a Petri dish containing LB Agar to a 1L flask containing LB medium and incubated at 30 °C and 120 rpm overnight in a shaking incubator.

Cells for the anaerobic experiments were cultured in serum bottles containing degassed anaerobic growth medium and closed with thick blue butyl rubber stoppers and aluminium crimp seals. As with the aerobic culture studies, the medium was also inoculated by transfer of a single aerobically grown colony from a Petri dish containing LB Agar. The cultures were also placed in a shaking incubator at 30 °C and 120 rpm until they reached the desired cell density. Throughout the study, media were prepared using Milli-Q water ($\geq$ 18.2 ΩM cm). 0.22-μm-filtered ultra-high-purity N_2 gas was injected into the headspace of the bottle, used to flush the syringes prior to use, and injected into the culture bottle to compensate for subsequent sample withdrawal.

3.2.3 Cr reduction experiments

A series of experiments were performed to determine the rates of reduction of Cr(VI) to Cr(III), and the associated isotope fractionations by microbial action. In each experiment, dissolved Cr(VI) was combined with the microbial culture under different conditions, and the experiments run while Cr(VI) was reduced. The remaining Cr(VI) in solution was separated using anion exchange chromatography and the isotope composition was measured by thermal ionisation mass spectrometry (TIMS).

The experiments with different pH, electron donors, electron donor concentrations, and different species were conducted aerobically in 150 mL Erlenmeyer flasks. When cells reached the late exponential state, they were collected by centrifugation at 4100 rpm and 4 °C for 20 minutes. The cells were then washed 3-4 times using a 0.9 % sterile NaCl solution before adding to 50 mL of freshly made autoclaved minimal salts medium. The cell density was adjusted to 10^9 - 10^{10}/mL. For *Pseudomonas fluorescens* LB 300, glucose was the major electron donor employed in this study, except in the experiments with different electron donors, in which the effect of three other electron donors have also been investigated: citrate, acetate and propionate. For *Shewanella oneidensis* MR 1, sodium succinate was the principle electron donor. These electron donors have been widely used in many previous studies, and shown to efficiently mediate bacterial reduction [*Tekerlekopoulou et al.*, 2010; *Xu et al.*, 2011]. The pH of the media was adjusted using 1 M HCl or NaOH. The media were then incubated at set temperatures.

The impact of different electron donors were also investigated in the anaerobic experiments, in which the cells were first cultured in anaerobic growth medium and then transferred to the cell suspension medium. Throughout the study, 0.22-μm-filtered ultra-high-purity N_2 gas was also used to fill headspaces, flush the syringes prior to use, and injected to compensate for subsequent sample withdrawal.

At each time point, 1 mL of sample was taken and centrifuged at 9000 rpm at

4°C for 10 min. The supernatant was filtered (0.22 μm) to remove all cells, transferred to a clean Eppendorf tube and stored at -80°C before further treatment. The Cr(VI) and Cr(III) concentrations were measured by HPLC (Thermo scienctific^{TM} dionex^{TM} ICS−3000), using a Dionex IonPac CG5A (4 × 50mm) guard column, a Dionex IonPac CS5A (4 × 250 mm) column and a 375 μL reaction coil.

All experiments in this study were undertaken in triplicates.

3.2.4 Cr Isotope Analysis

The preparation method of samples for isotope composition determination largely followed that of *Ellis et al.* [2002]. A double-spike method was employed for correction of isotopic fractionation occurring during sample preparation and mass spectrometry. The double spike used is a mixture of ^{50}Cr and ^{54}Cr. Chromium isotope measurements were performed on a Thermo Finnigan Triton TIMS instrument. During the reduction experiments and the sample treatment period, it was assumed that no significant isotope exchange between Cr species occurred, as the equilibrium exchange reaction rates between Cr species were found to be very low in these conditions [*Wang et al.*, 2015]. The Data acquisition method used was modified from *Trinquier et al.* [2008].

3.3 Results

3.3.1 Biosorption and bioreduction

In order to determine the extent to which Cr(VI) was adsorbed onto cell surfaces, heat-killed cells were used as controls for each experiment. Less than 3% of the Cr (VI) was removed by the dead cells, indicating that observed reductions in Cr(VI) to Cr(III) were due to cellular activity (Fig. 3.1a).

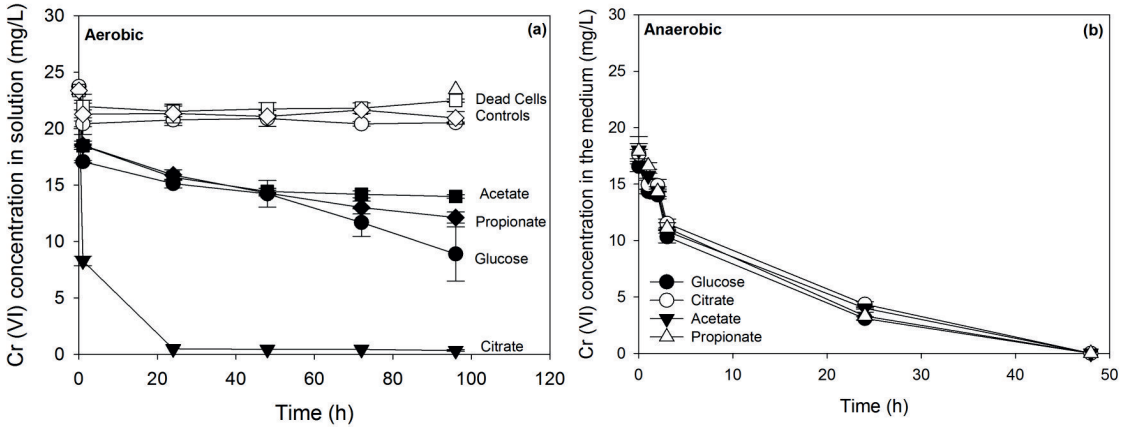


Figure 3.1: Chromium reduction experiments by *Pseudomonas fluorescens* LB 300 under aerobic conditions (a) and anaerobic conditions (b), using different compounds as electron donors. During aerobic reduction, the reduction rate was fastest with citrate as electron donor, and there were no significant differences for the other three donors (p>0.5). The reduction rates under anaerobic conditions were generally greater than that under aerobic conditions. There were no differences between different electron donors groups when the reduction occurred anaerobically (p>0.5). Uncertainties in the experiment were expressed as standard deviation between the triplicates in each experimental group. Controls were prepared with the same concentration of cells as in experimental groups, though the cells were thermally killed in controls. The dead cells controls in the anaerobic experiments were the same with that in the aerobic experiments.

3.3.2 Electron Donors and Respiration Pathways

The experiments with different electron donors were done with *Pseudomonas fluorescens* LB 300 (Fig. 3.1a) under both aerobic and anaerobic conditions. In the aerobic experiments, citrate promoted a significantly greater Cr reduction rate (15.1 mg·L^{-1}·hour^{-1}, p<0.01) compared to that of glucose (6.6 mg·L^{-1}·hour^{-1}), acetate (4.9 mg·L^{-1}·hour^{-1}) and propionate (4.8 mg·L^{-1}·hour^{-1}). However, under anaerobic conditions, reduction rates were not affected by the nature of the electron donors (Fig 3.1b). Generally, chromium reduction rates under anaerobic conditions were much greater, with over 70 % of chromium reduced within 24 hours (Fig. 3.1b), than that detected under aerobic conditions, where cultures took 72 hours to reduce approximately 50% of the chromium in the medium (Fig 3.1a).

In all experiments, δ^{53}Cr of the remaining Cr(VI) increased as the concentration

decreased; Cr(VI) became enriched in the heavier isotopes as microbial reduction proceeded (Fig. 3.2). In closed systems, such as experiments in this study, if the isotopic fractionation factor, α, is constant with time, and there is no subsequent isotope exchange between Cr(VI) and Cr(III), then the δ^{53}Cr value of the remaining Cr(VI) in the system evolves according to Rayleigh fractionation, which can be expressed as follows.

$$R_{Cr(VI)} = R^0_{Cr(VI)} f^{\alpha-1} \tag{3.4}$$

Where $R_{Cr(VI)}$ is the $\frac{^{53}Cr}{^{52}Cr}$ in the remaining Cr(VI); $R^0_{Cr(VI)}$ is the $\frac{^{53}Cr}{^{52}Cr}$ in the original Cr(VI) pool; α is the isotope fractionation factor; and f is the fraction of the Cr(VI) remaining after the reduction process.

By plotting values using a linearised equation, the best fit α values can be found by using linear regression [*Kitchen et al.*, 2012]. Uncertainties can be calculated as 2×standard errors of the best fit slopes. Our results are expressed in terms of ε (Eq. 3.3). For easy comparison, the δ^{53}Cr values were normalised to zero at the starting point of each experiment.

Under aerobic conditions, relatively small variations between fractionation factors were detected using different electron donors (Fig. 3.2a). The best-fit Rayleigh distillation relationship for the experiments with glucose, citrate, acetate and propionate yielded isotopic fractionation factors (ε) of -3.12±0.10 ‰, -4.32 ‰, -3.21±0.20 ‰ and -3.90±0.95 ‰, respectively. However, under anaerobic conditions, the variation in isotopic fractionation signatures as a result of using different electron donors was much more significant, despite the reduction rates being similar (Fig. 3.1b). The best-fit ε value was -4.96±0.37 ‰ for glucose, -4.77±0.45 ‰ for citrate, -3.24±0.17 ‰ for acetate, and -1.53±0.24 ‰ for propionate.

The extents of Cr reduction and the corresponding isotope fractionations under aerobic and anaerobic conditions are directly compared for each electron donor in Fig. 3.3. The best fit ε value for the combined aerobic and anaerobic rate is -4.71±0.38 ‰ for cultures with citrate (r^2 = 0.9875) and -3.26±0.13 ‰ for those

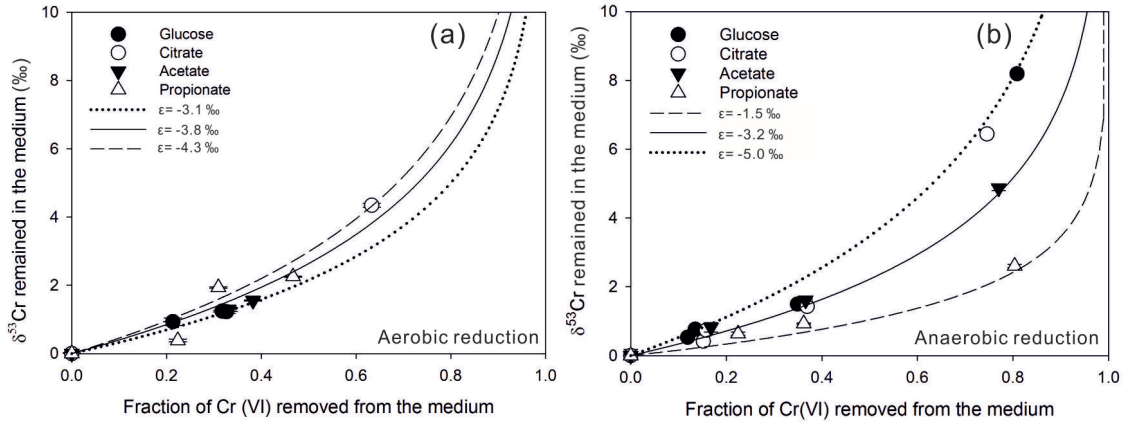


Figure 3.2: The impact of different electron donors on Cr isotope fractionation by *Pseudomonas fluorescens* LB 300. Under aerobic conditions, ε values for Rayleigh fractionation were ranging from -3.12 ‰ to -4.32 ‰, with the best fit value of 3.8 ‰ for all electron donors. Under anaerobic conditions, ε was -4.96, -4.77, -3.24 and -1.53 ‰ for experiments with glucose, citrate, acetate and propionate, respectively. Error bars are 2 × standard error for the measurement, which are generally smaller than the sizes of the icons.

with acetate ($r^2 = 0.9981$). However, greater differences were observed when glucose and propionate were the electron donors. With glucose, the isotopic fractionation factor increased from -3.12±0.10 ‰ under aerobic conditions to -4.96±0.37 ‰ (r^2 = 0.9607) under anaerobic conditions; when using propionate, it was much smaller under anaerobic (-1.53±0.24 ‰) than aerobic conditions (-3.90±0.95 ‰), which indicates that the respiration pathways can have a significant impact on microbial isotopic fractionation, and also that there are very different reduction mechanisms involving electron transfer processes.

Cr reduction with *Shewanella oneidensis* MR 1 was also examined. The anaerobic reduction rates of chromium were much faster for this species than under aerobic conditions, but much lower than that recorded for *Pseudomonas fluorescens* LB 300 (Fig. 3.4a). However, despite the significant difference in the reduction rates under aerobic and anaerobic conditions, the Cr isotope fractionations were very similar in all growth conditions examined for *Shewanella oneidensis* MR 1 (Fig 3.4b). Best fit Rayleigh distillation curves correspond to ε of -3.43±0.05 ‰ (r^2 = 0.99) under

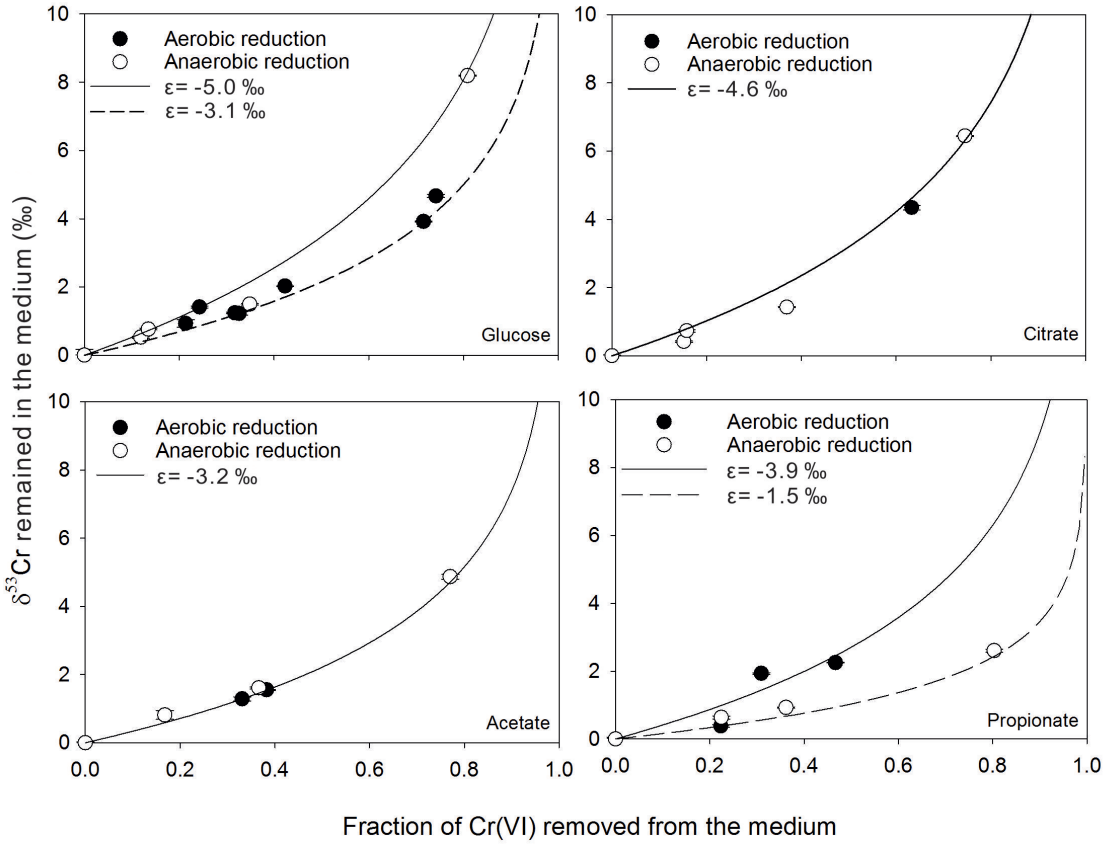


Figure 3.3: The impact of different respiration pathways on Cr isotope fractionation by *Pseudomonas fluorescens* LB 300. Data are the same as in Fig. 3.2. Rayleigh distillation curves corresponding to the fractionation factors were plotted here to compare the difference between aerobic and anaerobic reductions. A significant difference in the fractionation factor for aerobic and anaerobic reduction is found when glucose and propionate are the electron donor, but not acetate and citrate. Error bars are 2 × standard error for the measurement, which are generally smaller than the sizes of the icons.

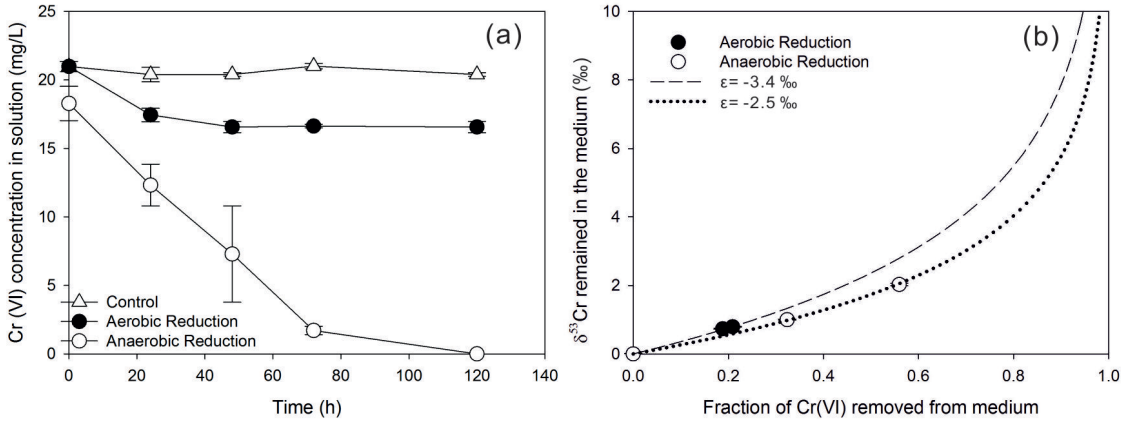


Figure 3.4: (a)Comparison of the aerobic and anaerobic reduction of Cr (VI) by *Shewanella oneidensis* MR 1, with sodium succinate as the electron donor. An autoclaved control was prepared under the same lab conditions with the same concentration of cells as in experimental groups, but the cells in the control group were thermally killed. Error bars are shown as the standard deviations between the triplicates in each experimental group. (b): Chromium isotope fractionation results from both aerobic and anaerobic reduction experiments with *Shewanella oneidensis* MR 1. Rayleigh distillation curves are shown corresponding to the fractionation factor ε = -3.4 for aerobic reduction and -2.5‰ for anaerobic reduction. Error bars are 2 × standard error for the measurement, which are generally smaller than the sizes of the icons.

aerobic, and -2.47±0.07 ‰ (r^2 = 0.99) under anaerobic, conditions. The best-fit value for both experiments together is -2.6 ‰ (r^2 = 0.98).

3.3.3 Electron Donor Concentration

During the 96 hours of incubation in this study, Cr reduction rates were fast within the first 48 hours and the fraction that has been reduced was higher in samples with greater glucose concentrations (Fig. 3.5a). There was little reduction in the experiments with no electron donor in the medium, indicating that Cr was not the sole energy source.

As bacterial Cr(VI) reduction proceeded with glucose as the electron donor, the δ^{53}Cr value increased to 4.67 ‰ (Fig. 3.5b). The best fit Rayleigh distillation curve corresponds to ε = -3.16±0.34 ‰ for all experiments in this study.

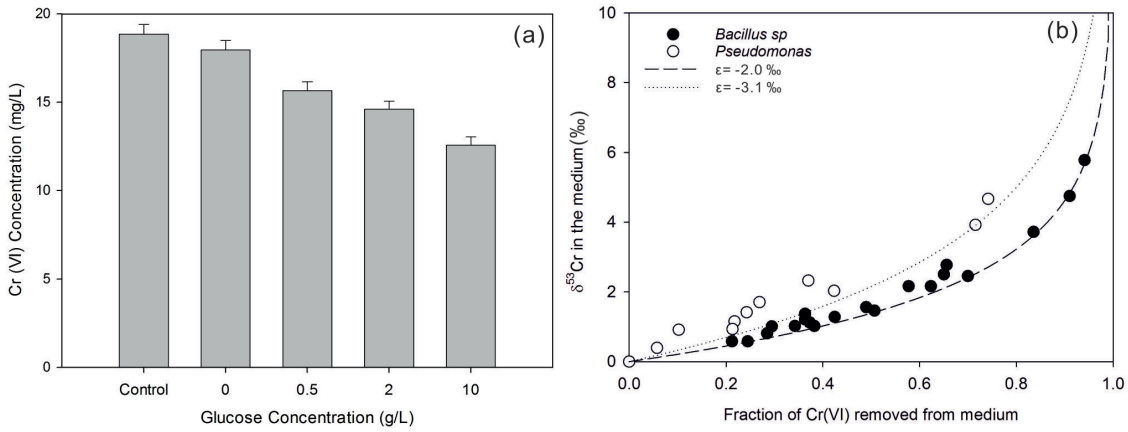


Figure 3.5: (a): 48 hour chromium reduction experiments with *Pseudomonas fluorescens* LB 300, and using different concentrations of the electron donor, glucose. The fraction of Cr(VI) reduced was larger in groups with higher concentrations of glucose. Uncertainties shown in the experiment are the standard deviations between the triplicates in each experimental group. Controls were prepared with the same concentration of cells, though dead. (b):The fraction of Cr(VI) that has been reduced to Cr(III) versus the isotope composition of the remaining Cr(VI). The fractionation factor ε = -3.1 ‰ for all 5 experiments in this study, and is -2‰ in the study with *Bacillus sp.*.

3.3.4 pH

In this study, the optimal pH for *Pseudomonas fluorescens* was investigated by examining the growth and Cr reduction rates under a range of pH (4,6 and 8). The pH range was determined by the growth conditions of the bacteria; within this range, the redox state of Cr was unchanged and chemically stable in the medium, as determined by measuring the Cr(VI) concentration in the control medium (without bacteria). The dominant Cr(VI) species at pH 4 are $HCrO_4^-$ [*Pourbaix*, 1974], the fractions of which decrease with the increase of pH, as the fractions of CrO_4^{2-} increase [*Trama and Benoit*, 1960; *Zink et al.*, 2010]. At pH 4 and 6, the bacterial Cr(VI) reduction rates were similar, whilst at pH 8, the reduction rate was much faster within the first 24 hours, and the fraction of reduced Cr(VI) was also much greater than in the other two groups.

Isotope data from the pH experiments are presented in Fig 3.6b. Under all

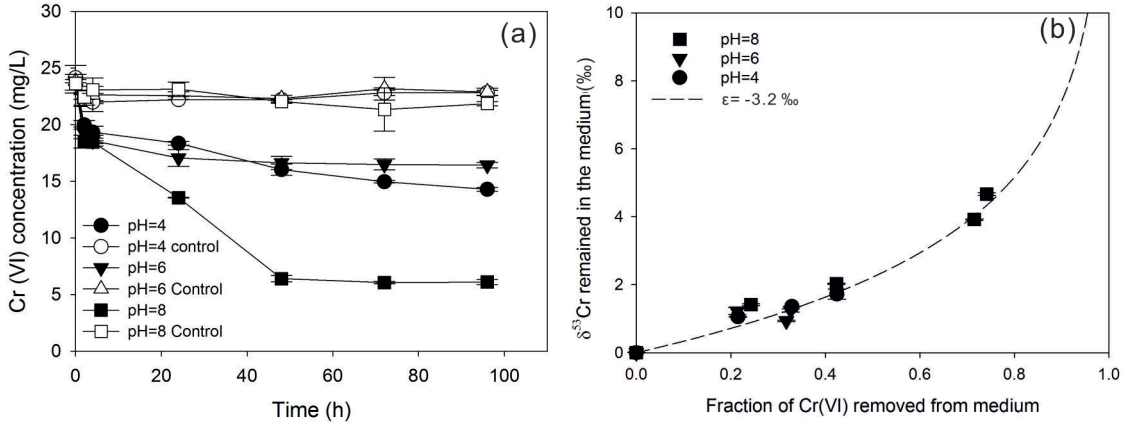


Figure 3.6: Chromium reduction experiments for *Pseudomonas fluorescens* LB 300 at different pH under aerobic conditions, with glucose as the electron donor. Controls were prepared with the same concentration of cells though thermally killed. Uncertainties are the standard deviation between the triplicates in each group. (a): Cr(VI) was reduced at all pH conditions, though reduction was much faster, and occurred to a much greater extent, at pH = 8. (b): The fraction of Cr(VI) reduced to Cr(III) versus the isotope composition of Cr of the remaining Cr(VI). A single Rayleigh distillation curve corresponding to the fractionation factor ε = -3.2‰ (dashed line) is plotted. Error bars are shown as 2 × standard error for the measurement, which are smaller than the sizes of the icons.

conditions, with the reduction of Cr(VI), the δ^{53}Cr value increased. There are no significant differences with respect to pH (ε = -3.21±0.18 under all pH conditions), and all data points from the three experiments fit on one Rayleigh distillation curve of the δ^{53}Cr value versus the fraction of Cr that has been removed. Although the reduction rate of chromium by *Pseudomonas fluorescens* LB 300 varied with pH, the isotope fractionation factor was consistent, indicating that pH and the speciation of Cr(VI) had little impact on chromium isotope fractionations generated by the bacteria, which also suggests that the reduction pathways of Cr(VI) were identical under different pH conditions.

3.4 Discussion

3.4.1 Electron Donors and Respiration Pathways

In our study, the nature of electron donors is found to be of great importance in affecting Cr reduction rates and isotope fractionation under both aerobic and anaerobic conditions. *Wang and Shen* [1995] have also conducted both aerobic and anaerobic reduction studies of chromium, employing the same bacteria (*Pseudomonas fluorescens* LB 300) and only glucose as the electron donor, and reported similar rates under aerobic conditions. However, unlike this study, they were unable to detect reduction of chromium by the bacteria under anaerobic conditions. The effect of electron donors on Cr reduction are also dependent on the bacterial species, reflecting different bacterial metabolic pathways of reduction. That is to say, the electron donor that is effective in catalysing Cr reduction by one bacteria may not be as useful for other bacterial species. For instance, *Xu et al.* [2011] investigated Cr (VI) reduction by *Pannonibacter phragmitetus* Lsse-09, and found different electron donors, such as lactate, acetate, formate, pyruvate, citrate and glucose, were responsible for different reduction rates, especially under aerobic conditions. Of the electron donors tested in their study, acetate resulted in the greatest reduction rate.

Electron donors are also found to be important for microbial reduction of other elements. For example, in a previous study, S isotope fractionation during sulphate reduction is found to be directly proportional to molecular hydrogen as electron donor and inversely proportional to reduction rate with lactate and ethanol as electron donors [*Kaplan and Rittenberg*, 1964]. However, far less is known of the extent that different electron donors impact Cr isotope fractionation. So far, the only data available, reported by *Sikora et al.* [2008], shows that, two different electron donors, formate and lactate, had little impact on anaerobic bacterial Cr isotope fractionation by *Shewanella oneidensis* MR-1. Compared with the control groups, where no elec-

tron donors were added, the reduction rates from those with low concentrations (less than 100 μM) of formate and lactate were almost the same or even lower than that in the control group, indicating that the bacteria may use their endogenous reserves [*Cheung and Gu*, 2007] as electron donors under all of these conditions. No isotope data from the control group has been reported to help investigate this hypothesis. The present study, for the first time shows that, in substantial concentrations, different electron donors result in different Cr isotope fractionations, especially under anaerobic conditions. The difference that electron donors induced, in terms of bacterial isotope fractionation, reflected the different reduction pathways. However, the underlying mechanisms remain uncertain. As multiple enzymes have been found to catalyse efficiently Cr(VI) reduction in microbial systems [*Michel et al.*, 2001, 2003], such as various types of C-cytochromes, [Fe]-hydrogenase and other metalloenzymes containing hemes or (Fe/S) centers, it is highly likely that multiple reduction pathways co-exist in the same bacteria each pathway may have a different kinetically induced fractionation factor, and the efficiencies of these pathways may be impacted by different electron donors.

In this study, the different isotopic fractionation factors generated by *Pseudomonas* (used the same electron donor) in the presence and absence of oxygen indicate that the respiration pathways can have a significant impact on microbial isotopic fractionation, and also that there are very different reduction mechanisms involving electron transfer processes. For aerobes, the reductase for Cr(VI) is associated with the cell membrane and can mediate the transfer of electrons from NADH to chromate [*Bopp and Ehrlich*, 1988]; the reductases in many other bacteria capable of reducing Cr(VI) are soluble in the cytosol [*Cheung and Gu*, 2007]. ChrR, one of the best studied reductases of *Pseudomonas putida*, functions as a 50-kDa dimer and demonstrates NADH-dependent reductase activity that protects against chromate toxicity. It transiently reduces Cr(VI) with a one-electron shuttle to form Cr(V), followed by a two electron transfer to generate Cr(III). YieF Cr(VI) reductase, a well

characterised protein extracted from *E.coli*, is similar to ChrR in terms of kinetic and physicochemical properties, but is unique in that it catalyzes the reduction of Cr(VI) to Cr(III) via a four-electron transfer in which three electrons are consumed in reducing Cr(VI) to Cr(III) and the other one is transferred to molecular oxygen, generating ROS. YieF is regarded as a more effective enzyme than ChrR in reducing Cr(VI). The production of these enzymes is an adaptive mechanism promoted by recent chromate exposure, and their reduction of Cr(VI) is through co-metabolism, which requires other substrates in addition to Cr(VI). The types of electron donors may impact the Cr(VI)-reducing enzymes produced, which then impacts the reduction pathway and isotope fractionation for Cr(VI). The reduction activities of anaerobes have been reported to be associated with electron transfer systems that catalyse the electron shuttle along the respiratory chains [*Cheung and Gu*, 2007]. In the absence of oxygen, Cr(VI) can serve as a terminal acceptor for many electron donors such as carbohydrates, proteins, fats, hydrogen, and even endogenous electron reserves. Under anaerobic conditions, it has been demonstrated that the cytochromes are responsible for the enzymatic reduction of different metals, such as Fe(III) and Cr(VI). Several types of c_3 cytochromes were found responsible for Cr(VI) reduction in bacteria [*Lovley*, 1995; *Michel et al.*, 2001, 2003; *Sundararajan et al.*, 2011].

These studies of enzymes provide evidence that the bacteria can use several different pathways to reduce Cr, dependent upon the environmental conditions and the electron donors, which in turn modify the isotopic fractionation factors as revealed in this study. This indicates that Cr isotope fractionation depends on electron donor and respiration pathways, so under well-controlled lab conditions, it can be clear indicator of reduction mechanisms. Based on this study, further research can be conducted towards mixed populations and environmental samples, to better characterise Cr isotope fractionation and transfer it to tools for use in the environment.

3.4.2 Electron Donor Concentration

The concentration and distribution of electron donors vary considerably in the environment, and this can have a significant impact on microbial metabolic rates, especially for aerobic bacteria [*Xu et al.*, 2011]. In this study, the concentration of glucose has great impact on bacterial Cr reduction rates but no significant impact on Cr isotope fractionation. *Xu et al.* [2015] also investigated the effect of glucose concentration on Cr reduction activity by *Bacillus sp.*(Black circles in Fig 3.5b) and also found its impact on isotope fractionation was insignificant, with a best fit ε value of 2.00±0.21 ‰. The different ε values determined in these two studies may be due to the difference in bacterial species investigated.

Sikora et al. [2008] reported that the concentration of lactate affected the isotopic fractionation factor during Cr reduction by *Shewanella oneidensis* MR-1. A greater fractionation factor was observed at lower electron concentration when the reduction rate was slower. However, in the present this study, such a relationship was not found under the experimental conditions employed. Previous studies have indicated that external electron donors have a much greater impact on microbial reduction rates during aerobic than anaerobic reduction [*Xu et al.*, 2011]. This is because under anaerobic conditions, some bacteria can use internally-stored reserves as electron donors, so even if there are no external electron donors, it is still possible to reduce Cr(VI). *Sikora et al.* [2008] study was undertaken under anaerobic conditions, and great Cr reduction rates were also found in their control groups (no electron donors), indicating *Shewanella oneidensis* MR-1 can get electrons from the endogenous reserves to catalyse the reduction of Cr. Thus the different fractionation factors reported between low and high lactate concentrations might reflect reduction pathways that utilized different electron donors.

3.4.3 pH

pH is known to be a significant factor governing the chemical state of chromium [*Zink et al.*, 2010]. It is also a critical factor in determining the optimum conditions for bacterial growth and metabolism (i.e. bacteria have their preferential pH conditions for growth).

In this study, both the reduction rate and the fraction of reduced Cr(VI) was much greater at pH 8 than at pH 4 or 6. Similar trends were also observed by *Wang and Shen* [1995] for both *Pseudomonas fluorescens* and *Bacillus sp.*. The different reduction rates determined at different pH may be due to Cr toxicity. Cr(VI) is able to penetrate cellular membranes and induce oxidative stress that damages cell membranes and DNA-protein complexes, and alters the physiological functions of bacteria and other biota [*Xu et al.*, 2004, 2005]. Many previous studies regarding Cr(VI) have confirmed that a decrease in the pH resulted in increased toxicity of Cr(VI) to various species, such as earthworms [*Sivakumar and Subbhuraam*, 2005], common carp [*Stouthart et al.*, 1995] and rainbow trout [*Van Der Putte et al.*, 1981]. To explain these observations, it has been suggested that the level of acute Cr(VI) toxicity is attributable to the speciation of Cr, where $HCrO_4^-$ is much more toxic than CrO_4^{2-}, because a) monovalent ions tend to be more readily taken up by the cells than divalent ions, and b)$HCrO_4^-$ is more oxidizing and reactive than CrO_4^{2-} [*Trama and Benoit*, 1960; *Van Der Putte et al.*, 1981]. Since the dominant species of Cr(VI) changes with pH, it may be either that the bacterial Cr(VI) reduction activity is impacted by the levels of toxicity of the different species, or that the bioavailability of the different Cr(VI) species are different under those pH conditions.

Importantly, the consistent isotope fractionation factor found at all different pH suggests that pH and the speciation of Cr(VI) had little impact on bacterial chromium isotope fractionations, which also indicates that the reduction pathways of Cr(VI) were identical under different pH conditions.

3.4.4 Bacterial species

Several genera of bacteria have been reported to have the ability to reduce chromium, but there have been few studies focused on comparing Cr isotopic fractionation associated with the reduction process by different species, as reported here in Fig. 3.7.

Basu et al. [2014] studied several Cr(VI) reducing bacteria, and found that the Cr isotope fractionation factor ε was -3.03 for *G. sulfurreducens*, -2.17‰ for *Shewanella. sp*, -3.14‰ for *P.stutzeri* and -3.01‰ for *D. vulgaris*, respectively. In our study, the fractionation factor for *Pseudomonas fluorescens* LB 300 fell in the range of -1.5 to - 5 ‰ and was -2.5‰ for *Shewanella oneidensis* MR 1. *Sikora et al.* [2008] also studied *Shewanella oneidensis* MR 1, the same strain reported here, but the fractionation factor found is different in these the two studies. *Sikora et al.* [2008] used formate and lactate as the electron donors. The fractionation factor was -4.3 when the electron donor concentration was low and -1.8 when it was high. In this study, sodium succinate was used as the electron donor and the fractionation factor was -2.5 ‰. The difference in the chromium isotopic fractionation may be due to the different electron donors employed, which further proves that the importance of different electron donors in catalysing Cr isotope fractionations.

Han et al. [2012] also investigated Cr isotope fractionation by an aquifer-derived bacterium *Pseudomonas stutzeri* RCH2 under denitrifying conditions and found the Cr(VI) was reduced at a very high rate (about 75% within 2 hours). The data presented in their study revealed a small δ^{53}Cr value range and considerable variance, suggesting additional processes were affecting Cr reduction and isotope fractionation in that study.

Overall, after analysing all the data available, the chromium isotope fractionation factors resulting from bacterial reduction are found to lie in quite a narrow range. A best fit for all the data yields a value of about -3.3‰ (Fig. 3.7; ex-

cluding the *Han et al.* [2012] data). Some abiotic Cr(VI) adsorption and reduction data are also plotted in Fig. 3.7. The fractionation factors due to adsorption processes are quite distinct from those due to reduction. The fractionation factors due to abiotic reduction processes are quite variable depending on the reductants and experimental conditions, and overlap with the ε range from bacterial reduction processes. Although variable, the ε range is still small enough to help effectively quantify reduction processes.

3.5 Conclusion

The isotope fractionation factors ε of chromium by microbial reduction range from -1.53 to -4.96 ‰, with a mean value at -3.3 ‰. Changes in pH and substrate concentration had little significant impact on the fractionation factors under the experimental conditions employed. However, different electron donors and bacterial respiration pathways had significant effects on microbial metabolism, thus affecting chromium isotope fractionation. It has been generally assumed that lower cell specific reduction rates would result in higher fractionation factors [*Basu et al.*, 2014; *Habicht and Canfield*, 1997; *Sikora et al.*, 2008]; however, it was not always the case in this study. Different reduction pathways, which affect the rates of reduction, may be responsible for the observed differences in the fractionation factors. Since the range of values for ε for different species and conditions is relatively small, a mean value can be used for interpreting Cr isotope variations in more complex natural environment. Nonetheless, the clearly resolved isotopic variations determined by high-precision mass spectrometry can be utilised to probe biological processes, by clearly distinguishing biological pathways. This is a significant finding since it suggests that isotope signatures can be used as a powerful diagnostic tool for microbial activities under a range of environmental conditions. Our study contributes to the understanding of Cr isotope behaviour and the role of bacteria in different

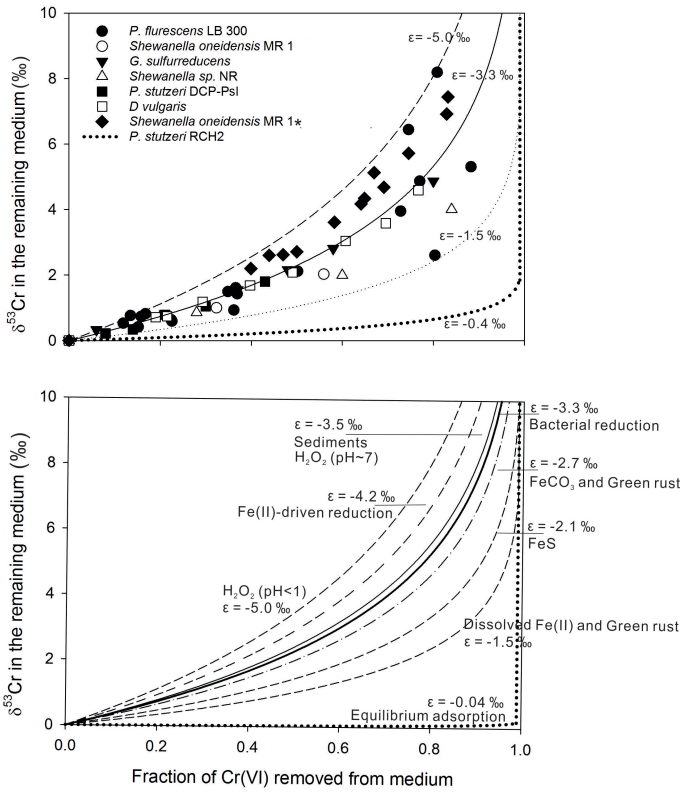


Figure 3.7: Upper panel: Isotope results from anaerobic reduction experiment with different species of bacteria. Zero point normalization for each study was made to remove the difference in initial δ^{53}Cr of the standards. The black and white circles represent *Pseudomonas fluorescens* LB 300 and *Shewanella oneidensis* MR 1 from this study. Data for *G. sulfurreducens*, *Shewanella. sp*, *P.stutzeri* and *D. vulgaris* were from *Basu et al.* [2014] The black diamonds represent the data from *Sikora et al.* [2008], also for *Shewanella oneidensis* MR 1. Black dots represent the data from *Han et al.* [2012] (ε = -0.4 ‰. Rayleigh distillation model was applied for all species. A Rayleigh distillation fractionation factor ε = -2 ‰ fits the data for *Shewanella. sp*, while ε = -4.3 fits that for the *Sikora et al.* [2008] data for *Shewanella oneidensis* MR 1. The isotope data from our study and *Basu et al.* [2014] study fall on a single Rayleigh distillation model with best fit ε = -2.8 ‰ (r^2=0.98). The best fit ε for all data points in this figure was -3.3 ‰ (solid line, r^2= 0.86). Lower panel: Rayleigh distillation curves corresponding to fractionation factors from various abiotic Cr(VI) reduction experiments. All the data fall between ε = -1.5 ‰ and -5 ‰. Data on bacterial reduction is from this study, with FeS, $FeCO_3$, and Green rust are from *Basu and Johnson* [2012], with dissolved Fe(II) and Green rust is from *Dossing et al.* [2011], with H_2O_2 and Fe(II)-driven reduction is from *Kitchen et al.* [2012], with natural sediments are from *Ellis et al.* [2002] and *Basu and Johnson* [2012], and will equilibrium adsorption is from *Ellis et al.* [2004]

.

environments. Our study confirms the potential of Cr isotopic fractionation as an environmental diagnostic tool for assessing Cr cycling patterns in nature and also for monitoring the bio-remediation of chromium contaminated sites.

Chapter 4

Cr isotope fractionation during metal-mineral-microbe interactions

4.1 Introduction

Chromium occurs naturally in aqueous environment by weathering and leaching of rocks, and can originate from industrial anthropogenic sources, such as stainless steel production and engine corrosion prevention. Cr(VI) and Cr(III) are the most common and stable species of chromium in the natural environment. Cr(VI) is very reactive and has high solubility, while Cr(III) is less reactive and less soluble in water [*Garcia et al.*, 1994]. When the redox conditions of the surrounding environment changes, Cr species may be converted accordingly, and such conversion can be studied by using Cr isotopes. Cr has 4 stable isotopes. The lighter isotopes are known to be enriched in the products during redox reactions, because they are more reactive than the heavier ones [*Ellis et al.*, 2002]. Therefore, when Cr(VI) in solution is reduced to less soluble and less reactive Cr(III), it is removed from the solution, leaving behind Cr(VI) in solution with a heavier isotope composition.

The extent of fractionation is usually measured by the fractionation factor, and different processes may have different fractionation factors. Therefore, the extent of fractionation provides information on what process was involved.

Chromium isotope data are usually reported as relative deviations from a standard reference material (for instance, NIST SRM 979) in parts per thousand (per mil or ‰):

$$\delta^{53}Cr = [\frac{(^{53}Cr/^{52}Cr)_{sample}}{(^{53}Cr/^{52}Cr)_{standard}} - 1] \times 1000‰ \tag{4.1}$$

Elevated δ^{53}Cr values of Cr(VI) provide evidence for Cr(VI) reduction and therefore can be employed to indicate the extent of Cr(VI) reduction [*Ellis et al.*, 2002], which is particularly useful in monitoring the reduction processes in anthropogenic contaminant plumes [*Berna et al.*, 2010]. The oxidation conditions in the environment may impact Cr oxidation states and isotope composition in different Cr species, therefore, Cr isotope composition in the sedimentary deposits may reflect atmospheric oxygen levels in the past, which also makes it an useful indicator of paleo-environment [*Frei and Polat*, 2013; *Frei et al.*, 2013]. However, to improve the exploitation Cr isotope signatures as a diagnostic tool of reduction processes in different environments, the relationship between environmental conditions and Cr isotope fractionation factors are very important, but has not been well characterised.

Both biotic and abiotic reduction are important in controlling the behaviour of Cr in the environment. Abiotic reduction occurs both in the aqueous phase and on mineral surfaces. For example, *Zink et al.* [2010] reported Cr reduction by hydrogen peroxide in aqueous media under highly acidic and circum neutral conditions, with fractionation factors lying between -3.5 ‰ and -5.0 ‰, respectively. *Basu and Johnson* [2012] conducted Cr reduction experiments with a range of different minerals, and have reported fractionation factors ranging from -2.11 to -3.91 ‰. In addition to redox reactions, adsorption may also be considered an important process in inducing chromium isotope fractionation. *Ellis et al.* [2004] investigated the

effects of sorption during transport of Cr(VI) and found that stable isotope fractionation caused by kinetic adsorption processes is significant; however, equilibrium fractionation of Cr stable isotopes is negligible.

In all the abiotic reactants with Cr, Fe is very important. It is very common in the environment and is the most abundant trace element in marine and terrestrial organisms. Of all redox states of iron, both Fe(II) and Fe(III) can be thermodynamically stable under specific environments. When Fe(III) is reduced to Fe(II), it has the electrochemical potential to reduce Cr(VI) to Cr(III). Although unstable in oxic environments, aqueous Fe(II) commonly occurs in aquifers and other reducing waters. In the ancient oceans prior to the Great Oxidation event, Fe(II) was the most abundant iron species in aqueous environments, therefore, understanding its influence on Cr(VI) reduction is very important for interpreting Cr isotope data obtained in paleo-redox studies. Previous studies were focused on Cr - Fe interactions and the influence this has on isotope fractionation. Reactions in both aqueous phase and on solids have been studied, eg. *Dossing et al.* [2011] reported ε of -3.0 to - 4.4 ‰ for reduction by aqueous Fe(II) at circum-neutral pH, and -1.5 ‰ when simultaneously reduced by dissolved Fe(II) and Fe(II)+Fe(III) green rust. *Kitchen et al.* [2012] also conducted Cr(VI) reduction experiments with aqueous Fe(II) and found ε to be -4.2 ‰ at a pH values ranging between 4 and 5.3. *Basu and Johnson* [2012] conducted Cr(VI) reduction experiments using Fe(II)-doped goethite, FeS, green rust, siderite and reduced sediments from a permeable reactive barrier; the fractionation factors ranged between -2.11 to -3.91 ‰.

Other than isotope data from Cr abiotic reactions, there are also some data available on Cr isotope fractionation by microbes. Changes in isotope fractionations due to microbial activity provide valuable insight into the mechanisms of metal cycling, and can be used to quantify biogeochemically-mediated redox processes [*Basu et al.*, 2014; *Han et al.*, 2012; *Sikora et al.*, 2008]. *Sikora et al.* [2008] were the first to investigate the impact of microbial reduction on Cr isotope fractionation by

Shewanella oneidensis MR 1 and found that the isotope fractionation factor ranged from 4.0 to 4.5 ‰ when reduction rates were low and were 1.8 ‰ when higher. *Han et al.* [2012] investigated ε during reduction by *Pseudomonas stutzeri* RCH2 under both aerobic and denitrifying conditions, and reported it to be 2 ‰ under aerobic, and 0.4 ‰ under denitrifying, conditions. *Basu et al.* [2014] examined chromium reduction by a metabolically diverse group of bacteria, and suggested that stronger isotopic fractionation was induced during Cr(VI) reduction under electron-donor-poor conditions. In our previous work, we investigated microbial Cr(VI) reduction under various environmental conditions, and found that the types of electron donors utilised and bacterial respiration pathways have a significant impact on microbial Cr isotope fractionation [*Zhang et al.*, 2016].

Previous studies on Cr isotopes are either focused on pure abiotic reactions, such as Cr reduction by different minerals, or only on biological reactions, such as reduction by suspended bacteria. Seldom study has considered combined metal-mineral-microbe interactions, which are very important in the heterogeneous and near surface environment [*Chorover et al.*, 2007; *Sparks*, 2005]. Microbial processes can be significantly influenced by the presence of minerals, including nutrient acquisition, cell adhesion, biofilm formation and energy generation [*Brown et al.*, 2008; *Hochella*, 2002]. Environmental contaminants, such as metals, may also be adsorbed onto mineral surfaces, and can then be transformed by microbial activity [*Chorover et al.*, 2007; *Gadd*, 2010; *Huang et al.*, 2004; *Kraemer et al.*, 1999]. Moreover, mineral surfaces may have different physico-chemical properties depending on the aqueous environment, including micro-topography, surface composition, surface charge, and hydrophobicity, which may also affect the biology of microbes. The properties of minerals play an important role in microbial attachment, which are critical in affecting colonization, biofilm formation, and microbial metabolic processes [*Brown et al.*, 2008; *Gadd*, 2010; *Vaughan et al.*, 2002].

Cr isotope signatures may be very useful when study metal-mineral-microbe in-

teractions. For example, *Stewart et al.* [2007] studied microbial-mediated chromate reduction in alkaline soil water systems which has iron mineral presented, and discovered that the percentage of Fe(II) increased when nearly all the chromate had been reduced. Although it was suggested that Cr(VI) reduction was mediated by direct enzymatic processes, it is also possible that the reduction of Cr(VI) was caused by Fe(II) produced from microbially mediated iron reduction, because many bacteria capable of reducing Cr(VI) are also Fe reducers. These different processes can be investigated by measuring Cr isotope fractionation, because Cr isotope fractionation factor generated by Fe(II) reduction and enzymatic reduction may be different.

While essential, there is limited information available on the impact of the presence of minerals, particularly Fe minerals, on bacterial Cr reduction activity and the consequent isotope fractionation.

The present study attempts to fill this gap by conducting bacterial Cr(VI) reduction experiments in the presence of different forms of Fe, including aqueous Fe(II), aqueous Fe(III), and two iron minerals, goethite and hematite. The main objective of this study is to determine the impact of these different minerals and aqueous Fe species on bacterial Cr reduction activity and the correspondent isotope fractionation factors generated, in order to better understand Cr behaviour during metal-mineral-microbe interactions and better characterise Cr isotope signatures as an environmental diagnostic tool.

4.2 Materials and Methods

4.2.1 Bacteria

The facultative anaerobes *Shewanella oneidensis* MR-1 (MR-1) and *Pseudomonas fluorescens* LB 300 (LB 300), which are common and representative in the environment, were selected for this study. *Shewanella oneidensis* MR-1 (MR-1) was purchased from NCIMB Ltd (NCIMB 14063) and *Pseudomonas fluorescens* LB 300

(LB 300) was kindly provided by Prof. Yi-Tin Wang at the department of Civil Engineering, University of Kentucky [*Wang and Shen*, 1995].

4.2.2 Cr reduction experiments

Anaerobic studies were conducted to determine the impacts of aqueous iron and iron minerals on the rate of reduction of Cr(VI) to Cr(III), and on the associated isotope fractionation by microbial action. In each experiment, dissolved Cr(VI) was combined with a microbial culture along with some form of Fe (Table 4.1), and aliquots of the medium were periodically removed and analysed while Cr(VI) was being actively reduced. Adsorption of Cr(VI) on bottles, cells and minerals were negligible [*Ellis et al.*, 2004; *Zhang et al.*, 2016]. Adsorption of Cr(III) on bottles and cells were also negligible [*Zhang et al.*, 2016], but the adsorption on minerals were not investigated. However, since isotope exchange between Cr(VI) and Cr(III) species are demonstrated to be insignificant under experimental conditions in this study [*Wang et al.*, 2015], the adsorption of Cr(III) does not have any impact on our data. The remaining Cr(VI) in solution was separated using ion exchange chromatography and the isotope fractionation was determined.

The anaerobic growth medium and cell suspension medium used was largely as described by *Myers and Nealson* [1988]. The composition of the growth media is as follows: 9.0 mM $(NH_4)_2SO_4$, 5.7 mM K_2HPO_4, 3.3 mM KH_2PO_4, 2.0 mM $NaHCO_3$, 1.01 mM $MgSO_4$, $CaCl_2$, 67.2 μM Na_2EDTA, 56.6 μM H_3BO_3, 10.0 μM NaCl, 5.4 μM $FeSO_4$, 5.0 μM $Ni(NH_4)_2(SO_4)_2$, 5.0 μM $CoSO_4$, 3.87 μM Na_2MoO_4, 1.5 μM Na_2SeO_4, 1.26 μM $MnSO_4$, 1.04 μM $ZnSO_4$, 0.2 μM $CuSO_4$, 20μg L-arginine HCl, 20 μg L-glutamine, and 40μg DL-serine in milli-Q water. The cell suspension medium contained 1.9 mM K_2HPO_4, 2.5 mM KH_2PO_4, 1 mM $MgCl_2$ and 32 mM NaCl. With sodium succinate applied as the source of carbon.

Cells were cultured in large serum bottles containing degassed anaerobic growth medium and sealed with thick butyl rubber stoppers and aluminum crimp seals.

The medium was inoculated by transferring a single aerobically-grown colony. The cultures were placed in a shaking incubator at 30 °C and 120 rpm until a desired cell density was reached. All media were prepared using Milli-Q water ($\geq$ 18.2 ΩM cm). Ultra-high-purity N_2 gas (0.22 μm filtered) was used to fill headspaces, flush syringes prior to use, and inject into culture bottles to compensate for subsequent sample aliquot withdrawals.

Several forms of Fe were investigated, including aqueous Fe(III), aqueous Fe(II), goethite, and hematite. Goethite is an iron(III) oxyhydroxide (FeO(OH)), and hematite is an iron(III) oxide (Fe_2O_3). Both of goethite and hematite are common in the environment and in some studies have been shown to be bioavailble by bacteria such as *Shewanella oneidensis* [*Lower et al.*, 2001], *Geobacter sulfurreducens* [*Wu et al.*, 2009], *Shewanella putrefaciens* CN32[*Liu et al.*, 2001], and *Shewanella alga* BrY [*Roden and Zachara*, 1996], although this has been challenged by other studies [*Cutting et al.*, 2009], which shows that in crystalline form of iron is not available and only amorphous coating or nanoscale granular substrates can be bioreduced. Nonetheless it is feasible that their presence in the environment, particularly where amorphous coating are likely to be present, may significantly impact on Cr reduction process both biotically and abiotically. Prior to the experiments, both goethite and hematite were cleaned in an ultrasonic bath (with 18.2 ΩM cm water) for 30 mins and dried at 40 °C until of constant weight. Both minerals have been characterised by using an X-ray Diffraction (XRD) instrument and a Raman microspectroscopy.

The Cr(VI) reduction experiments were all conducted in triplicate to account for the variability in microbial systems. In the experiments, the cell cultures were washed with 0.9% degassed sterile NaCl solution and transferred to 100 mL serum bottles containing degassed cell suspension medium, closed with thick blue butyl rubber stoppers and aluminum crimp seals. The cell density was adjusted to 10^9 - 10^{10} / mL. Then 20 mg/L Cr(VI), aqueous $FeCl_3$ solution, $FeCl_2$ solution, goethite and hematite were also added into the media, respectively, depending on the exper-

iments (Table 4.1).

At each time point, aliquots were taken from each sample, filtered sterile (0.22 μm), transferred to a clean Eppendorf tube, and stored at -80 °C before further treatment. The Cr(VI) and Cr(III) concentrations were measured simultaneously by HPLC (Thermo Scienctific^{TM} Dionex^{TM} ICS−3000).

A parallel experiment was done to analyse the role of Fe in this study. The experiments were done at the same conditions under which the Cr reduction experiments were undertaken. Minimal salts medium (1.9 mM K_2HPO_4, 2.5 mM KH_2PO_4, 1 mM $MgCl_2$ and 32 mM NaCl) was used, with sodium succinate (2.43 g/L) as the electron donor. The cell numbers were counted at the beginning of the experiments (3×10^9 cells/mL for Pseudomonas, and 2×10^9 cells/mL for Shewanella in experiment with goethite; 5×10^{10} cells/mL for Pseudomonas, and 4×10^{10} cells/mL for Shewanella in the experiments with hematite). During the experiment, due to the presence of minerals in the medium, it was difficult to determine the cell numbers by either optical density measurement or plate counting, but assuming growth was similar to previous experiments, the cell number would not have significantly changed during the period of the Cr reduction experiments. Therefore, it is assumed that the cell number remained at approximately the same level throughout the experiments (around 10^9 cells/mL in experiments with goethite and 10^{10} cells/mL in experiments with hematite). These numbers are used when normalising Fe(III) reduction rates to cell specific values. Throughout the study, the generation of Fe(II) was monitored by using ferrozine as described previously [*Carter*, 1971].

4.2.3 Cr isotope analysis

The preparation method of samples for isotope composition determination essentially employed the procedure reported by *Ellis et al.* [2002]; *Zhang et al.* [2016]. A double spike method was used to correct for isotopic fractionation during sample preparation and mass spectrometry. The double spike was enriched in ^{50}Cr and

^{54}Cr. Chromium isotope measurements were performed on a Thermo Finnigan Triton Thermal Ionization Mass Spectrometer (TIMS). The Data acquisition routine is modified from that of *Trinquier et al.* [2008]. The long-term instrumental reproducibility was determined by measuring a spiked Cr standard and the δ^{53}Cr value is 0±0.049 ‰.

4.2.4 Characterization of bacteria-mineral interaction by SEM

To gain a better understanding of the metal-microbe-mineral interactions in this study, the bacterial cells were imaged using a JEOL JSM-6390 Scanning Eletron Microscope (SEM), after 24 hours of incubation with Fe minerals and 20 mg/L Cr(VI). The samples from each experimental group were primarily fixed by using 2.5 % glutaraldehyde in a 0.1 M phosphate buffer at pH 7.2 - 7.4 and incubated at room temperature for 1 hour [*Gluenz et al.*, 2015]. They were then washed several times with phosphate buffer and fixed with 1 % OsO_4 buffer at 4 °C. After being washed several times with Milli-Q water, the samples were dehydrated with different concentrations of EtOH under ambient conditions and then dried using HMDS (Hexamethyldisilazane). Finally, they were mounted on carbon adhesive tape on SEM stubs and coated with gold before being examined by SEM at 10 kV.

4.3 Results

All experimental results are tabulated in the Appendix.

4.3.1 Fe minerals

Raman spectroscopy patterns of the two minerals are presented in Fig. 4.1, with the distinguishing Raman shifts (wavenumbers) labelled in bold numbers. The goethite spectra show both strong and weak bands at ∼248, ∼303, ∼391, ∼483, and ∼551 cm^{-1}, with the band at 303 and 391 cm^{-1} being the strongest. These values are in

good agreement with previously published values of ∼247, ∼300, ∼385, ∼482, and ∼550 cm^{-1} [*Das and Hendry*, 2011; *de Faria et al.*, 1997; *Hanesch*, 2009; *Legodi and de Waal*, 2007; *Oh et al.*, 1998; *Thibeau et al.*, 1978]. The hematite spectra show strong bands at ∼226, ∼300, and ∼410 cm^{-1}, and other weak bands at ∼248, ∼503, and ∼616 cm^{-1}. These measured values correspond to previously published values where well-resolved hematite bands were noted at ∼225, ∼245, ∼300, ∼412, ∼500, and ∼612 [*Das and Hendry*, 2011; *de Faria et al.*, 1997; *Hanesch*, 2009; *Legodi and de Waal*, 2007; *Oh et al.*, 1998; *Thibeau et al.*, 1978]. The strongest band at ∼666 cm^{-1} was not observed in previous studies. This band may be due to the contamination of other minerals, such as magnetite and calcium sulphate, for which a band at ∼667 was reported [*Antunes et al.*, 2014; *Das and Hendry*, 2011; *de Faria et al.*, 1997; *Hanesch*, 2009; *Legodi and de Waal*, 2007; *Oh et al.*, 1998; *Thibeau et al.*, 1978].

XRD patterns of the minerals are presented in Fig. 4.2, and were compared to standards database and published literature values. Hematite was characterised by peaks at 2θ of ∼25°, ∼39°, and ∼42° [*Das and Hendry*, 2011]. Other than hematite, small amount of anhydrous calcium sulphate was also detected. Goethite was characterised by peaks at 2θ of ∼18°, ∼21°, and ∼26° [*Das and Hendry*, 2011]. Small amount of bassanite was also detected in the goethite sample. Magnetite has not been detected by the XRD, so the band at 666 in Raman spectrums may be due to calcium sulphate.

To investigate the effects of goethite and hematite on microbial Cr reduction, the rates of Cr(VI) reduction are plotted in Figure 4.4. To compensate for the variability of the microbial system, every experiment in the study has been performed with side-by-side triplicate runs, and all concentration data reported here are the average values for each group, with uncertainties given as the standard deviation on the three values. The control group (with no Fe) contained only the minimal salts medium with bacteria and 20mg/L Cr(VI). During the experiment, the dissolved Cr(VI)

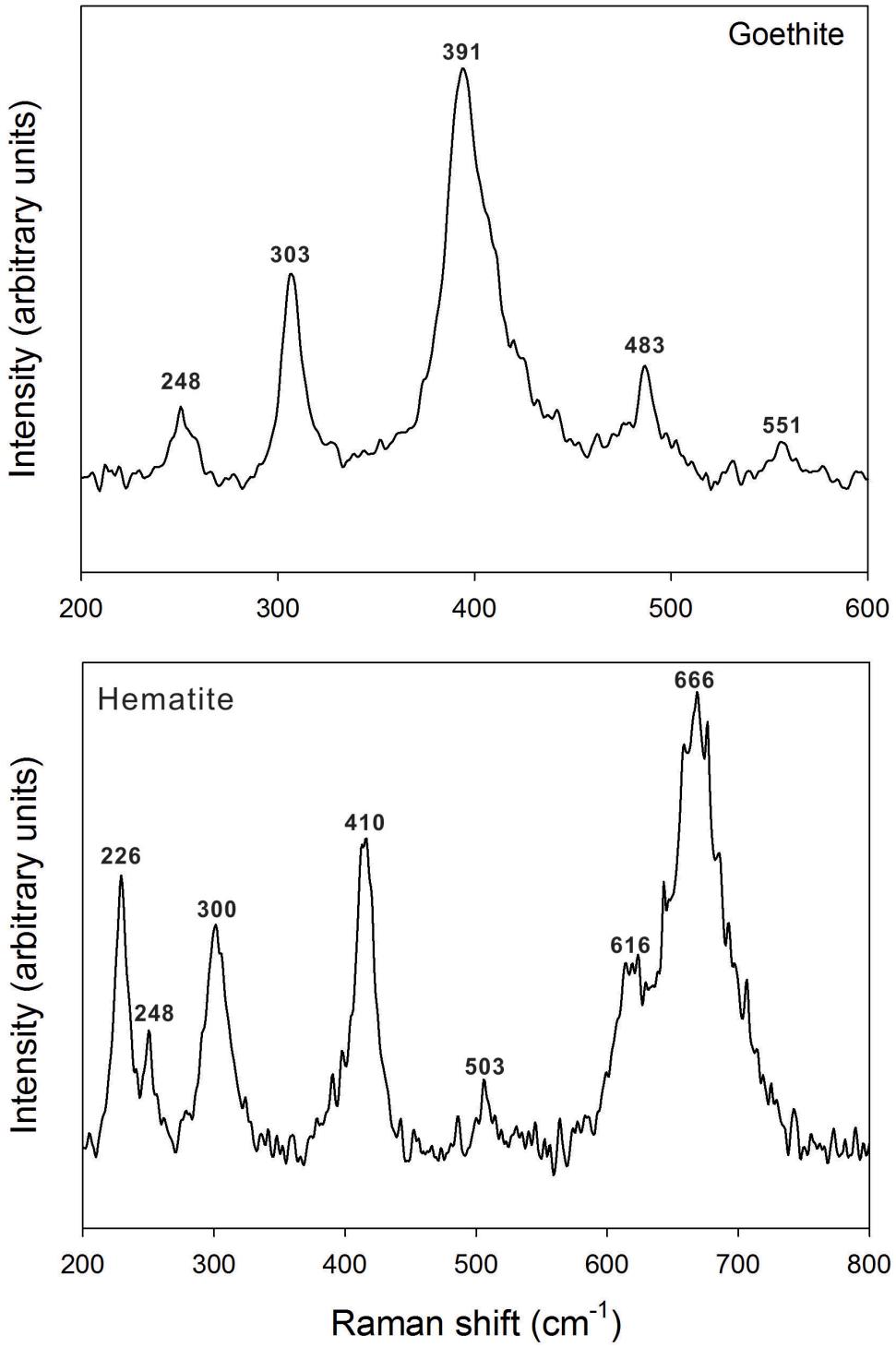


Figure 4.1: Raman spectra of the minerals phases used in this study.

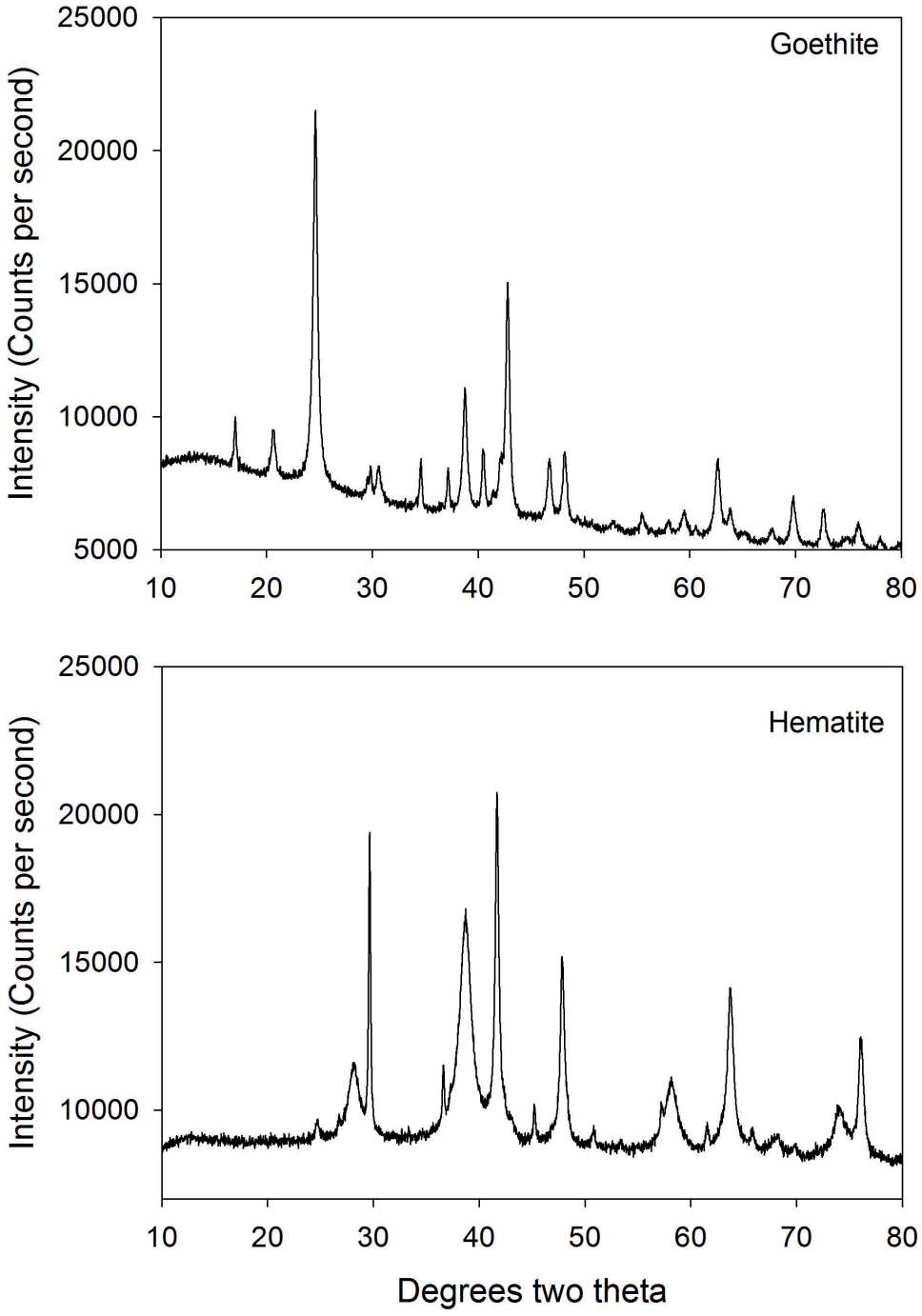


Figure 4.2: XRD spectrum of the minerals used in this study.

concentration progressively decreased in all experiments. Compared to the control group, the presence of either goethite or hematite inhibited the reduction of Cr(VI) by *Pseudomonas*, with the reduction rates in the groups with minerals much lower than those without any minerals. The control group reduced 80% of the Cr(VI) in the medium in the first 4 hours, whereas the groups with minerals present reduced only 50%.

Cell specific reduction rate is Cr(VI) reduction rate over cell numbers. In this study, cell numbers were controlled to be constant in each group, and were monitored by measuring optical density at the beginning and end of the experiments. The data from the Cr(VI) reduction experiments appear to have a constant rate for each group, and follow exponential decay, with the average Cr(VI) half-life for each group shown in Table 4.1. Cell specific reduction rates for each group are also shown in Table 4.1.

In contrast to the experiments with *Pseudomonas*, with *Shewanella*, the minerals greatly promoted bacterial Cr(VI) reduction activity. It took more than 72 hours to reduce 20 mg/L Cr(VI) in the control group (No Fe), whilst in the groups with minerals, all the Cr(VI) was reduced within 24 hours. The calculated cellular reduction rates were one magnitude greater when minerals were in the medium, and the Cr(VI) half-life for the experiments with minerals were much shorter (Table 4.1). Of the two minerals that were used in this study, goethite promoted a more significant increase in the reduction rate of Cr(VI).

Throughout the Cr(VI) reduction experiments, no Fe(II) was detected by the ferrozine assay for both bacteria and minerals when Cr(VI) is in presence in the solution (Fig.4.3). In the control experiments with only minerals in the medium (no Cr), Fe(II) was generated in the presence of the bacteria with both hematite and goethite (Fig. 4.3). It has to be noted that Fe (II) was detected from *Pseudomonas* after 15 days in the experiments with hematite, and 28 days in the experiments with goethite (due to the sampling frequency, no sampling has been done between 96

Table 4.1: Cell specific reduction rates and isotopic fractionation factors

Experiments	**Cell specific reduction rate** (10^{-10}mg·h^{-1}·Cell^{-1})	ε (‰)	**Half-life** (Hours)
P. fluorescens			
No Fe	4.62±0.08	-2.56±0.51	1.65
Aqueous Fe(III)	5.64±0.09	-3.00±0.82	1.57
Goethite	3.70±0.59	-2.96±0.19	3.43
Hematite	1.64±0.07	-4.26±0.71	4.66
Aqueous Fe(II)	2.94±0.02	-3.39±1.99	1.05
Goethite and Fe(II)	2.70±0.00	-3.24±0.39	0.68
Hematite and Fe(II)	1.71±0.56	-3.29±0.28	0.88
S. oneidensis			
No Fe	0.29 ± 0.07	-2.47 ± 0.07	30.34
Aqueous Fe(III)	0.30 ± 0.02	-2.34 ± 0.07	54.09
Goethite	2.59 ± 0.95	-2.13 ± 0.41	1.78
Hematite	1.65 ± 1.12	-2.27 ± 0.29	2.59

All experiments were done in triplicates.

Errors for cell-specific reduction rates are shown as standard deviations between the triplicates.

ε: Isotope fractionation factor. Errors are calculated based on least-squares fitting method.

All isotope analysis consist of measurement of 800 isotope ratios.

hours and 28 days in goethite experiments). Assuming the Fe(II) was generated by live cells, Fe(III) reduction rates by *Pseudomonas* ($1.8\pm1\times10^{-13}$ mg Fe(II)/hour/cell for goethite and $1.5\pm0.2\times10^{-14}$ mg Fe(II)/hour/cell for hematite) were found to be much slower than those by *Shewanella* ($9.2\pm5.4\times10^{-12}$ mg Fe(II)/hour/cell for goethite and $2.0\pm0.1\times10^{-12}$ mg Fe(II)/hour/cell for hematite). It cannot be distinguished here whether the observed Fe(II) was generated by living cells of *Pseudomonas*, or by reductants released from the dead cells.

The isotope compositions of dissolved Cr(VI) throughout the experiments are plotted in Figure 4.5. Significant isotopic fractionation associated with microbial Cr(VI) removal was observed in every experiment, with or without Fe-bearing minerals in the medium. The δ^{53}Cr values of the remaining Cr(VI) increased progressively from the initial δ^{53}Cr (0 ± 0.11‰) as the reaction advanced (Fig. 4.5).

In this study, Cr (VI) reduction experiments were performed in a well-mixed, closed environment. If the isotopic fractionation factor α is consistent over time under these conditions, the δ^{53}Cr value of the remaining Cr(VI) in the system evolves according to a Rayleigh relationship, which can be expressed as:

$$R_{Cr(VI)} = R^0_{Cr(VI)} f^{\alpha-1} \tag{4.2}$$

where $R_{Cr(VI)}$ is the $^{53}Cr/^{52}Cr$ ratio of the remaining Cr(VI), and $R^0_{Cr(VI)} = {}^{53}Cr/^{52}Cr$ is that of the original Cr(VI) pool, α is the isotope fractionation factor, where $\alpha = (^{53}\mathrm{Cr}/^{52}\mathrm{Cr})_{Cr(III)}/(^{53}\mathrm{Cr}/^{52}\mathrm{Cr})_{Cr(VI)}$, and f is the fraction of the Cr(VI) remaining after reduction.

The best-fit for α values can be found by plotting a linearised version of the equation of Eq.4.2 by linear regression [*Kitchen et al.*, 2012]. These are shown in the Appendix. Uncertainties were calculated as 2×standard errors on the best-fit slopes. The results are expressed as ε

$$\varepsilon = (\alpha - 1) \times 1000‰ \tag{4.3}$$

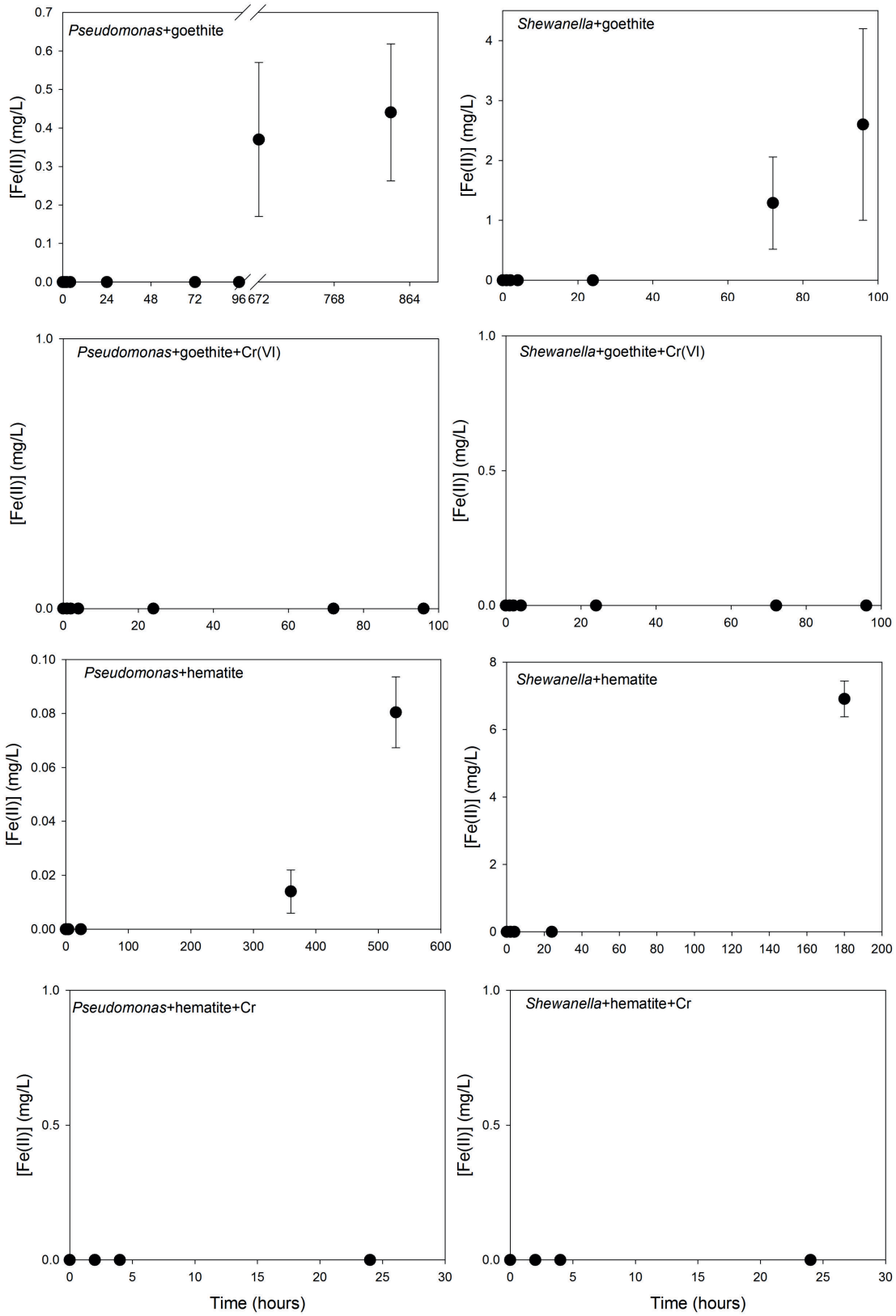


Figure 4.3: Both *Pseudomonas fluorescens* LB 300 and *Shewanella oneidensis* MR 1 are found to be able to reduce goethite and hematite. In the precence of Cr(VI), no Fe(II) was detected to be generated by either bacteria.

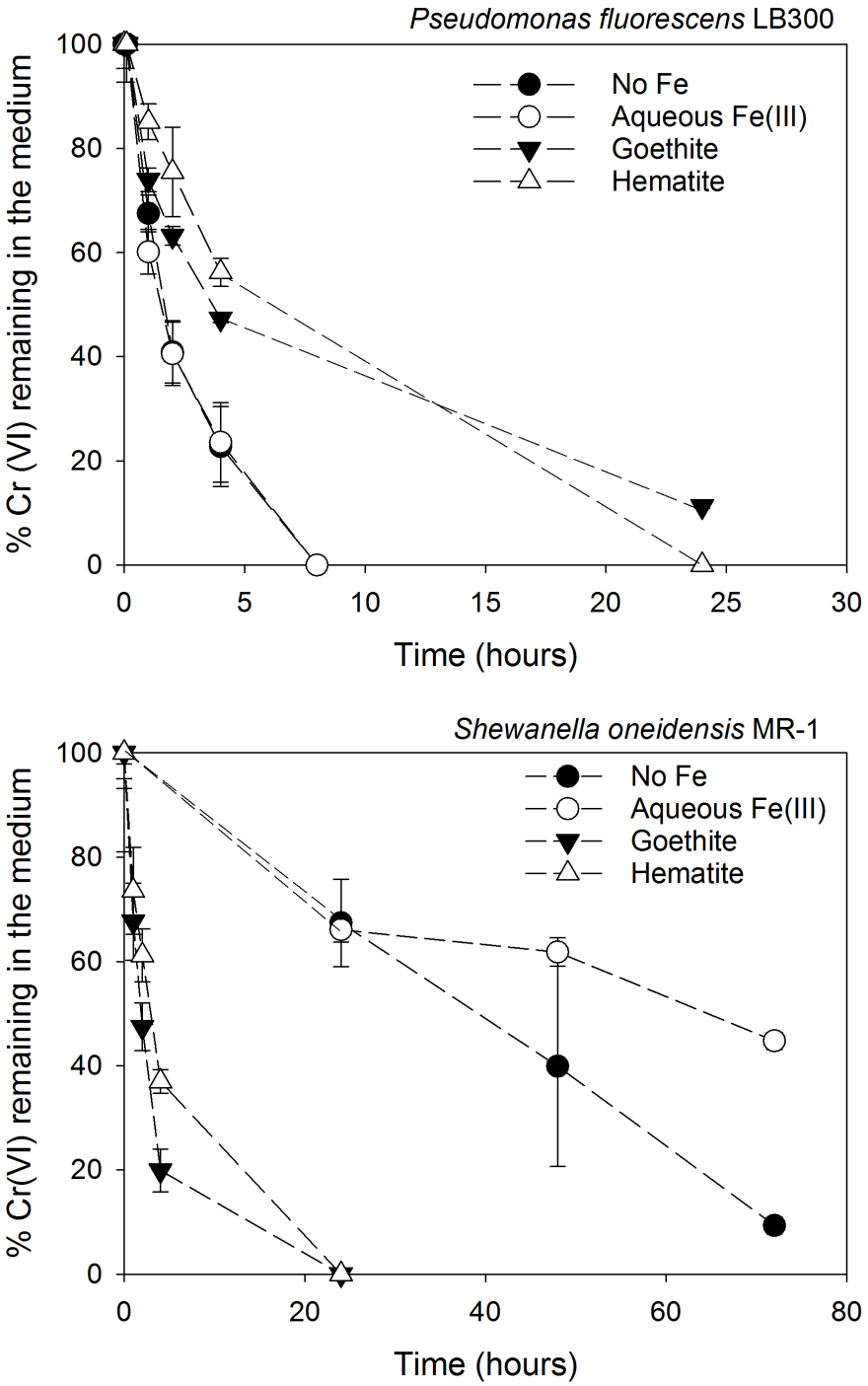


Figure 4.4: Microbial chromium reduction experiments with *Pseudomonas fluorescens* LB 300 (upper panel) and *Shewanella oneidensis* MR 1 (lower panel), in the presence of aqueous Fe(III) or iron minerals. Uncertainties are shown as standard deviations between the triplicates in each group. Note difference in x-axis scale between the two panels.

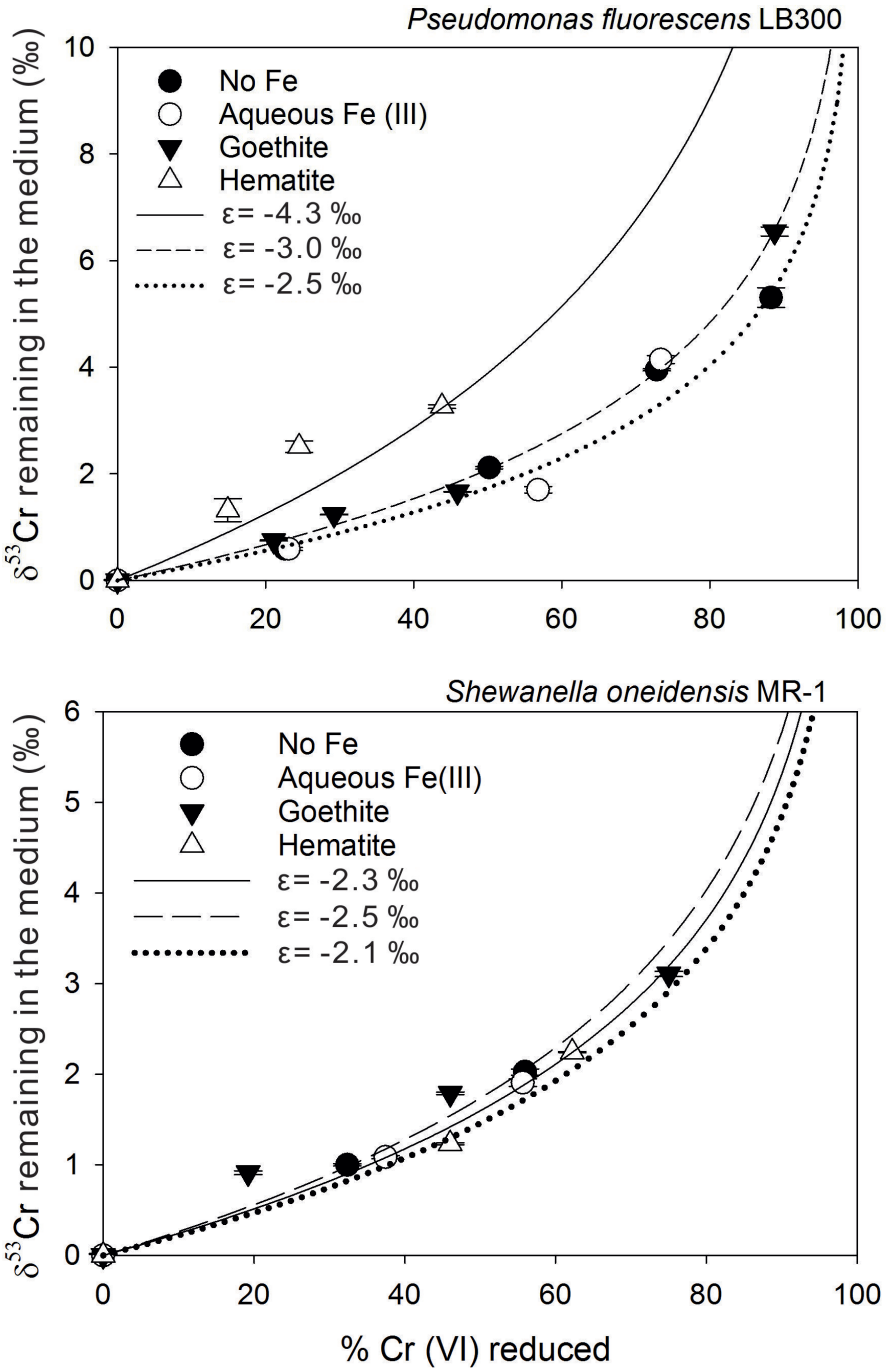


Figure 4.5: Observed isotopic fractionations during microbial Cr(VI) reduction experiments using *Pseudomonas fluorescens* LB 300 (upper panel) and *Shewanella oneidensis* MR 1 (lower panel). Uncertainties were shown at 2 × of standard deviations of the isotope measurement.

.

In most cases, ε is very close to the difference in δ^{53}Cr between the Cr(VI) reactant and the reaction product Cr(III) flux in per mil, so that:

$$\varepsilon \approx \delta_{react} - \delta_{prod} \tag{4.4}$$

.

For *Pseudomonas*, there was no significant difference between the control group and the group with goethite. The fractionation factors, determined by fitting Rayleigh distillation curves to the data (Eq. 4.2), were -2.56±0.51 and -2.96±0.19 ‰ for the two groups, respectively, indicating that the presence of goethite did not have a significantly detectable impact on chromium isotope behaviour. The group with hematite had a greater fractionation factor (-4.26 ‰).

For *Shewanella*, the isotopic fractionation factor was -2.47±0.07 ‰ for the samples without iron , and was -2.13±0.41 and -2.27±0.29 ‰ for those with goethite and hematite, respectively. This shows that the presence of these two minerals did not have a noticeable effect on the microbial chromium isotope fractionation and had little influence on microbial Cr reduction pathways.

4.3.2 Aqueous Fe(III)

In this study, a titration experiment has been done that $FeCl_3$ was added into minimal salts medium containing succinate. No precipitation was observed in the experiment when Fe concentration was up to 10 mM/L. In this study, the initial Fe(III) concentration was 1 mM/L. In the reduction experiment with *Pseudomonas*, the presence of aqueous Fe(III) in the medium has no detectable impact on the reduction process (Fig. 4.4). The reduction rate was similar in the experiment without Fe(III); both were very fast (Table 4.1), with all the chromium being reduced within the first 8 hours. The decrease in Cr(VI) concentration with time in both

control and aqueous Fe(III) groups fit a model of first-order reaction with similar average Cr(VI) half-lives (Table 4.1). In the study with *Shewanella*, there was also no significant difference ($p > 0.05$) between the control group (no iron) and the group with aqueous Fe(III).

The Cr isotope data for *Pseudomonas* and *Shewanella* are both shown in Fig. 4.5. The best-fit fractionation factor for *Pseudomonas* is -3.00±0.82 ‰, and -2.34±0.07 ‰ for *Shewanella* with aqueous Fe(III) in the medium; both of these are essentially indistinguishable from that in the control groups. Overall, this indicates that soluble Fe(III) has little effect on chromium isotope fractionation by bacteria.

4.3.3 Fe(II)

To investigate further the influence of iron, experiments added with aqueous Fe(II) were conducted (Fig. 4.6). Two distinct processes have been observed: a rapid initial loss followed by a more slowly reduction. The reduction rate was found to be extremely fast in all of the groups with added Fe(II); about 65 % of Cr(VI) was reduced in the first minute. After this initial rapid loss, the rest of the Cr(VI) was gradually reduced by the bacteria (*Pseudomonas*) in the following 4 hours. The reduction process in the second process fits a first-order decay model, with a much shorter Cr(VI) half-life (Table. 4.1). There were no significant differences ($p > 0.05$) in the bacterial reduction rates in samples having only aqueous Fe(II) and those with Fe(II) and Fe(III) minerals (Fig. 4.6, Table 4.1).

The Cr isotope data are presented in Fig. 4.6 for all experiments that involved Fe(II). After the quick initial loss, subsequent reduction of chromium was due to microbial activity, and Cr isotope fractionation factors were much higher. The best-fit ε value for microbial reduction (the second slope) was about -3.3 ‰ in all groups with Fe(II) (considering the point of initial loss as the start of microbial reduction, solid line in Fig. 4.6), regardless of whether there were any minerals in the system. The presence of iron minerals or aqueous iron species in the environment

does not appear to significantly affect the magnitude of microbial Cr(VI) isotope fractionation.

4.3.4 SEM Analysis

Selected images are shown in Fig. 4.7. Suspended cells of *Pseudomonas* and *Shewanella* in the two control groups, without minerals and Cr(VI), are illustrated in Figs. 4.7A and 4.7B, respectively. *Pseudomonas* revealed rough surfaces and possessed multiple polar flagella, aiding the motility of the cells [*O'Toole and Kolter*, 1998a,b]. The flagella are also found to be essential for bacteria to reach and adhere on abiotic surfaces [*O'Toole and Kolter*, 1998a,b]. *Pseudomonas* is about 1 to 2 μm in size, and is smaller than *Shewanella*, which is about 2 to 3 μm. The cell surfaces of *Shewanella* were much smoother compared to *Pseudomonas*. Furthermore, some nanowires produced by *Shewanella*, which have been reported to be conductive and able to transfer electrons extracellularly [*Pirbadian et al.*, 2014], are also observed in this study and presented in Fig. 4.7B and Fig. 4.8(white arrows).

Figs. 4.7C and 4.7E show the attachment of *Pseudomonas* onto goethite and hematite surfaces after the experiments. With both minerals, it was very clear that the bacteria produced many flagella and extracellular polymeric substances (EPS), that helped the cells adhere to the grain surfaces and to each other. The attached cells formed several layers on the mineral surfaces.

The interaction of *Shewanella oneidensis* MR 1 with the two minerals is shown in Figs. 4.7D (with goethite) and 4.7F (with hematite). The species is known to form biofilms under various conditions [*Thormann et al.*, 2004]; however, compared with *Pseudomonas*, the attachment of *Shewanella* on the mineral surfaces were much looser. This bacteria were found to produce very thin nanowires in this study, but no EPS was observed.

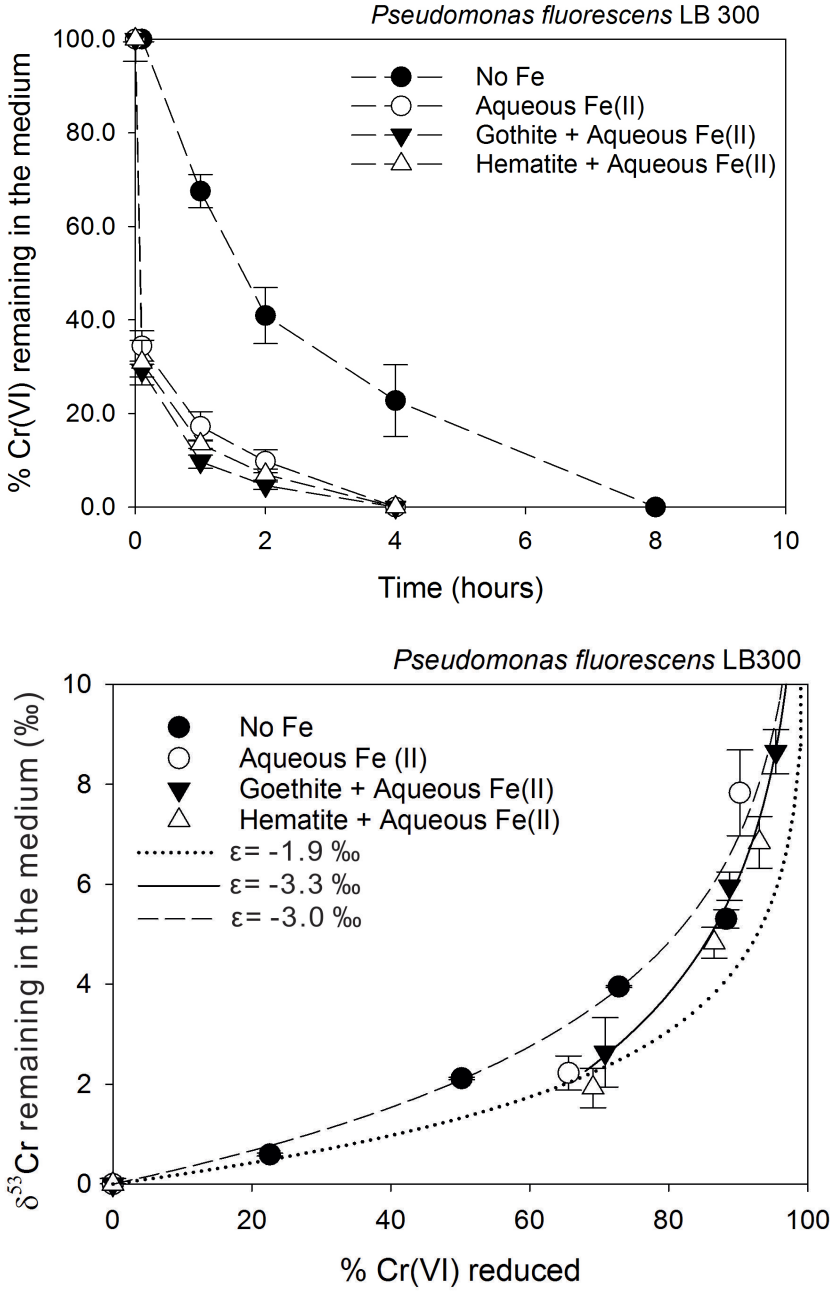


Figure 4.6: Upper panel: The impact of aqueous Fe(II) on Cr(VI) reduction in experiments using *Pseudomonas fluorescens* LB 300, with different iron minerals in the system. Lower panel: Corresponding δ^{53}Cr vs. Cr(VI) reduced during the experiments. Cr reduction and isotope fractionation in the experiments with Fe(II) involve a two-step process; the initial loss of Cr is from abiotic reduction by aqueous Fe(II), and the following reduction is caused by bacteria. The dotted-line shows the Rayleigh distillation curve for abiotic Cr isotope fractionation by aqueous Fe(II), and the solid line represents that for microbial Cr isotope fractionation (considering the point of initial loss as the start of microbial reduction). Note the difference in x-axis scale between the two panels

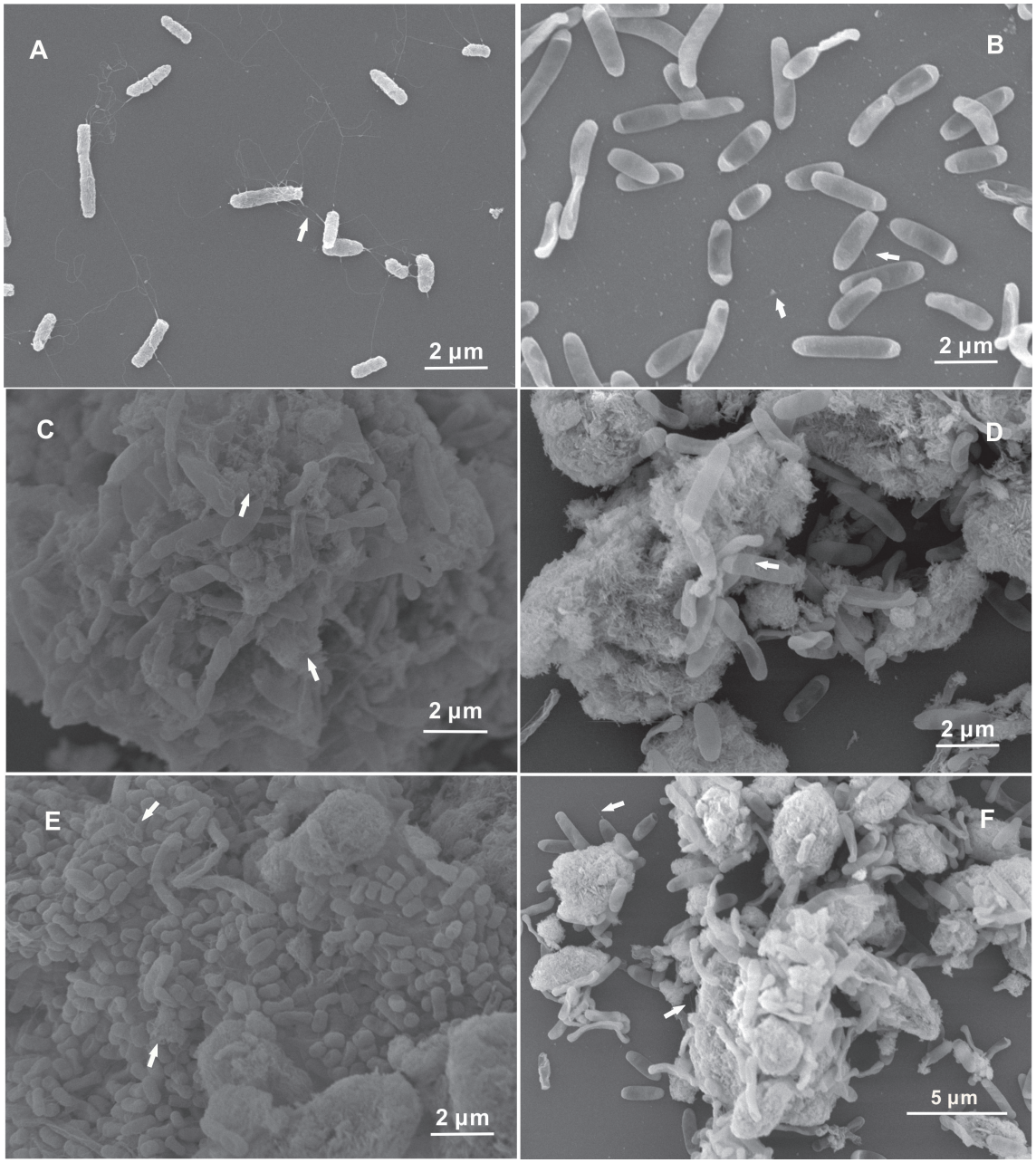


Figure 4.7: SEM images. A: Suspended cells of *Pseudomonas fluorescens* LB 300, with multiple flagella aiding their mobility (White arrows). B: Suspended cells of *Shewanella oneidensis* MR 1. The cells were flat and have thick polars. The cells produced nanowires to help electron transfer (white arrows). C: The attached cells of *Pseudomonas fluorescens* LB 300 on goethite surfaces. The flagella produced and EPS helped the attachment of the cells to the abiotic surfaces and also to each other (white arrows). D: The cells of *Shewanella oneidensis* MR 1 attached on goethite surfaces. No EPS was observed, but the cells produced some nanowires (white arrows). E: The cells of *Pseudomonas fluorescens* LB 300 attached on hematite surfaces. The flagella produced and EPS helped the attachment of the cells onto the abiotic surfaces and also to each other (white arrows). The cells attached closely and formed several layers of biofilm. F: The loosely attached cells of *Shewanella oneidensis* MR 1 on hematite surfaces. No EPS was observed, but the cells produced some nanowires (white arrows).

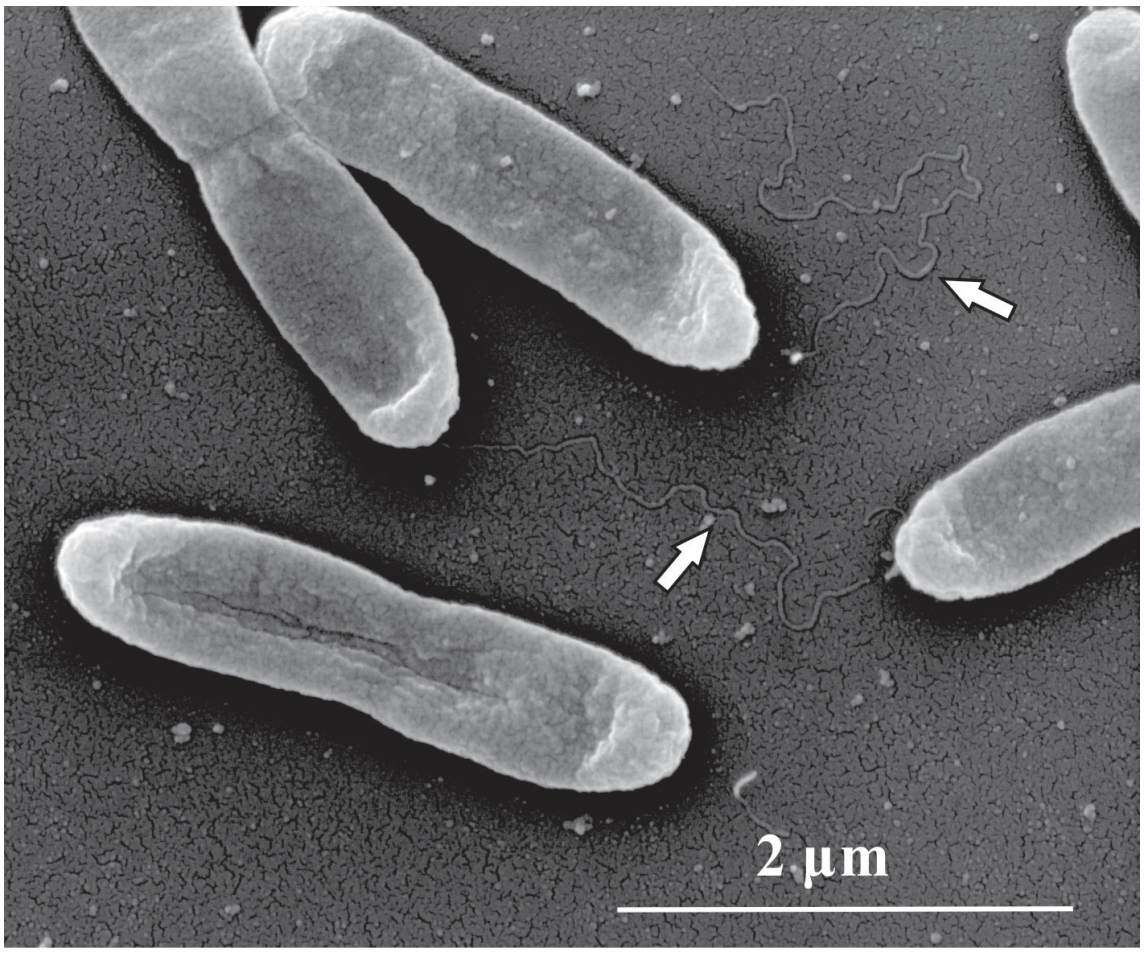


Figure 4.8: SEM images of *Shewanella oneidensis* MR 1. The cells were flat and have thick polars. The cells produced nanowires to help electron transfer (white arrows) [*El-Naggar et al.*, 2010; *Gorby et al.*, 2006; *Pirbadian et al.*, 2014].

4.4 Discussion

4.4.1 Is biogenic Fe(II) contributing to Cr(VI) reduction?

In this study, we observed very different effects of iron oxides on microbial Cr reduction rates by the two different bacteria: the presence of minerals largely increased the reduction rates by *Shewanella* but significantly slowed down the rates by *Pseudomonas*. There are several possibilities for explaining these observations that can be considered. It is possible that, when Cr(VI) and Fe(III) are both present in the system, the bacteria reduce Fe(III) first, generating Fe(II), which then reduces Cr(VI) abiotically. In the reduction experiments with both an Fe(III)-bearing mineral and Cr(VI) in solution, no Fe(II) was detected by the Ferrozine assay throughout the experimental period. However, Fe(II) may still have been generated by the bacteria; it may be possible that the biogenic Fe(II) was quickly re-oxidised by Cr(VI), and so was an electron shuttle in the system. In this case, the rates of Cr(VI) reduction depend on the rates of Fe(II) generated by the bacteria.

For *Pseudomonas fluorescens*, it is not clear whether the observed Fe(III) reduction was due to the living cells or reductant from the dead cells. It is possible that this bacteria cannot reduce either goethite or hematite, therefore, no biogenic Fe(II) had any contribution to Cr reduction in this study. Even if the bacteria can reduce both minerals, the rates were extremely slow in this study: $1.8\pm1\times10^{-13}$ mg/L Fe(II)/hour/cell for goethite, and $1.5\pm0.2\times10^{-14}$ mg/L Fe(II)/hour/cell for hematite. With about 10^{10} cells in each of the experiments, about 2×10^{-3} mg/L Fe(II) can be generated by *Pseudomonas fluorescens* per hour from goethite, and about 1.5×10^{-4} mg/L Fe(II) from hematite. Even if we assume that the reaction of Fe(II) reducing Cr(VI) is extremely fast, which has been suggested in previous studies [*Buerge and Hug*, 1999; *Kitchen et al.*, 2012], with such a low rate to generate Fe(II), the Cr(VI) reduction should have taken at least 20000 hours in the

experiments with goethite, and even longer in the experiments with hematite. In the experimental period of 24 hours, a maximum amount of 0.048 mg/L of Fe(II) can be generated to reduce about 0.15 mg/L Cr(VI), which is less than 0.1% of the total Cr(VI) reduced. Therefore, even though there are considerable uncertainties in the values used, the reduction of Cr(VI) by bacterially reduced is several orders of magnitude lower than the rate of Cr(VI) observed, and so is still unlikely to be the main reductant for Cr(VI) in this study.

For *Shewanella oneidensis* MR-1, a known iron-reducer, similar calculations can be made. The bacteria generate Fe(II) at a rate of $\pm 5.4 \times 10^{-12}$ mg/L/hour/cell for goethite, and $2.0 \pm 0.1 \times 10^{-12}$ mg/L/hour/cell for hematite in this study. The bacteria (10^{10} cells) can generate 0.1 mg/L Fe(II) from goethite per hour, and 0.02 mg/L Fe(II) from hematite. In the experimental period of 24 hours, Shewanella oneidensis can generate 2.4 mg/L Fe(II) from goethite and 0.48 mg/L Fe(II) from hematite. At such rates, only less than 5% of Cr(VI) may be reduced by the biogenic Fe(II). However, since the uncertainties in the number of cells, and so in the total Fe(III) reduction rates may be large, the biogenic Fe(II) could have made a substantial contribution to Cr(VI) reduction. Here Cr isotope data provides some insight. If the bacteria reduced Fe(III) first, generating Fe(II), which then reduced Cr(VI), the isotope fractionation factor should be close to -1.5 ‰ [*Dossing et al.*, 2011], which was determined in abiotic Cr(VI) reduction experiments with Fe(II) at pH conditions close to those in this study. If Cr(VI) reduction was due to bacterial activity, then the isotope fractionation factors measured in the presence of minerals should be -2.470.07‰, as shown in Table 4.1. In this study, the results are consistent with a Cr isotope fractionation factor of -2.13 0.41‰ in the presence of goethite, and -2.270.29‰ in the presence of hematite. These values are indistinguishable from the value from bacterial Cr isotope fractionation factor, and so it is possible that Cr(VI) reduction was completely due to bacterial activity. However, considering the uncertainties in the isotope data, it is also possible that biogenic Fe(II) had

some contribution to Cr(VI) reduction. In the presence of mineral phases, Cr(VI) reduction rates were an order of magnitude larger than that in the absence of minerals, and such an increase in reduction by an order of magnitude can clearly not be explained by abiotic Cr(VI) reduction given the isotope constraints. Therefore, another mechanism may also have a substantial contribution to accelerate Cr(VI) reduction rates by *Shewanella*.

4.4.2 Microbe-mineral interactions

If Fe(III) reduction does not have a substantial contribution to Cr(VI) reduction, then why does the presence of goethite and hematite in the system inhibit Cr(VI) reduction by *Pseudomonas*, while increasing that of *Shewanella*? Here we hypothesise that the two bacteria use different pathways for Cr(VI) reduction, and those pathways may have been impacted by the presence of mineral surfaces, and in particular by the effect of attachment of bacteria onto the surfaces

Most bacteria, including *Pseudomonas* and *Shewanella*, are negatively charged, and both goethite and hematite have positive surface charge under neutral pH conditions [*Kumpulainen et al.*, 2008; *Pan et al.*, 2004; *Plaza et al.*, 2001; *Zeltner and Anderson*, 1988], so the bacteria can naturally adhere to the mineral surface by electrostatic attachment. This has been confirmed by imaging the samples with SEM (Fig. 4.7). The Cr(VI) employed in this study was in the form of a dichromate anion which, for the same reason, may also partially accumulate around the mineral surface. However, the electron-transfer pathways and the production of effective Cr reduction enzymes may have differed for the two strains under the growth conditions employed.

Although the reduction mechanism for Cr(VI) by either bacteria has not been fully understood, several studies have been carried out previously to provide some perspective. *Bopp and Ehrlich* [1988] looked into chromate reduction by *Pseudomonas fluorescens*, and demonstrated there was chromate reductase activity in

the S_{32} fraction rather than in the S_{150} fraction (both fractions contained soluble enzymes and were obtained by centrifuging cell-free extracts at different speeds), suggesting that the enzymes necessary for transferring electrons from NADH to chromate are membrane-bound. With the attachment of the bacteria to mineral surfaces, or the formation of biofilms, the active contactable surface area between cell membranes and dissolved Cr(VI) decreases, reduces the interaction between Cr(VI) and available membrane-associated enzymes, resulting in observed lower reduction rates. The multiple flagella that *Pseudomonas fluorescens* LB 300 have are important in this process, as they were found to be essential for the bacteria to reach and interact with abiotic surfaces; mutants lack the ability to produce flagella have worse attachment on abiotic surfaces and also have worse ability to form biofilms [*O'Toole and Kolter*, 1998a,b].

Previous studies of *Shewanella oneidensis* MR-1 have revealed two distinctive enzymatic reduction pathways. *Myers et al.* [2000] extracted all the enzymes from cells to determine their reductase activity and demonstrated that the dominant proteins exhibiting enzymatic Cr(VI) reduction are localised on the inner-most layer of the bacterial membrane; thus, Cr(VI) reduction by those enzymes would first involve the transportation of Cr(VI) across the cell membrane, and then reduction inside the cell. *Lies et al.* [2005], showed that the cells also had the ability to generate soluble electron carriers, or mediators, which can reduce iron at a distance. Since Cr(VI) has a higher redox potential than Fe(III), it is likely that such electron shuttles are also effective in reducing Cr(VI), particularly within biofilms [*Lies et al.*, 2005]. Enzymatic studies with other sulfate-reducing bacteria have also demonstrated that multiple enzymes can be responsible for Cr(VI) reduction [*Michel et al.*, 2001, 2003]. In addition to membrane-bound cytochromes, other metalloenzymes that contain hemes or (Fe/S) centers possess metal reductase activity, and these could also contribute to Cr(VI) reduction as well. Furthermore, in the presence of Cr(VI), a portion of both cytochrome c and periplasmic proteins are found to leak

out of the cell, and may then lead to Cr(VI) reduction in the aqueous phase [*Michel et al.*, 2001]. Other than enzymatic reduction processes for electron transfer, it has recently been demonstrated that *Shewanella oneidensis* MR-1 can produce bacterial nanowires that provide an extracellular electron transport pathway [*El-Naggar et al.*, 2010; *Gorby et al.*, 2006; *Pirbadian et al.*, 2014]. Such nanowires were also found in this study (Fig. 4.7B, white arrows). The nanowires from *Shewanella oneidensis* MR-1 are extensions of the outer and periplasmic membrane, which includes the multiheme cytochromes responsible for extracellular electron transfer [*Pirbadian et al.*, 2014]. These can therefore reduce Cr(VI) over a much greater volume. Since electrons can travel along the nanowires, any change in the surrounding environment which impacts nanowire formation or the electron transfer gradient is likely to influence Cr(VI) reduction. In this study, while attachment of *Shewanella oneidensis* MR-1 may have resulted in a decrease in the direct reduction of Cr(VI) by the membrane-bound enzymes, the formation of biofilms should not affect the release of water soluble enzymes nor the generation of electron shuttles within the biofilm matrix, and the presence of the mineral surfaces may provide better reaction boundaries because of surface charge, enhances the electron transfer activity of nanowires, contributing to the greater reduction rate observed in our study.

To summarise, Cr(VI) reduction pathways are demonstrated in Fig. 4.9; three main reduction pathways seem to play a role. 1) Both *Pseudomonas fluorescens* LB 300 and *Shewanella oneidensis* MR-1 have membrane-bound enzymes that are responsible for Cr(VI) reduction. As illustrated in Fig. 4.9A, if the enzymes are on the outer membrane, Cr(VI) can be reduced directly from outside the cell. By contrast, if the enzymes are localised on the inner membrane, Cr(VI) has to be transported into the cell and then reduced. In this pathway, if cells are attached and stack on the mineral surface, the contactable surface area between bacteria and Cr(VI) decreases, and Cr(VI) reduction rates also decrease. 2) Bacteria can use self-made nanowires for electron transfer. Even if the cells are immobilised, they can

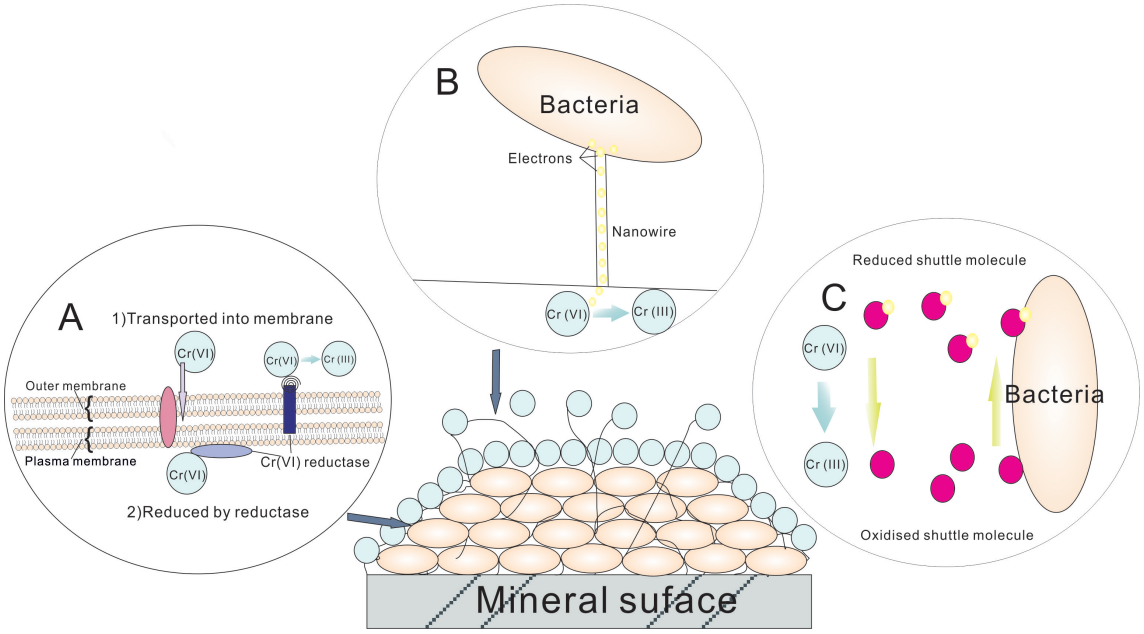


Figure 4.9: Three possible pathways for microbial Cr(VI) reduction. A: The enzymes responsible for Cr(VI) reduction are membrane-bound. If the enzymes are on the outer membrane, Cr(VI) can be reduced on the surface of the cell. However, if they are on the inner-membrane of the bacteria, Cr(VI) needs to be transported into the cell first, and then be reduced. B: *Shewanella oneidensis* MR 1 can produce nanowires to facilitate electron transfer processes. The nanowires are extensions of outer and periplasmic membrane, and they can aid electron transfer between bacteria and mineral substrate, bacteria and metals, and between two bacteria. C: *Shewanella oneidensis* MR 1 can also produce soluble "electron shuttles" to aid electron transfer at a distance.

still transfer electrons to Cr(VI) over long distances (see Fig. 4.9B). The electron transfer processes can be between bacteria and abiotic substrates, or even between two different bacteria. The electron transfer process in this pathway may have been enhanced by the mineral, by introducing the positive-surface-charged interactive boundaries which change the electron transfer gradient along the bacteria nanowires. 3)Bacteria can produce extracellular electron shuttles or water-soluble enzymes for Cr(VI) reduction (see Fig. 4.9C). This pathway may not be significantly impacted by the presence of the minerals.

Pathway 1 is the most important for *Pseudomonas fluorescens* [*Bopp and Ehrlich*, 1988], which is why a significant decrease of Cr(VI) reduction was observed in the experiment in the presence of minerals (Fig. 4.4). There is no information on the

conductivity of the flagella produced by this specific bacteria. However, even if the flagella are conductive and able to transfer electrons extracellularly, they can not provide the dominant electron transfer pathway for this bacteria, based on our observations of the reduction experiments in the presence of minerals. Therefore, it is likely that the multiple flagella *Pseudomonas* produced mainly aid bacterial motility, not electron transfer. For *Shewanella oneidensis* MR-1, the three pathways have all been shown to be responsible for Cr(VI) reduction [*Gorby et al.*, 2006; *Lies et al.*, 2005; *Myers et al.*, 2000], but the relative importance of the three pathways have not been investigated before. In this study, the presence of the minerals clearly increase the Cr(VI) reduction rates by this bacteria, indicating that the electron transfer has been significantly enhanced. From the three pathways, only the nanowire mechanism will be enhanced by the presence of minerals. This is, then, the possible reason for the greater reduction rate observed in our study, and so the dominant pathway for *Shewanella oneidensis* MR-1. Further study can be done to better address this possibility.

4.4.3 The impact of iron

In this study, we have focused on the impacts of both Fe(II) and Fe(III) on chromium cycling in anoxic environments. In previous experiments utilizing the same bacteria, fast initial loss of Cr(VI), as observed here (Fig. 4.6), was never reported. The fast initial loss of Cr(VI) concentration with a low isotope fractionation factor clearly can be ascribed to the abiotic reaction with Fe(II).

$$Cr(VI) + 3Fe(II) \xrightarrow{electron\ transfer} \mathrm{Cr(III)} + 3Fe(III) \tag{4.5}$$

The existence of Fe(II) is one of the main factor that control Cr(VI) cycling in the environment. In the anoxic zones of modern environments, Fe(III) oxides are readily reduced and provide significant electron sinks for both chemical and biological

processes, generating aqueous Fe(II) and solid-phase Fe(II)-bearing minerals. These minerals include siderite, vivianite and geologically significant mixed-valence Fe(II)-Fe(III) minerals, such as magnetite and green rust. The solubility and stability of both Fe(III) and Fe(II) are dependent upon the prevailing pH in the environment. When pH decreases, the solubility of Fe(III) and the stability of Fe(II) are enhanced. At a pH below 4.0, Fe(II) exists as an aqueous species, even in the presence of oxygen. Studies of various aquatic and sedimentary systems have shown that Fe(II) undergoes both biotic and abiotic oxidation in the environment. Iron redox cycling can alter the geochemistry of soils and sediments, causing the degradation of organic matter, mineral dissolution and weathering, thus affecting the formation of geologically important minerals, as well as the mobilization or immobilization of various anions and cations.

Chromium isotope fractionation during reduction of Cr(VI) by aqueous Fe(II) has been investigated previously by *Dossing et al.* [2011] and *Kitchen et al.* [2012]. The fractionation factors were found to be -1.5 ‰ when pH ranged between 6.8 and 8.1 [*Dossing et al.*, 2011], and -4.2 ‰ when pH ranged between 4.0 to 5.3 [*Kitchen et al.*, 2012]. In our study, the pH in the buffer solution was always kept around 7, which is closer to the conditions used by *Dossing et al.* [2011]. The best-fit Rayleigh distillation curve is shown as the dotted line in figure 4.6, with ε = -1.9 ‰, and the δ^{53}Cr values are consistent with *Dossing et al.* [2011]. After the initial Cr(VI) loss, the further reduction of chromium occurs due to microbial activity, and the best-fit ε value for the microbial reduction is -3.3 ‰ in all groups with Fe(II), regardless of whether there were any minerals in the system. The presence of iron minerals or aqueous iron species in the environment does not affect microbial Cr(VI) isotope fractionation, indicating the reduction pathways are the same under these conditions.

In the experiment with *Pseudomonas* and hematite, a higher isotope fractionation factor was observed, which is possibly due to both microbial fractionation

and a mineral adsorption fractionation. The fractionation factors for adsorption on goethite and hematite were not investigated in this study; however, *Ellis et al.* [2004] have done adsorption experiments with γ-Al_2O_3 and goethite, and found Cr(VI) stable isotope fractionation caused by sorption was negligible. Therefore, it is proposed here that Cr isotope fractionation by adsorption on hematite may also be insignificant, and the greater fractionation factor determined in this study was due to the impact of mineral on bacterial activity. Such impact may be due to the physiochemical property of this mineral, including solubility, reduction potential, and surface area. Further study is needed to better address this issue.

4.5 Conclusions

Although metal-mineral-microbe interactions are important in the natural environment, there are limited data available on the specific processes involved. In this study, we obtained the first batch of isotope data about the impact of different forms of Fe, including aqueous Fe(III), aqueous Fe(II), goethite and hematite, on microbial Cr reduction processes and isotope fractionation.

The presence of either goethite or hematite inhibited Cr(VI) reduction rates by the bacterium *Pseudomonas fluorescens* LB 300, but accelerated those by *Shewanella oneidensis* MR 1. These differences are possibly related to the way bacteria attach to the minerals, as well as differences in the underlying reduction mechanism of the two bacteria. The Cr isotopic fractionation factors are independent of the presence of the minerals for *Shewanella*. However, for *Pseudomonas*, the value of ε was higher in the presence of hematite. Under the same lab conditions, the isotope fractionation factors for different bacteria are also different. This indicates that the species of bacteria and the types of minerals in the environment may have significant impact on microbial Cr fractionation factors. Therefore, to better estimate the extent of Cr reduction in particular environments, data from natural samples

are required. For example, where isotope shifts are used to determine the extent of Cr removal by microbial reduction at sites of contamination [*Ellis et al.*, 2002], site-specific ε values should be obtained from experiments using natural samples and the local microbial populations.

Aqueous Fe(III) in the solution did not have a detectable effect on either bacterial Cr reduction rates nor the Cr isotopic fractionation factors, indicating that reduction of Cr(VI) occurs prior to that of Fe(III). By contrast, the presence of aqueous Fe(II) induced a rapid abiotic reduction of Cr, but has little impact on the bacterial Cr reduction rates or isotopic fractionation.

SEM images confirmed that the attachment of *Pseudomonas fluorescens* LB 300 onto mineral surfaces was much tighter than that of *Shewanella oneidensis* MR 1, and this was most likely due to the flagella on the cell surfaces. These images also showed that *Shewanella oneidensis* MR 1 produced bacterial nanowires in the process, which may be essential for electron transfer for this bacteria.

Overall, bacterial Cr isotope fractionation processes are independent of the presence of aqueous iron, but may be impacted by the presence of minerals in the surrounding environment. In addition, the results in this study show that Cr isotopes are useful to help distinguish between different reduction processes, and indicate that the dominant Cr(VI) reduction pathway for *Pseudomonas fluorescens* LB 300 may involve membrane-bound enzymes, while for *Shewanella oneidensis* MR 1 it may be via extracellular electron transfer.

Chapter 5

Monitor Cr toxicity and remediation process-combining a whole-cell bioreporter and Cr isotope techniques

5.1 Introduction

Hexavalent chromium is a common contaminant in the environment, as a consequence of its wide application in industry, such as for corrosion inhibition, electroplating, paints, pigment manufacturing and leather tanning [*Desai et al.*, 2008]. Various experimental studies showed that Cr(VI) has very high solubility and bioavailablity [*Antonini and Roberts*, 2007; *Dayan and Paine*, 2001]. Moreover, toxicity studies demonstrated that Cr(VI) could induce oxidative stress in cells, causing DNA damage, gene mutation, sister chromatid exchange, chromosomal aberrations, cell transformation and dominant lethal mutations in a number of targets in both animal and human cells [*Xu et al.*, 2004, 2005]. In humans, the lethal oral dose of soluble chromates is considered to be 50 - 70 mg/kg body weight [*Dayan and Paine*,

2001]. The acute poisoning of Cr(VI) can induce vomiting, diarrhoea, haemorrhage and blood loss into the gastrointestinal tract, which can cause cardiovascular shock, and the longer toxic effect in humans are liver and kidney necrosis [*Dayan and Paine*, 2001].

In the environment, Cr(VI) pollution can alter the structure of soil microbial communities, as well as reduce microbial growth and enzymatic activity. Lab-based studies have indicated that it can also cause cellular oxidative stress in cells of microorganisms, and the cellular defence against the toxicity involves activation of antioxidant mechanisms [*Ackerley et al.*, 2006]. The toxicity of Cr(VI) towards microorganisms can also inhibit the biodegradation of other organic pollutants. For example, in a study with natural samples, Cr(VI) was found to alter microbial compositions, which affected the soil biodegradation potential [*Kourtev et al.*, 2006]. As in mammalian cells, in bacteria Cr(VI) is still highly toxic at the extracelluar level because it can rapidly enter the cytoplasm. Its toxicity in the cytoplasm is mainly related to the reduction process that generates free radicals [*Ramirez-diaz et al.*, 2008].

Cr(VI) can be reduced to Cr(III), which is generally found to have much lower bioavailability and much lower toxicity than Cr(VI) [*Dayan and Paine*, 2001; *Zhang et al.*, 2011]. However, studies have found that it is toxic to microbes by causing DNA damage [*Plaper et al.*, 2002] or changing the pH [*Garcia et al.*, 1994] in the surrounding environment. However, Cr(III) is more insoluble than Cr(VI) and more surface-reactive, and so much less mobile and less biovailable.

Because of the seriousness of Cr(VI) pollution and its alarming effects on human health, Cr was classified as class A human carcinogen by the US Environmental Protection Agency (USEPA) [*Desai et al.*, 2008] and health standards are generally not exceeded in unpolluted areas. Monitoring and control of pollutant Cr are clearly very important.

Remediation of pollutant Cr(VI) commonly involves transformation to less toxic

and less mobile oxidation states. Compared with most conventional physicochemical methods, biological Cr(VI) detoxification is an eco-friendly and cost-effective alternative in various environments and in industry. Many microorganisms, such as *Bacillus. sp* [*Pan et al.*, 2014], *Pseudomonas.sp* [*Park et al.*, 2000], *Escherichia coli* [*Ackerley et al.*, 2004b] and *shewanella. sp* [*Hossain et al.*, 2005], have proved to have great ability to adapt to, and colonize, noxious metal-polluted environments, and to transform the oxidation state of Cr. However, microbes have their own limitations towards highly toxic contaminants, which can cause severe damage to their functions or even their viabilities. Therefore, the assessment of environmental risks to microbial communities associated with aqueous and soil contamination is very important both before instigating any bioremediation plans and with remediation progresses. Therefore, a rapid and efficient method to evaluate the potential toxic impact is required.

Bacterial whole cell bioreporters have been developed in recent years. They have been found to be efficient, cost-effective, sensitive and selective to toxic materials, to reflect the bioavailability and genotoxicity of hazardous compounds [*van der Meer and Belkin*, 2010], and can be used *in situ* as an efficient alternative to complex, costly and labour intensive chemical analysis or animal tests. The whole cell bioreporter ADPWH_*rec*A involves the soil bacterium *Acinetobacter baylyi*ADP1 as the host, and has a chromosomal insertion of the promoterless *lux*CDABE cassette form *Photorhabdus luminescens* [*Huang et al.*, 2005], which is controlled by the SOS-inducible *rec*A promoter. The chromosomally based ADPWH_*rec*A bioreporter expresses bioluminescence in the presence of DNA-damaging compounds [*Huang et al.*, 2005]. It has been applied in various studies to test the toxicity of a variety of chemical compounds including polycyclic aromatic hydrocarbons and other groundwater contaminants [*Song et al.*, 2009].

Whole cell bioreporters are usually sensitive to toxic compounds, and it is generally assumed that the toxic effect on toxic-resistant bacteria is smaller than that on

sensitive bioreporters [*Fulladosa et al.*, 2006]. This is a very important assumption. When bioreporters are used for indicating toxicity level of certain environment, if they are viable in that environment, it means toxic-resistant microbes can be viable as well, and bioremediation is possible for such environment. The toxicity of a compound is largely dependent on its concentration. Although the genotoxicity of chromium has been studied over many years, there are limited data using whole cell bioreporters to indicate the toxicity of different chromium species at different initial concentrations. This is addressed in this study.

Monitoring of the progress of soil and groundwater remediation is typically done by mapping of Cr(VI) concentrations over the remediation site. However, the reduction of Cr(VI) concentrations can be caused by various reasons, such as dilution in groundwater, adsorption on soil particles or bioreduction. Identifying the mechanism that decreases Cr(VI) concentrations is essential for estimating the long term effect of remediation on a particular site. This can be done by monitoring Cr isotope fractionation [*Zhang et al.*, 2016].

Chromium has 4 isotopes. Isotopic fractionations are represented by the $^{53}Cr/^{52}Cr$ ratio, which is generally reported as relative deviations from a standard (e.g., the NIST SRM 979) in parts per thousand (per mil or ‰):

$$\delta^{53}Cr = [\frac{(^{53}Cr/^{52}Cr)_{sample}}{(^{53}Cr/^{52}Cr)_{standard}} - 1] \times 1000‰ \tag{5.1}$$

.

The lighter isotopes have lower dissociation energy, and so one common feature in many redox reactions is that the lighter isotopes are more reactive and are concentrated in the reaction products. Such features were observed in many previous studies [*Basu and Johnson*, 2012; *Kitchen et al.*, 2012; *Zink et al.*, 2010]. The elevated δ^{53}Cr values of the remaining Cr(VI) provide evidence for Cr(VI) reduction, and further can be employed to indicate the extent of Cr(VI) reduction [*Ellis et al.*, 2002]. The extent of Cr isotope fractionation is usually measured by the fraction-

ation factor, and different processes may have different fractionation factors. For example, microbial reduction of Cr preferentially removes lighter isotopes from the dissolved phase [*Basu et al.*, 2014; *Sikora et al.*, 2008], whilst dilution of the contaminant or adsorption results in an unchanged isotope composition [*Ellis et al.*, 2004]. Therefore, the extent of fractionation provides information on what process was involved.

In microbial Cr reduction processes, microbes progressively reduce Cr(VI) to Cr(III), which is less reactive and less mobile. Isotope exchanges between Cr(VI) and Cr(III) are negligible [*Wang et al.*, 2015], which means the products will not re-equilibrate with the original reactants. Since the lighter isotopes of Cr are enriched in the products, they will be progressively depleted in the original Cr(VI) pool. This scenario can be described by means of one of the Rayleigh equations [*Rayleigh*, 1896].

$$R_{Cr(VI)} = R^0_{Cr(VI)} f^{\alpha-1} \tag{5.2}$$

Where $R_{Cr(VI)}$ is the $\frac{^{53}Cr}{^{52}Cr}$ ratio in the remaining Cr(VI), $R^0_{Cr(VI)}$ is that in the original Cr(VI) pool. α is the isotope fractionation factor, where

$\alpha = (^{53}\mathrm{Cr}/^{52}\mathrm{Cr})_{Cr(III)}/(^{53}\mathrm{Cr}/^{52}\mathrm{Cr})_{Cr(VI)}$ during the reaction process. f is the fraction of the Cr(VI) remaining after reduction. As f decreases, $R_{Cr(VI)}$ increases, and so measurement of $R_{Cr(VI)}$ can be used to calculate f. Note that once fractionation occurs, there is no isotope exchange between Cr(III) and Cr(VI) that would alter this relationship [*Wang et al.*, 2015].

To make Cr isotopes a useful indicator of the extent of reduction, information about the mechanisms of Cr isotope fractionation is required, including a value for α. *Sikora et al.* [2008] reported microbial Cr isotope fractionation factor ranged from 4.0 to 4.5 ‰ when reduction rates were low and were 1.8 ‰ when higher. *Han et al.* [2012] investigated ε during reduction by *Pseudomonas stutzeri* RCH2 under both aerobic and denitrifying conditions, and reported it to be 2 ‰ under aerobic, and 0.4 ‰ under denitrifying, conditions. *Basu et al.* [2014] examined chromium

reduction by a metabolically diverse group of bacteria, and suggested that stronger isotopic fractionation was induced during Cr(VI) reduction under electron-donor-poor conditions. Our previous study has demonstrated the relationship between several important environmental conditions and Cr isotope signatures, and showed that the types of electron donors utilised and bacterial respiration pathways have a significant impact on microbial Cr isotope fractionation [*Zhang et al.*, 2016]; however, the impact of different Cr(VI) initial concentrations and their correspondent toxicity on bacterial Cr isotope fractionation has not yet been well studied. Therefore, this study focuses on determining the levels of Cr toxicity and their impact on Cr isotope fractionation by bacteria. For that purpose, a whole cell bioreporter was used to indicate the toxicity of different species of Cr over a range of concentrations, and Cr isotope fractionation by bacterial reduction was determined at different initial concentrations. These two techniques are shown to provide an effective monitor of the extent of Cr(VI) reduction and toxicity in the environment with various concentrations of Cr(VI), and with further development could become an important tool in the area of bioremediation.

5.2 Materials and methods

5.2.1 Chromium toxicity tests

To determine the right range of Cr initial concentrations for bacterial reduction experiments, a chromium toxicity test was done by using a whole cell bioreporter, *Acinetobacter baylyi* ADPWH_*rec*A. In the toxicity tests, the whole bioreporter was cultured in the presence of different species of Cr with different initial concentrations. The growth and bioluminescence of the bioreporters in different groups were monitored over the period of experiments. The level of Cr toxicity was then determined by comparing the growth rates and bioluminenscence generation with the control group. All experiments were done in triplicate.

5.2.1.1 Preparation of the bioreporter

All chemicals in this study were analytical-grade reagents (Sigmal Aldrich, USA). LB medium (Luria-Bertani medium) and LBK medium (LB medium with 10 μg kanamycin mL^{-1}) were used for cultivation of the strains and induction studies.

The strain was first recovered from -80 °C and incubated on LB agar plate (supplemented with 10 μg kanamycin mL^{-1}) at 30 °C overnight. One colony was then transferred and incubated in 5 mL LBK medium in a shaking incubator at 150 rpm, 30 °C, for 12-14 hours. Before the experiment, the strain was harvested by centrifugation at 4000 rpm for 20 minutes. The cells were then re-suspended in 5 mL fresh LB medium and diluted by a factor of 10 with fresh LB medium for the experiments.

5.2.1.2 chromium sample preparation

Potassium dichromate, potassium chromate and chromium chloride solutions with different concentrations were prepared. The concentrations of the stock solutions were 50, 200, 400 and 1000 mg chromium/L. Milli-Q water ($\geq$ 18.2 ΩM cm) was used in one group as a blank control (data shown as Control in all figures). Mitomycin C (MMC) from streptomyces caespitosus, which is a known toxin to the bioreporters, was used as a positive control in the experiment to ensure the bioreporter are functioning normally (data not shown).

5.2.1.3 Bioreporter response measurement

Aliquots of 180 μl ADPWH_*rec*A and 20 μl chromium solutions were transferred to, and mixed in, a 96-well microplate (black with clear bottom, Greiner, Germany) to generate concentrations in the wells of 0, 5, 20, 40 and 100 mg/L for all of the three different chromium solutions. Milli-Q water and mitomycin C (1×10^{-6} M) were used as the negative and positive controls. Bioluminescent intensity and optical density were both measured with a Bio-tek Synergy 2 HT plate reader every 30 minutes at

30 °C over 6 hours. Each group in these experiments contained triplicate samples and every measurement was done three times.

In this study, the intensity of bio-luminescence expressed by the control group was considered to be the baseline. The toxicity of Cr was evaluated using the induction ratio, which can be calculated using the following equation:

$$The\ induction\ ratio = \frac{Bioluminescent\ intensity_{induced}}{Bioluminescent\ intensity_{control}} \tag{5.3}$$

The detection limit is defined as the lowest concentration of Cr(VI) causing a significant induction ratio response relative to the negative control (p<0.01).

In the presence of DNA damaging compounds that cause genotoxicity to cells, the intensity of bio-luminescence increases with an increase in the toxicity level. In this case, the induction ratio is greater than 1. However, when the toxicity level is exceeded to the extent that seriously damages cell functions, the bio-luminescence will decrease, and in this case, the induction ratio is less than 1.

5.2.2 Cr reduction experiments

Cr reduction experiments were conducted with *Pseudomonas fluorescens* LB 300, which is common in the environment and can resist high Cr concentrations [*Wang and Shen*, 1995]. LB (Luria Bertani) Broth (Sigma Aldrich) and Minimal salts medium (0.03g NH_4Cl, 0.03g K_2HPO_4, 0.05g KH_2PO_4, 0.01g NaCl and 0.01 g $MgSO_4$ in 1 L of Milli-Q water) were employed in the study. Before the aerobic reduction experiments, bacteria were cultured by transferring a single colony grown aerobically in a Petri dish containing LB Agar to a 1 L flask containing LB medium and incubated at 30 °C and 120 rpm overnight. To compensate for the variability of microbial systems, all experiments in this study were done in triplicate.

The aerobic reduction experiments were conducted in 150 mL Erlenmeyer flasks. When cells reached the late exponential state, they were collected by centrifugation

at 4100 rpm and 4 °C for 20 minutes. The cells were then washed 3-4 times using 0.9 % sterile NaCl solution before being added to 50 mL of fresh minimal salts medium and incubated at 30 °C and 120 rpm. The cell density was adjusted to 10^9 - 10^{10}/mL. Glucose was employed as the electron donor in the study, which was prepared as solution and sterilised by passing through a 0.22 μm membrane. A Cr (VI) solution was prepared by dissolving potassium di-chromate in sterilized Milli-Q water and filtering the solution through 0.22 μm membrane before the experiments.

During the experiments, Cr(VI) was reduced by the bacteria aerobically, and Cr(III) was produced. Periodically, 1 mL of sample was taken and centrifuged at 9000 rpm at 4°C for 10 min. The supernatant was sterile filtered (0.22 μm) and transferred to a clean Eppendorf tube and stored at -80°C before further treatment. The Cr(VI) and Cr(III) concentrations were measured simultaneously by HPLC (Thermo Scienctific^{TM} Dionex^{TM} ICS$-$3000).

5.2.3 Cr isotope measurements

Cr isotopes were measured by a thermal ionization mass spectrometer (Thermo Finnegan Triton TIMS instrument). The preparation method of samples for isotope composition determination largely followed that of *Ellis et al.* [2002]; *Zhang et al.* [2016]. A double isotope spike method was employed for correction of isotopic fractionation during sample preparation and mass spectrometry. The data acquisition method is modified from *Trinquier et al.* [2008].

5.3 Results

5.3.1 Determination of Cr toxicity

In this study, growth kinetic curves of ADPWH_*rec*A with different concentrations of Cr_2O_7, CrO_4 and Cr(III) are shown in Figure 5.1.

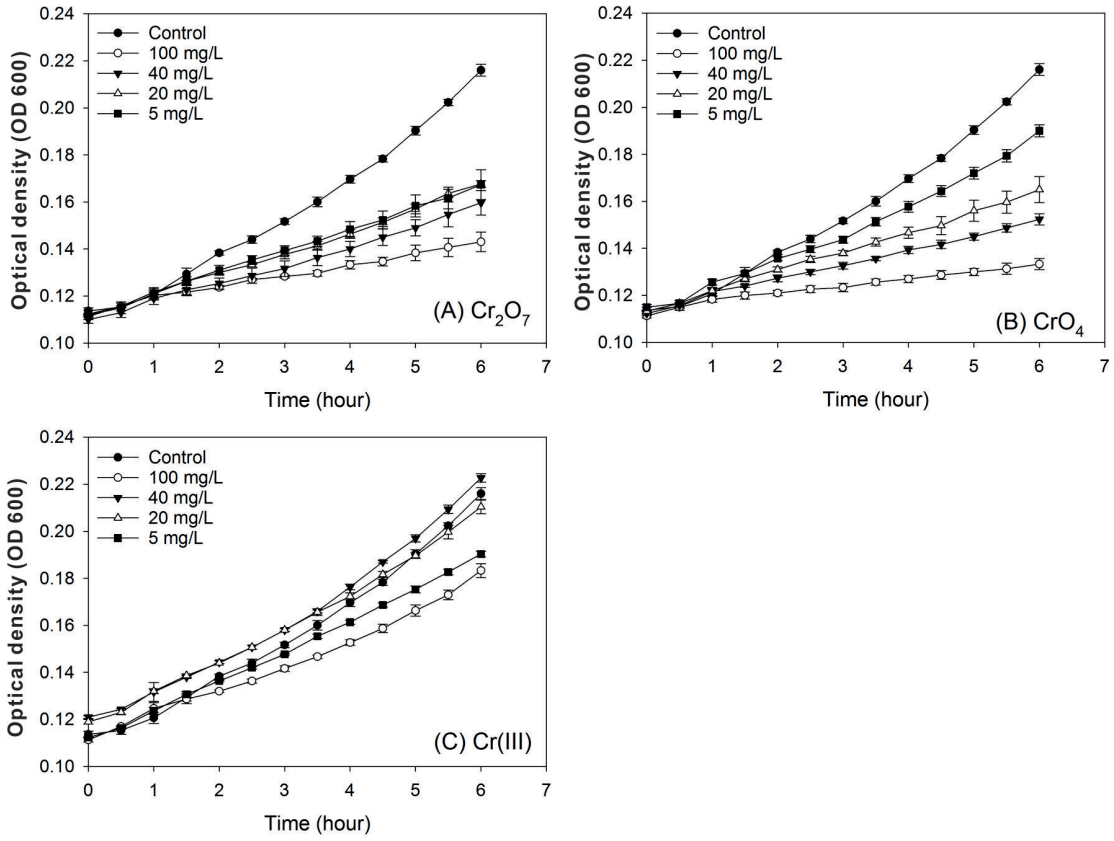


Figure 5.1: Growth curve of the ADPWH_*rec*A with different concentrations of $K_2Cr_2O_7$ (A), K_2CrO_4 (B) and Cr(III) (C). Higher concentrations of $K_2Cr_2O_7$ and K_2CrO_4 affected the growth of the ADPWH_*rec*A to a larger extent. Error bars represent the standard deviation of 3 replicates.

The optical density of each group at 600 nm wavelength (OD600), measured over the experimental period, is related to cell number in each group and provides an indicator of bacterial growth. Note that variations of OD600 can only indicate the change of total number of cells, but not number of viable cells. In all groups in this study, OD600 value rises with time, showing that cell number is increasing in all groups; however, the rate of increase is different. In Fig. 5.1A-5.1B, the control group is shown for comparison, which only contained the bacteria in LB medium. Compared with the control group, the growth rates from all groups containing Cr(VI), regardless of the species, were much slower, indicating that Cr(VI) inhibits the growth of ADPWH_*rec*A. Growth rates were found to be lower when Cr(VI) concentration was higher, indicating greater inhibition with concentration.

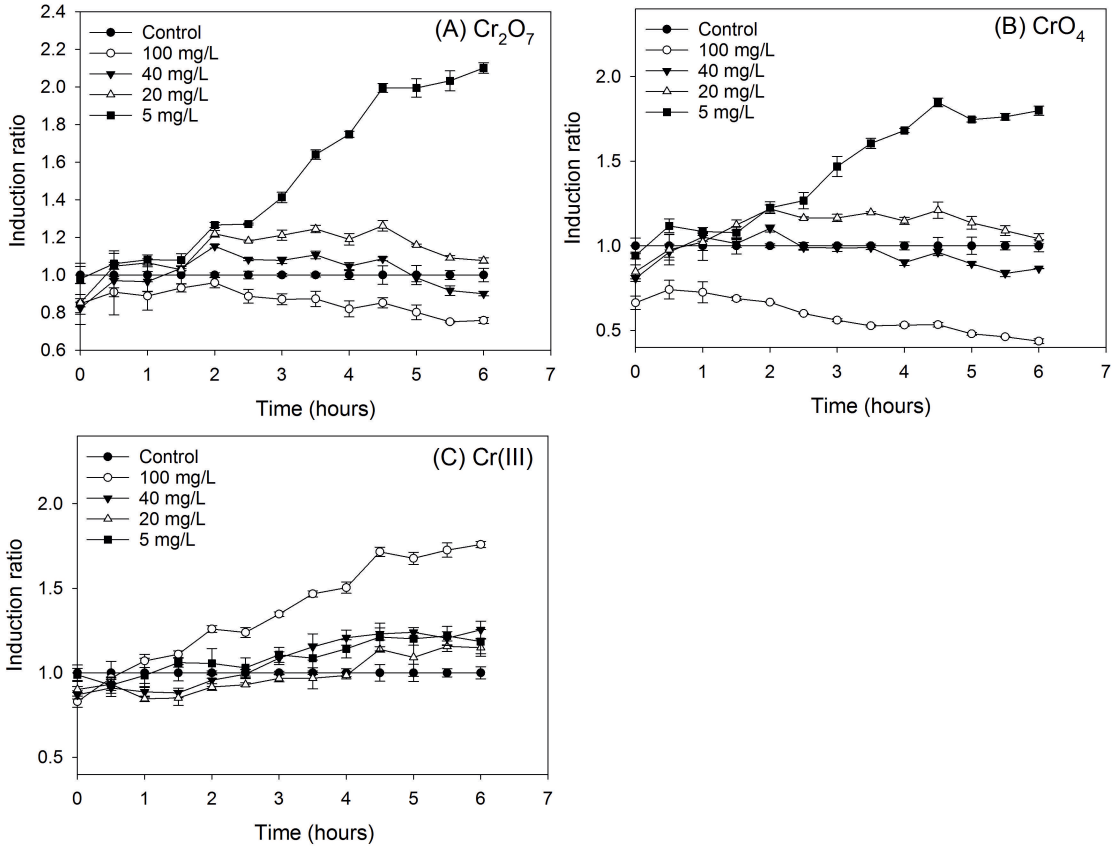


Figure 5.2: The induction ratio measured throughout the experiments are shown for the different Cr species and for different concentrations. Low concentration of Cr(VI) (5 mg/L) from $K_2Cr_2O_7$ (A) and K_2CrO_4 (B) induce bioluminescence of the ADPWH_*rec*A, while high concentrations of Cr(VI) (100 mg/L) inhibit it. Higher concentrations of Cr(III) (C) induce more bioluminence of the ADPWH_*rec*A. Error bars represent the standard deviation of 3 replicates.

The growth rates from groups with different concentrations of Cr(III) are shown in Figure 5.1C. Cr(III) has a blue colour which interferes with optical density measurement, so the initial OD600 values for groups with different Cr(III) concentrations are different. In this case, growth rates were compared by calculating the slope of each curve, and were found to be close to each other. No significant differences are observed between the control group and Cr(III)-treated groups at all time points (p>0.05), indicating that Cr(III) concentrations have little impact on bacterial growth across the experimental values.

The induction rate (IR) values for ADPWH_*rec*A responses over a 6 hour exposure to different species of chromium in the solution are shown in Fig 5.2. For each

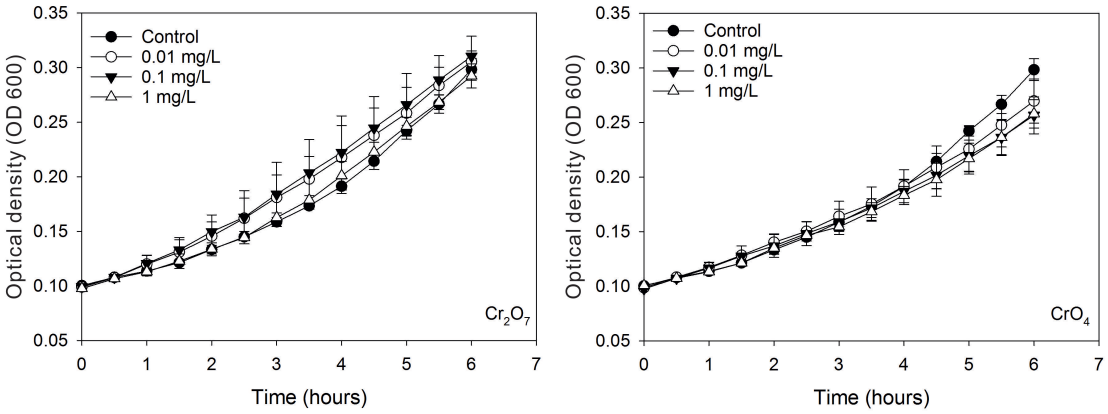


Figure 5.3: Growth curve of the ADPWH_*rec*A with different concentrations (< 5 mg/L) of $K_2Cr_2O_7$ and K_2CrO_4. There were no significant difference between each group at such low Cr(VI) concentration levels

group, bioluminescence generated by cells tends to increase at the beginning, and then decreases, depending on the physiology of bacteria. In the experiments, 5mg/L of Cr(VI) in solution significantly induced bioluminescence of the bioreporter (IR >1, p<0.05), indicating that Cr(VI) exerted genotoxicity in water (Fig 5.2A and Fig 5.2B). Another experiment with low Cr concentrations were also done to confirm the sensitivity of the bioreporter, and it was shown that low concentration of Cr (< 1 mg/L) does not have significant impact on bacterial growth (Fig 5.3). The induction ratio is proportional to the dose when initial Cr(VI) concentration $\ngeq$ 5 mg/L (Fig 5.4). However, higher concentrations ($\geq$20 mg/L) of Cr(VI) from both Cr_2O_7 and CrO_4 show great inhibition on bioluminescence of the ADPWH_*rec*A. Compared to the control group, the bioluminescence from both groups with 100 mg/L Cr(VI) were much suppressed from the beginning of the experiment (IR < 1), and the induction ratios to the control group decreased over the experimental period (Fig 5.2A and Fig 5.2B), indicating the function of the bacteria was severely damaged. Compared to Cr_2O_7, CrO_4 shows greater inhibition of bioluminescence with the same concentration of Cr(VI), indicating that CrO_4 may be more toxic to ADPWH_*rec*A than Cr_2O_7.

In the experiment with Cr(III), although bacteria growth rates were similar to

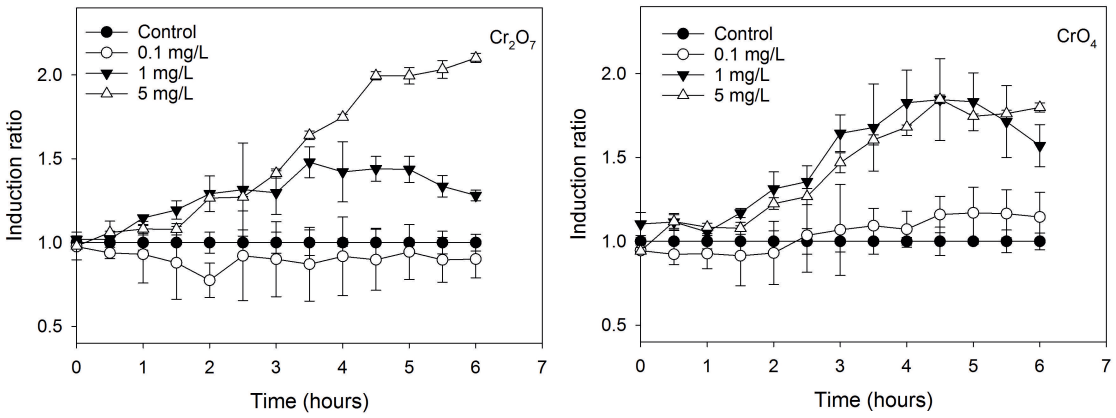


Figure 5.4: Response of ADPWH_*rec*A to different concentrations of $K_2Cr_2O_7$ and K_2CrO_4 at 6 hours of experiment. The induction ratio is proportional to the dose.

that of the control, the IR values of groups with 20, 40 and 100 mg/L Cr(III) showed that there was inhibition of bioluminescence at the beginning of the experiment, but the induction ratio increased over the experimental period and bioluminescence was induced for all concentrations of Cr(III) (Fig 5.2C). The dose response curve shows that higher concentrations of Cr(III) can cause greater induction of bioluminescence (Fig 5.7C) with time, indicating that Cr(III) can be genotoxic at high concentrations.

5.3.2 Bacterial Cr(VI) reduction experiments

Cr reduction experiments by *Pseudomonas fluorescens* LB 300 were conducted over a Cr(VI) concentration range from 5 to 40 mg/L (Fig. 5.5). Control groups in this study contained the same amount of dead cells of *Pseudomonas* as in experimental groups. A fast drop of Cr(VI) concentration in control groups was observed, which was due to adsorption of Cr(VI) on the cells. After the initial loss, Cr(VI) concentrations in control groups remained constant. In experimental groups, Cr(VI) was reduced by the bacteria over the experimental period, with a faster reduction rate within the first 24 hours. After the fast removal of Cr in the first hour, the reduction rate slowed down. About 50 % Cr(VI) was reduced in the groups containing initially 40 mg/L and 20mg/L Cr(VI). Complete Cr(VI) reduction was only observed

in the experimental group initially containing 5mg/L Cr(VI). The reduction rate of Cr(VI) was found to be higher at higher initial Cr(VI) concentrations (Fig. 5.5), which reflects bacteria adapting to the toxic environment.

5.3.3 The application of Cr isotopes

The isotope data are presented in Fig. 5.6. With the reduction of Cr(VI), the δ^{53}Cr value increased, indicating that the produced Cr(III) had a lighter isotopic composition.

Cr (VI) reduction experiments in this study were conducted in a well mixed, closed environment. In such a system, if the isotopic fractionation factor, α, is constant with time, the δ^{53}Cr value of the remaining Cr(VI) in the system evolves according to the Rayleigh relationship, which can be expressed as in EQ. 5.2.

The best fit α values can be found by plotting the linearised equation and using a linear regression for the plots[*Kitchen et al.*, 2012]. Uncertainties can be calculated as 2×standard errors of the best fit slopes.

The results were expressed as ε.

$$\varepsilon = (\alpha - 1) \times 1000‰ \tag{5.4}$$

The fractionation factor ε was -3.08±0.51 ‰ when the initial Cr(VI) concentration was 5 mg/L, -3.12±0.10 ‰ when it was 20 mg/L, and was -2.57±0.39 ‰ when it was 40 mg/L. The lower fractionation factor at high concentration may reflect the impact of chromium toxicity. However, since the differences between the groups having various initial Cr(VI) concentrations are small, it means that the isotope techniques can be applied over a wide range of Cr(VI) concentration.

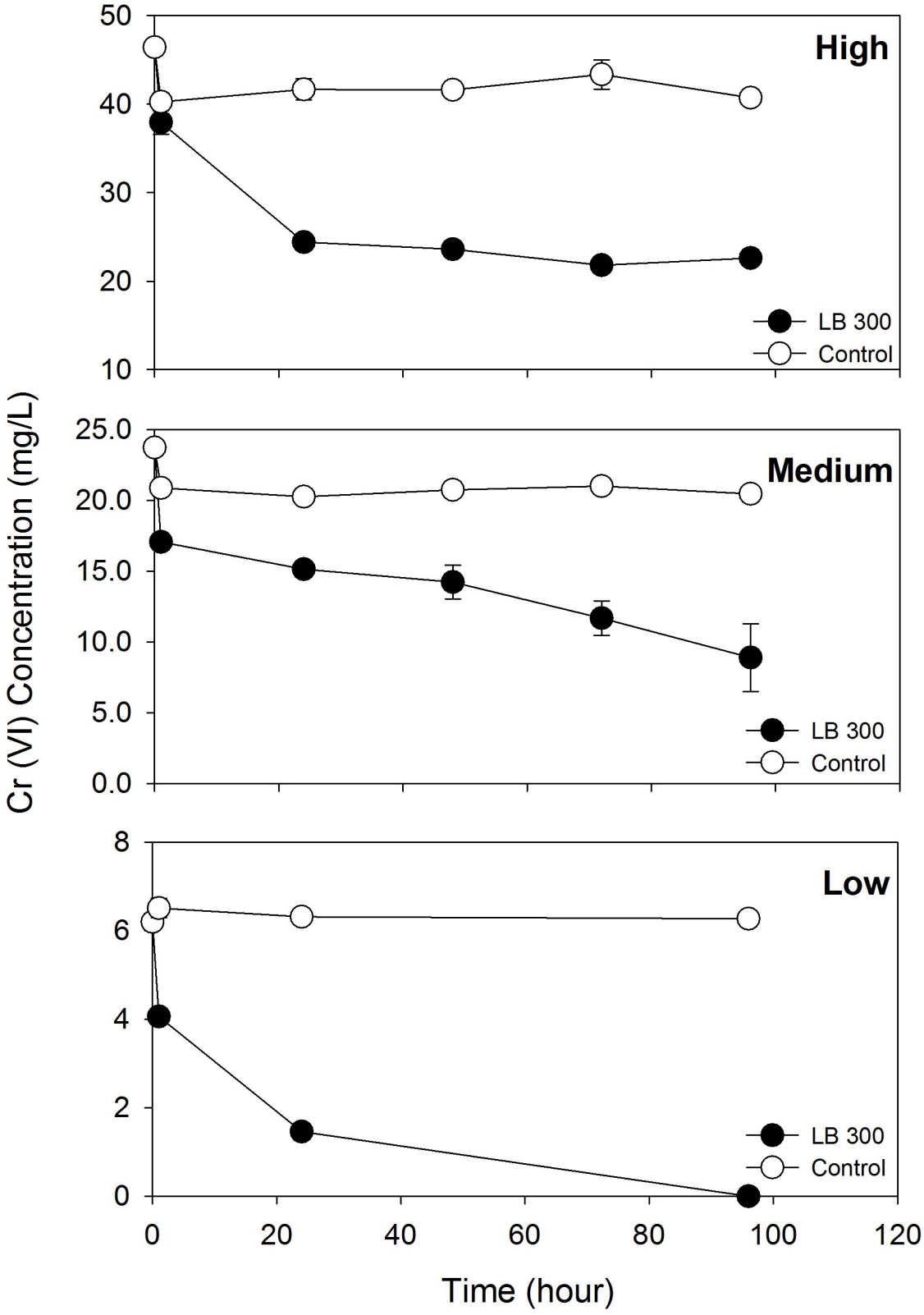


Figure 5.5: Chromium reduction experiments by *Pseudomonas fluorescens* LB 300 at high (40 mg/L), medium (20 mg/L) and low (5 mg/L) initial Cr concentration. Uncertainties in the experiment are expressed as standard deviation between the triplicates in each experimental group. Controls were prepared with the same amount of dead cells. Uncertainties are shown as standard deviation between the triplicates in each group.

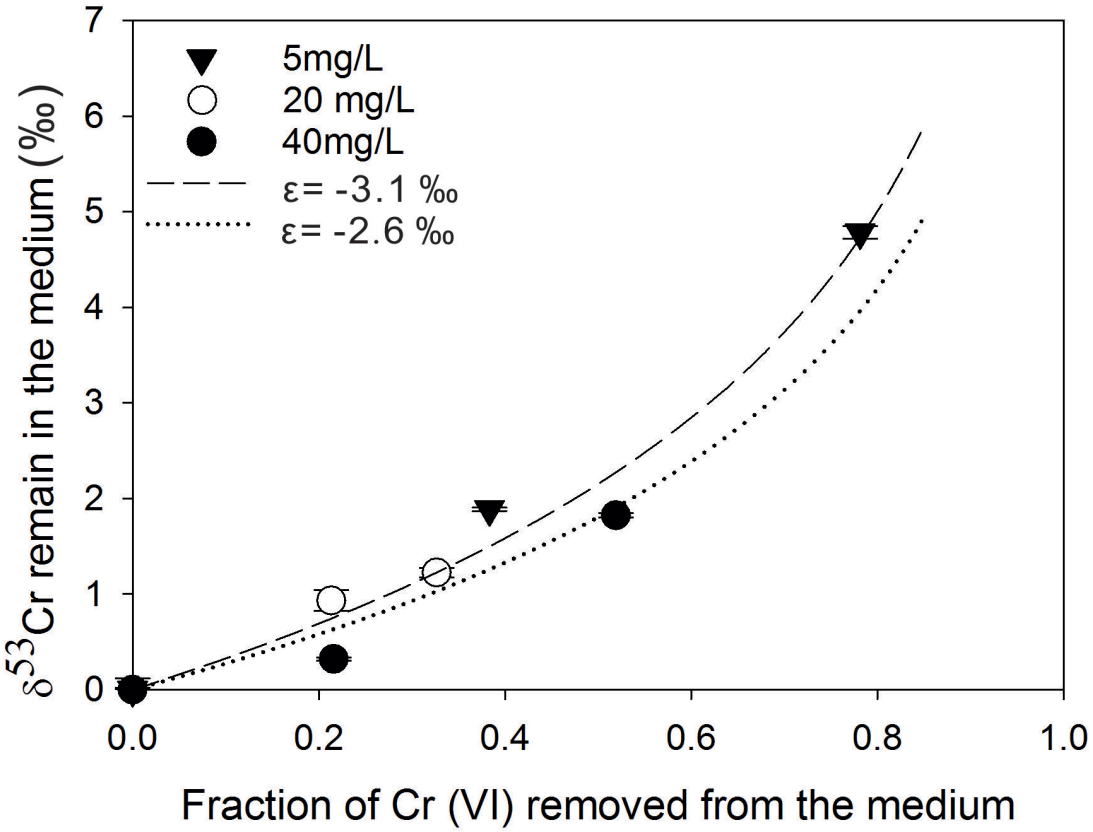


Figure 5.6: Isotope fractionation when reduced by *Pseudomonas fluorescens* LB 300 with different starting concentration of chromium. The fractionation factor ε = -3.1‰ when initial Cr (VI) was low or at medium level, and -2.6‰ when it was high. Uncertainties are shown as 2 × standard deviation for the measurement.

5.4 Discussion

Cr(VI) is toxic to most living organisms. Previous studies demonstrated that it can cause cellular oxidative stress and defense against its toxicity centres on activation of antioxidant mechanisms [*Ackerley et al.*, 2006]. It was also found that a soil microbial community responded to chromate pollution through changes in community structure, metabolic activity and also the selection of Cr(VI) resistance. Different microbes have different resistance to Cr toxicity, for example, *Pseudomonas* strains were found to be able to resist up to around 200 mg Cr(VI), and, cyanobacteria were found to be much more sensitive to chromium [*Viti et al.*, 2006].

Compared to Cr(III), Cr(VI) more readily penetrates cellular membranes and induces oxidative stress that causes cell membrane damages [*Xu et al.*, 2004]. When Cr(VI) enters into cells, it reacts with the intracellular reductants and generates the short lived intermediates Cr(V) and/or Cr(IV) that are ultimately reduced to Cr(III) in cells [*Xu et al.*, 2004, 2005]. In the cytoplasm, some of the Cr(V) generated can be reoxidized to Cr(VI) and produce a reactive oxygen species (ROS) that can easily combine with DNA-protein complexes; Cr(IV) is able to bind to cellular material, altering their physiological functions. Studies have shown that Cr(VI) could be transported through mammalian cell membranes by the carboxylate, sulphate and phosphate carrier systems.[*Bopp and Ehrlich*, 1988; *Michel et al.*, 2003].

Although there were many studies concerning the toxicity of Cr(VI), whole bioreporters have not been utilised to assess the toxicity of Cr species and concentrations. Among the known whole cell bioreporters, the enteric microorganism *E.coli* has been the most utilized [*Ackerley et al.*, 2006; *Llagostera et al.*, 1986]. However, it is not ideal for genotoxicity assessments in natural environments, because it requires an incubation temperature at 37 °C. Instead, the whole cell bioreporter ADPWH_*rec*A, which used the soil bacterium *Acinetobacter baylyi*ADP1 as the host, has a greater potential to assess the ambient environments. It has been shown to have high

sensitivity, specificity (to DNA damage), and robustness in various environments. Moreover, it is able to detect not only genotoxicity but also cytotoxicity, and has been used in various studies to test a variety of chemical compounds, including polycyclic aromatic hydrocarbons and other groundwater contaminants [*Song et al.*, 2009].

The chromosomally based ADPWH_*rec*A bioreporter can express bioluminescence in the presence of DNA damaging compounds. In the toxicity assessment in this study, a low concentration (5 mg/L) of Cr(VI) was found to induce a significant increase in the intensity of biolumenescence, whilst higher concentrations (20, 40 and 100 mg/L) decreased it, indicating that such high concentrations of Cr(VI) exceeded the cellular DNA repair capability. Similar discoveries were made with mitomycin C (MMC), which damages DNA by cross-linking DNA or protein [*Song et al.*, 2009]. In previous studies, it was found that a higher concentration of MMC induced a higher intensity of bioluminescence until the concentration was over 3 μM, when bioluminescence induction started to decrease [*Song et al.*, 2009, 2014].

The IR values from different groups after the experiments are shown in Fig 5.7. The dose response curve clearly shows that a higher Cr(VI) concentration causes greater inhibition to the generation of bioluminescence by the bacteria. In the presence of genotoxins, ADPWH_*rec*A can be induced to express bioluminescence and the induction ratio is then proportional to the dose (Fig. 5.4). However, in this study with Cr(VI) concentration over 5 mg/L, bioluminescence was clearly inhibited by higher concentrations of Cr(VI) (Fig. 5.2), which indicates that it is the cytotoxicity of Cr(VI), rather than genotoxicity, that is affecting the cells. A further evidence is that bacterial growth rate decreases at higher Cr(VI) concentration (slope of the growth curve, Fig. 5.1). It is also important to note that an increase of OD600 value can only indicate the increase to total cell number, but not viable cell number. It is highly possible that the number of viable cells that can generate bioluminescence decreased with higher Cr(VI) concentration, which results in a lower

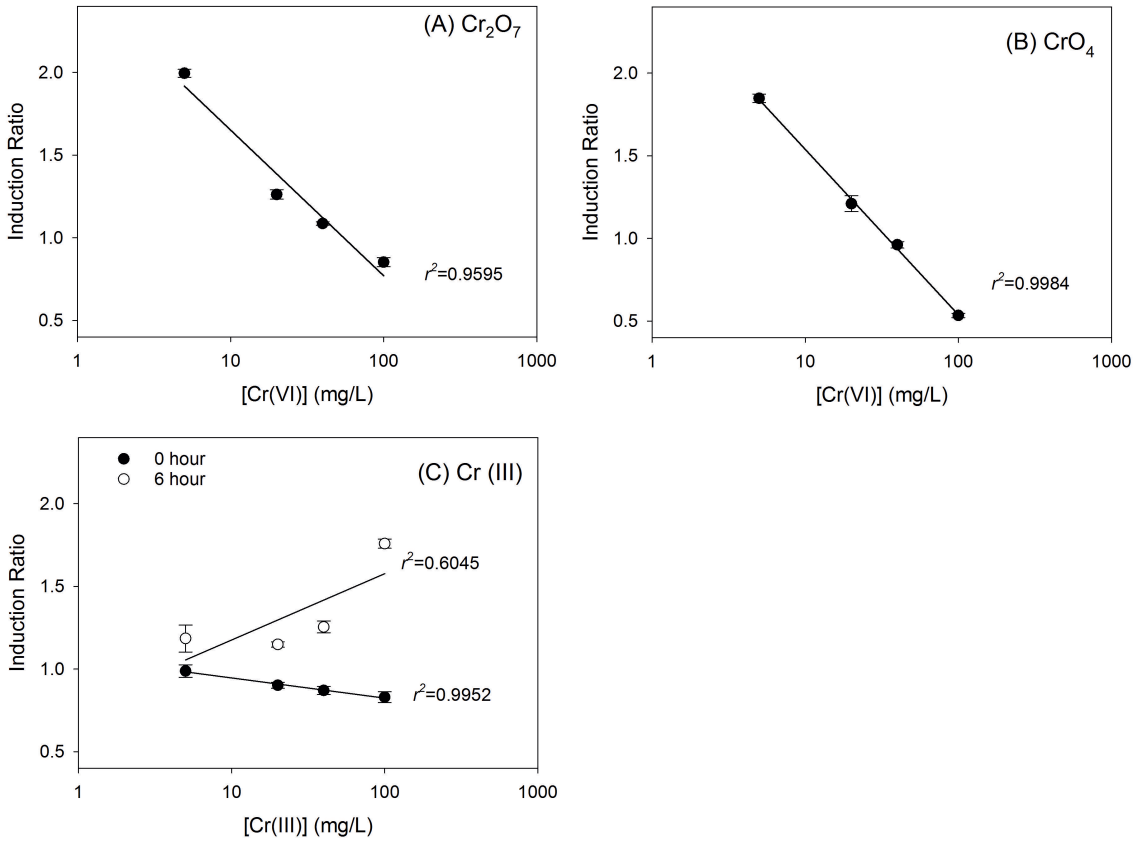


Figure 5.7: The response of ADPWH_*rec*A to different concentrations of $K_2Cr_2O_7$ (A) and K_2CrO_4 (B) after 6 hours of exposure and the response of ADPWH_*rec*A to different concentration of Cr(III) (C) in solution at time 0 and after 6 hours. The linear regression curve of the dose-responses are shown (solid line) respectively. Error bars represent the standard deviation of 3 replicates.

IR value compared with the control group. *Song et al.* [2014] have observed that Cr(VI) could be inhibiting the bioluminescence of another *Acinetobacter baylyi* based light-off bioreporter when the dose exceeded 5200ng/assay (26mg/L), which is in agreement with this study. The induction ratio from the experimental groups with 20 and 40 mg/L Cr(VI) were between 0.8 to 1.2, which is caused by the combination of both bioluminescence induction and inhibition of growth. It can be concluded from the results that Cr(VI) is both genotoxic and cytotoxic depending on the dose level.

Comparing Cr(VI) species, it is evident from Fig. 5.2 that CrO_4^{2-} was slightly more toxic to the bioreporter, especially at the highest concentration (100 mg/L).

However, this result is at odds with that of *Francisco et al.* [2010], in whose study dichromate was more toxic than chromate to the chromium-resistant and reducing strain *Ochrobactrum tritici* 5bvl1. This may be due to the difference in physiology between different species, especially between chromium resistant bacteria and non-resistant bacteria. A previous study indicated that the bioassay would be insensitive to Cr(VI) in either acute or chronic toxicity test if Cr(VI) reducing bacteria were used [*Fulladosa et al.*, 2006]. The bioreporter used in this study is a Cr non-resistant bacteria.

After reduction, Cr(III) is produced. Although Cr(III) is required for proper sugar and fat metabolism, some studies showed it could also be toxic to microbes by causing DNA damage [*Plaper et al.*, 2002] or changing pH [*Garcia et al.*, 1994] in the surrounding environment. Intracellular studies indicated that Cr(III)-DNA adducts and related hydroxyl radical oxidative DNA damage have a central role in originating the genotoxicities. In this study, the toxicity of Cr(III) was also assessed and demonstrated to be much lower than the toxicity of Cr(VI) (Figs. 5.1 and 5.2). However, although Cr(III) does not have a significant impact on bacterial growth ($p > 0.5$), the IR value increased with Cr(III) concentration, indicating it has genotoxicity to the bioreporter, particularly at the highest concentration (100 mg/L). These results suggested that even if Cr(VI) is reduced to Cr(III) by the bacteria, if the original concentration is too high, it may still cause a great problem to the environment, and therefore other techniques should be used to further immobilise Cr at such high concentration levels before it is released into the environment.

Cr isotopes were demonstrated to be good indicators of microbial Cr(VI) reduction. Various bacteria are reported to be able to reduce Cr(VI), and the corresponding isotope fractionation factors have been determined [*Basu and Johnson*, 2012; *Sikora et al.*, 2008; *Zhang et al.*, 2016], with ϵ value ranging between 1.5 ‰ to 5.0 ‰ and mean value of 3.3 ‰ [*Zhang et al.*, 2016]. The impact of a series of different environmental parameters on microbial Cr(VI) reduction and isotope frac-

tionation has been assessed in previous studies [*Zhang et al.*, 2016]. It was shown that pH and electron donors concentration do not have significant impact on microbial Cr isotope fractionation; however, the species of microbes, microbial respiration pathways involved, the type of electron donors, and the presence of some minerals significantly impacted bacterial Cr isotope fractionation [*Zhang et al.*, 2016]. Since there are big variations in Cr isotope fractionation factors, it is important to constrain Cr isotopes to different environments. In nature, the concentrations of Cr are very variable. It is between 25 to 5000 ng/L in rivers and lakes, and is about 5 to 900 ng/L in sea waters [*Bradl*, 2005]. In Cr contaminated sites, its concentration can be around 30 mg/L [*Stewart et al.*, 2007, 2010] or much higher [*Pinon-Castillo et al.*, 2010]. Since Cr(VI) concentrations vary in different environments, understanding the impact of its concentration on bacterial reduction and the consequent isotopic fractionation is necessary in order to better constrain Cr isotopes as an environmental diagnostic tool. However, this has not yet been studied before.

Although the toxicity of Cr_2O_7 and CrO_4^{2-} may be different to bacteria, the difference in speciation of Cr(VI) is shown to have insignificant impact on bacterial Cr isotope fractionation [*Zhang et al.*, 2016]. Therefore, in this study, Cr(VI) reduction experiments were only conducted with different concentrations of Cr_2O_7, by a Cr(VI) reducing bacteria *Pseudomonas fluorescens* LB 300. Higher reduction rates were found at higher initial concentrations, reflecting that bacteria adapted to the toxic environment. Similar results were also obtained in other studies [*Wang and Shen*, 1995]. Microbes used in bioremediation usually are highly resistant to the targeting toxic compounds. In this study, the bacteria used in the reduction experiment is also a species that can resist Cr toxicity to quite a high concentration [*Wang and Xiao*, 1995]. However, to ensure the sensitivity of bioreporters, the strains used always have a low tolerance to the toxic compounds. Therefore, if the Cr concentration in a particular site does not exceed the level in which Cr(VI) can severely damage the bioreporter, bioremediation can still be planned at such a site.

However, if the bioreporter is significantly damaged or killed by the toxins in a contaminated site, other physical or chemical remediation methods should be planned instead of using biological remediation methods.

In this study, the growth kinetic curves for the bioreporter from the 5 mg/L Cr(VI) group and the 20 mg/L Cr(VI) group showed no significant difference ($p > 0.05$) between each other; the group with 40 mg/L Cr(VI) has much lower growth rates (Fig5.1A). These results are consistent with the Cr isotope results, in which the fractionation factor was lower in 40 mg/L Cr(VI) group (2.57±0.39 ‰, Fig 5.6) than in the other two groups with lower Cr initial concentration (3.13±0.17 ‰, Fig 5.6). The small difference in the Cr isotopic fractionation factors between each group indicates that the reduction mechanisms may be similar under those conditions with different Cr initial concentrations. The toxicity of Cr(VI) at these concentrations do not have great impact on the microbially mediated Cr isotope fractionation, and therefore it can be used for indicating the extent of bioreduction at remediation sites. However, some other factors, such as bacteria species or mineral type in the contaminated area, may still have an impact on microbial Cr isotope fractionation [*Zhang et al.*, 2016]. Therefore, to better use Cr isotopes to accurately estimate the extent of Cr(VI) reduction, some lab experiments on natural samples are still required.

5.5 Conclusion

In this study, the toxicity of different species of Cr have been assessed using the whole cell bioreporter ADPWH_*rec*A over a wide range of concentrations. The bioreporter was found to be sensitive to both Cr(VI) and Cr(III). It can indicate genotoxicity of Cr(VI) at low concentration levels (< 5 mg/L) and cyto-toxicity at high concentration levels. Genotoxicity was also found with Cr(III), especially at the highest concentration (100mg/L). Cr bioreduction experiments were also conducted

at different high initial concentrations, and Cr isotope compositions were measured throughout the experiments. The isotopic fractionation factors obtained from the reduction experiments were found to be insensitive to different initial concentrations, indicating that bacteria use a similar reduction mechanism under these conditions, and the isotope technique can be applied to monitor the bioremediation process to estimate the extent of Cr reduction.

The study showed that the whole cell bioreporter ADPWH_*rec*A and Cr isotopes can be combined to first indicate the toxicity of Cr and provide background information to help plan a remediation strategy, and more importantly, to monitor the effectiveness of the end-point of bioremediation processes.

Chapter 6

Synthesis and Directions for Future Research

6.1 Summary of previous studies

The behaviour of Cr is quite complicated in the environment, and can be controlled by many different abiotic and biotic processes. The abiotic processes include adsorption by mineral surfaces, reduction by inorganic and organic reductants both in the dissolved phase and on mineral surfaces, and co-precipitation with other metals or carbonates. The biotic processes include reduction and incorporation by microbes, and uptake and transfer through food chains. The dominant process that controls Cr migration is dependent on the conditions in the surrounding environment. It has been well demonstrated that chromate is reduced by Fe(II), sulfides, and organic materials in the environment [*Kota and Stasicka*, 2000; *Stanin*, 2004]. The role of Fe(II) is especially important when biological activity is limited [*Fendorf and Li*, 1996]. Fe(II)(aq) concentrations and Fe(II)-bearing solids are prevalent under anoxic conditions, and they can dramatically affect Cr chemistry under such conditions. It was observed that Fe(II) species were the major reductant of Cr(VI) in sands or gravels of a suboxic aquifer under mildly reducing conditions [*Stanin*,

2004]. However, Fe(II) may not have a significant influence on Cr(VI) reduction in oxygenated systems, because aqueous Fe(II) may be oxidized to Fe(III) by dissolved O_2 at all but highly acidic pH (<3) [*Fendorf and Li*, 1996]. However, dissolution of Fe(II)-bearing minerals may significantly impact the reduction of Cr(VI) to Cr(III) even in oxygenated systems [*Eary and Rai*, 1989]. Cr(VI) reduction by Fe(II) has been reported to be a much faster process [*Dossing et al.*, 2011; *Kitchen et al.*, 2012; *Stanin*, 2004] than the observed biological process [*Wielinga et al.*, 2001].

Sulfides can be another major factor to reduce Cr(VI) to Cr(III). Some dissolved sulfides can be release to the environment through discharge of industrial wastes, the decomposition of organic matter, and sulfate reduction [*Stanin*, 2004]. *Kim et al.* [2001] have reported the reaction stoichiometry, kinetics, and mechanism for Cr(VI) reduction by hydrogen sulfide, and suggested a three-step mechanism: formation of an inner-sphere chromate-sulfide intermediate complex ($H_2O_4Cr^{VI}S^{2-}$), intramolecular electron transfer to form Cr(IV) species, and subsequent fast reactions leading to Cr(III). *Chen et al.* [2015] investigated the effects of pH on Cr(VI) reduction by Fe(II) and sulfide compounds, and observed that the sum of Cr(VI) removal by single Fe(II) and S(-II) was similar to that by the mixtures at pH 3.0-5.0 and pH 12.0. However, the removal of Cr(VI) by the mixtures was more effective than the sum of the single-species removals at pH 7.0-9.0. They suggested that the promoting effect was primarily attributed to the catalysis of ferric ion generated during the reduction process [*Chen et al.*, 2015].

As an essential micronutrient at low concentrations and a well-known toxin at high concentrations, Cr can interact with microbial communities in many ways. It can help microbes survive by facilitating glucose synthesis, and can also be toxic to them by inducing oxidative stress in cells. Any interactions with microbes may cause an isotope composition change in certain Cr species. For example, microbial reduction of Cr(VI) to Cr(III) results in an enrichment of light isotopes in the products(Cr(III)) and therefore a depletion of light isotopes in the Cr(VI) species. In

principle, different Cr(VI) reduction pathways by microbes can generate different isotope fractionation factors. If those isotope fractionation factors can be characterised and related to specific reduction processes, a better understanding of the mechanisms for Cr(VI) reduction can be obtained. In this study, the focus was on microbial control of Cr in the environment. The primary intention of this study is to establish isotope fractionation as an effective means to provide insight into the prevailing conditions in the habitat such as redox, pH, and concentration, and help further establish the technique for identifying environmental processes.

For this purpose, I have conducted Cr reduction experiments with two different bacteria, under a series of well controlled lab conditions. Some of the conditions, pH and electron donor concentration for instance, had a significant impact on bacterial Cr reduction rates but no detectable impact on Cr isotope fractionation. However, there also are some conditions that only have a great impact on the isotope fractionation factors but not on the reduction rates of Cr by bacteria. The most significant parameters that affected bacterial Cr isotope fractionation factors, as determined in this study, were bacterial species, their respiration pathways and the electron donors employed. Although the first intention was to investigate the difference in Cr isotope fractionation factors induced by biotic and abiotic processes, it turns out that the factors for these two sets of processes overlap with each other. The bacterial Cr isotope fractionation factors ranged from -1.5 ‰ to -5.0 ‰. Reported isotope data from abiotic reduction experiments are also mostly within that range, with the only exception being the data from *Ellis et al.* [2004] with respect to the equilibrium adsorption process. As was mentioned in Chapter 3, the inverse relationship between cellular-specific reduction rates and isotope fractionation factors, which was proposed in many previous studies [*Basu et al.*, 2014; *Sikora et al.*, 2008; *Wing and Halevy*, 2014], was not observed in this study. However, after plotting available data from various abiotic Cr reduction experiments by different reductants, an inverse relationship between the reduction rates and isotope fractionation factors

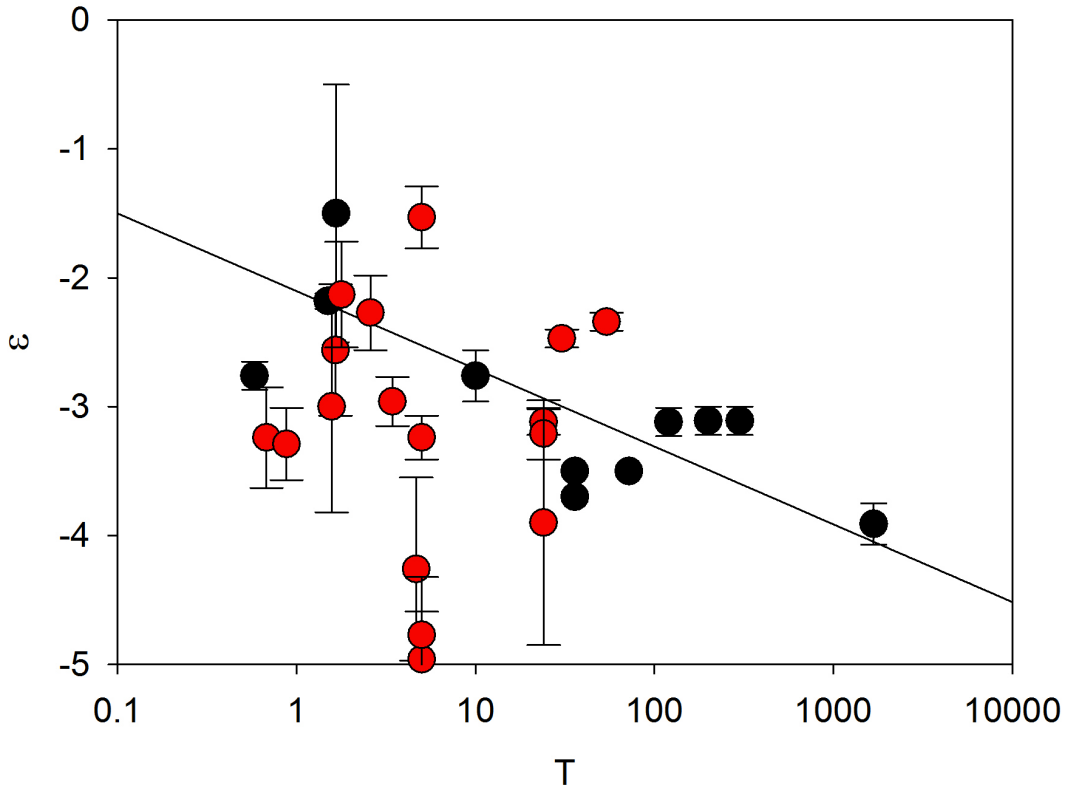


Figure 6.1: The relationship between Cr isotope fractionation factors and the half life of the reaction for abiotic Cr reduction experiments (black circles). The data are from *Ellis et al.* [2002], *Dossing et al.* [2011], *Basu and Johnson* [2012] and *Kitchen et al.* [2012]. Red circles are Cr isotope fractionation factors generated by bacterial Cr(VI) reduction from this study

was detected. Fig. 6.1 shows the relationship between isotope fractionation factors and the half life of the reaction. It is clear that the longer it takes to reduce Cr, the greater the isotope fractionation factor.

The nature of isotope fractionation factors in those reduction processes are impacted by the kinetic and mass-dependent effects. It must be noted that such relationship has also been reported for biotic reactions in some previous studies for Cr and S [*Basu et al.*, 2014; *Sikora et al.*, 2008; *Wing and Halevy*, 2014], but not observed in some other studies [*Kaplan and Rittenberg*, 1964; *Zhang et al.*, 2016]. In biotic reations, the inverse relationship between isotope fractionation factors and reduction rates may indicate kinetic fractionation of isotopes, but the reason for

such relationship was not fully understood and requires more study.

For those abiotic reactions, the relationship between isotope fractionation factors and reduction rates (in Fig. 6.1) may also indicate kinetic fractionation rather than equilibrium fractionation of Cr isotopes in those studies, and the isotope ratio shifts likely reflects the kinetic isotope effect accompanying the breakage of Cr-O bonds of the Cr(VI) oxyanions. However, in the natural environment, equilibrium fractionation of isotopes may be dominant. If the fractionation factors obtained from those abiotic studies only reflected kinetic isotope fractionation, more studies may be required to help determine whether these results are applicable to the natural environment.

To date, although it has been suggested that lighter isotopes are more reactive, but the extent to which these isotopes are more reactive compared to the heavier ones is unknown. We also do not know how different environmental factors can affect the behaviours of different elements, and how they impact the isotope fractionation processes. These questions certainly require more study.

6.2 Directions of future study

It is not possible to distinguish biotic and abiotic reduction processes by using Cr isotope data from the environment, especially when we consider the great variation of conditions in different environments. However, one can still have a picture of what may be the dominant process, when having some on-site data available, for example, the pH, temperature, and salinity. These parameters are important for both abiotic and biotic processes.

It may be particularly useful if data of concentrations and isotopic compositions are available for some other elements. For instance, Fe isotope data may provide useful complementary information. Fe isotopes have been studied for many decades, and it has been shown that microbial Fe(III) reduction produces the largest quan-

tities of isotopically distinct Fe by several orders of magnitude relative to abiotic reactions [*Johnson et al.*, 2008]. Fe and Cr are both redox sensitive, and many bacteria that are able to reduce Cr are also able to reduce iron [*Myers and Nealson*, 1990]. For the same species of bacteria, the mechanism for microbial iron reduction and Cr reduction may be similar [*Gorby et al.*, 2006; *Myers and Myers*, 1992; *Myers and Nealson*, 1990; *Myers et al.*, 2000; *Viamajala et al.*, 2002]. Moreover, Fe limitation is found to impact microbial S isotope fractionation [*Sim et al.*, 2012] by impairing the synthesis of cytochromes and hydrogenases, and hence reducing the flow of electrons to the sulphate reduction system. Such Fe limitation may also impact microbial Cr reduction system, because cytochromes and hydrogenases are also found to be responsible for Cr reduction in many species of bacteria [*Michel et al.*, 2001, 2003; *Myers and Myers*, 1992; *Sundararajan et al.*, 2011]. By combining information on different isotope systems (eg. Fe, S, Mo, Cd, and Cr etc.) in the environment, it may allow an integrated look into the biogeochemical cycling that occurred in nature [*Frei et al.*, 2013; *Johnson et al.*, 2008].

To remediate Cr-contaminated water and soils, the initial stages are often accomplished in a relatively short period of time by removing contaminant sources, removing highly contaminated shallow soils, or installing a low permeability cap. After that, remediation of the subsurface may require much longer time and substantial financial resources. Common strategies for Cr remediation include the no action option, pump-and-treat remediation, soil solidification/stabilization, and bioremediation [*Jeyasingh and Philip*, 2005; *Palmer and Wittbrodt*, 1991]. To find the optimal remedial strategies for the contaminated sites, some understanding of the physical and chemical processes affecting the migration and chemical state of Cr is required. For example, advection, dispersion, and diffusion are physical processes affecting the rate at which Cr can migrate in the subsurface. Redox reactions, chemical speciation, adsorption/desorption phenomena, and precipitation/dissolution reactions can control the transformation and mobility of Cr. Cr isotope variations are shown to

have potential to be diagnostic of specific processes [*Basu and Johnson*, 2012; *Ellis et al.*, 2002, 2004; *Kitchen et al.*, 2012], and such information have direct implication to the design of the remedial system. For example, Cr-contaminated groundwater could be remediated by passing through an engineered geochemical barrier, which contains a material that reacts with the Cr to enhance its removal. Ideally, such barrier should promote the reduction of Cr(VI) and the precipitation of Cr(III). However, some materials in the barrier may also adsorb Cr(VI). Adsorption reactions can only retard the rate of Cr(VI) migration through the barrier; it cannot prevent the migration of Cr(VI). Therefore, it is useful to distinguish between the reduction and adsorption of Cr(VI) in order to better evaluate such strategies. This can be easily done by measuring the variation of Cr isotopes [*Ellis et al.*, 2002, 2004]. Other examples may involve strategies such as the pump-and-treat method, which is one of the most commonly used methods for aquifer remediation. This strategy pumps contaminated water to the surface for treatment either on site or at treatment plant. By monitoring Cr isotopes from water in the extraction well, one may be able to determine the reduction capacity along the flow path [*Berna et al.*, 2010], or to tell whether any solid phase precipitates such as CaCrO4 and BaCrO4 have contributed to the Cr(VI) concentration by dissolution [*Palmer and Wittbrodt*, 1991]. Such information is important to determine the operation time for the pump-and-treat strategy, and to decide whether chemical enhancement should be added in the strategy. For sites with relatively low concentration of Cr(VI), bioremediation may be another option. Such strategy uses naturally occurring organisms to transform hazardous substances into less toxic substances, which can be applied both *in situ* and *ex situ*. Bioremediation has limitations that the contaminants have to be in a form that are bioavailable to microbes, and the toxicity level cannot be too high, otherwise it will significantly affect the efficiency of treatment. Therefore, the proper sites can be determined firstly by measuring the bioavailability and the toxicity level of Cr(VI) by microbial bioreporters, which have been described in chapter

5; secondly, by determining whether bioreduction is a more dominant process onsite. Many previous studies have demonstrated that the isotope signatures generated by abiotic reduction and biotic reduction are different [*Ellis et al.*, 2002; *Sikora et al.*, 2008]. By conducting site specific analysis, one may be able to determine whether bioreduction has great potential, further more to determine whether the remediation process can be accelerated by introducing more nutrients and oxygen to enhance the growth of the microorganisms capable of treating pollution.

Under well controlled conditions, I found distinctive Cr isotope fractionation factors generated by bacteria when using different electron donors, reflecting different bacterial Cr reduction pathways. This finding indicates the possibility of using isotope signatures as a tool to probe specific biochemical processes. Such possibility has not been widely considered before, but may be of great value with more studies being done.

To date, the mechanisms of microbial Cr reduction have not been well characterised. There are at least three important pathways for bacterial Cr reduction processes (chapter 4). The first involves proteins that are either membrane-bound or inside cells. This pathway requires direct contact between the bacteria and the metal. If the protein bound to the outer-membrane, the electron transfer process may occur on the cell surface; otherwise, reduction requires at least two steps. First is the transportation of Cr into the cell, and second is the electron transfer between the electron donors and acceptors, facilitated by enzymes. The second pathway is by producing extracellular electron shuttles to complete the electron transfer process. For example, *Shewanella oneidensis* MR-1 was demonstrated to be able to use flavin as an electron shuttle to facilitate long distance indirect electron transfer to the substrate [*Kotloski and Gralnick*, 2013]. The third pathway involves the production of the so-called 'nanowires'. The nanowires for *Shewanella oneidensis* MR-1 are believed to be extensions of the membrane compartments, and are found to have the ability for long distance electron transfer [*El-Naggar et al.*, 2010].

Different microbes can employ different electron transfer pathways for Cr(VI) reduction [*Christl et al.*, 2012; *Michel et al.*, 2001, 2003; *Myers et al.*, 2000; *Sultan and Hasnain*, 2012]. This has also been proved in my study, where the two species of bacteria generated different isotope fractionation factors for Cr(VI) reduction [*Zhang et al.*, 2016]. More interestingly, some species of microbes may be able to use multiple pathways simultaneously. The three electron transfer pathways for Cr reduction have been proposed separately in previous studies [*Gorby et al.*, 2006; *Lies et al.*, 2005; *Myers et al.*, 2000], but they have not been summarised and compared with each other. To my knowledge, no study has yet been done to determine when bacteria use different pathways and why they shift electron transfer pathways. Understanding the mechanisms of how different microbes obtain and transfer electrons can help understand complex biogeochemical processes, such as nutrient cycling, microbial dissolution of minerals, and biomineralisation. In my study, different Cr isotope fractionation factors were observed providing indirect evidence of different reduction mechanisms. However, further studies are still required to gain more direct evidence for microbial Cr reduction mechanisms. Based on my observation and hypothesis, there are several directions that can be explored to achieve a better understanding of the electron transfer processes. Such studies can also be applied to other elements, including Fe and S.

6.2.1 Intracellular or extracellular reactions?

Understanding the mechanisms of microbial metabolic pathways is useful for both studies of microbiology and geochemistry. Specifically, it is important to distinguish between the intracelluar and extracellular electron transfer pathways for microbes. Understanding the dominant pathway can provide a better perspective when assessing the biogeochemical processes in the natural environment. For example, extracellular electron transfer pathways allow microbes to transfer electrons to mineral surfaces without attaching to them, in which way long-distance microbial dissolution

of minerals can take place. With the change of specific environmental conditions, the dominant metabolic pathways for microbes may also change, which may have a great impact on their interactions with the abiotic environment [*Shimizu*, 2013]. However, microbial metabolic pathways are complicated and species dependent, and have not been well characterised with regard to different environments. Hence, more studies are required to address it.

There are several ways that may be useful in future studies trying to distinguish different electron transfer pathways. The first one involves using mutants that lack some electron transfer functions and use isotope signatures to indicate the difference between different pathways. For instance, *Gorby et al.* [2006] used a mutant of *Shewanella oneidensis* MR-1 to study the function of bacterial nanowires. Such mutants lack the *mtr*C and *omc*A genes that control decaheme cytochrome c complex production [*Gorby et al.*, 2006]. Although they can still produce extracelluar structures that have a similar appearance to those nanowires produced by wild-type MR-1, the conductivity of those structures are extremely poor. Their findings indicate that the mutants lose the ability to employ nanowires for electron transfer. However, they are still able to use other electron transfer pathways. As mentioned in Chapter 4, *Shewanella oneidensis* MR-1 is believed to be able to use all three pathways for electron transfer processes [*Gorby et al.*, 2006; *Lies et al.*, 2005; *Myers et al.*, 2000], and each pathway may generate a unique isotope fractionation factor during electron transfer processes. By conducting Cr(VI) (or other elements, such as Fe(III)) reduction experiments with both the mutants and the wild-type strains, and measuring the isotope fractionation factors, one may be able to obtain valuable information to help distinguish different reduction pathways. Also by comparing the isotope signatures obtained from the lab with those detected in the natural environment, one may be able to find the dominant pathways in nature under different conditions.

Other than using isotopes, distinguishing intracellular from extracellular path-

ways may also be achieved by using heavy water labelling. The work of *Berry et al.* [2014] demonstrated that, after treatment with 40% heavy water, physiologically active cells can be rapidly identified with Raman microspectroscopy, by measuring cellular D incorporation. When bacteria employ intracellular pathways to transfer electrons, they have to be metabolically active, and therefore can be detected by deuterium labelling. That is to say, comparing the Raman spectra of the cells that are in the control group (without Cr) with those actively reducing Cr, it is possible to see an increase of the D peak in the cells in the Cr reduction group. If the cells are using extracellular electron transfer pathways, they may incorporate the similar amount of heavy water as in the control group, because the electron transfer processes are taking place outside the cells. But this need to be further confirmed with more lab based experiments.

6.2.1.1 Study of intracellular pathways-the role of metals

The intracellular pathway for electron transfer is a complex process, which may involve many different enzymes. The enzymatic study for Cr(VI) reduction has been carried out for many years, with several useful enzymes discovered and characterised [*Michel et al.*, 2001, 2003]. But Cr isotope measurements have not been used to help understand the role of individual proteins in isotope fractionation. Thus, further study can be carried out to determine the reduction of Cr by individual enzymes and the correspondent isotope fractionation factors. If Cr isotope signatures generated by different enzymes can be well characterised, they may be used to indicate specific biological processes by different enzymes. Such a study may involve extraction and separation of useful enzymes, determination of their functions in Cr reduction processes, characterisation of the enzymatic reduction processes, finding the corresponding genome frames, and determination of Cr isotope fractionation factors. Based on the experimental results, quantitative models may be built up to determine Cr isotope behaviour under more complex environmental conditions,

and to predict Cr cycling patterns in the environment. A similar model has been proposed by *Wing and Halevy* [2014] for microbial S reduction. These techniques can also be expanded to study microbial metabolism of other metals, to find potential roles of different metals in metalloproteins formation and function, and even to study microbe-driven activities in the human body.

6.2.1.2 Study of extracellular pathways

The two major extracellular electron transfer pathways, via electron shuttles (ESs) or nanowires, have been studied for several decades [*Gorby et al.*, 2006; *Lies et al.*, 2005]. However, only limited data are available to explain the mechanisms involved. There are still many questions; for example, how do bacteria produce electron shuttles or nanowires? What triggers their production? What is the structure for the nanowires? To answer these questions, more research needs to be done.

Electron shuttles are compounds that can be reduced and re-oxidised. They can transfer electrons between bacteria and extracellular electron donors or acceptors. Common electron shuttles include flavin, phenazines and humic substances [*Lies et al.*, 2005]. Future studies on electron shuttles should focus on their structure, production, transformation and distribution.

Bacterial nanowires are found in many species, including *Geobacter*, *Shewanella*, *Synechocystis*, and *Pelotomaculum* [*Boesen and Nielsen*, 2013; *El-Naggar et al.*, 2010; *Gorby et al.*, 2006; *Pirbadian et al.*, 2014; *Reguera et al.*, 2005]. Although it has been demonstrated that these bacteria can use their wires for electron transfer, the mechanisms involved are not clear yet. Two hypotheses, metal-like conductivity (MLC) and superexchange conductivity (SEC), have been proposed in previous studies [*Boesen and Nielsen*, 2013; *Vargas et al.*, 2013]. In the former hypothesis, the pilus produced by bacteria has electron-conductive properties and has cytochromes attached that mediate electron transfer to the final acceptor. In the latter, heme groups in cytochromes play the most important role in the process, and the electrons

hop between those aligned with the pilus. Further study can be designed to test these hypotheses, by addressing the structures and functions of nanowires.

6.2.2 Applications

Although this study was focused on Cr, the research methods and implications are not restricted to this element. There are many elements that have different oxidation states in the environment, such as Mo, Fe, and S. The methods in this study, as well as those suggested for future research, can also be applied to these elements. With more and more isotope fractionation factors of different elements characterised, our knowledge of geochemical processes can be enhanced, and we will be able to know more about the interactions between the biosphere and the environment.

Isotope techniques can also be used to monitor remediation processes for heavy metals, such as Cr and Cd [*Berna et al.*, 2010; *Wasylenki et al.*, 2014], or to trace the migration of the contaminants [*Frei et al.*, 2014].

Moreover, the similar application of isotope techniques as in this study can also be applied to those concerning microbial processes in human body [*Monachese et al.*, 2012]. For example, human gastrointestinal bacteria such as *Lactobacillus*, are able to bind and detoxify some heavy metals in human body from food contamination [*Monachese et al.*, 2012]. Isotope techniques may be useful to help understand the mechanisms involved in such detoxification processes. In addition, isotope signatures may also be useful as indicators of specific disease, such as breast cancer [*Larner et al.*, 2015].

The study about extracellular electron transfer processes is also applicable in technology development, including bioremediation, biosensor development, and optimisation of the activity of microbial fuel cells.

References

Ackerley, D. F., C. F. Gonzalez, C. H. Park, R. Blake, A. Keyhan, and A. Matin (2004a), Chromate-reducing properties of soluble Flavoproteins from *Pseudomonas putida* and *Escherichia coli*, *Applied and Environmental Microbiology*, *70*(2), 873–882.

Ackerley, D. F., C. F. Gonzalez, M. Keyhan, R. Blake, and A. Matin (2004b), Mechanism of chromate reduction by the Escherichia coli protein, NfsA, and the role of different chromate reductases in minimizing oxidative stress during chromate reduction, *Environmental Microbiology*, *6*(8), 851–860.

Ackerley, D. F., Y. Barak, S. V. Lynch, J. Curtin, and A. Matin (2006), Effect of chromate stress on *Escherichia coli* K-12, *Journal of Bacteriology*, *188*(9), 3371–3381.

Antonini, J. M., and J. R. Roberts (2007), Chromium in stainless steel welding fume suppresses lung defense responses against bacterial infection in rats, *Journal of Immunotoxicology*, *4*(2), 117–127.

Antunes, V. H., A. Candeias, M. J. Oliveira, and M. Carvalho (2014), Characterization of gypsum and anhydrite ground layers in 15th and 16th centries portuguese paintings by raman spectroscopy and other techniques, *Journal of Raman Spectroscopy*, *45*, 11–12.

Banerjee, D., and H. W. Nesbitt (1999), Oxidation of aqueous Cr(III) at birnessite

surfaces: Constraints on reaction mechanism, *Geochimica Et Cosmochimica Acta*, *63*(11-12), 1671–1687.

Baralkiewicz, D., and J. Siepak (1999a), Chromium, nickel and cobalt in environmental samples and existing legal norms, *Polish Journal of Environmental Studies*, *8*(4), 201–208.

Baralkiewicz, D., and J. Siepak (1999b), Speciation analysis of chromium(III) and (VI) in natural water samples by graphite furnace atomic absorption spectrometry, *Chemia Analityczna*, *44*(5), 879–884.

Basu, A., and T. M. Johnson (2012), Determination of Hexavalent Chromium Reduction Using Cr Stable Isotopes: Isotopic Fractionation Factors for Permeable Reactive Barrier Materials, *Environmental Science & Technology*, *46*(10), 5353–5360.

Basu, A., T. M. Johnson, and R. A. Sanford (2014), Cr isotope fractionation factors for Cr(VI) reduction by a metabolically diverse group of bacteria, *Geochimica et Cosmochimica Acta*, *142*(0), 349–361.

Beard, B. L., and C. M. Johnson (1999), High precision iron isotope mmeasurement of terrestrial and lunar materials, *Geochimica Et Cosmochimica Acta*, *63*, 1653–1660.

Berna, E. C., T. M. Johnson, R. S. Makdisi, and A. Basui (2010), Cr stable isotopes as indicators of Cr(VI) reduction in groundwater: A detailed time-series study of a point-source plume, *Environmental Science & Technology*, *44*(3), 1043–1048.

Berry, D., E. Mader, T. K. Lee, D. Woebken, Y. Wang, D. Zhu, M. Palatinszky, A. Schintlmeister, M. C. Schmid, B. T. Hanson, N. Shterzer, I. Mizrahi, I. Rauch, T. Decker, T. Bocklitz, J. Popp, C. M. Gibson, P. W. Fowler, W. E. Huang, and M. Wagner (2014), Tracking heavy water (D2O) incorporation for identifying and

sorting active microbial cells, *Proceedings of the National Academy of Sciences, E*, 194–203.

Bigeleisen, J., and M. G. Mayer (1947), Calculations of equilibrium constants for isotopic exchange reactions, *Journal of Chemical Physics*, *15*, 261–267.

Bni, r., R. Karosi, and J. Posta (2007), Speciation of hexavalent chromium in waters by liquid liquid extraction and GFAAS determination, *Microchemical Journal*, *85*(1), 103–108.

Boesen, T., and L. P. Nielsen (2013), Molecular dissection of bacterial nanowires, *mBio*, *4*(3), e00,270–12, doi:10.1128/mBio.00270-13.

Bopp, L., and H. Ehrlich (1988), Chromate resistance and reduction in *Pseudomonas fluorescens* strain LB300, *Archives of Microbiology*, *150*(5), 426–431.

Bopp, L., A. M. Chakrabarty, and H. Ehrlich (1983), Chromate resistance plasmid in *Pseudomonads fluorescens.*, *Journal of Bacteriology*, *155*(3), 1105–1109.

Bradl, H. (2005), *Heavy Metals in the Environment: Origin, Interaction and Remediation*, Academic Press.

Brown, G. E., T. Trainor, and A. M. Chaka (2008), *Chemical Bonding at Surfaces and Interfaces*, chap. Geochemistry of mineral surfaces and factors affecting their chemical reactivity, pp. 457–509, Elsevier.

Buerge, I. J., and S. J. Hug (1999), Influence of mineral surfaces on Chromium(VI) reduction by Iron(II), *Environmental Science & Technology*, *33*(23), 4285–4291.

Campanella (1996), *Element speciation in bioinorganic chemistry*, Wiley Interscience, New York.

Canfield, D. E. (2001), Biogeochemistry of sulfur isotopes, *Stable Isotope Geochemistry*, *43*, 607–636.

Carter, P. (1971), Spectrophotometric determination of serum iron at the submicrogram level with a new reagent (ferrozine), *Analytical Biochemistry*, *40*, 450–458.

Chen, J., R. Chen, and M. Hong (2015), Influence of pH on hexavalent chromium reduction by Fe(II) and sulfide compounds, *Water Science and Technology*, *72*(1), 22–28.

Cheng, Y. J., F. B. Yan, F. Huang, W. S. Chu, D. M. Pan, Z. Chen, J. S. Zheng, M. J. Yu, Z. Lin, and Z. Y. Wu (2010), Bioremediation of Cr(VI) and Immobilization as Cr(III) by *Ochrobactrum anthropi*, *Environmental Science & Technology*, *44*(16), 6357–6363.

Cheung, K., and J. Gu (2007), Mechanism of hexavdalent chromium detoxification by microorganisms and bioremediation application potential: A review, *International Biodeterioration & Biodegradation*, *59*, 8–15.

Chirwa, E. N., and Y. T. Wang (2000), Simultaneous chromium(VI) reduction and phenol degradation in an anaerobic consortium of bacteria, *Water Research*, *34*(8), 2376–2384.

Chorover, J., R. Kretzschmar, F. Garcia-Pichel, and D. L. Sparks (2007), Soil biogeochemical processes within the critical zone., *Elements*, *3*, 321–326.

Christl, I., M. Imseng, E. Tatti, J. Frommer, C. Viti, L. Giovannetti, and R. Kretzschmar (2012), Aerobic Reduction of Chromium(VI) by *Pseudomonas corrugata* 28: Influence of Metabolism and Fate of Reduced Chromium, *Geomicrobiology Journal*, *29*(2), 173–185.

Ciavatta, C., C. Manoli, L. Cavani, C. Franceschi, and P. Sequi (2012), Chromium-containing organic fertilizers from tanned hides and skins: A review on chemical, environmental, agronomical and legislative aspects, *Journal of Environmental Protection*, *3*(11), 1532–1541.

Cutting, R. S., V. S. Coker, J. W. Fellowers, J. R. Lloyd, and D. J. Vaughan (2009), Mineralogical and morphological constraints on the reduction of Fe(III) minerals by *Geobacter sulfurreducens*, *Geochimica Et Cosmochimica Acta*, *73*(14), 4004–4022.

Das, S., and M. J. Hendry (2011), Application of raman spectroscopy to identify iron minerals cocommon found in mine wastes, *Chemical Geology*, *290*, 101–108.

Dayan, A., and A. Paine (2001), Mechanisms of chromium toxicity, carcinogenicity and allergenicity: Review of the literature from 1985 to 2000, *Human and Experimental Toxicology*, *20*, 439–451.

de Faria, D. L. A., S. V. Silva, and M. T. de Oliveira (1997), Raman microspectroscopy of some iron oxides and oxyhydroxides, *Journal of Raman Spectroscopy*, *28*, 873–878.

Desai, C., K. Jain, and D. Madamwar (2008), Evaluation of *in vitro* Cr(VI) reduction potential in cytosolic extracts of three indigenous *Bacillus sp* isolated from Cr(VI) polluted industrial landfill, *Bioresource Technology*, *99*(14), 6059–6069.

Dossing, L. N., K. Dideriksen, S. L. S. Stipp, and R. Frei (2011), Reduction of hexavalent chromium by ferrous iron: A process of chromium isotope fractionation and its relevance to natural environments, *Chemical Geology*, *285*(1-4), 157–166.

Druhan, J. L., C. I. Steefel, M. E. Conrad, and D. J. DePaolo (2014), A large column analog experiment of stable isotope variations during reactive transport: I. A comprehensive model of sulfur cycling and delta S-34 fractionation, *Geochimica Et Cosmochimica Acta*, *124*, 366–393.

Eary, L., and D. Rai (1989), Kinetics of chromate reduction by ferrous ions derived from hematite and biotite at 25 °C, *American Journal of Science*, *289*, 180–213.

El-Naggar, M. Y., G. Wanger, K. M. Leung, T. D. Yuzvinsky, G. Southam, J. Yang, W. M. Lau, K. H. Nealson, and Y. A. Gorby (2010), Electrical transport along bacterial nanowires from *shewanella oneidensis* MR-1, *Proceedings of the National Academy of Sciences*, *107*(42), 18,127–18,131.

Ellis, A. S., T. M. Johnson, and T. D. Bullen (2002), Chromium isotopes and the fate of hexavalent chromium in the environment, *Science*, *295*(5562), 2060–2062.

Ellis, A. S., T. M. Johnson, and T. D. Bullen (2004), Using chromium stable isotope ratios to quantify Cr(VI) reduction: Lack of sorption effects, *Environmental Science & Technology*, *38*(13), 3604–3607.

Fein, J. B., D. A. Fowle, J. Cahill, K. Kemner, M. Boyanov, and B. Bunker (2002), Nonmetabolic reduction of Cr(VI) by bacterial surfaces under nutrient-absent conditions, *Geomicrobiology Journal*, *19*(3), 369–382.

Fendorf, S., and G. Li (1996), Kinetics of chromate reduction by ferrous iron, *Environmental Science & Technology*, *30*, 1614–1617.

Feng, X. H., L. M. Zhai, W. F. Tan, W. Zhao, F. Liu, and J. Z. He (2006), The controlling effect of pH on oxidation of Cr(III) by manganese oxide minerals, *Journal of Colloid and Interface Science*, *298*(1), 258–266.

Fengdorf, S. E. (1995), Surface reactions of chromium in soils and waters, *Geoderma*, *67*, 55–71.

Francisco, R., A. Moreno, and P. V. Morais (2010), Different physiological responses to chromate and dichromate in the chromium resistant and reducing strain *Ochrobactrum tritici* 5bvl1, *Biometals*, *23*, 713–725.

Frei, R., and A. Polat (2013), Chromium isotope fractionation during oxidative weathering-Implications from the study of a Paleoproterozoic (ca. 1.9 Ga) paleosol, Schreiber Beach, Ontario, Canada, *Precambrian Research*, *224*, 434–453.

Frei, R., C. Gaucher, D. Stolper, and D. E. Canfield (2013), Fluctuations in late Neoproterozoic atmospheric oxidation Cr isotope chemostratigraphy and iron speciation of the late Ediacaran lower Arroyo del Soldado Group (Uruguay), *Gondwana Research*, *23*(2), 797–811.

Frei, R., D. Poir, and K. M. Frei (2014), Weathering on land and transport of chromium to the ocean in a subtropical region (Misiones, NW Argentina): A chromium stable isotope perspective, *Chemical Geology*, *381*(0), 110–124.

Fulladosa, E., V. Desjardin, J. C. Murat, R. Gourdon, and I. Villaescusa (2006), Cr(VI) reduction into Cr(III) as a mechanism to explain the low sensitivity of *Vibrio fischeri* bioassay to detect chromium pollution, *Chemosphere*, *65*(4), 644–650.

Gadd, G. M. (2010), Metals, minerals and microbes: geomicrobiology and bioremediation, *Microbiology*, *156*, 609–643.

Galer, S. J. G. (1999), Optimal double and triple spiking for high precision lead isotopic measurement, *Chemical Geology*, *157*(3-4), 255–274.

Gao, X. D., and D. G. Schulze (2010), Chemical and mineralogical characterization of arsenic, lead, chromium, and cadmium in a metal-contaminated histosol, *Geoderma*, *156*(3-4), 278–286.

Garcia, M. T., I. Ribosa, L. Perez, and J. S. Leal (1994), The environmental-impact of chromium salts - ecotoxicity and inhibition of surfactant biodegradation, *Toxicological and Environmental Chemistry*, *44*(3-4), 225–232.

Gluenz, E., R. J. Wheeler, L. Hughes, and S. Vaughan (2015), Scanning and three-dimensional electron microscopy methods for the study of *Trypanosoma brucei* and *Leishmania mexicana* flagella, *Methods in Cell Biology*, *127*, 509–542.

Gorby, Y. A., S. Yanina, J. S. Mclean, K. M. Rosso, D. Moyles, A. Dohnalkova, T. J. Beveridge, I. S. Chang, B. H. Kim, K. S. Kim, D. E. Culley, S. B. Reed, M. F. Romine, D. A. Saffarini, H. E. A., L. Shi, D. Elias, D. W. Kennedy, G. Pinchuk, K. Watanabe, S. Ishii, B. Logan, K. H. Nealson, and J. K. Fredrickson (2006), Electrical conductive bacterial nanowires produced by *Shewanella oneidensis* Strain MR-1 and other Microorganisms, *Proceedings of the National Academy of Sciences*, *103*(30), 11,358–11,363.

Guha, H., K. Jayachandran, and F. Maurrasse (2001), Kinetics of chromium (VI) reduction by a type strain Shewanella alga under different growth conditions, *Environmental Pollution*, *115*(2), 209–218.

Habicht, K. S., and D. E. Canfield (1997), Sulfur isotope fractionation during bacterial sulfate reduction in organic-rich sediments, *Geochimica Et Cosmochimica Acta*, *61*(24), 5351–5361.

Han, R. Y., L. P. Qin, S. T. Brown, J. N. Christensen, and H. R. Beller (2012), Differential isotopic fractionation during Cr(VI) reduction by an aquifer-derived bacterium under aerobic versus denitrifying conditions, *Applied and Environmental Microbiology*, *78*(7), 2462–2464.

Hanesch, M. (2009), Raman spectroscopy of iron oxides and oxy(hydroxides) at lower laser power and possible application in environmental magnetic studies, *Geophysical Journal International*, *177*, 941–948.

Harrison, A. G., and H. G. Thode (1958), Mechanism of the bacterial reduction of sulphate from isotope factionation studies, *Transactions of the Faraday Society*, *54*, 84–92.

Hart, S. R., and A. Zindler (1989), Isotope fractionation laws: A test using calcium, *International Journal of Mass Spectrometry and Ion Processes*, *89*, 287–301.

He, M. Y., X. Y. Li, H. L. Liu, S. J. Miller, G. J. Wang, and C. Rensing (2011), Characterization and genomic analysis of a highly chromate resistant and reducing bacterial strain *Lysinibacillus fusiformis* ZC1, *Journal of Hazardous Materials*, *185*(2-3), 682–688.

Hochella, M. (2002), Sustaining earth: thoughts on the present and future roles in mineralogy in environmental science, *Mineral magazine*, *66*, 627–652.

Hoefs, J. (2004), *Stable isotope geochemistry*, Springer-Verlag Berlin Heidelberg New York.

Hossain, M. A., M. Alam, D. Yonge, and P. Dutta (2005), Finite element modeling of cr(vi) reduction by shewanella oneidensis mr-1 employing the dual-enzyme kinetic model, *Computers & Geosciences*, *31*(10), 1286–1292.

Huang, P., M. Wang, and M. Wang (2004), Mineral-organic-microbial interactions, in *Encyclopedia of soils in the environment*, edited by D. Hillel, C. Rosenzweig, D. Powlson, K. Scow, M. Singer, D. Sparks, and J. Hatfield, pp. 486–499, Elsevier.

Huang, W. E., H. Wang, H. Zheng, L. Huang, A. Singer, I. Thompson, and A. Whiteley (2005), Chromosomally located gene fusions constructed in Acinetobacter sp. ADP1 for the detection of salicylate, *Environmental microbiology*, *7*, 1339–1348.

Izbicki, J. A., T. D. Bullen, P. Martin, and P. Schroth (2012), Delta chromium-53/52 isotopic composition of native and contaminated groundwater, mojave desert, usa., *Applied Geochemistry*, *27*, 841–853.

Jeyasingh, J., and L. Philip (2005), Bioremediation of chromium contaminated soil: optimization of operating parameters under laboratory conditions, *Journal of Hazardous Materials*, *118*(1-3), 113–120.

Jiang, B., D. Zhu, Y. Song, D. Zhang, Z. Liu, X. Zhang, W. E. Huang, and G. Li (2015), Use of a whole-cell bioreporter, *Acinetobacter baylyi*, to estimate the geno-

toxicity and bioavailability of chromium(VI)-contaminated soils, *Biotechnol Letters*, *37*, 343–348.

Johnson, C. M., and B. L. Beard (1999), Correction of instrumentally produced mass fractionation during isotopic analysis of Fe by thermal ionization mass spectrometry, *International Journal of Mass Spectrometry*, *193*, 87–99.

Johnson, C. M., B. L. Beard, and E. Roden (2008), The iron isotope fingerprints of redox and biogeochemical cycling in modern and ancient earth, *Annual Review of Earth and Planetary Sciences*, *36*, 457–493.

Johnson, T. M., and T. D. Bullen (2004), Mass-dependent fractionation of selenium and chromium isotopes in low-temperature environments., *Geochemistry of Non-Traditional Stable Isotopes*, *55*, 289–317.

Joutey, N., W. Sayel, H. Bahafid, and N. El-Ghachtouli (2015), Mechanisms of hexavalent chromium resistance and removal by microorganisms, *Reviews of Environmental Contamination and Toxicology*, *233*, 45–69.

Kantar, C., Z. Cetin, and H. Demiray (2008), *In situ* stabilization of chromium(VI) in polluted soils using organic ligands: The role of galacturonic, glucuronic and alginic acids, *Journal of Hazardous Materials*, *159*(2-3), 287–293.

Kaplan, I. R., and S. C. Rittenberg (1964), Microbiological fractionation of sulphur isotopes, *Journal of General Microbiology*, *34*(2), 195–212.

Kieber, R. J., and G. R. Helz (1992), Indirect photoreduction of aqueous chromium(VI), *Environmental Science & Technology*, *26*(2), 307–312.

Kim, C., Q. Zhou, B. L. Deng, E. C. Thornton, and H. Xu (2001), Chromium(VI) reduction by hydrogen sulfide in aqueous media: stoichiometry and kinetics, *Environmental Science & Technology*, *35*(11), 2219–2225.

Kitchen, J. W., T. M. Johnson, T. D. Bullen, J. M. Zhu, and A. Raddatz (2012), Chromium isotope fractionation factors for reduction of Cr(VI) by aqueous Fe(II) and organic molecules, *Geochimica Et Cosmochimica Acta*, *89*, 190–201.

Kota, J., and Z. Stasicka (2000), Chromium occurrence in the environment and methods of its speciation, *Environmental Pollution*, *107*(3), 263 – 283, doi:http://dx.doi.org/10.1016/S0269-7491(99)00168-2.

Kotloski, N. J., and J. A. Gralnick (2013), Flavin Electron Shuttles Dominate Extracellular Electron Transfer by *Shewanella oneidensis*, *mBio*, *4*(1), e00,553–12, doi:10.1128/mBio.00553-12.

Kourtev, P. S., C. H. Nakatsu, and A. Konopka (2006), Responses of the anaerobic bacterial community to addition of organic c in chromium(VI)- and iron(III)-amended microcosms, *Applied and Environmental Microbiology*, *72*(1), 628–637.

Kraemer, S. M., S. F. Cheah, R. Zapt, J. D. Xu, K. N. Raymond, and G. Sposito (1999), Effect of hydroxamate siderpphores on fe release and Pb(II) adsorption by goethite, *Geochimica Et Cosmochimica Acta*, *63*, 3003–3008.

Kumpulainen, S., F. Von der Kammer, and T. Hofmann (2008), Humic acid adsorption and surface charge effects on schwertmannite and goethite in acid sulphate waters, *Water Re*, *42*(8-9), 2051–2060.

Landrot, G., M. Ginder-Vogel, K. Livi, J. P. Fitts, and D. L. Sparks (2012), Chromium(III) oxidation by three poorly crystalline manganese(IV) oxides. 2. solid phase analyses, *Environmental Science & Technology*, *46*(21), 11,601–11,609.

Larner, F., L. N. Woodley, S. Shousha, A. Moyes, E. Humphreys-Williams, S. Strekopytov, A. N. Halliday, M. Rehkamper, and R. C. Coombes (2015), Zinc isotopic compositions of breast cancer tissue, *Metallomics*, *7*, 112–117, doi:10.1039/C4MT00260A.

Legodi, M. A., and D. de Waal (2007), The preparation of magnetite, goethite, hematite and maghemite of pigment quality from mill scale iron waste., *Dyes and Pigments*, *74*, 161–168.

Libes, S. M. (1992), *An Introduction to marine Biogeochemistry*, John Viley & Sons, Inc.

Lies, D. P., M. E. Hernandez, A. Kappler, R. E. Mielke, J. A. Gralnick, and D. K. Newman (2005), *Shewanella oneidensis* MR-1 uses overlapping pathways for iron reduction at a distance and by direct contact under conditions relevant for biofilms, *Applied and Environmental Microbiology*, *71*(8), 4414–4426.

Liu, C. X., S. Kota, J. M. Zachara, J. K. Fredrickson, and C. K. Brinkman (2001), Kinetic analysis of the bacterial reduction of goethite, *Environmental Science & Technology*, *35*(12), 2482–2490.

Llagostera, M., S. Garrido, R. Guerrero, and J. Barbe (1986), Inducation of SOS genes of *Escherichia coli* by chromium compounds, *Environmental mutagenesis*, *8*(4), 571–577.

Lovley, D. R. (1995), Microbial reduction of iron, manganese, and other metals, *Advances in Agronomy*, *54*, 175–231.

Lower, S. K., M. F. HoHochella, and T. J. Beveridge (2001), Bacterial recongnition of mineral surfaces: Nanoscale Internactions between shewanella and α-FeOOH, *Science*, *292*(5520), 1360–1363.

May, T. W., and R. H. Wiedmeyer (1998), A table of polyatomic interferences in ICP-MS, *Atomic Spectroscopy*, *19*(5), 150–155.

Michel, C., M. Brugna, C. Aubert, A. Bernadac, and M. Bruschi (2001), Enzymatic reduction of chromate: comparative studies using sulfate-reducing bacteria.

key role of polyheme cytochromes c and hydrogenases., *Applied Microbiology and Biotechnology*, *55*(1), 95–100.

Michel, C., M. T. Giudici-Orticoni, F. Baymann, and M. Bruschi (2003), Bioremediation of chromate by sulfate-reducing bacteria, cytochromes c3 and hydrogenases, *Water Air and Soil Pollution*, *3*(3), 161–169.

Monachese, M., J. P. Burton, and G. Reid (2012), Bioremediation and tolerance of humans to heavy metals through microbial processes: a potential role for probiotics?, *Applied and Environmental Microbiology*, *78*(18), 6397–6404.

Myers, C. R., and J. M. Myers (1992), Localization of Cytochromes to the Outer-Membrane of Anaerobically Grown *Shewanella-Putrefaciens* MR-1, *Journal of Bacteriology*, *174*(11), 3429–3438.

Myers, C. R., and K. H. Nealson (1988), Bacterial manganese reduction and growth with manganese oxide as the sole electron-acceptor, *Science*, *240*(4857), 1319–1321.

Myers, C. R., and K. H. Nealson (1990), Respiration-Linked Proton Translocation Coupled to Anaerobic Reduction of Manganese(IV) and Iron(III) in *Shewanella-Putrefaciens* MR-1, *Journal of Bacteriology*, *172*(11), 6232–6238.

Myers, C. R., B. P. Carstens, W. E. Antholine, and J. M. Myers (2000), Chromium(VI) reductase activity is associated with the cytoplasmic membrane of anaerobically grown *Shewanella putrefaciens* MR-1, *Journal of Applied Microbiology*, *88*(1), 98–106.

Naik, U. C., S. Srivastava, and I. S. Thakur (2012), Isolation and characterization of *Bacillus cereus* IST105 from electroplating effluent for detoxification of hexavalent chromium, *Environmental Science and Pollution Research*, *19*(7), 3005–3014.

Oh, S. J., D. C. Cook, and H. E. Townsend (1998), Characterization of iron-oxides cocommon formed as corrosion products on steel, *Hyperfine Interactions*, *112*, 59–65.

O'Toole, G. A., and R. Kolter (1998a), Flagellar and twiching motility are necessary for *Pseudomonas aeruginosa* biofilm development., *Molecular Microbiology*, *30*, 295–304.

O'Toole, G. A., and R. Kolter (1998b), The initiation of biofilm formation in *Pseudomonas fluorescens* WCS365 proceeds via multiple, convergent signaling pathways: a gene analysis, *Molecular Microbiology*, *28*, 449–461.

Palmer, C. D., and P. R. Wittbrodt (1991), Processes affecting the remediation of chromium-contaminated sites, *Environmental Health Perspectives*, *92*, 25–40.

Pan, X., Z. Liu, Z. Chen, Y. Cheng, D. Pan, J. Shao, Z. Lin, and X. Guan (2014), Investigation of Cr(VI) reduction and Cr(III) immobilization mechanism by planktonic cells and biofilms of *Bacillus subtilis* ATCC-6633, *Water Research*, *55*(0), 21–29.

Pan, Z., P. Somasundaran, N. J. Turro, and S. Jockusch (2004), Interactions of cationic dendrimers with hematite mineral, *Colloids and Surfaces A: Physicochemical and Engineering Aspects*, *238*, 123–126.

Park, C. H., M. Keyhan, B. Wielinga, S. Fendorf, and A. Matin (2000), Purification to homogeneity and characterization of a novel *Pseudomonas putida* chromate reductase, *Applied and Environmental Microbiology*, *66*(5), 1788–1795.

Pfeffer, C., S. Larsen, J. Song, M. Dong, F. Besenbacher, R. L. Meyer, K. U. Kjeldsen, L. Schreiber, Y. A. Gorby, M. Y. El-Naggar, K. M. Leung, A. Schramm, N. Risgaard-Petersen, and L. P. Nielsen (2012), Filamentous bacteria transport-electrons over centimetre distances, *Nature*, *491*, 218–221.

Pinon-Castillo, H. A., E. M. S. Brito, M. Goni-Urriza, R. Guyoneaud, R. Duran, G. V. Nevarez-Moorillon, J. F. Gutierrez-Corona, C. A. Caretta, and G. E. Reyna-Lopez (2010), Hexavalent chromium reduction by bacterial consortia and pure strains from an alkaline industrial effluent, *Journal of Applied Microbiology*, *109*(6), 2173–2182.

Pirbadian, S., S. E. Barchinger, K. M. Leung, H. S. Byun, Y. Jangir, R. A. Bouhenni, S. B. Reed, M. F. Romine, D. A. Saffarini, Y. A. Gorby, J. H. Golbeck, and M. Y. El-Naggar (2014), *Shewanella oneidensis* MR-1 nanowires are outer membrane and periplasmic extensions of the extracellular electron transport components, *Proceedings of the National Academy of Sciences*, *111*(35), 12,883–12,888.

Plaper, A., S. Jenko-Brinovec, A. Premzl, J. Kos, and P. Raspor (2002), Genotoxicity of trivalent chromium in bacterial cells. possible effects on DNA topology, *Chemical Research in Toxicology*, *15*(7), 943–949.

Plaza, R. C., F. Gonzalez-Caballero, and A. V. Delgado (2001), Electrical surface charge and potential of hematite/yttrium oxide core-shell colloidal particles, *Colloid Polymer Science*, *279*, 1206–1211.

Pourbaix, M. (1974), *Atlas of Electrochemical Equilibria in Aqueous Solutions*, NACE International (National Association of Corros.

Raddatz, A., T. M. Johnson, and T. McLing (2010), Cr stable isotopes in snake river plain aquifer groundwater: evidence for natural reduction of dissolved Cr(VI), *Environmental Science & Technology*, *45*, 502–507.

Ramirez-diaz, M., C. Diaz-Perez, E. Vargas, H. Riveros-Rosas, J. Campos-Garcia, and C. Cervantes (2008), Mechanisms of bacterial resistance to chromium compounds, *Biometals*, *21*, 321–332.

Rayleigh, S. R. S. (1896), Theoretical considerations respecting the separation of gases by diffusion and similar processes, *Philosophical Magazine Series 5*, *42*(259).

Reguera, G., K. McCarthy, T. Mehta, J. Nicoll, M. T. Tuominen, and D. R. Lovley (2005), Extracellular electron transfer via microbial nanowires, *Nature*, *435*, 1098–1101.

Risgaard-Petersen, N., A. Revil, P. Meister, and L. P. Nielsen (2012), Sulfur, iron, and calcium cycling associated with natural electric currents running through marine sediment, *Geochimica Et Cosmochimica Acta*, *92*, 1–13.

Rock, M. L., B. R. James, and G. R. Helz (2001), Hydrogen peroxide effects on chromium oxidation state and solubility in four diverse, chromium-enriched soils, *Environmental Science & Technology*, *35*(20), 4054–4059.

Roden, E., and J. M. Zachara (1996), Microbial reduction of crystalline iron(III) oxides: influence of oxide surface area and potential for cell growth, *Environmental Science & Technology*, *30*, 1618–1628.

Rotaru, M., J. L. Birck, and C. J. Allegre (1992), Clues to early solar system history from chromium isotopes in carbonaceous chondrites, *Nature*, *358*(6386), 465470.

Rudge, J. F., B. C. Reynolds, and B. Bourdon (2009), The double spike toolbox, *Chemical Geology*, *265*, 420–431.

Rudnick, R. L., and S. Gao (2003), Composition of the Continental Crust, *Treatise on Geochemistry*, *3*, 659, doi:10.1016/B0-08-043751-6/03016-4.

Russel, W. A., D. A. Papanastassiou, and T. A. Tombrello (1978), Ca isotope fractionation on the earth and other solar system materials, *Geochimica Et Cosmochimica Acta*, *42*, 1075–1090.

Schauble, E. A. (2004), Applying stable isotope fractionation theory to new systems, *Geochemistry of Non-Traditional Stable Isotopes*, *55*, 65–111.

Shimizu, K. (2013), Metabolic regulation of a bacterial cell system with emphasis

on *Escherichia coli* metabolism, *ISRN Biochemistry*, *2013*(Artical ID 645983), doi:http://dx.doi.org/10.1155/2013/645983.

Siebert, C., T. F. Ngler, and J. D. Kramers (2001), Determination of molybdenum isotope fractionation by double-spike multicollector inductively coupled plasma mass spectrometry, *Geochemistry, Geophysics, Geosystems*, *2*(7), 1032.

Sikora, E. R., T. M. Johnson, and T. D. Bullen (2008), Microbial mass-dependent fractionation of chromium isotopes, *Geochimica Et Cosmochimica Acta*, *72*(15), 3631–3641.

Sim, M. S., T. Bosak, and S. Ono (2011), Large sulfur isotope fractionation does not require disproportionation, *Science*, *333*(6038), 74–77.

Sim, M. S., S. Ono, and T. Bosak (2012), Effects of iron and nitrogen limitation on sulfur isotope fractionation during microbial sulfate reduction, *Applied and Environmental Microbiology*, *78*(23), 8368–8376.

Sivakumar, S., and C. Subbhuraam (2005), Toxifcity of chrmium (III) and chromium (VI) to the earthworm *Eisenia fetida*, *Ecotoxicology and Environmental Safety*, *62*(1), 93–98.

Song, Y., G. Li, S. Thornton, L. P. Thompson, S. Banwart, and H. W. Lerner, D. N (2009), Optimization of bacterial whole cell bioreporters for toxicity assay of environmental samples, *Environmental s*, *43*, 7931–7938.

Song, Y., B. Jiang, S. Tian, H. Tang, Z. Liu, C. Li, J. Jia, W. E. Huang, X. Zhang, and G. Li (2014), A whole-cell bioreporter approach for the genotoxicity assessment of bioavailability of toxic compounds in contaminated soil in China, *Environmental Po*, *195*, 178–184.

Sparks, D. L. (2005), Toxic metals in the environment: the role of surfaces, *Elements*, *1*, 193–196.

Stanin, F. T. (2004), *The transport and fate of chromium(VI) in the Environment*, chap. Chapter5, pp. 167–214, CRC Press.

Stewart, D. I., I. T. Burke, and R. Mortimer (2007), Stimulation of microbially mediated chromate reduction in alkaline soil-water systems, *Geomicrobiology Journal*, *24*(7-8), 655–669.

Stewart, D. I., I. T. Burke, D. V. Hughes-Berry, and R. A. Whittleston (2010), Microbially mediated chromate reduction in soil contaminated by highly alkaline leachate from chromium containing waste, *Ecological Engineering*, *36*(2), 211–221.

Stouthart, A. H. H. X., F. A. T. Spanings, R. A. C. Lock, and S. E. Wendelaar Bonga (1995), Effects of water pH on chromium toxicity to early life stages of the common carp (*Cyprinus carpio*), *Aquatic Toxicology*, *32*(1), 31–42.

Sultan, S., and S. Hasnain (2012), Chromium (VI) reduction by cell free extract of Ochrobactrum anthropi isolated from tannery effluent, *Bulletin of Environmental Contamination and Toxicology*, *89*(1), 152–157.

Sundararajan, M., A. J. Campbell, and I. H. Hillier (2011), How do enzymes reduce metals? the mechanism of the reduction of Cr(VI) in chromate by cytochrome c7 protein proposed from DFT calculations, *Faraday Discussions*, *148*, 195–205.

Tekerlekopoulou, A. G., G. Tsiamis, E. Dermou, S. Siozios, K. Bourtzis, and D. V. Vayenas (2010), The effect of carbon source on microbial community structure and Cr(VI) reduction rate, *Biotechnology and Bioengineering*, *107*(3), 478–487.

Thibeau, R. J., C. W. Brown, and Heidersbach (1978), Raman spectra of possible corrosion products of iron, *Applied Spectroscopy*, *32*, 532–535.

Thode, H. G., H. Kleerekoper, and D. McElcheran (1951), Isotope fractionation in the bacterial reduction of sulphate., *Research*, *4*, 581–582.

Thormann, K. M., R. M. Saville, S. Shukla, D. A. Pelletier, and A. M. Spormann (2004), Initial Phases of biofilm formation in *Shewanella oneidensis* MR-1, *Journal of Bacteriology*, *186*(23), 8096–8104.

Trama, F. B., and R. J. Benoit (1960), Toxicity of hexavalent chromium to bluegills, *Water Environment Control Federation*, *32*(8), 868–877.

Trinquier, A., J. L. Birck, and C. J. Allegre (2008), High-precision analysis of chromium isotopes in terrestrial and meteorite samples by thermal ionization mass spectrometry, *Journal of Analytical Atomic Spectrometry*, *23*(12), 1565–1574.

van der Meer, J., and S. Belkin (2010), Where microbiology meets microengineering: design and applications of reporter bacteria, *Nature Reviews Microbiology*, *8*, 511–522.

Van Der Putte, I., M. A. Brinkhorst, and J. H. Koeman (1981), Effect of pH on the acute toxicity of hexavalent chrmium to rainbow trout (*Salmo gairdneri*), *Aquatic Toxicology*, *1*(2), 129–142.

Vargas, M., N. S. Malvankar, P.-L. Tremblay, C. Leang, J. A. Smith, P. Patel, O. Snoeyenbos-West, K. P. Nevin, and D. R. Lovley (2013), Aromatic amino acids require for pili conductivity and long-range extracellular electron transport in *Geobacter sulfurreducens*, *mBio*, *4*(2), e00,210–13, doi:http://dx.doi.10.1128/mBio.00105-13.

Vaughan, D. J., R. A. D. Pattrick, and R. A. Wogelius (2002), Minerals, metals and molecules: ore and environmental mineralogy in the new millenium., *mineral magazine*, *66*, 653–676.

Viamajala, S., B. M. Peyton, W. A. Apel, and J. N. Petersen (2002), Chromate reduction in *Shewanella oneidensis* MR-1 is an inducible process associated with anaerobic growth, *Biotechnology Progress*, *18*(2), 290–295.

Viti, C., A. Mini, G. Ranalli, G. Lustrato, and L. Giovannetti (2006), Response of microbial communities to different doses of chromate in soil microcosms, *Applied Soil Ecology*, *34*(2-3), 125–139.

Viti, C., E. Marchi, F. Decorosi, and L. Giovannetti (2014), Molecular mechanisms of Cr(VI) resistance in bacteia and fungi, *FEMS Microbiology Reviews*, *38*(4), 633–659.

Wang, W., and Q. Zhang (2013), Dioxin and phthalate uptake and assimilation by green mussel *Perna viridis*, *Environmental Pollution*, *178*, 455–462.

Wang, X., T. M. Johnson, and A. S. Ellis (2015), Equilibrium isotopic fractionation and isotopic exchange kinetics between Cr(III) and Cr(VI), *Geochimica et Cosmochimica Acta*, *153*(0), 72–90.

Wang, Y. T., and H. Shen (1995), Bacterial reduction of hexavalent chromium, *Journal of Industrial Microbiology*, *14*(2), 159–163.

Wang, Y.-T., and C. Xiao (1995), Factors affecting hexavalent chromium reduction in pure cultures of bacteria, *Water Research*, *29*(11), 2467–2474.

Wanner, C., U. Eggenberger, D. Kurz, S. Zink, and U. Mader (2012), A chromate-contaminated site in southern Switzerland Part 1: site characterization and the use of Cr isotopes to delineate fate and transport., *Applied Geochemistry*, *27*, 644–654.

Wasylenki, L. E., J. W. Swihart, and S. J. Romaniello (2014), Cadmium isotope Fractionation during adsorption to Mn oxyhydroxide at low and high ionic strength, *Geochimica Et Cosmochimica Acta*, *140*, 212–226.

Whalley, C., A. Hursthouse, S. Rowlatt, P. Iqbal-Zahid, H. Vaughan, and R. Duran (1999), Chromium speciation in natural waters drainining contaminated land, Glasgow, U.K., *Water Air and Soil Pollution*.

Wielinga, B., M. M. Mizuba, C. M. Hansel, and S. Fendorf (2001), Iron promoted reduction of chromate by dissimilatory iron-deducing bacteria, *Environmental Science & Technology*, *35*(3), 522–527.

Wing, B. A., and I. Halevy (2014), Intracellular metabolite llevel shape sulfur isotope fractionation during microbial sulfate respiration, *Proceedings of the National Academy of Sciences*, *111*(51), 18,116–18,125.

Wu, L., B. L. Beard, and E. C. M. Roden, E.E.Roden (2009), Influence of pH and dissolved Si on Fe isotope fractionation during dissimilatory microbial reduction of hematite, *Geochimica Et Cosmochimica Acta*, *73*, 5584–5599.

Xu, F., T. Ma, L. Zhou, Z. Hu, and L. Shi (2015), Chromium isotopic fractionation during Cr(VI) reduction by *Bacillus sp.* under aerobic conditions, *Chemosphere*, *130*(0), 46–51.

Xu, L., M. F. Luo, W. L. Li, X. T. Wei, K. Xie, L. J. Liu, C. Y. Jiang, and H. Z. Liu (2011), Reduction of hexavalent chromium by Pannonibacter phragmitetus LSSE-09 stimulated with external electron donors under alkaline conditions, *Journal of Hazardous Materials*, *185*(2-3), 1169–1176.

Xu, X., H. Li, and J. Gu (2004), Reduction of hexavalent chromium by ascorbic acid in aqueous solutions., *Chemos*, *57*, 609–613.

Xu, X., H. Li, J. Gu, and X. Li (2005), Kinetics of the reduction of chromium (VI) by vitamin C., *Environmental Toxicology and Chemistry*, *24*, 1310–1314.

Yahya, S. K., Z. A. Zakaria, J. Samin, A. S. S. Raj, and W. A. Ahmad (2012), Isotherm kinetics of Cr(III) removal by non-viable cells of *Acinetobacter haemolyticus*, *Colloids and Surfaces B-Biointerfaces*, *94*, 362–368.

Zayed, A., and N. Terry (2003), Chromium in the environment: factors affecting biological remediation, *Plant and Soil*, *249*(1), 139–156.

Zeltner, W. A., and M. A. Anderson (1988), Surface charge development at the goethite / aqueous solution interface: Effects of CO_2 adsorption, *Langmuir*, *4*(2), 469–474.

Zhang, Q., L. Y. Yang, and W. Wang (2011), Bioaccumulation and trophic transfer of dioxins in marine copepods and fish, *Environmental pollution*, *159*(12), 3390–3397.

Zhang, Q., K. Amor, S. J. G. Galer, I. Thompson, and D. Porcelli (2016), An chromium isotope proxy for bacterial reduction processes, *Geochimica Et Cosmochimica Acta*, *Submitted*.

Zink, S., R. Schoenberg, and M. Staubwasser (2010), Isotopic fractionation and reaction kinetics between Cr(III) and Cr(VI) in aqueous media, *Geochimica Et Cosmochimica Acta*, *74*(20), 5729–5745.

Appendix

In this study, experiments were done in triplicates, Cr concentration data were reported as the mean±s.d of the triplicate samples. Isotope measurement was done with one run of specific sample in each experimental group. All $\delta^{53}Cr$ value was obtained by measuring a spiked sample 800 times on TIMS, and the value was reported as mean±2×s.e. Uncertainties of ϵ were calculated based on the least square method. Original isotope data for chapter 3 are presented in Tables 1-14, for chapter 4 are presented in Tables 15-25, and for chapter 5 are presented in Table 26-28.

Table 1: Aerobic Cr(VI) reduction by *Pseudomonas fluorescens* LB 300 with glucose as the electron donor

Time	**Sample**	**[Cr(VI)]**	**Fraction removed**	**Fraction remaining**	lnF	$\delta^{53}Cr$	$ln(\frac{\delta^{53}Cr}{1000}+1)$
(Hour)		**(mg/L)**	**%**	**%**		**‰**	
0	A	23.74	0.00	100.00			
	B	23.74	0.00	100.00	-0.000000	0.00±0.01	0.000000
	C	23.74	0.00	100.00			
1	A	16.97	28.53	71.47			
	B	17.16	27.71	72.29	-0.324497	0.93±0.04	0.000927
	C	17.12	27.87	72.13			
24	A	15.56	34.44	65.56			
	B	14.86	37.42	62.58	-0.468654	1.49±0.03	0.001488
	C	15.00	36.82	63.18			
48	A	13.41	43.51	56.49			
	B	13.70	42.31	57.69			
	C	15.59	34.32	65.68			
72	A	12.37	47.90	52.10			
	B	12.41	47.73	52.27	-0.648691	1.95±0.03	0.001950
	C	10.27	56.72	43.28			
96	A	10.22	56.96	43.04			
	B	10.58	55.42	44.58	-0.807967	2.53±0.09	0.002525
	C	7.20	69.66	30.34			

ε = -3.12±0.10‰

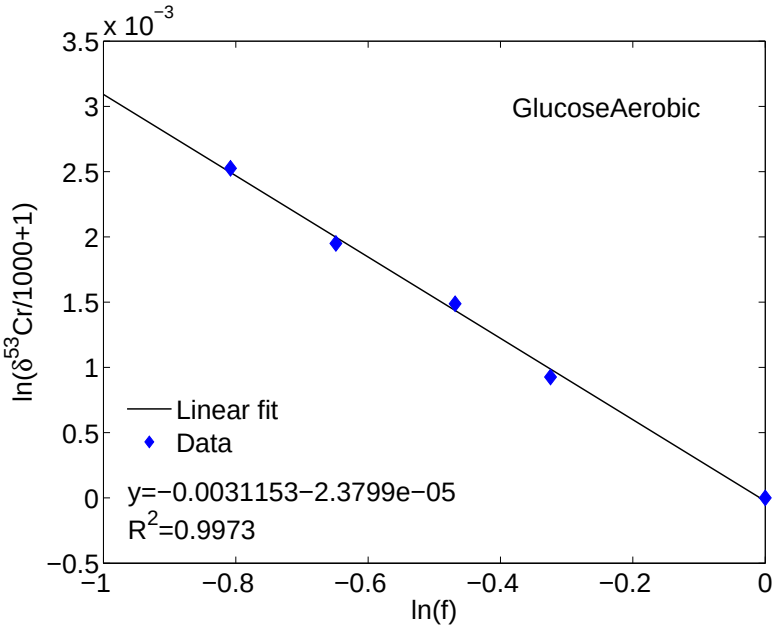


Figure 2: $\ln f$ vs. $\ln\left(\delta^{53}Cr/1000+1\right)$ for aerobic Cr(VI) reduction by *Pseudomonas* with glucose as the electron donor.

Table 2: Aerobic Cr(VI) reduction by *Pseudomonas fluorescens* LB 300 with citrate as the electron donor

Time	**Sample**	**[Cr(VI)]**	**Fraction removed**	**Fraction remaining**	lnF	$\delta^{53}Cr$	$ln(\frac{\delta^{53}Cr}{1000}+1)$
(Hour)		**(mg/L)**	**%**	**%**		**‰**	
0	A	23.74	0.00	100.00			
	B	23.74	0.00	100.00	-0.000000	0.00±0.02	0.000000
	C	23.74	0.00	100.00			
1	A	8.56	63.95	36.05			
	B	8.58	63.86	36.14	-1.017693	4.34±0.06	0.004331
	C	7.98	66.37	33.63			
24	A	0.49	97.93	2.07			
	B	0.49	97.93	2.07			
	C	0.49	97.93	2.07			
48	A	-	-	-			
	B	0.44	98.13	1.87			
	C	0.44	98.13	1.87			
72	A	-	-	-			
	B	-	-	-			
	C	-	-	-			
96	A	-	-	-			
	B	0.29	98.77	1.23			
	C	0.25	98.96	1.04			

ε = -4.32 ‰

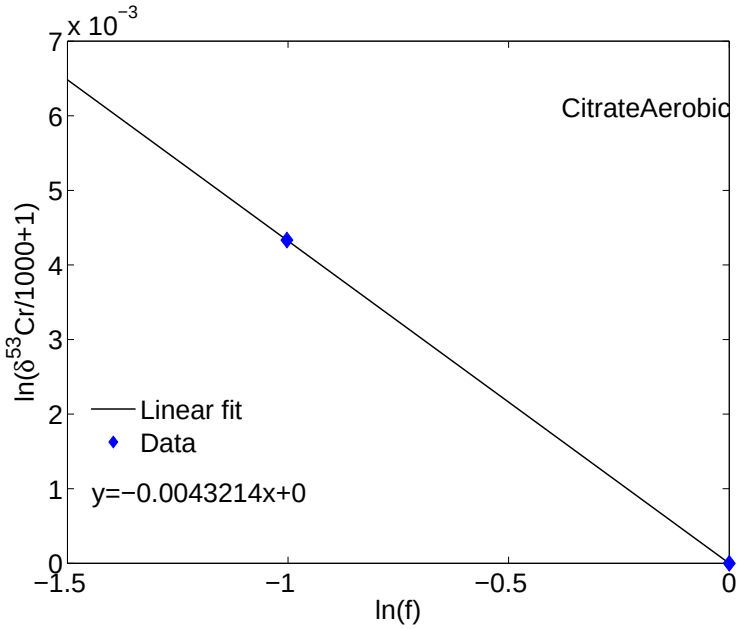


Figure 3: $\ln f$ vs. $\ln(\delta^{53}Cr/1000 + 1)$ for aerobic Cr(VI) reduction by *Pseudomonas* with citrate as the electron donor.

Table 3: Aerobic Cr(VI) reduction by *Pseudomonas fluorescens* LB 300 with acetate as the electron donor

Time	**Sample**	**[Cr(VI)]**	**Fraction removed**	**Fraction remaining**	lnF	$\delta^{53}Cr$	$ln(\frac{\delta^{53}Cr}{1000}+1)$
(Hour)		**(mg/L)**	**%**	**%**		**‰**	
0	A	23.38	0.00	100.00	-0.000000	0.00±0.02	0.000000
	B	23.38	0.00	100.00			
	C	23.38	0.00	100.00			
1	A	18.38	21.38	78.62			
	B	18.65	20.24	79.76			
	C	18.49	20.92	79.08			
24	A	15.64	33.10	66.90	-0.401984	1.29±0.06	0.001289
	B	15.47	33.83	66.17			
	C	15.96	31.74	68.26			
48	A	14.52	37.88	62.12			
	B	14.67	37.25	62.75			
	C	14.12	39.61	60.39			
72	A	14.44	38.23	61.77	-0.481776	1.55±0.02	0.001549
	B	13.85	40.76	59.24			
	C	14.27	38.99	61.01			
96	A	14.79	36.73	63.27			
	B	13.89	40.59	59.41			
	C	14.10	39.69	60.31			

ε = -3.21±0.20 ‰

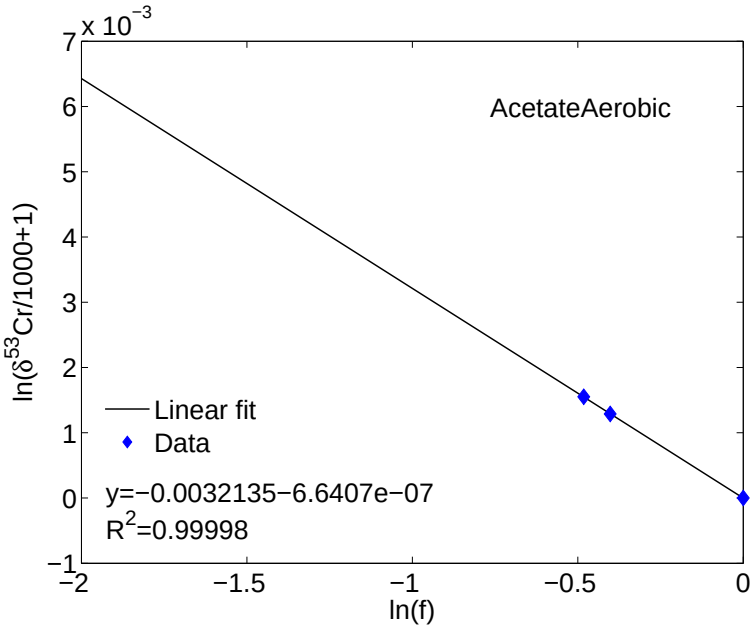


Figure 4: $\ln f$ vs. $\ln(\delta^{53}Cr/1000 + 1)$ for aerobic Cr(VI) reduction by *Pseudomonas* with acetate as the electron donor.

Table 4: Aerobic Cr(VI) reduction by *Pseudomonas fluorescens* LB 300 with propionate as the electron donor

Time	**Sample**	**[Cr(VI)]**	**Fraction removed**	**Fraction remaining**	lnF	$\delta^{53}Cr$	$ln(\frac{\delta^{53}Cr}{1000}+1)$
(Hour)		**(mg/L)**	**%**	**%**		**‰**	
0	A	23.38	0.00	100.00	-0.000000	0.00±0.02	0.000000
	B	23.38	0.00	100.00			
	C	23.38	0.00	100.00			
1	A	18.16	22.35	77.65	-0.252912	0.38±0.04	0.000380
	B	18.54	20.70	79.30			
	C	18.90	19.16	80.84			
24	A	16.15	30.91	69.09	-0.369824	1.94±0.02	0.001938
	B	15.35	34.33	65.67			
	C	16.18	30.79	69.21			
48	A	14.00	40.10	59.90			
	B	14.45	38.21	61.79			
	C	14.45	38.21	61.79			
72	A	13.47	42.40	57.60			
	B	12.38	47.07	52.93			
	C	13.19	43.59	56.41			
96	A	13.55	42.04	57.96			
	B	13.89	40.59	59.41	-0.628607	2.25±0.01	0.002247
	C	14.10	39.69	60.31			

ε = -3.90±0.95 ‰

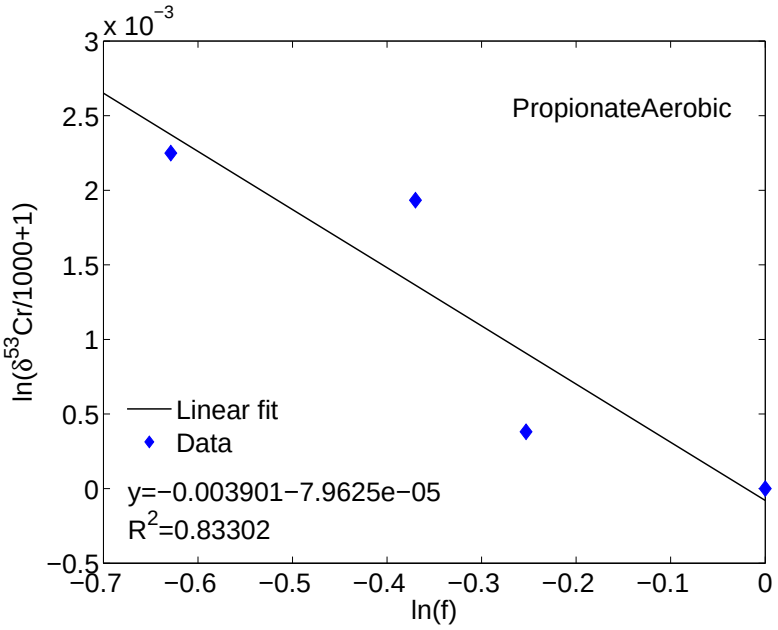


Figure 5: $\ln f$ vs. $\ln\left(\delta^{53}Cr/1000+1\right)$ for aerobic Cr(VI) reduction by *Pseudomonas* with propionate as the electron donor.

Table 5: Anaerobic Cr(VI) reduction by *Pseudomonas fluorescens* LB 300 with glucose as the electron donor

Time	**Sample**	**[Cr(VI)]**	**Fraction removed**	**Fraction remaining**	lnF	$\delta^{53}Cr$	$ln(\frac{\delta^{53}Cr}{1000}+1)$
(Hour)		**(mg/L)**	%	%		‰	
0	A	16.52	0.00	100.00	-0.000000	0.00±0.18	0.000000
	B	16.13	0.00	100.00			
	C	17.04	0.00	100.00			
1	A	14.56	11.89	88.11	-0.126579	0.52±0.03	0.000520
	B	14.16	12.18	87.82			
	C	14.29	16.13	83.87			
2	A	14.29	13.47	86.53	-0.144734	0.76±0.02	0.000760
	B	13.64	15.43	84.57			
	C	14.16	16.90	83.10			
3	A	10.76	34.88	65.12	-0.428876	1.49±0.02	0.001489
	B	9.71	39.79	60.21			
	C	10.50	38.41	61.59			
24	A	3.16	80.85	19.15	1.652804	8.19±0.02	0.008157
	B	2.90	82.01	17.99			
	C	3.16	81.44	18.56			

ε = -4.96±0.37‰

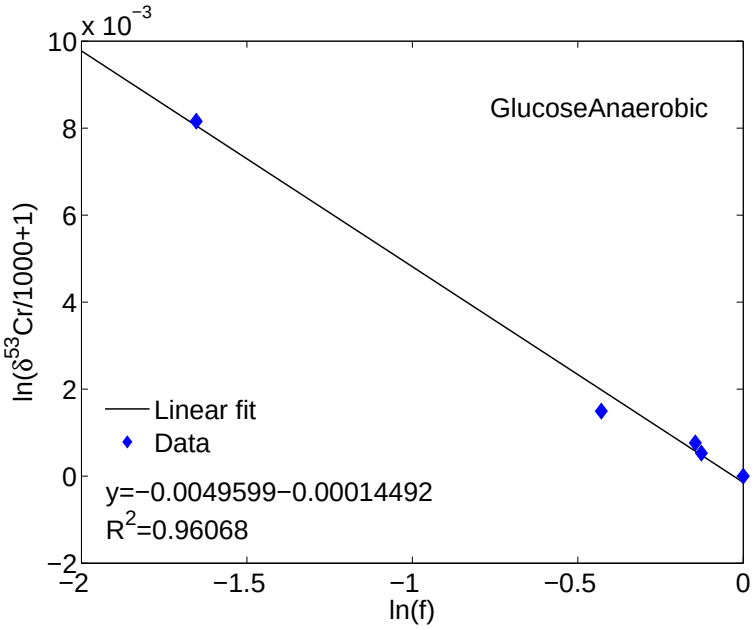


Figure 6: $\ln f$ vs. $\ln(\delta^{53}Cr/1000+1)$ for anaerobic Cr(VI) reduction by *Pseudomonas* with glucose as the electron donor.

Table 6: Anaerobic Cr(VI) reduction by *Pseudomonas fluorescens* LB 300 with citrate as the electron donor

Time	**Sample**	**[Cr(VI)]**	**Fraction removed**	**Fraction remaining**	lnF	$\delta^{53}Cr$	$ln(\frac{\delta^{53}Cr}{1000}+1)$
(Hour)		**(mg/L)**	**%**	**%**		**‰**	
0	A	18.09	0.00	100.00	-0.000000	0.00±0.02	0.000000
	B	17.31	0.00	100.00			
	C	17.57	0.00	100.00			
1	A	15.34	15.20	84.80	-0.164870	0.42±0.02	0.000420
	B	14.95	13.62	86.38			
	C	14.56	17.14	82.86			
2	A	15.47	14.48	85.52	-0.156371	0.73±0.04	0.000730
	B	14.42	16.65	83.35			
	C	14.69	16.40	83.60			
3	A	11.41	36.91	63.09	-0.460661	1.43±0.01	0.001429
	B	11.15	35.56	64.44			
	C	11.94	32.05	67.95			
24	A	4.60	74.55	25.45	-1.386473	6.44±0.01	0.006419
	B	4.21	75.67	24.33			
	C	4.21	76.03	23.97			

ε = -4.77±0.45‰

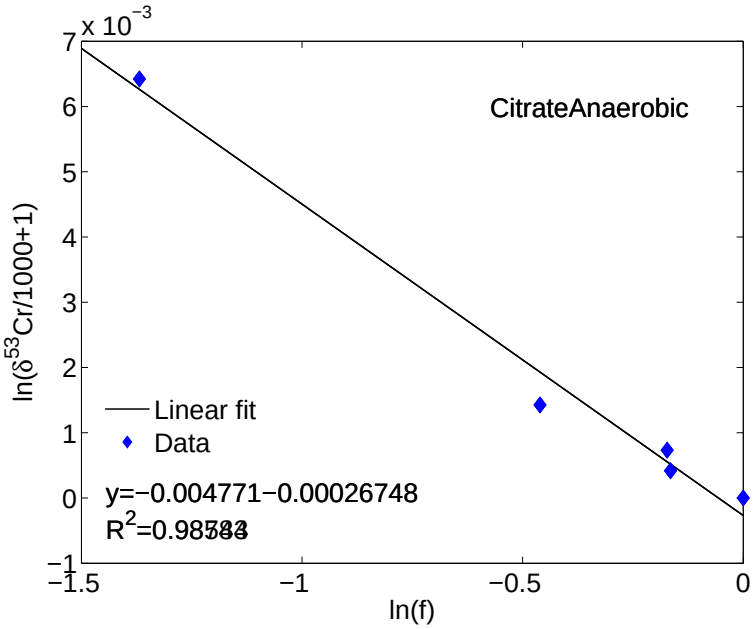


Figure 7: $\ln f$ vs. $\ln\left(\delta^{53}Cr/1000+1\right)$ for anaerobic Cr(VI) reduction by *Pseudomonas* with citrate as the electron donor.

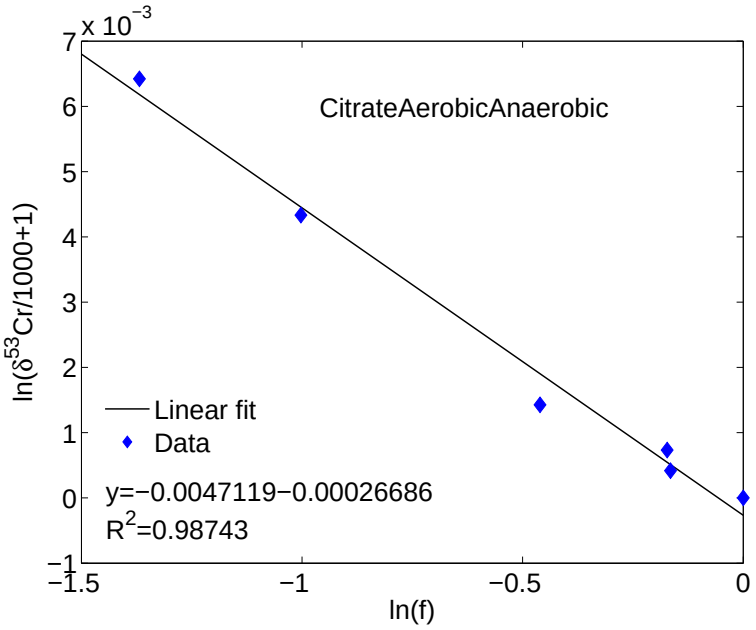


Figure 8: $\ln f$ vs. $\ln(\delta^{53}Cr/1000 + 1)$ for both aerobic and anaerobic Cr(VI) reduction by *Pseudomonas* with citrate as the electron donor.

Table 7: Anaerobic Cr(VI) reduction by *Pseudomonas fluorescens* LB 300 with acetate as the electron donor

Time	**Sample**	**[Cr(VI)]**	**Fraction removed**	**Fraction remaining**	lnF	$\delta^{53}Cr$	$ln(\frac{\delta^{53}Cr}{1000}+1)$
(Hour)		**(mg/L)**	**%**	**%**		**‰**	
0	A	17.17	0.00	100.00	-0.000000	0.00±0.02	0.000000
	B	19.40	0.00	100.00			
	C	17.44	0.00	100.00			
1	A	15.47	9.91	90.09			
	B	15.86	18.22	81.78			
	C	15.86	9.01	90.99			
2	A	14.29	16.77	83.23	-0.183601	0.82±0.13	0.000820
	B	14.42	25.65	74.35			
	C	14.56	16.52	83.48			
3	A	10.89	36.60	63.40	-0.455645	1.61±0.03	0.001609
	B	10.89	43.87	56.13			
	C	10.63	39.05	60.95			
24	A	3.95	77.00	23.00	-1.469864	4.87±0.07	0.004858
	B	4.08	78.97	21.03			
	C	3.95	77.35	22.65			

ε = -3.24±0.17‰

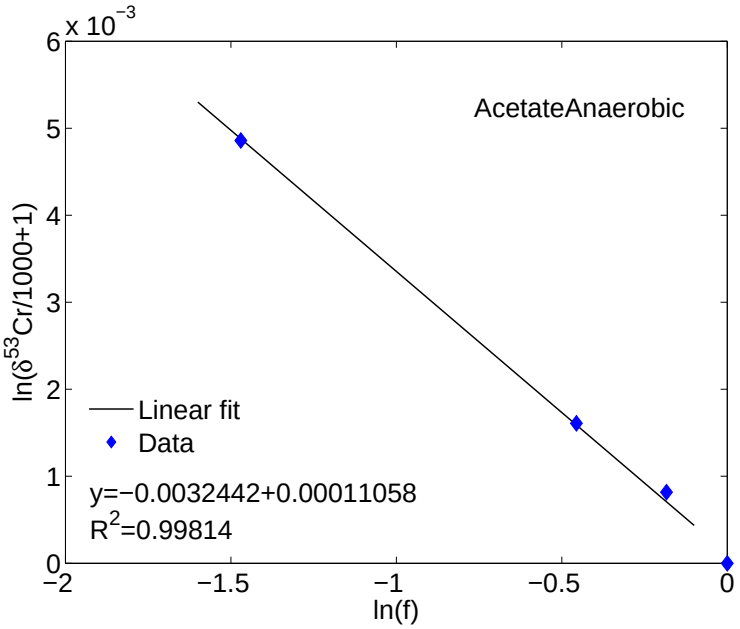


Figure 9: $\ln f$ vs. $\ln\left(\delta^{53}Cr/1000+1\right)$ for anaerobic Cr(VI) reduction by *Pseudomonas* with acetate as the electron donor.

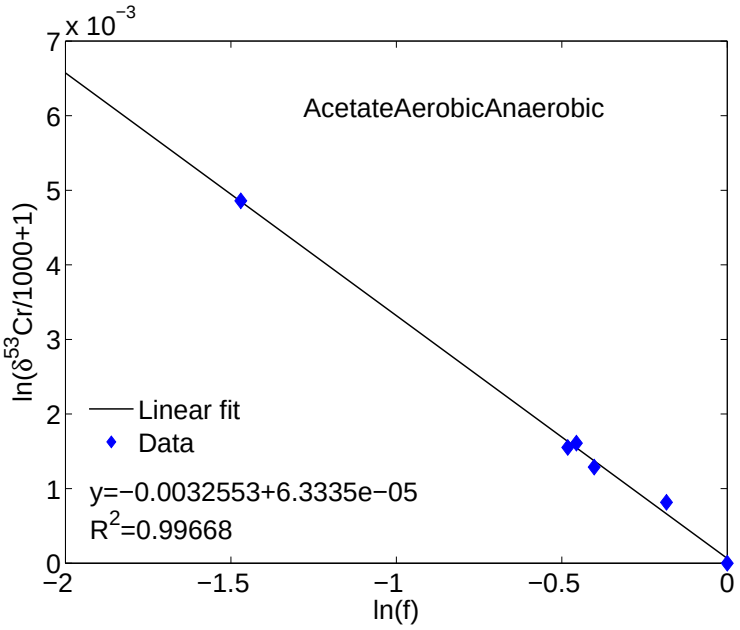


Figure 10: $\ln f$ vs. $\ln(\delta^{53}Cr/1000+1)$ for both aerobic and anaerobic Cr(VI) reduction by *Pseudomonas* with acetate as the electron donor.

Table 8: Anaerobic Cr(VI) reduction by *Pseudomonas fluorescens* LB 300 with propionate as the electron donor

Time	**Sample**	**[Cr(VI)]**	**Fraction removed**	**Fraction remaining**	lnF	$\delta^{53}Cr$	$ln(\frac{\delta^{53}Cr}{1000}+1)$
(Hour)		**(mg/L)**	**%**	**%**		**‰**	
0	A	18.09	0.00	100.00	-0.000000	0.00±0.05	0.000000
	B	17.17	0.00	100.00			
	C	18.48	0.00	100.00			
1	A	16.78	7.24	92.76			
	B	16.78	2.29	97.71			
	C	16.26	12.04	87.96			
2	A	14.03	22.44	85.52	-0.156371	0.63±0.05	0.000630
	B	14.16	17.54	83.35			
	C	14.82	19.84	83.60			
3	A	11.54	36.19	63.09	-0.460661	0.93±0.02	0.000930
	B	10.63	38.12	64.44			
	C	11.15	39.67	67.95			
24	A	3.56	80.34	25.45	-1.386473	2.60±0.05	0.002597
	B	2.90	83.10	24.33			
	C	3.43	81.47	23.97			

ε = -1.53±0.24‰

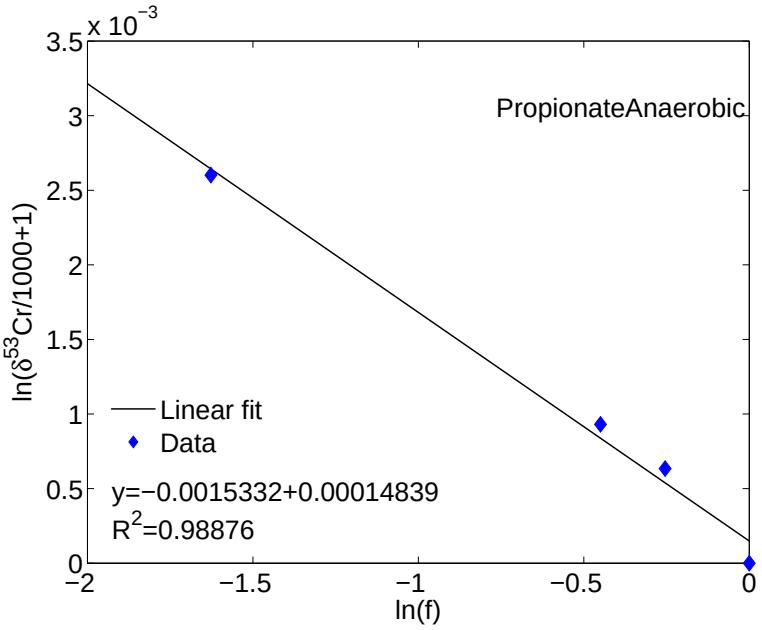


Figure 11: $\ln f$ vs. $\ln(\delta^{53}Cr/1000+1)$ for anaerobic Cr(VI) reduction by *Pseudomonas* with propionate as the electron donor.

Table 9: Aerobic Cr(VI) reduction by *Shewanella* with succinate as the electron donor

Time	**Sample**	**[Cr(VI)]**	**Fraction removed**	**Fraction remaining**	lnF	$\delta^{53}Cr$	$ln(\frac{\delta^{53}Cr}{1000}+1)$
(Hour)		**(mg/L)**	**%**	**%**		**‰**	
0	A	21.42	0.00	100.00	-0.000000	0.00±0.01	0.000000
	B	20.81	0.00	100.00			
	C	20.72	0.00	100.00			
24	A	18.00	14.21	85.79			
	B	17.21	17.97	82.03			
	C	17.12	18.39	81.67			
48	A	17.03	18.81	81.19	-0.208389	0.73±0.02	0.000730
	B	16.42	21.74	78.26			
	C	16.24	22.57	77.43			
72	A	16.60	20.90	79.10	-0.460661	0.79±0.01	0.000790
	B	16.51	21.32	78.68			
	C	16.77	20.06	79.94			

ε = -3.43±0.05‰

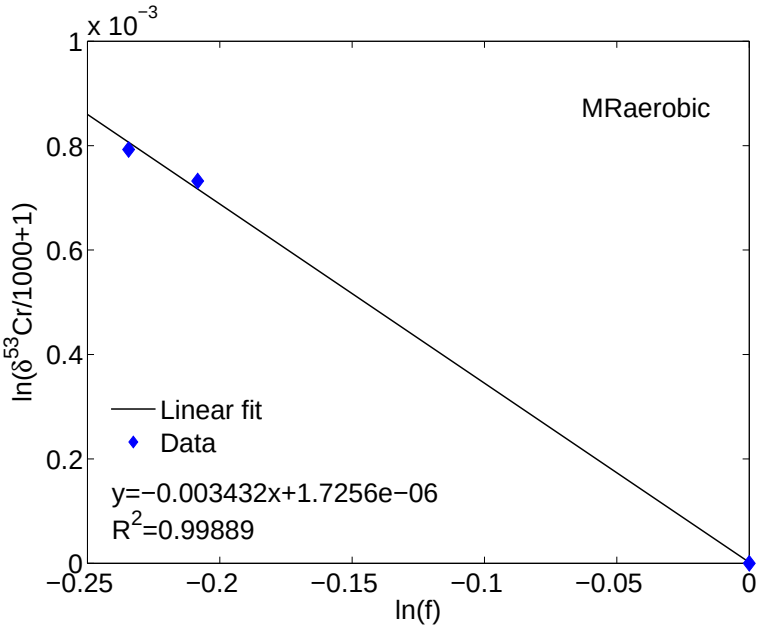


Figure 12: $\ln f$ vs. $\ln\left(\delta^{53}Cr/1000+1\right)$ for aerobic Cr(VI) reduction by *Shewanella* with succinate as the electron donor.

Table 10: Anaerobic Cr(VI) reduction by *Shewanella* with succinate as the electron donor

Time	**Sample**	**[Cr(VI)]**	**Fraction removed**	**Fraction remaining**	lnF	$\delta^{53}Cr$	$ln(\frac{\delta^{53}Cr}{1000}+1)$
(Hour)		**(mg/L)**	**%**	**%**		**‰**	
0	A	19.00	0.00	100.00			
	B	21.01	0.00	100.00			
	C	21.82	0.00	100.00	-0.000000	0.00±0.01	0.000000
24	A	11.63	38.78	61.22			
	B	14.66	30.25	69.75			
	C	14.76	32.37	67.63	-0.391101	1.00±0.01	0.001000
48	A	3.15	83.40	16.60			
	B	10.72	48.98	51.02			
	C	9.61	55.95	44.05	-0.819885	2.02±0.02	0.002018
72	A	1.14	94.02	5.98			
	B	1.74	91.71	8.29			
	C	1.14	94.79	5.21			

ε = -2.47±0.07‰

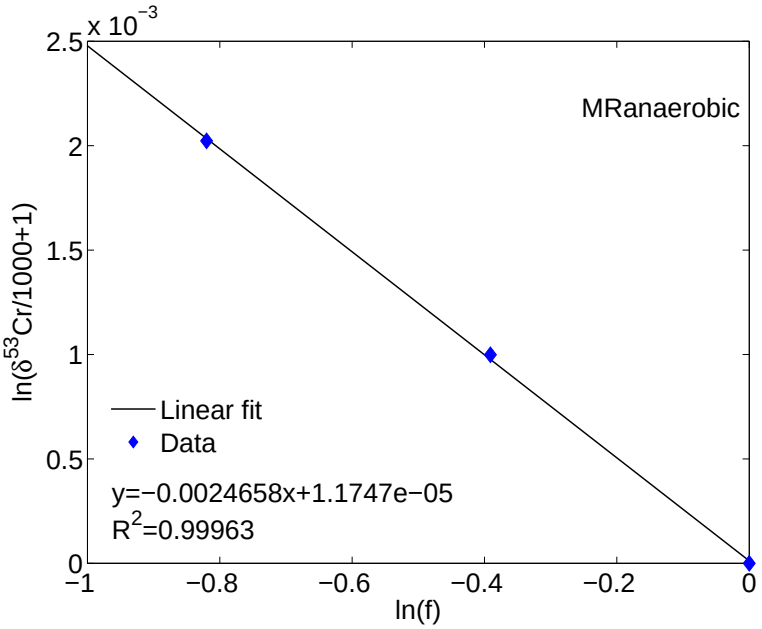


Figure 13: $\ln f$ vs. $\ln(\delta^{53}Cr/1000+1)$ for anaerobic Cr(VI) reduction by *Shewanella* with succinate as the electron donor.

Table 11: Aerobic Cr(VI) reduction by *Pseudomonas fluorescens* LB 300 with different concentrations of glucose as the electron donor (data at 48 hours)

[Glucose] (mg/L)	**Sample**	**[Cr(VI)]** (mg/L)	**Fraction removed** %	**Fraction remaining** %	lnF	$\delta^{53}Cr$ ‰	$ln(\frac{\delta^{53}Cr}{1000}+1)$
Time 0	A	20.00	0.00	100.00			
	B	20.00	0.00	100.00			
	C	20.00	0.00	100.00	-0.000000	0.00±0.01	0.000000
0	A	18.07	9.65	90.35			
	B	17.19	14.03	85.97			
	C	17.95	10.23	89.77	-0.107889	0.52±0.04	0.000523
0.5	A	15.84	20.81	79.19			
	B	14.94	25.32	74.68			
	C	15.65	21.75	78.25	-0.245213	0.76±0.05	0.000759
2	A	15.09	24.55	75.45			
	B	13.99	30.03	69.97			
	C	14.62	26.91	73.09	-0.313526	1.31±0.02	0.001313
10	A	13.14	34.32	65.68			
	B	11.89	40.54	59.46			
	C	12.57	37.15	62.85	-0.464360	1.93±0.01	0.001930

ε = -3.19±0.34‰, including all data from experiments that used glucose as the electron donor.

Table 12: Aerobic Cr(VI) reduction by *Pseudomonas fluorescens* LB 300 at pH 4

Time	**Sample**	**[Cr(VI)]**	**Fraction removed**	**Fraction remaining**	lnF	$\delta^{53}Cr$	$ln(\frac{\delta^{53}Cr}{1000}+1)$
(Hour)		**(mg/L)**	%	%		‰	
0	A	23.38	0.00	100.00	-0.000000	0.00±0.01	0.000000
	B	25.39	0.00	100.00			
	C	23.66	0.00	100.00			
2	A	19.76	15.48	84.52			
	B	20.43	19.55	80.45			
	C	19.78	16.38	83.62			
4	A	18.73	19.87	80.13			
	B	19.64	22.64	77.36			
	C	19.65	16.93	83.07			
24	A	18.25	21.95	78.05	-0.247861	1.05±0.01	0.001049
	B	18.54	26.97	73.03			
	C	18.28	22.70	77.30			
48	A	15.69	32.92	67.08	-0.399216	1.36±0.01	0.001359
	B	16.61	34.57	65.43			
	C	15.82	33.12	66.88			
72	A	14.54	37.79	62.21			
	B	14.44	43.11	56.89			
	C	14.66	38.01	61.99			
96	A	13.64	41.66	58.34	-0.538869	1.72±0.15	0.001719
	B	13.79	45.69	54.31			
	C	14.01	40.75	59.25			

ε = -3.08±0.32‰

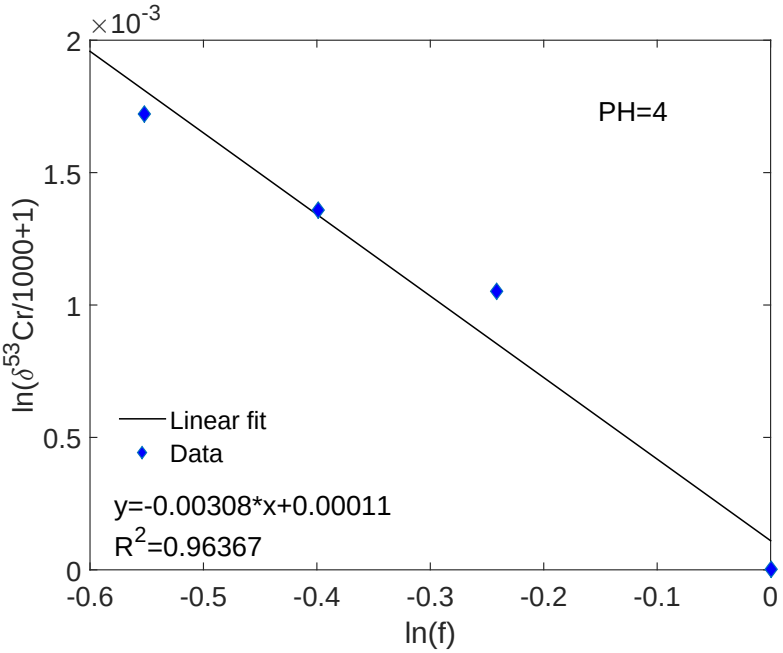


Figure 14: $\ln f$ vs. $\ln(\delta^{53}Cr/1000+1)$ for Cr(VI) reduction by *Pseudomonas* at pH 4.

Table 13: Aerobic Cr(VI) reduction by *Pseudomonas fluorescens* LB 300 at pH 6.

Time	**Sample**	**[Cr(VI)]**	**Fraction removed**	**Fraction remaining**	lnF	$\delta^{53}Cr$	$ln(\frac{\delta^{53}Cr}{1000}+1)$
(Hour)		**(mg/L)**	%	%		‰	
0	A	23.87	0.00	100.00	-0.000000	0.00±0.07	0.000000
	B	23.96	0.00	100.00			
	C	23.68	0.00	100.00			
2	A	18.75	21.33	78.67	-0.239939	0.93±0.11	0.000930
	B	19.78	17.02	82.98			
	C	19.33	18.93	81.07			
4	A	18.87	20.86	79.14			
	B	18.04	24.31	75.69			
	C	18.87	20.86	79.14			
24	A	16.27	31.74	68.26	-0.381826	1.24±0.02	0.001239
	B	17.21	27.81	72.19			
	C	17.72	25.67	74.33			
48	A	16.47	30.91	69.09			
	B	17.28	27.49	72.51			
	C	16.14	32.29	67.71			
72	A	16.05	32.65	67.35	-0.395290	1.22±0.05	0.001219
	B	17.00	28.67	71.33			
	C	16.42	31.11	68.89			
96	A	15.76	33.88	66.12			
	B	16.60	30.38	69.62			
	C	16.27	31.74	68.26			

ε = -3.14±0.21‰

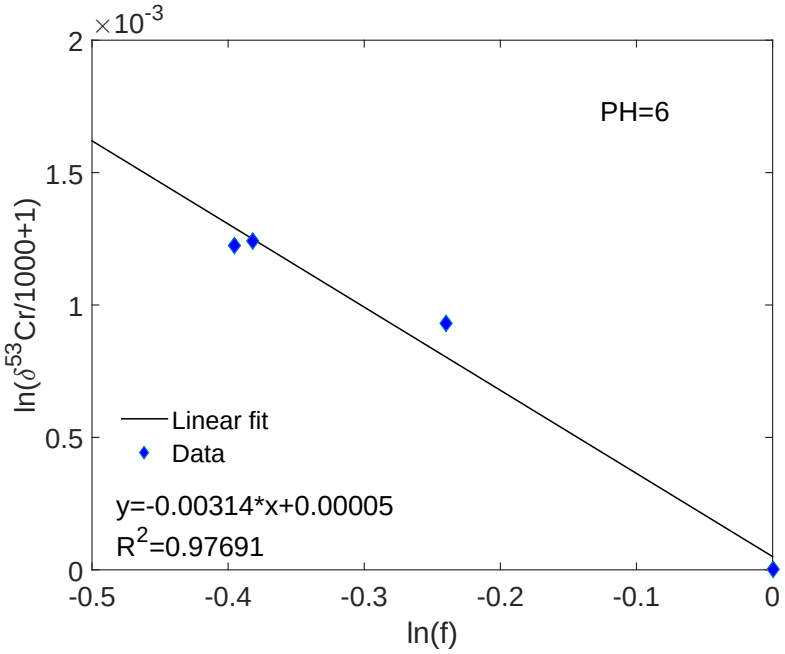


Figure 15: $\ln f$ vs. $\ln(\delta^{53}Cr/1000+1)$ for Cr(VI) reduction by *Pseudomonas* at pH 6.

Table 14: Aerobic Cr(VI) reduction by *Pseudomonas fluorescens* LB 300 at pH 8

Time	**Sample**	**[Cr(VI)]**	**Fraction removed**	**Fraction remaining**	lnF	$\delta^{53}Cr$	$ln(\frac{\delta^{53}Cr}{1000}+1)$
(Hour)		**(mg/L)**	%	%		‰	
0	A	23.57	0.00	100.00	-0.000000	0.00±0.01	0.000000
	B	24.48	0.00	100.00			
	C	22.83	0.00	100.00			
2	A	17.85	24.26	75.74	-0.277834	1.41±0.01	0.001409
	B	18.78	23.27	76.73			
	C	18.87	17.36	82.64			
4	A	18.38	22.01	77.99			
	B	18.40	24.85	75.15			
	C	18.61	18.48	81.52			
24	A	13.59	42.33	57.67	-0.550348	2.03±0.01	0.002028
	B	13.55	44.66	55.34			
	C	13.55	40.67	59.33			
48	A	6.71	71.54	28.46	-1.256538	3.92±0.01	0.003912
	B	6.35	74.07	25.93			
	C	6.17	72.99	27.01			
72	A	6.00	74.53	25.47			
	B	6.00	75.48	24.52			
	C	6.17	72.96	27.04			
96	A	6.32	73.16	26.84	-1.315285	4.67±0.04	0.004659
	B	5.87	76.00	24.00			
	C	6.11	73.23	26.77			

ε = -3.13±0.47‰

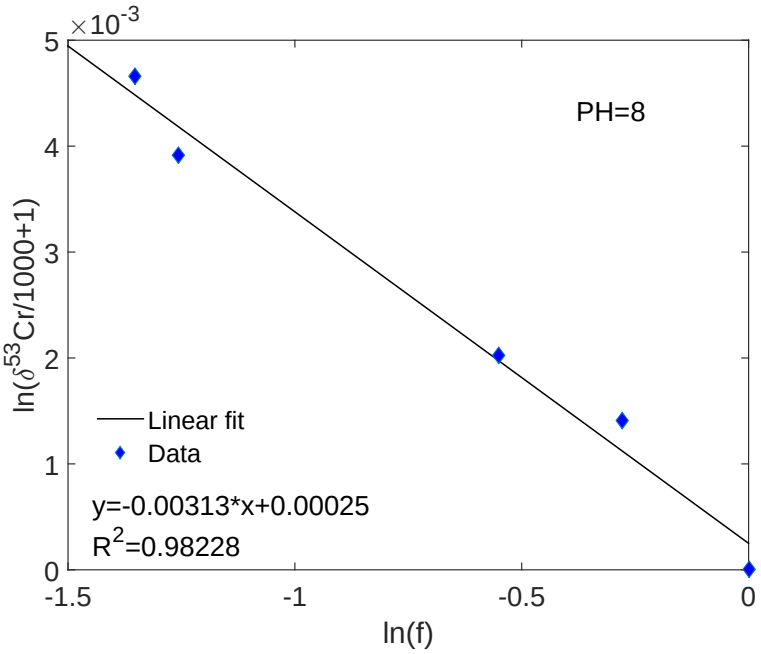


Figure 16: $\ln f$ vs. $\ln(\delta^{53}Cr/1000+1)$ for Cr(VI) reduction by *Pseudomonas* at pH 8.

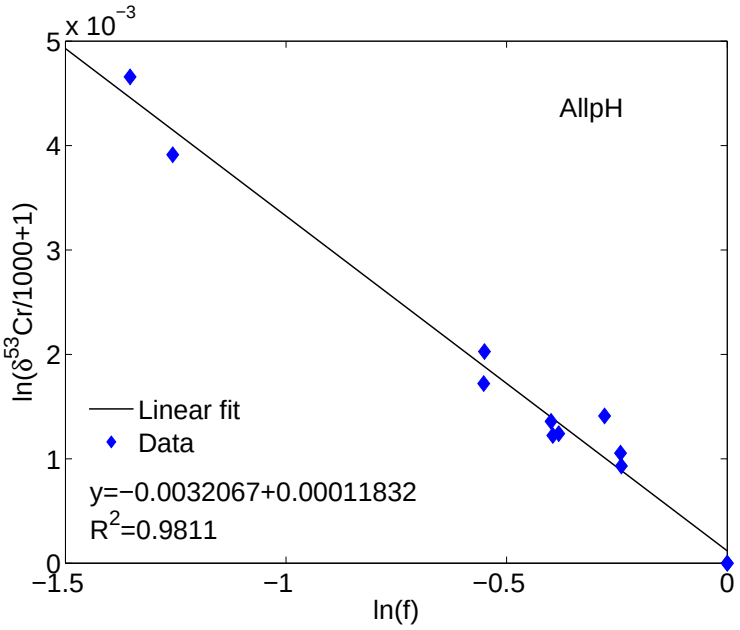


Figure 17: $\ln f$ vs. $\ln(\delta^{53}Cr/1000+1)$ for Cr(VI) reduction by *Pseudomonas* at different pH.

Table 15: Anaerobic Cr(VI) reduction by *Pseudomonas fluorescens* LB 300 without any mineral or aqueous iron species

Time	**Sample**	**[Cr(VI)]**	**Fraction removed**	**Fraction remaining**	lnF	$\delta^{53}Cr$	$ln(\frac{\delta^{53}Cr}{1000}+1)$
(Hour)		**(mg/L)**	%	%		‰	
0	A	18.28	0.00	100.00			
	B	18.28	0.00	100.00	0.000000	0.00±0.01	0.000000
	C	18.28	0.00	100.00			
0.1	A	14.18	22.43	77.57			
	B	14.15	22.58	77.42	-0.255928	0.59±0.03	0.000590
	C	14.31	21.70	78.29			
1	A	9.59	47.54	52.46			
	B	9.11	50.18	49.82	-0.696741	2.11±0.02	0.002112
	C	10.12	44.65	55.34			
2	A	5.80	68.27	31.73			
	B	4.97	72.81	27.19	-1.302344	3.94±0.02	0.0039414
	C	6.67	63.47	36.53			
4	A	3.03	83.42	16.58			
	B	2.14	88.27	11.73	-2.142691	5.31±0.18	0.005293
	C	4.32	76.32	23.68			

ε = -2.56±0.51‰

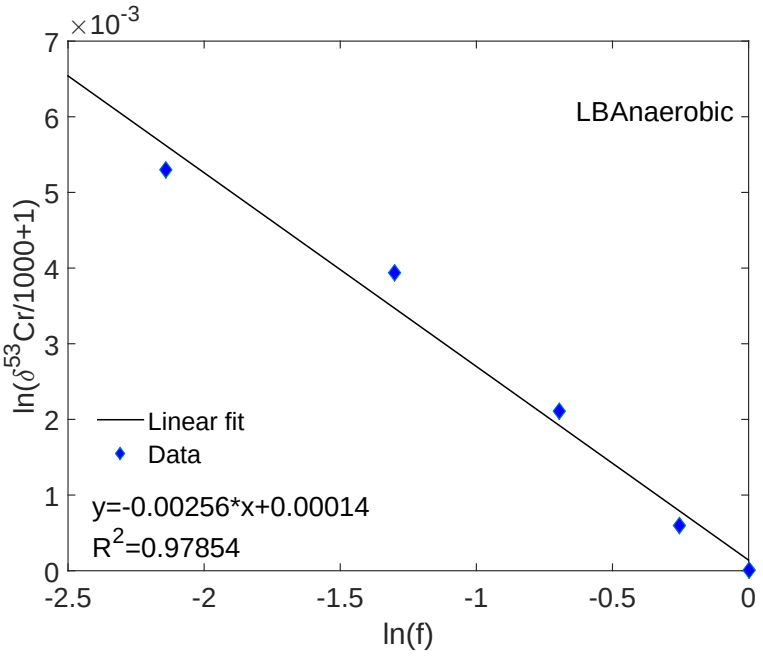


Figure 18: $\ln f$ vs. $\ln\left(\delta^{53}Cr/1000+1\right)$ for Cr(VI) reduction by *Pseudomonas* without any minerals or aqueous Fe species.

Table 16: Anaerobic Cr(VI) reduction by *Pseudomonas fluorescens* LB 300 in the presence of goethite

Time	**Sample**	**[Cr(VI)]**	**Fraction removed**	**Fraction remaining**	lnF	$\delta^{53}Cr$	$ln(\frac{\delta^{53}Cr}{1000}+1)$
(Hour)		**(mg/L)**	%	%		‰	
0	A	38.86	0.00	100.00	-0.000000	0.00±0.01	0.000000
	B	33.28	0.00	100.00			
	C	35.77	0.00	100.00			
1	A	30.40	21.08	78.92	-0.236696	0.75±0.01	0.000749
	B	30.79	7.48	92.52			
	C	29.22	18.30	81.70			
2	A	27.26	29.24	70.76	-0.345815	1.24±0.01	0.001236
	B	27.12	18.49	81.51			
	C	28.30	20.87	79.13			
4	A	20.84	45.89	54.11	-0.614210	1.66±0.01	0.001662
	B	20.97	36.98	63.02			
	C	21.36	40.27	59.73			
24	A	4.34	88.73	11.27	-2.182741	6.54±0.08	0.006524
	B	4.08	87.74	12.26			
	C	4.21	88.23	11.77			

ε = -2.96±0.19‰

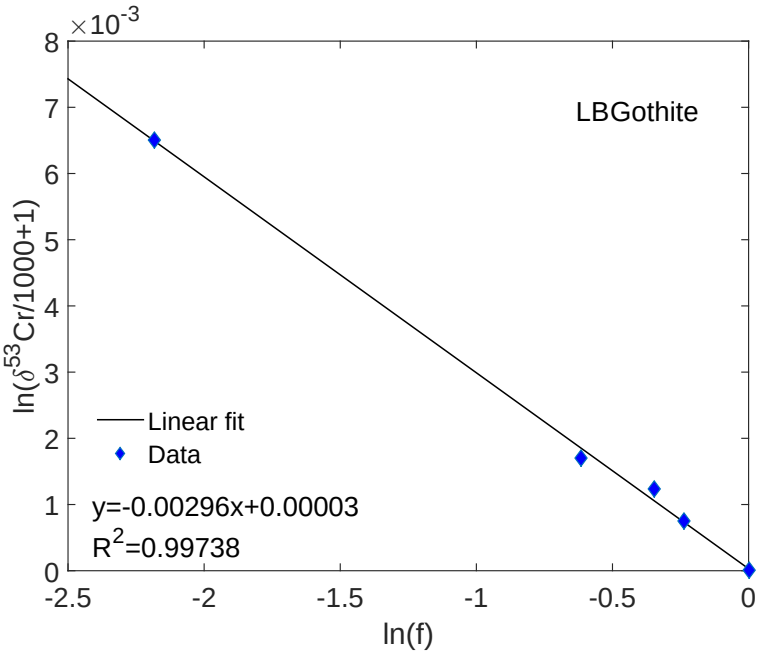


Figure 19: $\ln f$ vs. $\ln(\delta^{53}Cr/1000+1)$ for Cr(VI) reduction by *Pseudomonas* in the presence of goethite.

Table 17: Anaerobic Cr(VI) reduction by *Pseudomonas fluorescens* LB 300 in the presence of haematite

Time	**Sample**	**[Cr(VI)]**	**Fraction removed**	**Fraction remaining**	lnF	$\delta^{53}Cr$	$ln(\frac{\delta^{53}Cr}{1000}+1)$
(Hour)		**(mg/L)**	%	%		‰	
0	A	14.95	0.00	100.00	-0.000000	0.00±0.00	0.000000
	B	14.95	0.00	100.00			
	C	13.77	0.00	100.00			
1	A	10.36	30.72	69.28	-0.367014	1.32±0.21	0.0013181
	B	10.90	27.05	72.95			
	C	11.00	20.14	79.86			
2	A	9.35	37.45	62.55	-0.469203	2.51±0.10	0.0025053
	B	10.53	29.50	70.50			
	C	10.36	24.79	75.21			
4	A	6.79	54.57	45.43	-0.788998	3.26±0.04	0.0032552
	B	7.06	52.73	47.26			
	C	7.34	46.70	53.30			
24	A	0.00	100.00	0.00			
	B	0.00	100.00	0.00			
	C	0.00	100.00	0.00			

ε = -4.26±0.71‰

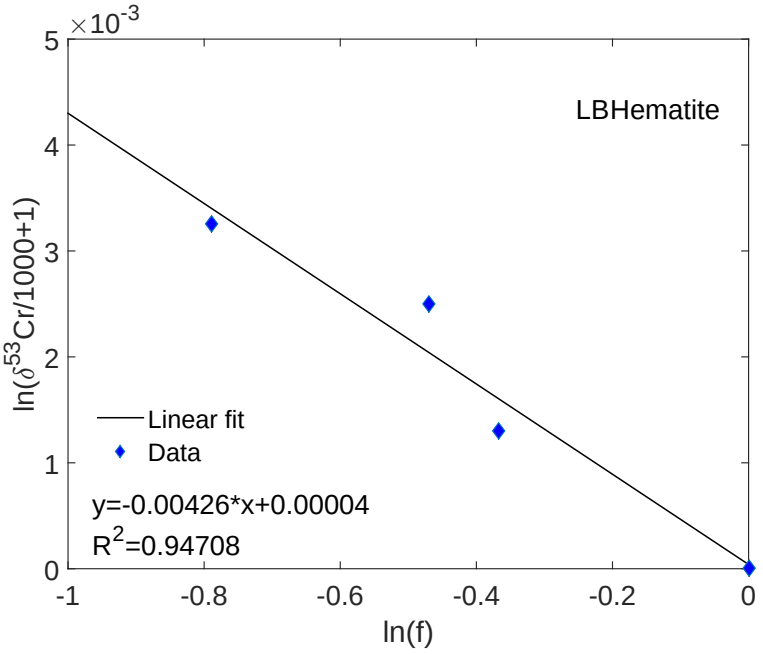


Figure 20: $\ln f$ vs. $\ln(\delta^{53}Cr/1000+1)$ for Cr(VI) reduction by *Pseudomonas* in the presence of haematite.

Table 18: Anaerobic Cr(VI) reduction by *Pseudomonas fluorescens* LB 300 aqueous Fe(III) in the medium

Time	**Sample**	**[Cr(VI)]**	**Fraction removed**	**Fraction remaining**	lnF	$\delta^{53}Cr$	$ln(\frac{\delta^{53}Cr}{1000}+1)$
(Hour)		**(mg/L)**	%	%		‰	
0	A	18.28	0.00	100.00			
	B	18.28	0.00	100.00	0.000000	0.00±0.01	0.000000
	C	18.28	0.00	100.00			
0.1	A	14.23	22.17	77.83			
	B	14.05	23.13	76.87	-0.263084	0.59±0.03	0.000590
	C	14.05	23.13	76.87			
1	A	9.11	50.16	49.84			
	B	7.90	56.80	43.20	-0.839403	1.70±0.06	0.001699
	C	8.03	53.48	46.52			
2	A	6.59	63.93	36.07			
	B	4.87	73.36	26.63	-1.322854	4.14±0.07	0.004133
	C	5.31	70.94	29.06			
4	A	4.41	75.86	24.14			
	B	2.24	87.71	12.28			
	C	3.28	82.01	17.99			

ε = -3.00±0.82‰

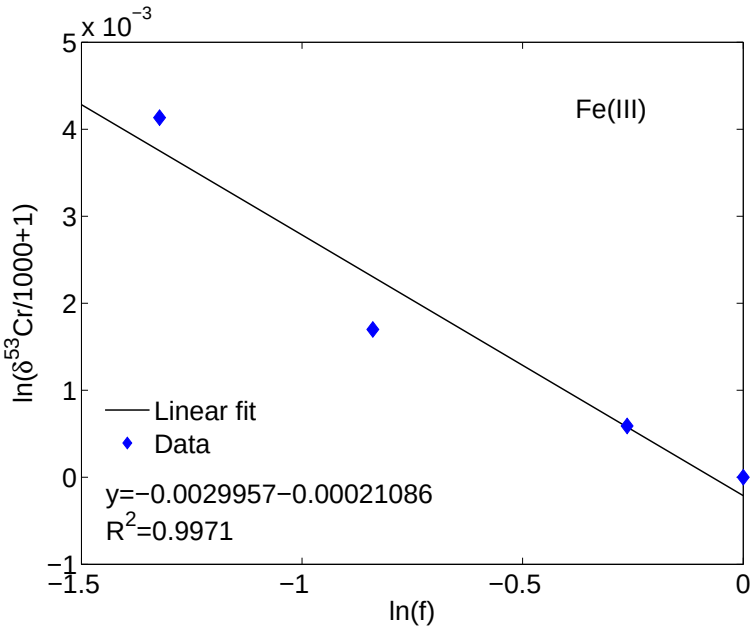


Figure 21: $\ln f$ vs. $\ln(\delta^{53}Cr/1000 + 1)$ for Cr(VI) reduction by *Pseudomonas* in the presence of aqueous Fe(III).

Table 19: Anaerobic Cr(VI) reduction by *Pseudomonas fluorescens* LB 300 aqueous Fe(II) in the medium

Time	**Sample**	**[Cr(VI)]**	**Fraction removed**	**Fraction remaining**	lnF	$\delta^{53}Cr$	$ln(\frac{\delta^{53}Cr}{1000}+1)$
(Hour)		**(mg/L)**	%	%		‰	
0	A	14.90	0.00	100.00	0.000000	0.00±0.01	0.000000
	B	14.90	0.00	100.00			
	C	14.90	0.00	100.00			
0.1	A	5.13	65.58	34.42	-1.066684	2.22±0.01	0.002219
	B	5.39	63.83	36.17			
	C	4.47	69.98	30.02			
1	A	2.57	82.76	17.24			
	B	1.91	87.16	12.84			
	C	1.69	88.65	11.35			
2	A	1.46	90.23	9.77	-2.325979	7.83±0.03	0.0078001
	B	1.06	92.87	7.13			
	C	0.75	94.98	5.02			

ε = -3.39±1.99‰

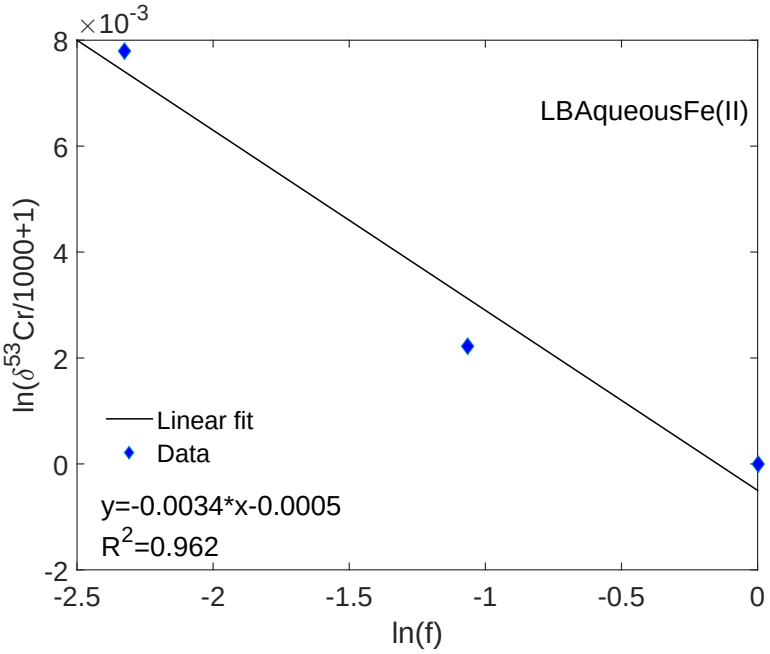


Figure 22: $\ln f$ vs. $\ln(\delta^{53}Cr/1000+1)$ for Cr(VI) reduction by *Pseudomonas* in the presence of aqueous Fe(II).

Table 20: Anaerobic Cr(VI) reduction by *Pseudomonas fluorescens* LB 300 with both aqueous Fe(II) and goethite in the medium

Time	**Sample**	**[Cr(VI)]**	**Fraction removed**	**Fraction remaining**	lnF	$\delta^{53}Cr$	$ln(\frac{\delta^{53}Cr}{1000}+1)$
(Hour)		**(mg/L)**	**%**	**%**		**‰**	
Original data							
0	A	14.90	0.00	100.00	0.000000	0.00±0.01	0.000000
	B	14.90	0.00	100.00			
	C	14.90	0.00	100.00			
0.1	A	4.34	70.86	29.14	-1.232989	2.64±0.02	0.0026323
	B	4.21	71.73	28.26			
	C	3.95	73.49	26.50			
1	A	1.68	88.74	11.26		5.96±0.01	
	B	1.44	90.32	9.68			
	C	1.27	91.46	8.54			
2	A	0.683	95.42	4.58		8.65±0.01	
	B	0.735	95.06	4.94			
	C	0.513	96.56	3.44			
Excluding abiotic reduction by Fe(II)							
0.1	A	4.34	0.00	100.00	0.000000	2.64±0.02	0.0026323
1	A	1.68	61.35	38.65	-0.950682	5.96±0.01	0.0059454
2	A	0.683	84.27	15.73	-1.849629	8.65±0.01	0.0086178

ε = -3.24±0.39‰ only for bacterial reduction

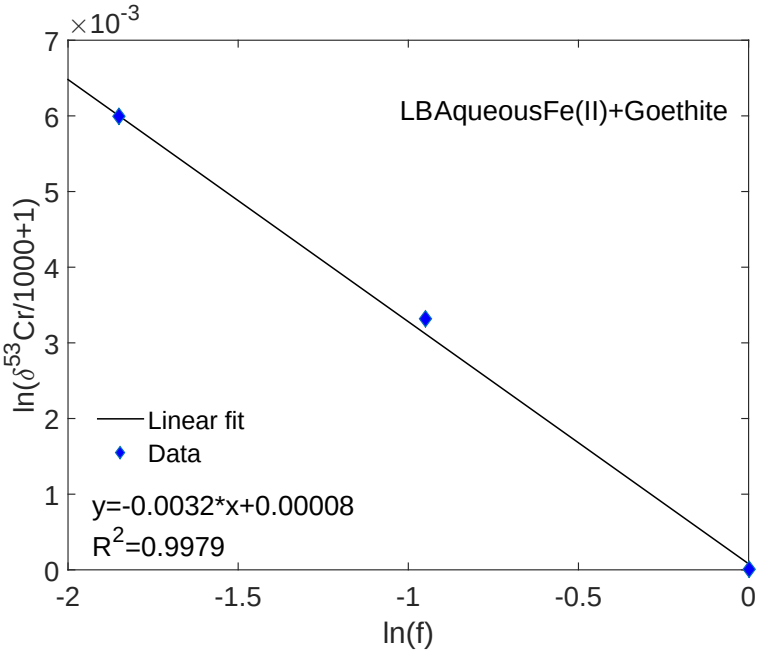


Figure 23: $\ln f$ vs. $\ln\left(\delta^{53}Cr/1000+1\right)$ for Cr(VI) reduction by *Pseudomonas* in the presence of both Fe(II) and goethite (excluding abiotic reduction by Fe(II)).

Table 21: Anaerobic Cr(VI) reduction by *Pseudomonas fluorescens* LB 300 with both aqueous Fe(II) and haematite in the medium

Time	**Sample**	**[Cr(VI)]**	**Fraction removed**	**Fraction remaining**	lnF	$\delta^{53}Cr$	$ln(\frac{\delta^{53}Cr}{1000}+1)$
(Hour)		**(mg/L)**	**%**	**%**		**‰**	
Original data							
0	A	14.90	0.00	100.00	0.000000	0.00±0.01	0.000000
	B	14.90	0.00	100.00			
	C	14.90	0.00	100.00			
0.1	A	4.60	69.10	30.90	-1.174427	1.92±0.01	0.001921
	B	3.29	77.89	22.11			
	C	3.56	76.13	23.87			
1	A	2.00	86.54	13.46		4.83±0.01	
	B	2.25	84.87	15.13			
	C	2.06	86.19	13.81			
2	A	1.04	93.04	6.96		6.84±0.02	
	B	1.17	92.16	7.84			
	C	1.38	90.76	9.24			
Excluding abiotic reduction by Fe(II)							
0.1	A	4.60	0.00	100.00	0.000000	1.92±0.01	0.001921
1	A	2.00	56.44	43.56	-0.831043	4.83±0.01	0.004818
2	A	1.04	77.49	22.51	-1.491046	6.84±0.02	0.006816

ε = -3.29±0.28‰ only for bacterial reduction

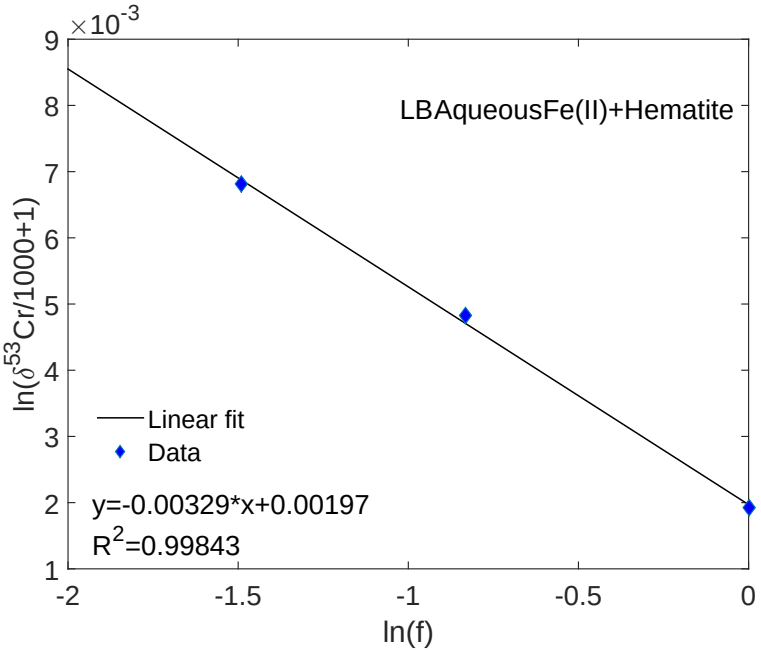


Figure 24: $\ln f$ vs. $\ln\left(\delta^{53}Cr/1000+1\right)$ for Cr(VI) reduction by *Pseudomonas* in the presence of both Fe(II) and Haematite (excluding abiotic reduction by Fe(II)).

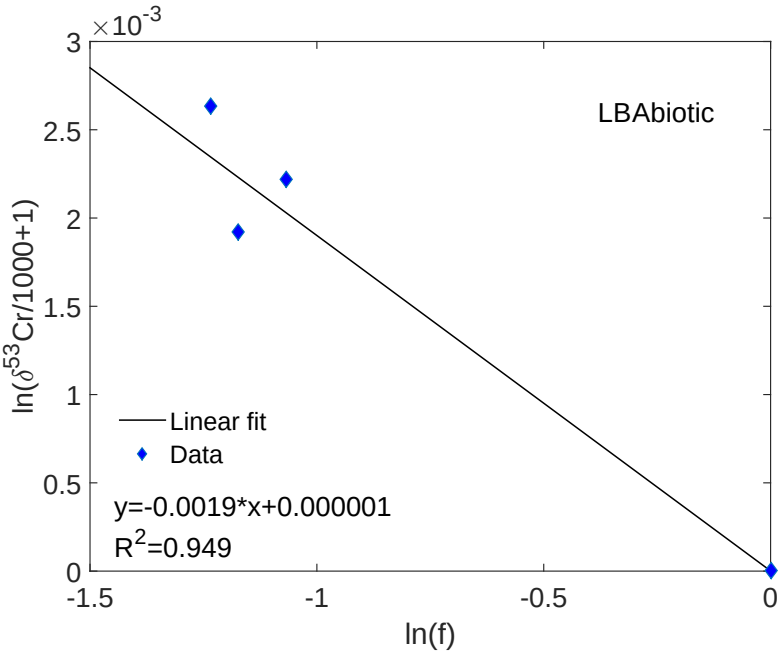


Figure 25: $\ln f$ vs. $\ln(\delta^{53}Cr/1000+1)$ for Cr(VI) abiotic reduction by Fe(II).

Table 22: Anaerobic Cr(VI) reduction by *Shewanella oneidensis* MR-1 without any mineral or aqueous iron species

Time	**Sample**	**[Cr(VI)]**	**Fraction removed**	**Fraction remaining**	lnF	$\delta^{53}Cr$	$ln(\frac{\delta^{53}Cr}{1000}+1)$
(Hour)		**(mg/L)**	%	%		‰	
0	A	19.00	0.00	100.00			
	B	21.01	0.00	100.00			
	C	21.82	0.00	100.00	0.000000	0.00±0.01	0.000000
24	A	11.63	38.77	61.22			
	B	14.66	30.25	69.75			
	C	14.76	32.37	67.63	-0.391101	1.00±0.01	0.000998
48	A	3.15	83.40	16.60			
	B	10.72	48.98	51.02			
	C	9.61	55.95	44.05	-0.819885	2.02±0.02	0.002022
72	A	1.14	94.02	5.98			
	B	1.74	91.71	8.29			
	C	1.14	94.79	5.20			

ε = -2.47±0.07‰

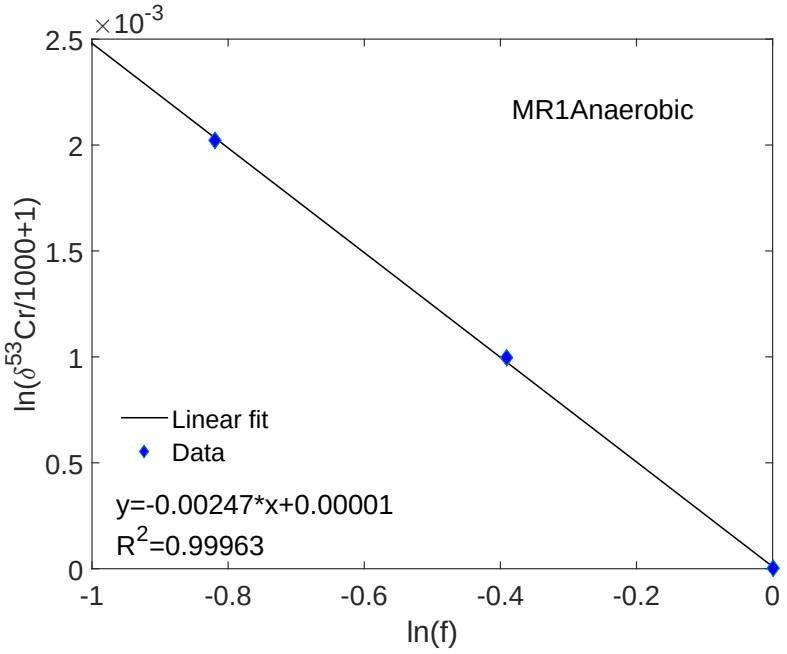


Figure 26: $\ln f$ vs. $\ln\left(\delta^{53}Cr/1000+1\right)$ for Cr(VI) reduction by *Shewanella* without any minerals or aqueous Fe species.

Table 23: Anaerobic Cr(VI) reduction by *Shewanella oneidensis* MR-1 with aqueous Fe(III) in the medium

Time	**Sample**	**[Cr(VI)]**	**Fraction removed**	**Fraction remaining**	lnF	$\delta^{53}Cr$	$ln(\frac{\delta^{53}Cr}{1000}+1)$
(Hour)		**(mg/L)**	%	%		‰	
0	A	20.91	0.00	100.00			
	B	21.41	0.00	100.00			
	C	19.40	0.00	100.00	0.000000	0.00±0.01	0.000000
24	A	13.14	37.15	62.85			
	B	13.95	34.86	65.14			
	C	13.04	32.77	67.23			
48	A	12.13	41.98	58.02			
	B	13.14	38.63	61.37			
	C	12.13	37.45	62.55	-0.469204	1.08±0.02	0.001084
72	A	5.98	71.41	28.59			
	B	9.11	57.47	42.52			
	C	8.60	55.65	44.34	-0.813057	1.90±0.04	0.001904

ε = -2.34±0.07‰

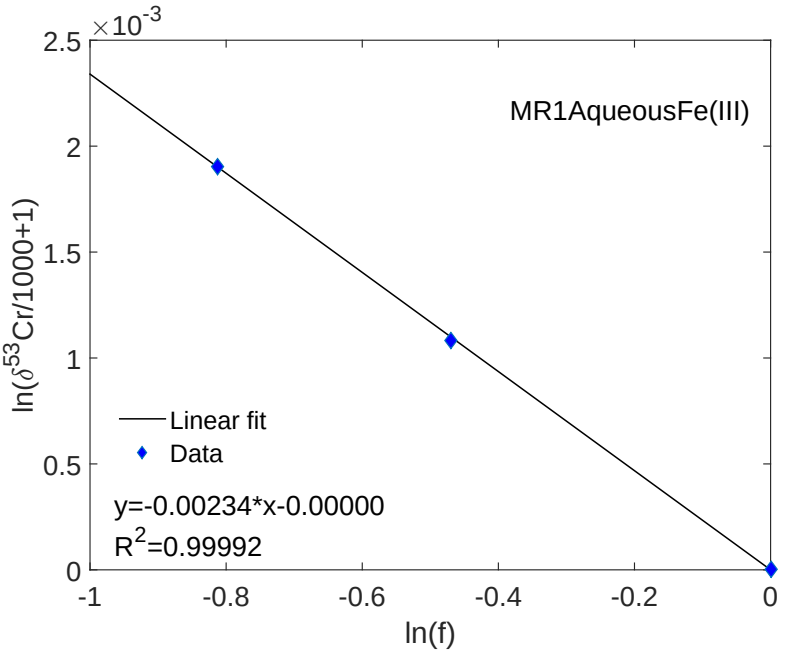


Figure 27: $\ln f$ vs. $\ln(\delta^{53}Cr/1000+1)$ for Cr(VI) reduction by *Shewanella* in the presence of aqueous Fe(III).

Table 24: Anaerobic Cr(VI) reduction by *Shewanella oneidensis* MR-1 with goethite in the medium

Time	**Sample**	**[Cr(VI)]**	**Fraction removed**	**Fraction remaining**	lnF	$\delta^{53}Cr$	$ln(\frac{\delta^{53}Cr}{1000}+1)$
(Hour)		**(mg/L)**	**%**	**%**		**‰**	
0	A	11.45	0.00	100.00	0.000000	0.00±0.01	0.000000
	B	11.45	0.00	100.00			
	C	15.69	0.00	100.00			
1	A	9.25	19.21	80.79	-0.21332	0.91±0.02	0.000912
	B	9.25	19.21	80.79			
	C	7.60	51.56	48.44			
2	A	6.18	46.03	53.97	-0.616556	1.79±0.01	0.001786
	B	6.66	41.83	58.16			
	C	5.48	65.07	34.93			
4	A	2.86	75.02	24.98	-1.387095	3.11±0.03	0.003102
	B	2.86	75.02	24.98			
	C	1.95	87.57	12.43			

ε = -2.13±0.41‰

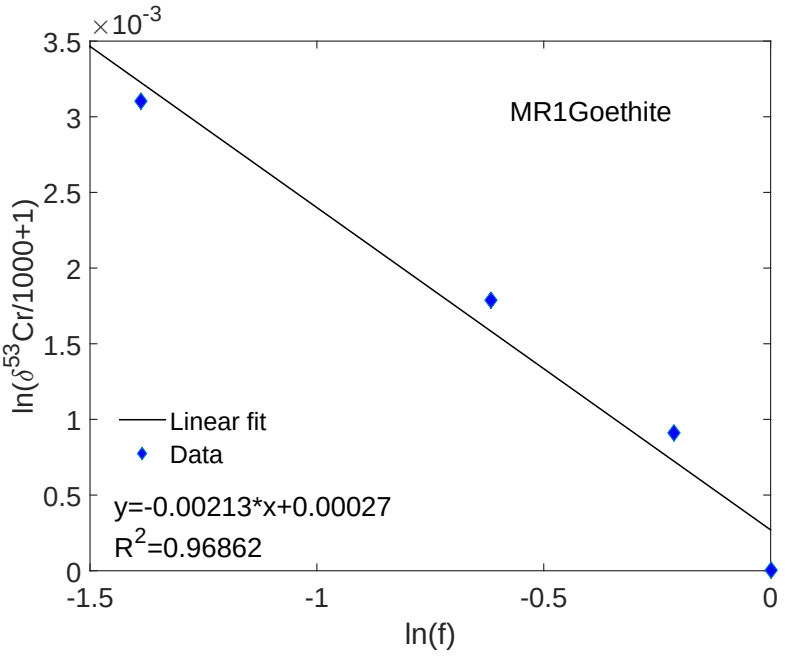


Figure 28: $\ln f$ vs. $\ln(\delta^{53}Cr/1000+1)$ for Cr(VI) reduction by *Shewanella* in the presence of goethite.

Table 25: Anaerobic Cr(VI) reduction by *Shewanella oneidensis* MR-1 with haematite in the medium

Time	**Sample**	**[Cr(VI)]**	**Fraction removed**	**Fraction remaining**	lnF	$\delta^{53}Cr$	$ln(\frac{\delta^{53}Cr}{1000}+1)$
(Hour)		**(mg/L)**	**%**	**%**		**‰**	
0	A	13.63	0.00	100.00	0.000000	0.00±0.01	0.000000
	B	13.28	0.00	100.00			
	C	13.05	0.00	100.00			
1	A	10.66	21.79	78.21			
	B	8.54	35.69	64.31			
	C	10.19	21.92	78.08			
2	A	7.36	46.00	54.00	-0.616186	1.23±0.01	0.001230
	B	8.54	35.69	64.31			
	C	8.54	34.56	65.44			
4	A	5.15	62.22	37.78	-0.973126	2.24±0.00	0.002241
	B	5.04	62.05	37.95			
	C	4.58	64.90	35.10			

ε = -2.27±0.29‰

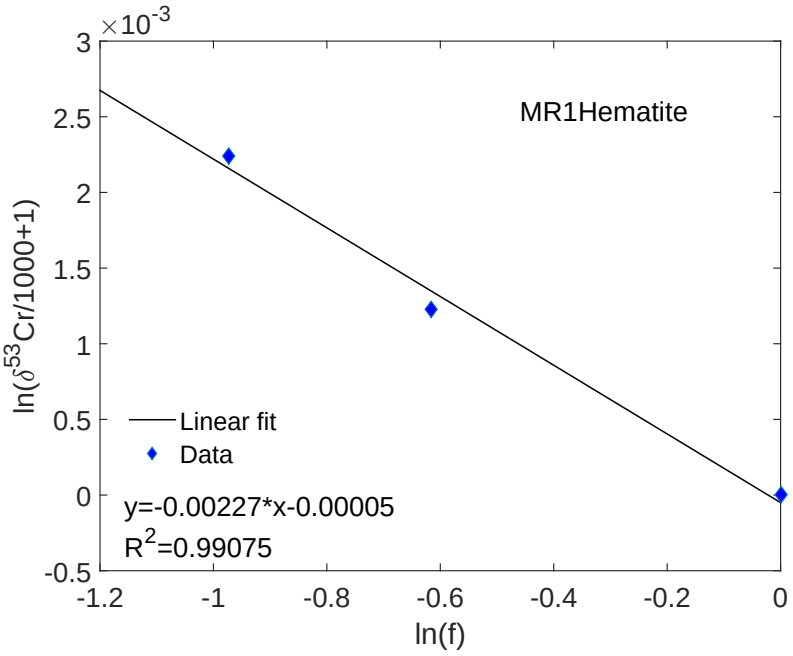


Figure 29: $\ln f$ vs. $\ln(\delta^{53}Cr/1000+1)$ for Cr(VI) reduction by *Shewanella* in the presence of haematite.

Table 26: Aerobic Cr(VI) reduction by *Pseudomonas fluorescens* LB 300 with different initial Cr(VI) concentration

Time	**Sample**	**[Cr(VI)]**	**Fraction removed**	**Fraction remaining**	lnF	$\delta^{53}Cr$	$ln(\frac{\delta^{53}Cr}{1000}+1)$
(Hour)		**(mg/L)**	**%**	**%**		**‰**	
High Cr(VI) initial concentration ε = -2.57±0.39‰							
0	A	46.42	0.00	100.00	0.000000	0.00±0.01	0.000000
	B	46.42	0.00	100.00			
	C	46.42	0.00	100.00			
1	A	36.40	21.59	78.41	-0.243204	0.32±0.02	0.000320
	B	38.52	17.02	82.98			
	C	38.94	16.13	83.87			
24	A	24.04	48.21	51.78			
	B	24.60	47.00	53.00			
	C	24.58	47.05	52.95			
48	A	24.46	47.31	52.69			
	B	22.73	51.04	48.96			
	C	23.64	49.07	50.93			
72	A	22.32	51.91	48.09	-0.732165	1.82±0.02	0.000182
	B	21.39	53.92	46.08			
	C	21.71	53.23	46.77			
96	A	22.20	52.18	47.82			
	B	22.80	50.88	49.12			
	C	22.43	51.68	48.32			

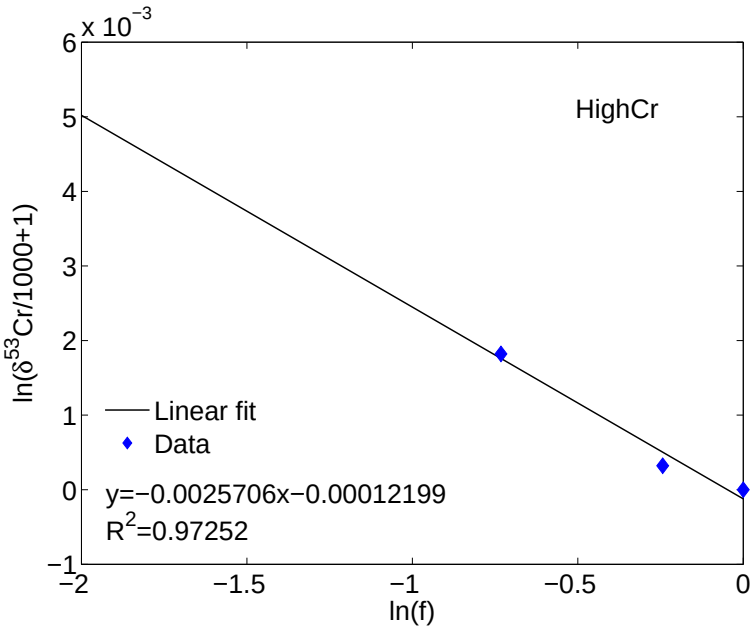


Figure 30: $\ln f$ vs. $\ln\left(\delta^{53}Cr/1000+1\right)$ for Cr(VI) reduction by *Pseudomonas* with high initial Cr concentration (40 mg/L).

Table 27: Aerobic Cr(VI) reduction by *Pseudomonas fluorescens* LB 300 with different initial Cr(VI) concentration

Time	**Sample**	**[Cr(VI)]**	**Fraction removed**	**Fraction remaining**	lnF	$\delta^{53}Cr$	$ln(\frac{\delta^{53}Cr}{1000}+1)$
(Hour)		**(mg/L)**	**%**	**%**		**‰**	
Medium Cr(VI) initial concentration *ε = -3.12±0.10‰							
0	A	23.74	0.00	100.00			
	B	23.74	0.00	100.00	-0.000000	0.00±0.01	0.000000
	C	23.74	0.00	100.00			
1	A	16.97	28.53	71.47			
	B	17.16	27.71	72.29	-0.324497	0.93±0.04	0.000927
	C	17.12	27.87	72.13			
24	A	15.56	34.44	65.56			
	B	14.86	37.42	62.58	-0.468654	1.49±0.03	0.001488
	C	15.00	36.82	63.18			
48	A	13.41	43.51	56.49			
	B	13.70	42.31	57.69			
	C	15.59	34.32	65.68			
72	A	12.37	47.90	52.10			
	B	12.41	47.73	52.27	-0.648691	1.95±0.03	0.001950
	C	10.27	56.72	43.28			
96	A	10.22	56.96	43.04			
	B	10.58	55.42	44.58	-0.807967	2.53±0.09	0.002525
	C	7.20	69.66	30.34			

* Same data from Table 1

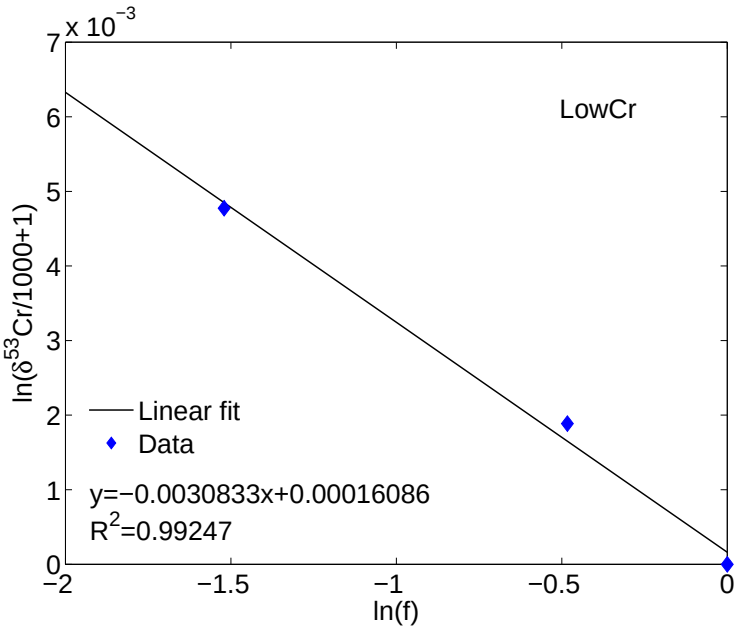


Figure 31: $\ln f$ vs. $\ln\left(\delta^{53}Cr/1000+1\right)$ for Cr(VI) reduction by *Pseudomonas* with low initial Cr concentration (5 mg/L).

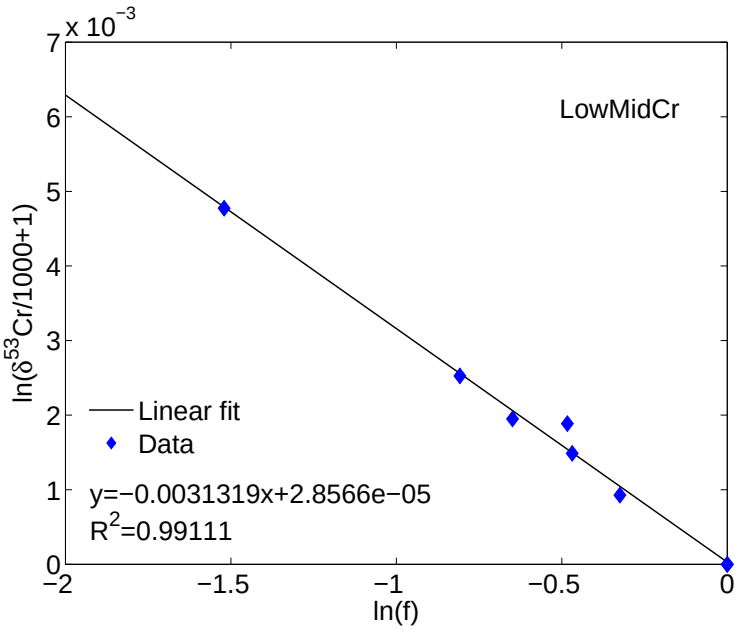


Figure 32: $\ln f$ vs. $\ln\left(\delta^{53}Cr/1000+1\right)$ for Cr(VI) reduction by *Pseudomonas* with both low (5 mg/L) and medium (20 mg/L) initial Cr concentration.

Table 28: Aerobic Cr(VI) reduction by *Pseudomonas fluorescens* LB 300 with different initial Cr(VI) concentration

Time	**Sample**	**[Cr(VI)]**	**Fraction removed**	**Fraction remaining**	lnF	$\delta^{53}Cr$	$ln(\frac{\delta^{53}Cr}{1000}+1)$
(Hour)		**(mg/L)**	%	%		‰	
Low Cr(VI) initial concentration ε = -3.08±0.51‰							
0	A	6.50	0.00	100.00	0.000000	0.00±0.01	0.000000
	B	6.50	0.00	100.00			
	C	6.50	0.00	100.00			
1	A	4.01	38.30	61.69	-0.482977	1.89±0.02	0.001885
	B	4.01	38.27	61.73			
	C	4.15	36.20	63.80			
24	A	1.42	78.14	21.86	-1.520399	4.78±0.07	0.004774
	B	1.44	77.86	22.14			
	C	1.51	76.73	23.27			